Universidade de Aveiro
2021

Patrícia Maria Veríssimo de Pinho e Silva

Toxicocinética de nanopartículas de prata em invertebrados bentónicos de água doce

Toxicokinetics of silver nanoparticles in freshwater benthic invertebrates

Universidade de Aveiro
2021

Patrícia Maria Veríssimo de Pinho e Silva

Toxicocinética de nanopartículas de prata em invertebrados bentónicos de água doce

Toxicokinetics of silver nanoparticles in freshwater benthic invertebrates

Tese apresentada à Universidade de Aveiro para cumprimento dos requisitos necessários à obtenção do grau de Doutor em Biologia e Ecologia das Alterações Globais, realizada sob a orientação científica da Doutora Susana Patrícia Mendes Loureiro, Professora Auxiliar com Agregação do Departamento de Biologia da Universidade de Aveiro, e coorientação do Doutor Cornelis Adrianus Maria van Gestel, Professor Catedrático do Departamento de Ciências Ecológicas da Faculdade de Ciências da Universidade Livre de Amesterdão, Países Baixos.

Apoio financeiro da FCT e do FSE no âmbito do III Quadro Comunitário de Apoio através de uma bolsa de doutoramento atribuída a Patrícia Maria Veríssimo de Pinho e Silva (PD/BD/52571/2014) e do projeto NanoFASE (União Europeia, programa Horizonte 2020, contrato nº 646002).

o júri

presidente

Doutor José Fernando Ferreira Mendes
Professor Catedrático da Universidade de Aveiro

Doutora Lúcia Maria Candeias Guilhermino
Professora Catedrática da Universidade do Porto

Doutora Martha Gerdina Vijver
Professora de Ecotoxicologia da Universidade de Leiden, Países Baixos

Doutora Elma Lahive
Investigadora do Centro de Ecologia e Hidrologia, Reino Unido

Doutora Susana Patrícia Mendes Loureiro (orientadora)
Professora Auxiliar com Agregação da Universidade de Aveiro

Doutor João Luís Teixeira Pestana
Investigador Auxiliar da Universidade de Aveiro

agradecimentos

São muitas as pessoas que estiveram envolvidas direta ou indiretamente neste trabalho, às quais estou imensamente grata!

Primeiro, um agradecimento muito especial à Susana! Obrigada por tudo o que me ensinou, pela (muita) paciência, entusiasmo, compreensão e ajuda nos momentos mais difíceis, e por fazer-me acreditar que sou capaz (sei que não foi fácil!). Muito obrigada pela oportunidade única de participar no NanoFASE!

A huge thank you to Kees! For being so kind and supportive, for your patience and willingness to always help me! I learned a lot from you!

Thank you to all my colleagues from the NanoFASE project, especially to the "mesocosm (aquatic and terrestrial) team"! I learned so much from you, it was an experience I will never forget!

Many thanks to Rudo, for all his help and never complaining about my endless samples!

To all my co-authors, thank you for all the essential help and contributions to this work, especially those whose support in this last phase was essential for me! Rui and Marija, thank you!

Um muito obrigada ao super técnico Abel, por sempre fazer todos os possíveis para nos ajudar, e pelo seu humor peculiar ;p

Carlinhos, obrigada pela ajuda e companhia nas horas infinitas no laboratório, pela tua amizade e, não menos importante, pelos teus "desencaminhanços" para um cafezinho rápido, que tanto precisava!

Zahra, I am very grateful for your friendship and support!

A todos os meus colegas de laboratório, do stress e call centre! Aos meus amigos do "Dirty Dancing", por todos os momentos que passamos dentro e fora do laboratório, os quais eu nunca irei esquecer! Bate vira!

Aos meus pais, avós, irmã e cunhadinho! Por todo o apoio, compreensão e por serem um refúgio!

Por fim, ao João…por tudo! Sem ti não seria possível! Obrigada por acreditares em mim!

palavras-chave

Nanopartículas de prata, nanopartículas de sulfeto de prata, invertebrados bentónicos, toxicocinética, bioacumulação, sedimentos de água doce, mesocosmos.

resumo

A indústria da nanotecnologia cresceu exponencialmente na última década, levando inevitavelmente à libertação de nanomateriais de engenharia (NME) para o meio ambiente. Os sedimentos podem ser importantes depósitos ambientais de NME, sendo uma potencial ameaça ao biota bentónico. Para uma nanotecnologia sustentável é necessária uma avaliação de risco ambiental robusta, de modo a garantir a preservação dos ecossistemas e, ao mesmo tempo, apoiar a inovação. Neste sentido, os estudos de bioacumulação e toxicocinética de NME têm sido altamente requisitados pelas entidades reguladoras. Com o objetivo de contribuir para esta temática, a presente tese tem como foco determinar e compreender a bioacumulação e toxicocinética de diferentes nanopartículas de prata pristinas (Ag NPs), nanopartículas de sulfeto de prata (Ag_2S NPs, usadas como modelo de uma forma de Ag NP ambientalmente envelhecida) e $AgNO_3$ em invertebrados bentónicos de água doce. As espécies ecologicamente relevantes *Physa acuta*, *Chironomus riparius* e *Girardia tigrina* foram escolhidas como organismos de teste e foram expostas às diferentes NPs por diferentes vias. No primeiro estudo, o caracol *P. acuta* foi exposto a 1) água contaminada (sem sedimento), 2) água contaminada com sedimento limpo e 3) sedimento contaminado. Os resultados revelaram rápida acumulação e depuração de Ag pelos caracóis no tratamento com Ag_2S NPs em todos os testes. A água foi a via de exposição de Ag predominante para a *P. acuta*. Também foi demonstrado que a biodisponibilidade da Ag para os caracóis foi muito influenciada pelas suas características e pela via de exposição. As larvas de *C. riparius* foram expostas às diferentes formas de Ag por meio de água, sedimento ou alimento. Os resultados revelaram consistentemente uma maior acumulação de Ag pelas larvas de quironomídeos, após a exposição a Ag_2S NPs, enquanto as larvas expostas às Ag NPs pristinas e ao $AgNO_3$ geralmente apresentaram uma toxicocinética semelhante. A acumulação de Ag pelas larvas foi mais bem explicada pela exposição a água, do que pela ingestão de partículas de sedimento, em ambos os testes de exposição via água e via sedimento. A exposição via alimento revelou acumulação de Ag apenas no tratamento com Ag_2S NP. No estudo seguinte, a *P. acuta* foi primeiro exposta a água contaminada com Ag (Ag_2S NP e $AgNO_3$) e alimentada com microalgas (limpas) e, subsequentemente, fornecida como alimento pré-exposto às planárias *G. tigrina*. Ambas as espécies revelaram maior acumulação de Ag no tratamento com $AgNO_3$ do que com Ag_2S NP.

resumo (cont.)

A acumulação de Ag pelos caracóis provavelmente ocorreu através da combinação de exposição à água e ingestão de microalgas. As planárias acumularam Ag via alimento em ambos os tratamentos com Ag_2S NP e $AgNO_3$, sem ser observado nenhum risco de biomagnificação na cadeia alimentar *P. acuta* → *G. tigrina*. Do nosso conhecimento, este é o primeiro estudo sobre a toxicocinética de NPs em planárias. Finalmente, um teste em mesocosmos foi efetuado em laboratório de modo a simular um ambiente de rio e avaliar a toxicocinética, bioacumulação e potencial biomagnificação da Ag_2S NP. Para além disso, foi avaliado se os testes de laboratório uni-específicos conseguem prever a bioacumulação de Ag no teste em mesocosmos. As espécies *G. tigrina, P. acuta e C. riparius* bioacumularam Ag nas exposições a Ag_2S NP e $AgNO_3$, mas revelaram concentrações internas de Ag mais elevadas na exposição a $AgNO_3$. A acumulação observada no tratamento com Ag_2S NP foi provavelmente na forma particulada, revelando biodisponibilidade desta forma de Ag, mais persistente e relevante num um cenário de exposição mais realista. Os testes de laboratório com uma espécie não foram geralmente capazes de prever com segurança a bioacumulação de Ag no sistema mais complexo dos mesocosmos. Além disso, não foi observado nenhum risco de biomagnificação no tratamento com Ag_2S NP neste cenário de exposição ambientalmente mais realista, no entanto, parece ter ocorrido na cadeia alimentar *P. acuta* → *G. tigrina* no tratamento com $AgNO_3$. Este foi o primeiro estudo a investigar a toxicocinética de Ag_2S NPs em invertebrados bentónicos num teste em mesocosmos de água doce. Este trabalho fornece dados importantes para a modelação da potencial exposição e bioacumulação de Ag após exposição a Ag NPs, incluindo Ag_2S NPs, em ambientes bentónicos de água doce. Os dados gerados na presente tese podem ser úteis em modelos preditivos para fins aplicados à nano regulação, contribuindo para o desenvolvimento da avaliação de risco ambiental de NME.

keywords

Silver nanoparticles, silver sulfide nanoparticles, benthic invertebrates, toxicokinetic, bioaccumulation, freshwater sediments, mesocosms.

abstract

The nanotechnology industry has grown exponentially in the last decade, inevitably leading to the release of engineered nanomaterials (ENMs) into the environment. Sediments can be important environmental sinks for ENMs, potentially threatening benthic biota. For a sustainable nanotechnology a robust environmental risk assessment is required to ensure the preservation of the ecosystems while supporting innovation. In line with this, studies on the bioaccumulation and toxicokinetics of ENMs have been highly requested by regulatory parties. Aiming to contribute to this subject, the present thesis focuses on determining and understanding the toxicokinetics of different pristine silver nanoparticles (Ag NPs), silver sulfide nanoparticles (Ag_2S NPs, used as model of an environmentally aged Ag NP form) and $AgNO_3$ in freshwater benthic invertebrates. The ecologically relevant species *Physa acuta*, *Chironomus riparius* and *Girardia tigrina* were chosen as test organisms and exposed to the different NPs through different routes. In the first study, the snail *P. acuta* was exposed to 1) contaminated water (without sediment), 2) contaminated water with clean sediment, and 3) contaminated sediment. Results revealed fast uptake and depuration of Ag from Ag_2S NPs by the snails in all experiments. Water exposure was the predominant Ag uptake route for *P. acuta*. It was also shown that bioavailability of Ag to the snails was greatly influenced by the Ag characteristics and by the exposure route. *C. riparius* larvae were exposed to the different Ag forms via water, sediment, or food. Results consistently revealed higher Ag uptake by the chironomid larvae upon exposure to Ag_2S NPs, while larvae exposed to pristine Ag NPs and $AgNO_3$ generally presented similar toxicokinetics. Uptake of Ag by the larvae was better explained by exposure to water than from the ingestion of sediment particles in both water and sediment exposure tests. Food exposure resulted only in Ag uptake in the Ag_2S NP treatment. For the next study, *P. acuta* was first exposed to Ag-spiked water (Ag_2S NP and $AgNO_3$) and fed with (clean) microalgae, and subsequently provided as pre-exposed food to the planarians *G. tigrina*. Both species revealed higher Ag uptake from $AgNO_3$ than from Ag_2S NP treatment. Uptake of Ag by the snails was probably via a combination of water exposure and ingestion of microalgae. Planarians accumulated Ag from the food in both Ag_2S NP and $AgNO_3$ treatments, but no apparent risk for biomagnification was observed in the food chain *P. acuta* → *G. tigrina*. To the best of our knowledge this is the first study investigating the toxicokinetics of NPs in planarians.

abstract (cont.)

Finally, an indoor mesocosm experiment simulating a stream environment was conducted to evaluate the toxicokinetics, bioaccumulation and biomagnification potential of Ag_2S NP. Furthermore, it was investigated whether single-species tests can predict Ag bioaccumulation in the mesocosm test. The species *G. tigrina*, *P. acuta* and *C. riparius* bioaccumulated Ag in both Ag_2S NP and $AgNO_3$ exposures, but showed higher internal Ag concentrations upon $AgNO_3$ exposure. The uptake observed in the Ag_2S NP treatment was probably in the particulate form, revealing bioavailability of this more environmentally persistent and relevant Ag nanoparticulate form in a more realistic exposure scenario. Single-species tests generally were not able to reliably predict Ag bioaccumulation in the more complex mesocosm system. Moreover, no risk for biomagnification was observed in Ag_2S NP treatment under this environmentally realistic exposure scenario, however it seemed to occur in the food chain *P. acuta* → *G. tigrina* in the $AgNO_3$ treatment. This was the first study investigating the toxicokinetics of Ag_2S NPs in benthic invertebrates in a freshwater mesocosm experiment. This work provides important data for modelling the potential exposure and bioaccumulation of Ag from Ag NPs exposures, including Ag_2S NPs, in freshwater benthic environments. The data generated in the present thesis may be useful for predictive models for nano regulation purposes, contributing to improving the environmental risk assessment of ENMs.

Table of Contents

List of Figures

List of Tables

Chapter 1

General Introduction

1. General introduction

1.1. Overview of nanomaterials: production, release and fate in the environment

Over the last two decades, we have witnessed impressive developments in the nanotechnology market, with an estimated global value to be of 55 billion US dollars by 2022 (Inshakova and Inshakov, 2017; Malakar et al., 2021). Nanomaterials were classified in 2011 by the European Commission (EC) as "a natural, incidental or manufactured material containing particles, in an unbound state or as an aggregate or as an agglomerate and where, for 50 % or more of the particles in the number size distribution, one or more external dimensions is in the size range 1 nm - 100 nm" (European Commission 2011). However, identifying ENMs according to this definition proved to be challenging due to the existing wide variety of ENMs (Mech et al., 2020). Therefore, this definition has been under review and new classifications for ENMs are being discussed under the EC.

Nanomaterials designed and produced for commercial purposes are designated as engineered nanomaterials (ENMs) (ISO, 2008). Materials or chemicals engineered at the nanoscale exhibit enhanced properties such as antimicrobial effects, increased conductivity, strength or ultraviolet protection (Ahamed et al., 2021). Consequently, ENMs became widely applied in different sectors, such as agrichemicals, personal care products, telecommunication, computing and energy (Malakar et al., 2021). On November 1st of 2020, there were 5,000 products containing ENMs registered at the online inventory Nanodatabase (www.nanodb.dk). Such high number indicates that ENMs have entered at consumerization, which means that nanotechnology and nano-enabled consumer goods became part of our everyday life (Hansen et al., 2020).

This extensive use inevitably leads to ENM releases into the environment and consequently to environmental and human exposure, which can occur during all stages of their life-cycle: from synthesis, to incorporation into consumer products, usage and end-of-life disposal and recycling (McGillicuddy et al., 2017; Wigger et al., 2020). For instance, releases at the manufacturing stage can occur when using high energy and temperature procedures to perform structural modification of the nano-enabled product. Examples of emissions during usage of nano-enabled products include the application of cosmetics and sunscreens, or the spraying of products (Martínez et al., 2021). Washing textiles with incorporated ENMs will also lead to their release into sewer systems. Mass flow studies indicate that only a limited amount of ENMs is likely to be directly release into the environment. The majority will be primarily discharged in management water facilities, such

as wastewater treatment plants (WWTPs), waste incineration and landfills, before reaching the environment (Wigger et al., 2020).

ENMs can be emitted to different environmental compartments such as air, water, sediment and soil and finally reach the biota. These compartments will act as “reactors”, in the sense that ENMs will undergo transformations (Svendsen et al., 2020). ENMs can be release to the air compartment when spraying products or when dealing with powder material. In the atmosphere, ENMs can behave like an aerosol and be transported until eventually be deposited, either by dry or wet deposition, into water bodies or soils, and also undergo transformations (e.g., condensation, photo-induced transformations) (John et al., 2017; Pachapur et al., 2016). ENMs can reach the soil compartment mostly through the deposition of sewage sludge on agricultural fields, and by the application of nanofertilizers and nanopesticides in crops, or application for soil remediation (Malakar et al., 2021). Several ENM transformations can occur in the soil compartment that will determine their mobility and deposition, such as heteroaggregation or homoaggregation, dissolution in soil pore water, attachment to soil particles, oxidation, etc (Pachapur et al., 2016). Leaching from soil to the groundwater and surface runoffs may constitute ENMs release pathways from the terrestrial into the aquatic compartment. ENMs may also be released into water bodies via WWTP effluents, untreated sewage, or through release from antifouling paints (Figure 1.1) (Malakar et al., 2021; Suhendra et al., 2020). In the water column, many transformations may take place as ENMs pass from the water phase to the sediment phase (Cross et al., 2015). Depending on the interactions, ENMs may aggregate and settle into sediments or migrate over long distances (Li et al., 2020). The interactions and transformations occurring in the aquatic environment, as well as the importance of sediments as sinks for ENMs and consequent risk to benthic invertebrates, will be explored in the following sections.

1.2. Nanomaterials in the aquatic compartment

1.2.1. Nanomaterial fate in the water column

In aquatic environments, ENMs can undergo a myriad of transformations that will depend on their intrinsic characteristics and on environmental properties, such as water chemistry, ionic strength, pH, colloids/NOM (natural organic matter) (Cross et al., 2015). Understanding the dynamic interplay of interactions/transformations between ENMs and the aquatic system is critical to predict the fate and subsequent exposure of pelagic and benthic organisms (Lead et al., 2018; Turan et al., 2019). In the water column, ENMs may behave

similarly to other colloids, thus the classical colloid theory of Derjaguin, Landau, Verwey, and Overbeek (DLVO) that describes the interactions between charged colloidal particles as a function of attractive (i.e., Van der Waals) and repulsive (i.e., electrostatic) forces, has also been applied to ENMs (Cross et al., 2015), although this theory proved to be unsatisfactory to predict colloid behaviour in complex natural systems (Tourinho et al., 2012). In suspension, ENMs may attach to each other (homoaggregation) or to suspended particulate matter (SPM), including organic matter (heteroaggragation) (Figure 1.1) (Williams et al., 2019). At environmentally realistic concentrations (<1 µg L^{-1}) and relevant time-scales, heteroaggregation is likely more important than homoaggregation (Lead et al., 2018).

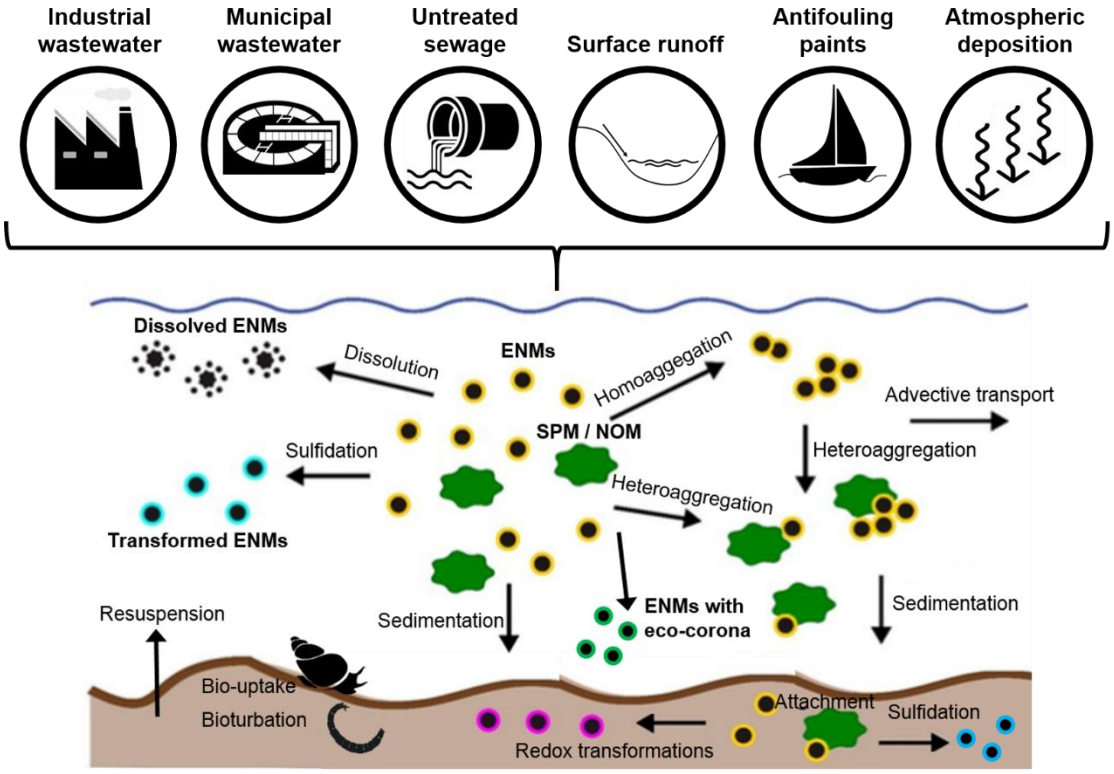

Figure 1.1. Engineered nanomaterial (ENM) fate processes and release pathways in the aquatic environment. Adapted from http://nanofase.eu/show/element_272.

In aquatic environments with high NOM concentrations, such as rivers or lakes, ENM behaviour will likely be dominated by complexation with NOM, because NOM concentrations probably are much higher than those of the ENMs (Cross et al., 2015). NOM has shown to stabilize ENMs against aggregation, through charge and steric repulsion (Lead et al., 2018). Since most of ENMs are expected to adsorb to NOM, ENM coating is likely to be replaced, for instance, by the binding of humic and fulvic acids, proteins and polysaccharides secreted by organisms, resulting in the formation of an environmental corona, the "eco-corona"

(Figure 1.1). This surface transformation may lead to passivation of charges with consequent changes of ENMs interactions, for instance, reducing the tendency of ENMs to aggregate to particulate matter (Spurgeon et al., 2020).

One important transformation process affecting ENM fate and consequently exposure to organisms in the aquatic media is dissolution. ENMs may undergo high dissolution into mainly an ionic form, such as ZnO ENMs, thus their fate, exposure and toxicity will be mostly attributed to ions. In turn, for ENMs with extremely low solubility, such as CeO_2 ENMs, the particulate form may be more important for their fate and toxicity. For ENMs with intermediate dissolution and solubility (e.g., Ag ENMs or CuO ENMs) both ionic and particle forms play important roles (Lead et al., 2018). Other surface reactions may also occur, such as oxidation via photooxidation (e.g., Ag ENMs to Ag_2O) or in the presence of organic ligands (e.g., Cu ENMs to CuO) (Williams et al., 2019). Due to their thermodynamic instability, the dissolution of small particles may involve a growth process known as the Ostwald ripening (Franklin et al., 2007). This process leads to the growth of larger particles at the consumption of smaller ones via the formation of intermediate mobile species (Gommes, 2019). Sulfidation is another surface reaction that may occur, which is of particular importance in systems with enhanced sulfide concentrations, such as in WWTPs or in sub-oxic or anoxic sediments (Figure 1.1). This reaction was mostly studied for Ag nanoparticles (Ag NPs), which are transformed into Ag sulfide NPs (Ag_2S NPs) by a core-shell formation, with gradual increase of the Ag_2S layer. This reaction may affect ENM surface charge, solubility and particle size (Lead et al., 2018).

1.2.2. Nanomaterial interactions with aquatic species

Due to the capacity of aquatic organisms to condition their environment, the interactions with biota may lead to further transformations of ENMs affecting their fate in surface waters. As mentioned earlier, interactions with biomolecules secreted by organisms may form an eco-corona (Nasser and Lynch, 2016; Spurgeon et al., 2020). Extracellular polymeric substances (EPS) are natural biopolymers secreted, for instance, by microalgae and other microorganisms, and are one of the main components of the NOM pool in aquatic environments. EPS-containing exudates will likely interact with ENMs forming an eco-corona, and also forming aggregates, which may result in flocculation in the water column and affect their sedimentation rates. Furthermore, it can also reduce exposure and toxicity to organisms in the water column, increasing exposure of benthic biota instead (Cross et al., 2015). When in sediments, resuspension of ENMs into the overlying waters can also happen due to the bioturbation activities of some sediment-dwelling species (Figure 1.1), potentially

shifting exposure from benthic to pelagic organisms (Cheng et al., 2019). This suggests that these processes can be important in coupling of benthic–pelagic ENM cycles in aquatic systems.

Species composition/diversity and abundance/density can have an important effect on the new properties ENMs may acquire. Selective feeding according to the species is an important aspect to consider. For instance, filter-feeders may alter the size distribution of natural inorganic colloids by selectively ingesting particles according to their filter mesh size (Cross et al., 2015). When ingested by organisms, ENMs may undergo transformations in the gastrointestinal tract during digestive processes and be excreted with different size, form or with a biological corona (bio-corona) (Cross et al., 2015; Monikh et al., 2021). The changes of ENM properties caused by biological entities are called biotransformation and are receiving growing attention (Pulido-Reyes et al., 2017). For example, ZnO NPs were biotransformed and excreted as dissolved Zn by the mussel *Mytilus galloprovincialis* (Montes et al., 2012). The crustacean *Daphnia magna* biotransformed CuO NPs and $CuSO_4$ into $Cu_3(PO_4)_2$ (Santos-Rasera et al., 2019). Mucus exudates secreted by organisms to prevent uptake may be deposited onto sediment surface beds and increase ENM bioavailability to benthic organisms (Cross et al., 2015).

1.2.3. Sediment environments as important sinks for nanomaterials

Fate studies revealed that heteroaggregation followed by sedimentation is likely to dominate ENM fate in natural water systems (Quik et al., 2012). Consequently, aquatic sediments are important final sinks for ENMs, and higher risk is attributed to benthic species than to pelagic ones (Selck et al., 2016). ENM characteristics and fate within sediments determine their bioavailability to benthic organisms. Once settled into sediment beds, ENM transformations may occur at the surface of the sediment or at the subsurface, following incorporation into sediments (Cross et al., 2015; Zhao et al., 2021). These transformations will depend on the new characteristics ENMs acquired so far, on (ecological) features of biota and on the geochemical properties of the sediments. Deposition of ENMs and attachment efficiency to sediment grains will depend on the pH and ionic strength, surface charge of the sediment minerals, and on the size and surface charge of the ENMs. This will also determine ENM mobility in sediments and availability in pore water (Cross et al., 2015). The coating of ENMs can determine their attachment efficiency. For instance, citrate-capped Ag NPs revealed higher attachment efficiency to quartz sand grains than PVP-capped Ag NPs (Badawy et al., 2013). Moreover, NOM plays a crucial role determining mobility and dissolution of ENMs within sediments and showed to either increase or reduce their mobility

(Cross et al., 2015). The presence of NOM reduced the prevalence of Ag^+ release from Ag NPs in sediment pore water (Akaighe et al., 2011; Liu and Hurt, 2010). Sulfidation within sediments is another process that can determine ENMs fate and bioavailability (Zhao et al., 2021). Sulfidation of Ag NPs may significantly reduce Ag^+ concentration, as Ag_2S NPs have very low solubility (He et al., 2019). Additionally, the Ag^+ released from Ag NPs may form smaller NPs by complexation with chloride present in pore waters, which can subsequently be sulfidised. Consequently, the distribution of ENMs in sediments or pore waters will influence exposure to benthic invertebrates (Cross et al., 2015; Lead et al., 2018).

1.3. Nanomaterial exposure to benthic invertebrates

Benthic invertebrates may be exposed to ENMs through several routes, such as associated with sediments in the different layers, in the pore water, overlying water or in food (Yoo et al., 2004). ENMs that do not penetrate into sediment surfaces may increase exposure to organisms that inhabit and feed on the surface layer of sediments (Cross et al., 2015), such as *Chironomus* species or freshwater gastropods. Conversely, organisms such as tubificid worms that feed in the deeper layers of sediments may be more exposed to ENMs that experience downward transportation in sediments (Cheng et al., 2019). ENMs undergoing higher dissolution and/or are transfer to sediment pore waters may be more available for transdermal uptake (Cross et al., 2015). Organisms such as pulmonate snails (e.g., *Lymnaea stagnalis, Physa acuta*) may also be exposed to ENMs in the water column, since these organisms are not exclusively in the sediment phase because they need to reach the surface to breathe (Kuehr et al., 2021a). Biofilms have shown to efficiently incorporate ENMs, thus deposit feeders like benthic grazers may be at particular risk when feeding on the biofilm at the sediment surface, with potential risks for trophic transfer (Cleveland et al., 2012; Park et al., 2018). Additionally, ecology, feeding habits and breathing type are some of the key factors of aquatic organisms that may determine uptake pathways of ENMs (Kuehr et al., 2021a).

1.3.1. Uptake of nanomaterials by benthic invertebrates

Within sediments, increased bioavailability of ENM aggregates to benthic filter-feeders is possible as aggregates can be retained in the filaments during filtration (Kuehr et al., 2021a). The uptake by the suspension-feeding bivalves *Crassostrea virginica* and *Mytilus edulis* of fluorescently labelled 100-nm polystyrene beads was especially enhanced by the formation of aggregates (Ward and Kach, 2009). Different respiratory modes may also

determine uptake. For instance, most freshwater gastropods are air-breathing pulmonates (pallial lung in the mantle cavity) and do not possess gills. They may take up dissolved contaminants through breathing to a lesser extent than gill-breathing species. Freshwater gastropods may also take up ENMs associated with food or passively through their soft body surfaces. Some bivalve species may accumulate ENMs through pedal feeding, which consists of a pinocytosis mechanism that can take up small particles by the surface of their foot. Amphipods may mainly take up ENMs through the dietary route or by respiration through the gills and trachea (Kuehr et al., 2021a). Dissolution also largely determines uptake. Several studies revealed lower uptake of the nanoparticulate form than the ionic counterpart (Kuehr et al., 2020; Kühr et al., 2018). Studies also show an important role of particle size, with nanosized or ionic form generally having a higher bioavailability than their microsized form (Pang et al., 2013). Different coatings and shapes also revealed different bioavailability and bioaccumulation of NPs. For instance, *L. stagnalis* uptake rate constants were higher for waterborne humic acid-coated Ag NPs than citrate Ag NPs, while upon dietary exposure higher accumulation was expected for citrate-coated Ag NPs (Croteau et al., 2011). The deposit feeder *Capitella teleta* showed preferential accumulation of rod-shaped compared to sphere- or platelet-shaped CuO NPs (Dai et al., 2015).

The formation of an eco-corona may also alter ENMs bioavailability and toxicity (Spurgeon et al., 2020). This corona may create a biological identity that is different from the original ENM synthetic identity, and can be an important feature determining the long-term fate of the ENMs (Pulido-Reyes et al., 2017). Studies suggests that the eco-corona may mitigate ENM toxicity, for instance, by reducing dissolution and bioavailability (Natarajan et al*.,* 2021). However, an increase in toxicity was also observed in exposures to NPs with an eco-corona. *D. magna* exposed to polystyrene NPs that were preincubated in conditioned medium to form an eco-corona (medium that contained *D. magna* to secret proteins before adding the polystyrene NPs), revealed higher NP uptake and toxicity, and also lower efficiency of NP removal from the gut (Nasser and Lynch, 2016). ENMs may also adsorb onto body surfaces, which may or may not result in transdermal uptake. However, in cases when transdermal uptake does not occur, ENMs may be available for dietary uptake by predators (Tangaa et al., 2016). Organisms can secret biogenic mucus that acts as barrier to ENM uptake. For example, it can be secreted at the body surface to prevent transdermal uptake, while gastrointestinal mucus can help preventing and/or selecting the uptake of ENMs into tissues (Cross et al., 2015).

Cellular uptake of ENMs has been the subject of a growing number of investigations during the past few years. While cellular uptake of ions derived from ENM dissolution may

follow the usual pathways for solutes, (e.g., ion channels, active transporters), for ENMs endocytosis seemed the prevalent cellular uptake mechanism (van den Brink et al., 2019). However, direct penetration of ENMs with sizes <10 nm has been indicated. The endocytic pathways for ENMs have been suggested to include mainly phagocytosis, macropinocytosis, clathrin-mediated, caveolin-mediated, and clathrin/caveolin-independent endocytosis (Pulido-Reyes et al., 2017). It is known that the cellular uptake pathway will be dependent of ENM size and charge. ENMs with a size of 50 nm were suggested as having the optimal size for a more efficient internalization and cellular uptake rates (Foroozandeh and Aziz, 2018). ENMs with a size >1 μm can be taken up non-specifically by macropinocytosis, and ENMs between 120-150 nm are endocytosed via the clathrin-mediated pathway (Kettiger et al., 2013). The upper limit size observed to use the latter internalization pathway was 200 nm (Rejman et al., 2004). The caveolae-mediated pathway was reported to usually endocytose ENMs of 50-100 nm (Gratton et al., 2008) but uptake of particles of 500 nm has also been reported (Rejman et al., 2004). Moreover, negatively charged ENMs showed a lower rate of endocytosis (probably via clathrin-/caveolae-independent endocytosis) (Dausend et al., 2008; Foroozandeh and Aziz, 2018), while positively charged ENMs can be rapidly internalized through clathrin-mediated endocytosis (Zhao et al., 2011). Neutral ENMs commonly use the caveolae-mediated mechanism (Panzarini et al., 2018). Shape may also determine cellular uptake, for instance, spherical Au NPs showed a 500% higher uptake than rod-shaped Au NPs of similar size (Chithrani et al., 2006).

1.3.2. Elimination of nanomaterials by benthic invertebrates

Following uptake, ENMs can be excreted or retained in the body. The internal fate of ENMs will depend on the detoxification strategies of the species, on the exposure concentrations and routes, and on the ENM properties. However, the rate at which organisms eliminate ENMs from the body will predominantly depend on their physiology (van den Brink et al., 2019). Upon uptake of metal ions released from dissolving ENMs, ions can be incorporated in metal storage granules. Intracellular compartmentalization has been reported as a strategy adopted by several species to deal with metals and ENMs and minimize their toxicity (van den Brink et al., 2019). ENMs can be accumulated in digestive tissues, such as in the hepatopancreas/digestive gland or gut epithelia. For instance, the marine mussel *M. galloprovincialis* and the freshwater crayfish *Orconectes virilis* stored CuO NP and Ag NPs, respectively, in their digestive glands (Brittle et al., 2016; Gomes et al., 2012). Desouky (2006) observed sequestration of metals in lysosomal granules in the

digestive gland of the freshwater snail *L. stagnalis*. These detoxification mechanisms help gastropods coping with exposures to high concentrations of metal ions and metallic ENMs avoiding toxicity, however, the resulting high body burdens may represent a risk for higher trophic levels (Kuehr et al., 2021a). Excretion via faeces may be a way to eliminate ENMs from the body by invertebrates. The vesicles of digestive cells may release the previously stored metals into the lumen of the alimentary canal or into the midgut gland to be excreted through faeces (Dallinger and Rainbow, 1993; van den Brink et al., 2019). Desouky (2006) suggests metal detoxification from the digestive gland of *L. stagnalis* may then occur via faeces or via basal exocytosis towards hemocytes. ENMs can also be rejected in pseudofaeces, which are mucus-bound substances with retained unwanted materials that are rejected by the gills of mussels and oysters, avoiding its ingestion. *M. galloprovincialis* filtered CeO_2 NPs from the water column and repackaged them in pseudofaeces (Montes et al., 2012).

Metal binding proteins, such as metallothioneins are another metal detoxification strategy present in many species (Amiard et al., 2006). Some studies have attributed slower elimination of Ag^+ to sequestration by MTs (Kuehr et al., 2021b). This also indicates that the fate of the nanoparticulate form and ions may be different within the same organism. García-Alonso et al. (2011) revealed different routes of cellular internalization and different *in vivo* fates of Ag once taken up by the estuarine polychaete *Nereis diversicolor* exposed to sediment spiked with citrate-capped Ag NPs and $AgNO_3$. Ag NPs were directly endocytosed into the gut epithelial cells and associated with organelles, heat denatured proteins and inorganic granules, whereas ionic Ag was found associated with the metallothionein fraction. The different intracellular fates of the nanoparticulate and ionic forms may lead to different elimination rates. Khan et al. (2012, 2015) reported a two-component efflux rate of Ag by the estuarine mudsnail *Peringia ulvae* exposed to Ag NPs, for which a "Trojan Horse" mechanism was suggested: a fast elimination of Ag (probably of the Ag NPs) followed by a slower efflux (probably of ionic Ag resulting from *in vivo* dissolution of the Ag NPs).

Even though ENMs are retained in the gut lumen, this not always results in internalization into the gut epithelial cells. The gut can act as a barrier to ENM uptake, for instance, by protective layers of cuticular or peritrophic membranes that can limit uptake of ENMs, or by removal of adsorbed ENMs to the gut epithelium surface through sloughing mucus. The basal lamina of epithelial cells is another barrier to cellular uptake of ENMs (van der Zande et al., 2020). However, if not excreted from the body it may also be considered as a possible dietary uptake route for predators. Invertebrates may possess other ways for sequestration and elimination of metals and ENMs, such as

biomineralization, which is the process by which organisms support the existing tissues (shells or exoskeletons) using minerals. During this process, metals or ENMs can be sequestered and incorporated into biological tissues (van den Brink et al., 2019). When moulting, metals and ENMs taken up can be eliminated from the body. *Chironomus riparius* seemed able to eliminate As and Zn during moulting and/or metamorphosis (Mogren et al., 2013; Timmermans et al., 1992). Nevertheless, further investigation is needed to evaluate the elimination of ENMs and metals by the processes of moulting or biomineralization (van den Brink et al., 2019).

1.4. Environmental Risk Assessment of nanomaterials

Environmental Risk Assessment (ERA) consists of comparing the predicted environmental concentrations (PECs) of a chemical in the environment with the concentration that causes no adverse effects (PNEC - predicted no-effect concentration) on the relevant receptors that may be exposed. Although the conventional ERA paradigm can be applied to ENMs, their nano-specific nature requires adaptations. From a regulatory point of view, data on ENM environmental release and exposure are necessary in order to estimate their environmental risks (Svendsen et al., 2020). However, as described in the previous sections, ENMs will undergo complex and dynamic transformations during their entire life-cycle, potentially reaching environmental receptors in unpredictable forms (Suhendra et al., 2020). Analytical techniques are needed for a reliable detection and characterization of ENMs in environmental matrices (Svendsen et al., 2020). Thus, predicting environmental concentrations and ENM forms that organisms can be potentially exposed to constitutes a key challenge for ERA (Giese et al., 2018; van den Brink et al., 2019). The use of environmental fate models (EFMs) and material flow analysis (MFA) can be alternatives for estimating PECs of ENMs (Wigger et al., 2020). It should be highlighted that, even though many challenges are still ahead, significant advances in understanding the environmental fate processes and exposure to ENMs have been made over the last decade (Svendsen et al., 2020). Several testing guidelines and guidance documents specific for ENMs are being updated and developed under the Organisation for Economic Co-operation and Development (OECD) Working Party on Manufactured Nanomaterials (WPMN) (Ahamed et al., 2021). Moreover, Oomen et al. (2018) provides an overview on the risk assessment frameworks developed specifically for ENMs, giving particular importance to frameworks directed towards decision-making and regulatory submissions at the national and European Union level. Bioaccumulation studies are mentioned as one of the issues that deserve special attention for improving current risk assessment frameworks.

Here, the framework delivered by the project NanoFASE - Nanomaterial Fate and Speciation in the Environment (European Commission Horizon 2020) is highlighted, with the present thesis being carried out within its scope (http://www.nanofase.eu/). NanoFASE aimed at delivering an integrated Exposure Assessment Framework by providing knowledge, new tools and models generated within the project (http://www.nanofase.eu/exposure_assessment_framework). With this framework, academia, regulators, and industry are able to assess the environmental fate of nanomaterials released from industrial nano-enabled products. The industry can use the information for a cost-effective safe-by-design approach of their nano-enable products. The goal is to integrate the generated models into the European Union System for the Evaluation of Substances (EUSES) model used within the European regulation on chemicals, REACH (Registration, Evaluation, Authorisation and Restriction of Chemicals). Furthermore, the review article of Svendsen et al. (2020) presents the state of the art and provides key principles for improving ENM-specific exposure modelling to support ERA. One of the key principles presented by Svendsen et al. (2020) is that "interactions with biota can affect ENM form and state". This concept was first introduced by NanoFASE and exposes the biota compartment as a "reactor" within ENM functional pathways. The different available ENM forms may experience distinct interactions with biota, such as different uptake rates and internal fates and may undergo biological-driven transformations, as explored in the previous sections of this Introduction. In this sense, another fundamental aspect for ERA of ENMs is understanding their toxicokinetics to determine their behaviour and risk to the biotic compartment. Determining their bioaccumulation potential and risk for biomagnification within food chains are also critical aspects to consider for the risk assessment of ENMs (Petersen et al., 2019), and are part of three main domains of the PBT assessment (persistence, bioaccumulation potential and toxicity) of chemicals required by REACH (Scheringer et al., 2013).

1.5. Toxicokinetic and bioaccumulation studies

Toxicity studies dominate the scientific literature on ENMs in aquatic or terrestrial organisms. These studies, however, do not provide sufficient information on the processes of uptake and bioaccumulation, that ultimately may lead to toxicity (Lead et al., 2018). Bioaccumulation studies are used to describe the concentration of a contaminant in relation to its external concentration in the surrounding environment. This may allow the estimation of the potential risk of exposure to contaminant concentration levels that may not be harmful upon short-term exposure but may be upon long-term exposure due to the continued uptake,

leading to exceedance of critical body concentrations (Pavlaki, 2016). However, bioaccumulation tests were originally developed for assessing the uptake of conventional solutes such as metals or lipophilic organic compounds. It assumes that a steady state is achieved between the internal chemical concentration in the tissues of the organism and in the exposure medium (Handy et al., 2018; van den Brink et al., 2019). This assumption, however, does not apply to ENMs because they are thermodynamically unstable and thus their behaviour cannot be described by chemical equilibrium (Oomen et al., 2018).

For metal ENMs, organisms can be exposed to the metal ions released from particle dissolution and/or to the nanoparticulate form. It has been assumed that if a ENM dissolves and releases metal ions, the accumulation and toxicity are likely to resemble that of exposure to the metal ion only (Croteau et al., 2014). This was supported by some studies, such as the toxicity of ZnO NPs to a microalgae which was explained from its dissolution, or the comparable uptake and elimination dynamics of ZnO NPs and aqueous Zn into an estuarine snail (Franklin et al., 2007; Khan et al., 2013). In turn, if the nanoparticulate form is taken up, its bioaccumulation and toxicity probably will differ from that of the ionic form (Croteau et al., 2014). Some studies have also supported this assumption, for instance, different bioaccumulation kinetics of Ag NPs and Ag^+ in *L. stagnalis* were observed, indicating that for accumulation the NP form was more important than the ionic form (Croteau et al., 2011). These studies were an indication that the modelling used for conventional chemicals need to be adapted for ENMs. However, in the lack of specific methods for ENMs, modelling approaches used for conventional chemicals have been applied to ENMs (van den Brink et al., 2019). The critical review of van den Brink et al. (2019) provides an analysis about the applicability of conventional modelling approaches to ENMs. For instance, the Biotic Ligand Model (BLM) is used to predict the bioavailability and toxicity of metal uptake from solution. Uptake and toxicity are not simply related to total metal concentrations in solution but rather related to the activity of metal ions, their complexation with the physiological site of action (biotic ligand) in the organism, and their interaction with competing ions in the exposure medium (Toro et al., 2001; van den Brink et al., 2019). This model seemed, however, to be less applicable to ENMs than to metal ions (van den Brink et al., 2019).

1.5.1. Toxicokinetic modelling of nanomaterials

Toxicokinetic-based biodynamic models have shown to be useful to investigate bioaccumulation of metals by organisms (Bourgeault et al., 2011). These models can help providing information on the ways chemicals, including ENMs, can be taken up and dealt with by the organisms, for instance, be stored or be eliminated from the body (Ardestani et

al., 2014; van den Brink et al., 2019). In the critical review of van den Brink et al. (2019), physiologically based pharmacokinetic (PBPK) models, or biodynamic models, were shown to have been successfully applied in uptake studies with ENMs. Toxicokinetics is the mathematical description of the time-course of chemical uptake, internal distribution, biotransformation and elimination in an organism, i.e. what the organism does with the toxicant (Ashauer and Escher, 2010). Moreover, different toxicokinetic models can be developed incorporating processes specifically related to accumulation, distribution, metabolism and excretion (ADME) of ENMs (Ashauer and Escher, 2010; van den Brink et al., 2019; Vijver et al., 2018). Briefly, to evaluate this, the experimental design consists in exposing the organisms to ENMs during an uptake phase, after which they are transferred to clean media for the elimination phase. The concentration of ENMs in the organism is measured at different time points during both phases (Carter et al., 2014). For the uptake phase, different exposure routes can be considered by exposing organisms to ENMs via water, sediment/soil or food. Additionally, simultaneous exposure routes can be accounted for (Pavlaki et al., 2018; Ribeiro et al., 2017). The one-compartment toxicokinetic model is the simplest approach and considers the organism as a single compartment, only assuming the kinetic processes of uptake and elimination. The uptake phase can be described by equation 1, including both uptake and elimination, since elimination also occurs during the uptake phase. When organisms are transferred to clean media for the elimination phase, elimination processes can be modelled by equation 2 (Ardestani et al., 2014; van den Brink et al., 2019).

Equation 1 → For the uptake phase ($0 \leq t \leq t_c$)

$$Q(t) = C_0 + \left(\frac{k1}{k2}\right) * C_{exp} * \left(1 - e^{(-k2*t)}\right)$$

Equation 2 → For the elimination phase ($t > t_c$)

$$Q(t) = C_0 + \left(\frac{k1}{k2}\right) * C_{exp} * \left(e^{(-k2*(t-t_c))} - e^{(-k2*t)}\right)$$

where Q(t) is the internal concentration in the organism at time t (e.g., µg Ag $g^{-1}_{organism}$ dry body weight), C_0 is the background concentration in the organism at time 0 (e.g., µg Ag $g^{-1}_{organism}$ dry body weight), C_{exp} is the concentration in the exposure media (e.g., µg Ag L^{-1} or mg Ag $kg^{-1}_{sediment}$), k1 is the uptake rate constant (e.g., L_{water} $g^{-1}_{organism}$ day^{-1} or $g_{sediment}$ $g^{-1}_{organism}$ day^{-1}), k2 is the elimination rate constant (e.g., day^{-1}), t is the sampling time (e.g.,

day), t_c is the time at which organisms were transferred from contaminated to clean medium (e.g., day).

Different versions of this model can be used according to some specificities, like applying different options to deal with C_0. For instance, animals may not have a background concentration of the ENMs ($C_0 = 0$) and so C_0 is removed from the equations 1 and 2, or when $C_0 > 0$ it may or may not be eliminated. For details of the equations used, see the review of Ardestani et al. (2014). Additionally, organisms may grow during the experiment. In those cases, a growth rate constant (k_{growth}) can be included in equations of both uptake and elimination phases (equations 3 and 4) of the toxicokinetic model to calibrate growth dilution (Figure 1.2) (Ardestani et al., 2014):

Equation 3 → For the uptake phase ($0 \leq t \leq t_c$)

$$Q(t) = C_0 + \left(\frac{k1}{k2 + k_{growth}}\right) * C_{exp} * \left(1 - e^{(-(k2+k_{growth})*t)}\right)$$

Equation 4 → For the elimination phase ($t > t_c$)

$$Q(t) = C_0 + \left(\frac{k1}{k2 + k_{growth}}\right) * C_{exp} * \left(e^{(-(k2+k_{growth})*(t-t_c))} - e^{(-(k2+k_{growth})*t)}\right)$$

It should be noted that the opposite may also occur, and organisms may lose weight during the experiments, for instance, due to food deprivation. As mentioned in section 1.3.2, some organisms have the ability to sequester metals or ENMs and store them in an inert form (e.g., in specialized tissues/organs such as in the hepatopancreas, or in granules), becoming biologically inactive (Figure 1.2) (Desouky, 2006; García-Alonso et al., 2011). For this, different approaches can be considered. For the first approach, kinetics of the uptake phase can be estimated using equation 1, whereas for the elimination phase an inert fraction (Fi, no dimension, ranging from 0 to 1) can be included in the equation, as follows in equation 5 (Tourinho et al., 2016; Vijver et al., 2006):

Equation 5 → For the elimination phase ($t > t_c$)

$$Q(t) = C_0 + \left(\frac{k1}{k2}\right) * C_{exp} * \left(Fi + (1 - Fi) * e^{(-k2*(t-t_c))}\right)$$

A second approach was suggested by van den Brink et al. (2019) in which a stored fraction (SF, no dimension, ranging from 0 to 1) is added in the equations of both the uptake

and elimination phases (equations 6 and 7), considering that organisms may also store ENMs during the uptake phase:

Equation 6 → For the uptake phase ($0 \leq t \leq t_c$)

$$Q(t) = C_0 + \left(C_{exp} * k1 * SF * t\right) + \left(C_{exp} * \left(\frac{k1}{k2}\right) * \left(1 - e^{(-k2*t)}\right) * (1 - SF)\right)$$

Equation 7 → For the elimination phase ($t > t_c$)

$$Q(t) = C_0 + \left(C_{exp} * k1 * SF * t_c\right) + \left(C_{exp} * \left(\frac{k1}{k2}\right) * \left(1 - e^{(-k2*t_c)}\right) * e^{(-k2*(t-t_c))} * (1 - SF)\right)$$

These two approaches assume that the metal or ENMs are not eliminated from the storage fraction over time, which may be difficult to meet from a physiological perspective (van den Brink et al., 2019). Thus, a third approach can be considered, using a two-compartment kinetic model. This model assumes that metals or ENMs are taken up from the exposure media and divided over a loosely-bound metal compartment and a storage compartment. For this, uptake and elimination rate constants from one compartment to the second compartment have to be included (Ardestani et al., 2014). For details on the equations used for the two-compartment model, see the review of Ardestani et al. (2014). It should be noted that to meet the requirements of using the two-compartment model it is necessary to measure the compound in the storage compartment, which can be difficult when dealing with small invertebrates. In such cases, the use of the one-compartment model with Fi or SF may be advisable. The two-compartment model can also be used to account for the biogenic formation of ENMs inside the exposed organism, including the rate at which ENMs are formed from the ionic metals taken up (Figure 1.2) (van den Brink et al., 2019).

In the case of ENMs that undergo dissolution and organisms are exposed to both ionic metal and nanoparticulate forms, such as in exposures to Ag NPs, a mixture exposure to both forms is a more likely scenario. In such scenario, the toxicokinetic model should include two uptake rate constants (k_{Ion} and k_{ENM} uptake rate constants, as seen in Figure 1.2) and two C_{exp} concentrations, one for the ionic form and the other for the nanoparticulate form (Figure 1.2). Obviously, this is only possible if concentrations of both forms are measured in the exposure media. Another situation can be the case of different elimination rates for ionic and NP forms because excretion rates can be form dependent (van den Brink et al., 2019).

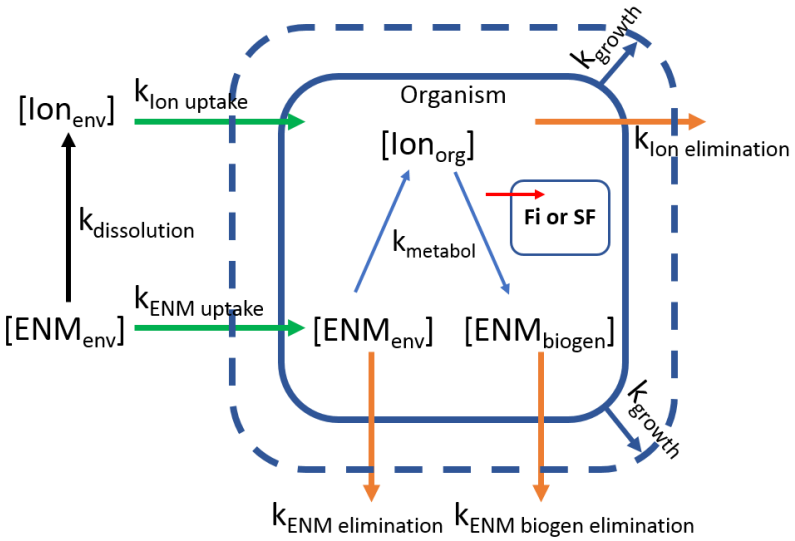

Figure 1.2. Schematic representation of the different forms of metal-based ENMs and kinetics of uptake and elimination. Forms of materials: [ENM_{env}]: concentration of ENMs in the environmental compartment (can be both in the environment and in the organism); [Ion_{env}]: concentration of the ionic form from the dissolution of the ENMs in the environmental compartment; [Ion_{org}]: concentration of the ionic form in the organism (may originate from uptake of Ion_{env} or from dissolution of ENM_{env} inside the organism); [ENM_{biogen}]: concentration of the biogenic particulate form; Fi or SF: inert fraction or stored fraction. The kinetic processes are: $k_{ENM\ uptake}$: uptake rate constant of ENM_{env}; $k_{Ion\ uptake}$: uptake rate constant of Ion_{env}; $k_{ENM\ elimination}$: elimination rate constant of ENM_{env}; $k_{Ion\ elimination}$: elimination rate constant of Ion_{org}; $k_{biogen\ elimination}$: elimination rate constant of ENM_{biogen}; $k_{dissolution}$: dissolution rate constant of ENM_{env} in the environmental compartment; $k_{metabol}$: transformation rate constant in the organism (can be dissolution of the ENM_{env} or biogenic formation of particulate materials); k_{growth}: rate constant for growth dilution. Red arrow: transport to the inert fraction or stored fraction. Adapted from van den Brink et al. (2019) with permission from the Royal Society of Chemistry (https://pubs.rsc.org/en/content/articlehtml/2019/en/c8en01122b).

As previously mentioned, it was seen that Ag NPs were eliminated faster while ionic Ag may be slowly excreted from the body of *P. ulvae* (Khan et al., 2015, 2012). For this, two elimination rate constants (k_{Ion} and k_{ENM} elimination rate constants, as seen in Figure 1.2) should be included in the model. The review of van den Brink et al. (2019) provides details on the equations and case studies showing the applicability of such models to ENM exposures. Additionally, simultaneous exposure routes are a likely scenario to occur in the environment and should also be covered in the modelling. This is of particular relevance, for instance, in benthic invertebrates that can be exposed to both water and sediment concentrations, or terrestrial invertebrates exposed to ENMs in soil and soil pore water. For that, different uptake rate constants should be applied accounting for each uptake route, as for the incorporation in the model of different uptake rate constants for ionic and NPs forms mentioned above. For ENMs, a decline in concentrations may also happen, for instance, decrease in ENM exposure concentration due to settlement from the water column during the uptake phase. In these situations, a decrease rate constant may be used to account for

the declining exposure concentration. For examples of these two scenarios (double exposure routes and decrease rate constant for ENM concentrations in the medium) and their application in equations, see Chapter 2 of this thesis.

1.5.2. Bioconcentration, bioaccumulation and biomagnification

Bioavailability of ENMs in exposure media and the physiological traits of the exposed species will have a crucial huge role determining ENM bioaccumulation. Bioavailability is the fraction of the chemical that is freely available to be taken up by the organism (Van Leeuwen et al., 2005). In bioaccumulation studies, different accumulation factors can be derived, which are dependent on the exposure routes, and can be designated as: bioconcentration factor (BCF), bioaccumulation factor (BAF) and biomagnification factor (BMF) (Uddin et al., 2020). The general definitions are given below:

Bioconcentration describes the process by which the organism takes up the chemical substance from the surrounding water only via dermal or respiratory pathways. **BCF** expresses the degree at which bioconcentration occurs, and is calculated as the ratio between the concentration of a chemical measured in the organism and that measured in the surrounding media at steady state (Arnot and Gobas, 2006; Kuehr et al., 2021a).

Bioaccumulation is the net result of the uptake of a chemical by the organism via all possible exposure routes in the surrounding environment (e.g., water, diet, sediment, or air). This process is expressed using the **BAF**, obtained as the ratio between the concentration of a chemical measured in the organism and that in the environment at steady state (Arnot and Gobas, 2006). **Biota-Sediment/Soil Accumulation Factors (BSAF)** can also be derived when accounting for concentrations in the sediment/soil (Ankley et al., 1992; van den Brink et al., 2019).

Biomagnification is the process in which the chemical concentration in the organism exceeds that of its diet, increasing along trophic levels. The degree of biomagnification is expressed by using **BMF**, estimated as the ratio of the chemical concentration in an organism to that in its diet at steady state (Arnot and Gobas, 2006).

However, as mentioned in the previous section, the steady state assumption cannot be applied to ENMs as they are not thermodynamically stable, and thus accumulation factors for ENMs should not be derived based on ratios between organisms and media (van den Brink et al., 2019). Instead, BCFs, BAFs and BMFs can be derived dynamically as the ratio between the uptake and elimination rate constants estimated from toxicokinetic models $\left(\frac{k1}{k2}\right)$, because k1 and k2 can be derived also without reaching the steady state (see section

1.5.1) (OECD, 2012; Pavlaki 2016). These factors are termed “kinetic BCF” or BCF_k, “kinetic BAF” or BAF_k, (Petersen et al., 2019) and “kinetic BMF” or BMF_k (OECD, 2012). It should be noted that the estimation of accumulation factors using the kinetic parameters cannot be made when the model includes a storage fraction (Fi or SF) (van den Brink et al., 2019).

1.6. Silver and silver sulfide nanoparticles as model nanomaterials

Within ENMs, extensive investigation has been particularly devoted to silver nanoparticles (Ag NPs), because they are one of the most incorporated ENMs in nano-functionalised products. According to predictions, Ag NP global production may reach 800 tons by 2025 (Pulit-Prociak and Banach, 2016). Ag NPs are particularly desirable for their antimicrobial properties, being applied in a wide range of consumer products (McGillicuddy et al., 2017; Pulit-Prociak and Banach, 2016). According to the investigation of Giese et al. (2018), the main product categories using Ag NPs are for medical purposes, textiles and consumer electronics, in this increasing order. This study reported that the most relevant source of Ag NPs is derived from textiles during washing processes, but cosmetics, cleaning agents and medical products also have a relevant contribution for Ag NP emissions, mainly through release via wastewaters (Giese et al., 2018). In the same work, PECs for Ag ENMs in sewage treatment effluent and surface freshwater were calculated to be in the range of 0.10-151 ng L^{-1} and 0-4.20 ng L^{-1}, respectively. These predicted values were similar to those measured in surface freshwaters (0-6.20 ng L^{-1}), but lower than those measured in sewage treatment effluent samples (0-1300 ng L^{-1}) collected from the Bavarian survey network of watercourses. PECs in freshwater sediments were estimated to be in the range of 0.19-471 µg kg^{-1}, considering 100% persistent of Ag ENMs (Giese et al., 2018).

In surface water, dissolution of Ag NPs may act like a major source of ionic Ag. It is assumed that uptake of Ag^+ released from Ag NP dissolution is the main pathway for accumulation and toxicity (Kuehr et al., 2020). Silver in all soluble forms was considered a priority surface water pollutant by the U.S. Environmental Protection Agency (EPA), due to its environmental impact and persistence (Brittle et al., 2016). Consequently, the increasing use and potential discharges of Ag NPs raised concerns regarding their environmental effects, either in their nanoparticulate form or of the ionic Ag released from these particles. Some studies have demonstrated that toxicity in Ag NP exposure may not be entirely attributed to the released Ag^+, but also to nano-specific effects. Ag NPs are known to cause genotoxicity, with the dominant mechanism being the generation of reactive oxygen species (ROS) (Ahamed et al., 2021). Upon cellular uptake, Ag NPs may translocate to the mitochondria and nucleus and induce alterations, such as oxidative stress, DNA damage,

genotoxicity and mitochondrial dysfunction. Consequently, apoptosis or necrosis may occur (Panzarini et al., 2018). The Ag ions released from endocytosed Ag NPs may also contribute to causing genotoxicity (Ahamed et al., 2021). The ecotoxicity of Ag NPs and Ag^+ to aquatic and terrestrial species has been the subject of extensive investigation in the past decade (see the reviews of Ahamed et al. (2021); Lead et al. (2018); Martínez et al. (2021); Turan et al. (2019)).

Once released into the environment, Ag NPs may undergo the transformations described in above (Figure 1.1) (Suhendra et al., 2020). As previously mentioned, Ag NPs are expected to rapidly transform into Ag_2S NPs during WWTP processes. Ag_2S NPs is the more environmentally relevant Ag NP form, since it is the dominant Ag species expected to be discharged into the environment and to eventually reach biota (He et al., 2019; Kaegi et al., 2015). Fletcher et al. (2019) measured Ag NP sulfidation product stability over two months and showed that it may result in stable products and cannot be a source of Ag^+ in natural waters. Thus, these Ag species are thought to mitigate the toxicity to organisms by limiting Ag^+ bioavailability and uptake due to their extremely low solubility. Several studies have supported that sulfidation of Ag NPs decreased their toxicity to a range of species, including *Caenorhabditis elegans* (nematode) (Levard et al., 2013; Starnes et al., 2015), *Lenma minuta* (duckweed) (Levard et al., 2013), *Fundulus heteroclitus* (killifish) (Levard et al., 2013), or *Danio rerio* (zebrafish) (Devi et al., 2015; Levard et al., 2013). However, some studies have shown Ag bioaccumulation upon exposure to Ag_2S NPs, indicating that the aged Ag NP form is still bioavailable (Baccaro et al., 2018; Clark et al., 2019; Kampe et al., 2018; Khodaparast et al., 2021). Studies also revealed that Ag_2S NPs can induce toxicity, which cannot be explained by Ag^+ due to its extremely low dissolution (Liu et al., 2018; Schultz et al., 2016). He et al. (2019) showed that Ag_2S NPs can potentially undergo transformations (photo-induced dissolution) that may lead to the release of Ag^+ and *in situ* formation of Ag^0 and Ag^0/Ag_2S NPs hetero-structures formed by photoreduction. These authors suggested that the formation of these NPs may potentially increase toxicity and consequently the safety of this Ag form may be overestimated in some cases. Furthermore, a study demonstrated that ozonation of a Ag_2S NP spiked effluent resulted in formation of AgCl, with consequent increase in Ag toxicity to the microalgae *Chlamydomonas reinhardtii*, reaching EC_{50} values comparable to those obtained for $AgNO_3$ (Thalmann et al., 2015). Additionally, Ag_2S NPs may be solubilised in the mildly acidic environments of digestive systems potentially leading to bioavailable Ag^+ (Kühr et al., 2018; Lee et al., 2000).

Considering this, future work is needed to understand at which extent Ag_2S NPs may mitigate Ag toxicity and what are the risks of their transformation products (Spurgeon et al.,

2020). It is also necessary to determine if the Ag_2S NPs can be incorporated into biological tissues and if that process is similar to that for dissolved metals (Clark et al., 2019), and also to investigate its potential for bioaccumulation and biomagnification. There is evidence that Ag NPs can biomagnified in the food chain to higher trophic levels (Xiao et al., 2019). In particular, Luo et al. (2016) observed that Ag NPs were transferred from *E. coli* to *C. elegans* and exerted high toxicity, causing germ cell death, affecting life span and reproductive integrity in the nematode.

1.7. Benthic invertebrates as model test organisms

Benthic macroinvertebrates are strongly recommended to assess aquatic ecosystem integrity, particularly looking at impacts of contaminants associated with sediments (Ferrari and Faburé, 2017). Benthic organisms can act as ecosystem engineers, so the functioning and health of benthic ecosystems depends on their abundance, species composition and diversity (Cross et al., 2015). These organisms are essential to the decomposition of organic matter, maintenance of clean water, primary production and to the uptake and transfer of materials (Palmer et al., 2000). Benthic organisms can be exposed to contaminants through water, sediment, sediment pore water and food (Cross, 2017). That said, understanding the risk that ENMs pose to benthic ecosystems not only is crucial to evaluate and predict localised effects of ENMs, but also to understand and predict the potential effects on the wider aquatic ecosystem (Cross et al., 2015). In this thesis, the species used are ecologically relevant and belong to different functional feeding groups to be representative of the different exposure routes by which benthic invertebrates would be exposed to ENMs in freshwater sediments.

1.7.1. *Physa acuta*

Physa acuta Draparnaud, 1805 is a freshwater pulmonate snail (Gastropoda: Physidae) (Figure 1.3). Native to North America, it is an invasive species that has widely spread over the last two centuries, becoming the world's most cosmopolitan freshwater gastropod (Dillon et al., 2002). These pond snails are hermaphroditic and relevant detritivores in lotic and lentic environments. Classified as "grazer-scrapers", they possess mouth parts appropriate for scraping off and consuming the organic layer, such as algae, fungi and dead organic matter attached to stones and rocks (Cheung and Lam, 1998). Pond snails are also a significant part of many fish and crayfish diet (Gomot, 1998) representing a relevant trophic link between primary producers and predators (Cheung and Lam, 1998).

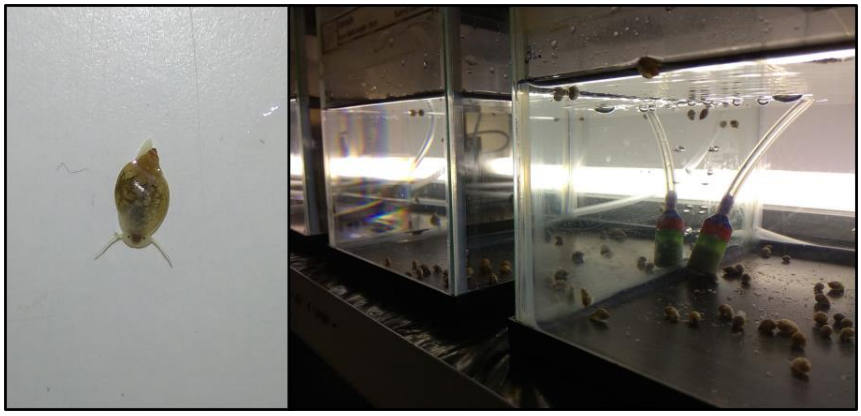

Figure 1.3. Adult *Physa acuta* (left) and *P. acuta* in aquariums (right) from laboratory cultures from the Applied Ecology and Ecotoxicology Research Group of the University of Aveiro. Source: Patrícia V. Silva.

Pond snails are easy to handle and to maintain in laboratory cultures, mainly due to their small size and easy reproduction (Gomot, 1998). It is possible to investigate the whole life cycle of *P. acuta*, from egg masses, embryos, juveniles and adults, in a range of endpoints (Gonçalves et al., 2017). Furthermore, previous studies have demonstrated the suitability of this species to ecotoxicological testing, and the toxicity of Ag NPs to this species has been addressed (Bernot and Brandenburg, 2013; Gonçalves et al., 2017; Justice and Bernot, 2014). As epibenthic species, these snails can be exposed to the overlying water, sediment and food, therefore are suitable organisms for bioaccumulation studies testing different exposure routes (De Jonge et al., 2010). Additionally, soft tissues and shells can be separately analysed, which has particular importance for studies on trophic transfer (Ramskov et al., 2015). This species was also selected as a suitable organism to assess bioaccumulation of metals due to its ability to accumulate high metal levels (Spyra et al., 2019). The hepatopancreas/digestive gland of gastropod molluscs is the main location of accumulation of metals and other xenobiotics and has shown to be the main target for Ag accumulation in freshwater snails (Bao et al., 2018; Desouky, 2006).

1.7.2. *Chironomus riparius*

Chironomid larvae are a prominent component of benthic macroinvertebrates belonging to the most abundant insect group in freshwater ecosystems (Nair et al., 2011). The non-biting midge *Chironomus riparius* Meigen, 1804 (Diptera, Chironomidae) is widely distributed in the northern hemisphere at temperate latitudes and inhabits both lotic and lentic environments (Figure 1.4). *C. riparius* undergoes full metamorphosis, having a short life-cycle that includes an aquatic phase (eggs, four larval stages and pupae) and a short aerial phase (non-feeding) as adult midges (Charles et al., 2004). The larvae of *C. riparius*

are sediment-dwelling and deposit-feeders (collector-gatherers), that feed on detritus deposited on the sediment surface (Armitage et al., 1995). Therefore, chironomid larvae are closely associated with surficial sediments and can be especially vulnerable to substances settled onto the sediment surface (Lee et al., 2016). Chironomids construct burrows in the upper layer of the sediment, and have a high bioturbation capacity (De Haas et al., 2005). Thus, *C. riparius* larvae are likely to accumulate contaminants through sediment ingestion, being considered relevant indicators of metal bioaccumulation in sediments (Bour et al., 2014; Dabrin et al., 2012). Chironomids are exposed to contaminants via different routes: sediments, sediment pore water and overlying water (Bervoets et al., 1997; Gimbert et al., 2018).

Figure 1.4. *Chironomus riparius* 4th instar larvae (left) and adult *Girardia tigrina* (right) from laboratory cultures from the Applied Ecology and Ecotoxicology Research Group of the University of Aveiro. Source: Patrícia V. Silva.

Chironomidae larvae and pupae have an important position in aquatic food chains. They are major food sources for many organisms living in the water column and sediments (e.g., crustaceans, fish or many other insects), which may potentially contribute to the re-transfer of contaminants to the water phase (Bour et al., 2017). Furthermore, the adult stages of *C. riparius* can be potential vectors for trophic transfer of contaminants to terrestrial predators, (e.g., other insects, birds or amphibians) (Ferrari and Faburé, 2017). This species is easy to maintain under laboratory conditions (Charles et al., 2004), and is widely used as model organism for standardized ecotoxicity testing for both water and sediment routes (OECD, 2010, 2004a, 2004b). Additionally, some studies have assessed the toxicity of Ag NPs to *C. riparius* larvae (Lee et al., 2016; Nair et al., 2013, 2011; Nair and Choi, 2012, 2011; Park et al., 2015).

1.7.3. *Girardia tigrina*

The free-living Platyhelminth *Girardia tigrina* Girard, 1850 (Tricladida, Dugesiidae) is a widespread freshwater planarian (or flatworm), originating from North America and introduced by human activities in Europe and other parts of the world (Figure 1.4). This species typically inhabits streams but can also be found in lakes or ponds. *G. tigrina* is a nocturnal carnivore, feeding on small invertebrates such as chironomid larvae, snails, oligochaetes, isopods, among others (Ilic et al., 2018). Planarians are also the food source of many fish, thus these organisms have an important dual role as prey and predator in aquatic food webs (Domingues, 2016; Saraiva et al., 2020). Planarians are secondary consumers in aquatic food chains, by contrast to other invertebrates used in ecotoxicological testing that usually are primary consumers or decomposers (Wu and Li, 2018). Planarians are much easier to culture and handle for laboratory experiments than other secondary consumers usually used, which tend to be vertebrates (e.g., fish, amphibians). Therefore, this species can be an advantage of using planarians in bioaccumulation tests, especially when looking at trophic transfer potential.

This species has negative phototaxis, tending to move away from light and is usually found under rocks or plant material (Noreña et al., 2015; Simão et al., 2020). Planarians display different behavioural responses to external stimuli and possess remarkable regenerative ability (Rink, 2013; Simão et al., 2020). They have a centralized brain and their nervous system exhibits similarities with that of vertebrates, making planarians a suitable model organism used in neurotoxicity, neuropharmacology, regeneration research, tumorigenicity, etc (Simão et al., 2020; Wu and Li, 2018). Wu and Li (2018) proposed freshwater planarian species as ideal organisms for ecotoxicological research because they are easily reared in the laboratory, can be obtained in large numbers and provide a variety of biological and behavioural characteristics that can be easily used as endpoints for ecotoxicological studies (e.g., regeneration capacity, locomotion, reproduction, feeding) (Oviedo et al., 2008; Wu and Li, 2018). Being epibenthic predator organisms, planarians can be exposed to contaminants adsorbed to sediments, in the water and in their preys (Simão et al., 2020). Even though the use of planarians in ecotoxicology is increasing and the toxicity of different substances has been assessed (e.g., metals, pesticides, PAHs, NPs) (Ermakov et al., 2019; Knakievicz and Ferreira, 2008; Leynen et al., 2019; Saraiva et al., 2020; Simão et al., 2020; Wu et al., 2011), studies on the bioaccumulation of contaminants are severely lacking.

1.8. Relevance and aims of the thesis

This study was undertaken as part of the work package on biota uptake of nanomaterials within the NanoFASE project (http://nanofase.eu/show/WP9_263). This work package focused on quantifying the uptake of ENMs in relevant aquatic and terrestrial species and assessing their bioaccumulation potential to higher trophic levels. This also included the evaluation of the effects of aged ENMs under environmentally relevant exposure scenarios, such as mesocosm experiments, in close collaboration with the work package on the environmental fate of ENMs in water and sediment compartments.

Considering this, the overarching aim of this thesis was to determine and understand the uptake and elimination kinetics of pristine and (simulated) aged Ag NPs and $AgNO_3$ in freshwater benthic invertebrates, under relevant environmental exposure scenarios. Due to the importance of freshwater sediments as sinks for ENMs, it is extremely relevant for the risk assessment to gather information on the kinetics of their bioaccumulation in benthic organisms (Selck et al., 2016). For this, ecological relevant benthic invertebrate species were chosen, covering for the different uptake routes that biota may be exposed to ENMs in benthic environments. It is of utmost importance to study the effect of ageing on the uptake and accumulation of ENMs by organisms. Studies have shown that Ag_2S NPs are the most relevant Ag nanoform in the environment (He et al., 2019; Kaegi et al., 2015). In order to fulfil this need, Ag_2S NPs synthetised *ab initio* to simulate an environmentally aged Ag NP form were used. Even though in the environment ENMs will be transformed, understanding the fate and effects of the original form is also necessary for risk assessment, as the transformation rates and behaviour are also dependent on the original ENM form (Lead et al., 2018). Therefore, in the present study pristine Ag NPs of different sizes and coatings were also tested. The toxicity of some of these Ag NPs to the test species used in the present work has been already investigated (Domingues, 2016; Gonçalves et al., 2017; Lopes, 2015). Furthermore, the NPs used were produced by partners of the project (AMEPOX Enterprise, Poland and Applied Nanoparticles (AppNano), Spain), and are applied in nano-enable products such as biocides and coatings from the health sector and paints (Ag NPs 3-8 nm and 60 nm; AMEPOX), and nanomedicines (Ag NP 50 nm; AppNano).

Another topic of relevance of the present thesis is the use of mesocosm experiments to evaluate the bioavailability and bioaccumulation of Ag_2S NPs. These experiments simulate more relevant and realistic environmental conditions and may be a link between laboratory and field exposure scenarios. Mesocosm results represent the combined behaviour of the entire system under certain conditions (Auffan et al., 2019), and so data derived from these

experiments may provide more realistic inputs to predictive models (Selck et al., 2016; Spurgeon et al., 2020). Furthermore, it is important to evaluate at which extent data derived by single-species bioaccumulation tests may predict uptake under more relevant scenarios, since most of the data available for risk assessment is derived from standardised single-species laboratory experiments. For this, comparison between these tests and mesocosm tests is needed.

In view of the foregoing, the specific aims of the present study were:

i) determine the toxicokinetics and bioaccumulation of different Ag NP forms (pristine and simulated aged forms) and $AgNO_3$ in the freshwater benthic invertebrates *Physa acuta*, *Chironomus riparius* and *Girardia tigrina* under different exposure routes;

ii) evaluate the bioavailability and bioaccumulation of Ag_2S NPs, and compare to that of pristine Ag NPs;

iii) evaluate potential biomagnification of Ag_2S NPs in single-species tests;

iv) determine toxicokinetics, bioaccumulation and biomagnification of Ag_2S NPs and $AgNO_3$ under mesocosm conditions;

v) evaluate if bioaccumulation under more realistic scenarios such as mesocosm experiments can be predicted by single-species bioaccumulation tests.

Data and models derived from this study were incorporated into the NanoFASE water-soil-organism (WSO) multimedia model (http://nanofase.eu/show/element_268), aiming at predicting the fate, speciation and bio-uptake of nanomaterials across space and in time, and were also included in case studies presented in the NanoFASE Exposure Assessment Framework.

1.9. Outline of the thesis

This work is divided into 6 chapters, 4 of which are in the format of scientific articles. This chapter, **Chapter 1**, is the current General Introduction in which an overview of the subject and general objectives of this thesis is provided.

Chapter 2 evaluates the toxicokinetics and bioaccumulation of different pristine Ag NPs and the simulated aged Ag_2S NPs (and $AgNO_3$) in the freshwater snail *Physa acuta*. Snails were exposed to different contamination scenarios such as spiked water, spiked water and clean sediment and spiked sediment. Moreover, the shell and soft tissue of the snails were analysed separately.

Chapter 3 investigates the toxicokinetics and bioaccumulation of different pristine Ag NPs and the simulated aged Ag_2S NPs (and $AgNO_3$) in the non-biting midge *Chironomus riparius*, under different exposure routes (spiked water and clean sediment, spiked sediment and spiked food). Exuviae and adult midges were also analysed to investigate potential transfer of Ag between life stages.

Chapter 4 evaluates the toxicokinetics and bioaccumulation of Ag_2S NPs and $AgNO_3$ in the planarian *Girardia tigrina* and *Physa acuta*. Snails were exposed through spiked water and clean food (microalgae) was provided. For the exposure of the planarians, *P. acuta* pre-exposed to Ag_2S NPs and $AgNO_3$ was provided as food item. Influence of gut depuration on internal Ag concentrations and toxicokinetics was evaluated. The potential biomagnification in the food chain snail → planarian was also assessed.

Chapter 5 investigates the toxicokinetics, bioaccumulation and potential biomagnification of Ag_2S NPs and $AgNO_3$ in an indoor stream mesocosm experiment, to infer on the bioaccumulation of the relevant aged Ag form in a more realistic stream environment. Data obtained in the mesocosm experiment were compared to that obtained in the previous chapters to evaluate if single-species tests data can predict bioaccumulation in the mesocosm exposure scenario.

Finally, **Chapter 6**, the General Discussion, provides a summary and an integrated discussion of the results obtained in the previous chapters. Suggestions for further research are also included.

1.10. References

Ahamed, A., Liang, L., Lee, M.Y., Bobacka, J., Lisak, G., 2021. Too small to matter? Physicochemical transformation and toxicity of engineered $nTiO_2$, $nSiO_2$, nZnO, carbon nanotubes, and nAg. J. Hazard. Mater. 404, 124107.

Akaighe, N., MacCuspie, R.I., Navarro, D.A., Aga, D.S., Banerjee, S., Sohn, M., Sharma, V.K., 2011. Humic acid-induced silver nanoparticle formation under environmentally relevant conditions. Environ. Sci. Technol. 45, 3895–3901.

Amiard, J.C., Amiard-Triquet, C., Barka, S., Pellerin, J., Rainbow, P.S., 2006. Metallothioneins in aquatic invertebrates: Their role in metal detoxification and their use as biomarkers. Aquat. Toxicol. 76, 160–202.

Ankley, G.T., Cook, P.M., Carlson, A.R., Call, D., Swenson, J.A., Corcoran, H.F., Hoke, R.A., 1992. Bioaccumulation of PCBs from Sediments by Oligochaetes and Fishes: Comparison of Laboratory and Field Studies. Can. J. Fish. Aquat. Sci. 49, 2080–2085.

Ardestani, M.M., Van Straalen, N.M., van Gestel, C.A.M., 2014. Uptake and elimination kinetics of metals in soil invertebrates: A review. Environ. Pollut. 193, 277–295.

Armitage, P.D., Cranston, P.S., Pinder, L.C. V., 1995. The Chironomidae - Biology and

Ecology of non-biting Midges.

Arnot, J.A., Gobas, F.A.P.C., 2006. A review of bioconcentration factor (BCF) and bioaccumulation factor (BAF) assessments for organic chemicals in aquatic organisms. Environ. Rev. 14, 257–297.

Ashauer, R., Escher, B.I., 2010. Advantages of toxicokinetic and toxicodynamic modelling in aquatic ecotoxicology and risk assessment. J. Environ. Monit. 12, 2056.

Auffan, M., Masion, A., Mouneyrac, C., de Garidel-Thoron, C., Hendren, C.O., Thiery, A., Santaella, C., Giamberini, L., Bottero, J.Y., Wiesner, M.R., Rose, J., 2019. Contribution of mesocosm testing to a single-step and exposure-driven environmental risk assessment of engineered nanomaterials. NanoImpact 13, 66–69.

Baccaro, M., Undas, A.K., De Vriendt, J., Van Den Berg, J.H.J., Peters, R.J.B., Van Den Brink, N.W., 2018. Ageing, dissolution and biogenic formation of nanoparticles: How do these factors affect the uptake kinetics of silver nanoparticles in earthworms? Environ. Sci. Nano 5, 1107–1116.

Badawy, A.M. El, Hassan, A.A., Scheckel, K.G., Suidan, M.T., Tolaymat, T.M., 2013. Key Factors Controlling the Transport of Silver Nanoparticles in Porous Media.

Bao, S., Huang, J., Liu, X., Tang, W., Fang, T., 2018. Tissue distribution of Ag and oxidative stress responses in the freshwater snail *Bellamya aeruginosa* exposed to sediment-associated Ag nanoparticles. Sci. Total Environ. 644, 736–746.

Ben-moshe, T., Dror, I., Berkowitz, B., 2010. Transport of metal oxide nanoparticles in saturated porous media. Chemosphere 81, 387–393.

Bernot, R.J., Brandenburg, M., 2013. Freshwater snail vital rates affected by non-lethal concentrations of silver nanoparticles. Hydrobiologia 714, 25–34.

Bervoets, L., Blust, R., De Wit, M., Verheyen, R., 1997. Relationships between river sediment characteristics and trace metal concentrations in tubificid worms and chironomid larvae. Environ. Pollut. 95, 345–356.

Bour, A., Mouchet, F., Cadarsi, S., Silvestre, J., Baqué, D., Gauthier, L., Pinelli, E., 2017. CeO_2 nanoparticle fate in environmental conditions and toxicity on a freshwater predator species: a microcosm study. Environ. Sci. Pollut. Res. 24, 17081–17089.

Bour, A., Mouchet, F., Verneuil, L., Evariste, L., Silvestre, J., Pinelli, E., Gauthier, L., 2014. Toxicity of CeO_2 nanoparticles at different trophic levels - Effects on diatoms, chironomids and amphibians. Chemosphere 120C, 230–236.

Bourgeault, A., Gourlay-Francé, C., Priadi, C., Ayrault, S., Tusseau-Vuillemin, M.H., 2011. Bioavailability of particulate metal to zebra mussels: Biodynamic modelling shows that assimilation efficiencies are site-specific. Environ. Pollut. 159, 3381–3389.

Brittle, S.W., Paluri, S.L.A., Foose, D.P., Ruis, M.T., Amato, M.T., Lam, N.H., Buttigieg, B., Gagnon, Z.E., Sizemore, I.E., 2016. Freshwater Crayfish: A Potential Benthic-Zone Indicator of Nanosilver and Ionic Silver Pollution. Environ. Sci. Technol. 50, 7056–7065.

Carter, L.J., Ashauer, R., Ryan, J.J., Boxall, A.B.A., 2014. Minimised bioconcentration tests: A useful tool for assessing chemical uptake into terrestrial and aquatic invertebrates? Environ. Sci. Technol. 48, 13497–13503.

Charles, S., Ferreol, M., Chaumot, A., Péry, A.R.R., 2004. Food availability effect on

population dynamics of the midge *Chironomus riparius*: A Leslie modeling approach. Ecol. Modell. 175, 217–229.

Cheng, D., Song, J., Zhao, X., Wang, S., Lin, Q., Peng, J., Su, P., Deng, W., 2019. Effects of chironomid larvae and *Limnodrilus hoffmeisteri* bioturbation on the distribution and flux of chromium at the sediment-water interface. J. Environ. Manage. 245, 151–159.

Cheung, C.C.C., Lam, P.K.S., 1998. Effect of Cadmium on the embryos and juveniles of a tropical freshwater snail, *Physa acuta* (Draparnaud, 1805). Wat. Sci. Tech. 38, 263–270.

Chithrani, B.D., Ghazani, A.A., Chan, W.C.W., 2006. Determining the size and shape dependence of gold nanoparticle uptake into mammalian cells. Nano Lett. 6, 662–668.

Clark, N.J., Boyle, D., Eynon, B.P., Handy, R.D., 2019. Dietary exposure to silver nitrate compared to two forms of silver nanoparticles in rainbow trout: Bioaccumulation potential with minimal physiological effects. Environ. Sci. Nano 6, 1393–1405.

Cleveland, D., Long, S.E., Pennington, P.L., Cooper, E., Fulton, M.H., Scott, G.I., Brewer, T., Davis, J., Petersen, E.J., Wood, L., 2012. Pilot estuarine mesocosm study on the environmental fate of Silver nanomaterials leached from consumer products. Sci. Total Environ. 421–422, 267–272.

Cross, R.K., 2017. The fate of engineered nanomaterials in sediments and their route to bioaccumulation. Univ. Exet. 1–210.

Cross, R.K., Tyler, C.R., Galloway, T.S., 2015. Transformations that affect fate, form and bioavailability of inorganic nanoparticles in aquatic sediments. Environ. Chem. 12, 627–642.

Croteau, M.N., Misra, S.K., Luoma, S.N., Valsami-Jones, E., 2014. Bioaccumulation and toxicity of CuO nanoparticles by a freshwater invertebrate after waterborne and dietborne exposures. Environ. Sci. Technol. 48, 10929–10937.

Croteau, M.N., Misra, S.K., Luoma, S.N., Valsami-Jones, E., 2011. Silver Bioaccumulation Dynamics in a Freshwater Invertebrate after Aqueous and Dietary Exposures to Nanosized and Ionic Ag. Environ. Sci. Technol. 45, 6600–6607.

Dabrin, A., Durand, C.L., Garric, J., Geffard, O., Ferrari, B.J.D., Coquery, M., 2012. Coupling geochemical and biological approaches to assess the availability of cadmium in freshwater sediment. Sci. Total Environ. 424, 308–315.

Dai, L., Banta, G.T., Selck, H., Forbes, V.E., 2015. Influence of copper oxide nanoparticle form and shape on toxicity and bioaccumulation in the deposit feeder, *Capitella teleta*. Mar. Environ. Res. 111, 99–106.

Dallinger, R., Rainbow, P. S., 1993. Ecotoxicology of metals in invertebrates. Lewis Publishers. United States of America.

Dausend, J., Musyanovych, A., Dass, M., Walther, P., Schrezenmeier, H., Landfester, K., Mailänder, V., 2008. Uptake mechanism of oppositely charged fluorescent nanoparticles in Hela cells. Macromol. Biosci. 8, 1135–1143.

De Haas, E.M., Kraak, M.H.S., Koelmans, A.A., Admiraal, W., 2005. The impact of sediment reworking by opportunistic chironomids on specialised mayflies. Freshw. Biol. 50, 770–780.

De Jonge, M., Blust, R., Bervoets, L., 2010. The relation between Acid Volatile Sulfides

(AVS) and metal accumulation in aquatic invertebrates: Implications of feeding behavior and ecology. Environ. Pollut. 158, 1381–1391.

Desouky, M.M.A., 2006. Tissue distribution and subcellular localization of trace metals in the pond snail *Lymnaea stagnalis* with special reference to the role of lysosomal granules in metal sequestration. Aquat. Toxicol. 77, 143–152.

Devi, G.P., Ahmed, K.B.A., Varsha, M.K.N.S., Shrijha, B.S., Lal, K.K.S., Anbazhagan, V., Thiagarajan, R., 2015. Sulfidation of silver nanoparticle reduces its toxicity in zebrafish. Aquat. Toxicol. 158, 149–156.

Dillon, R.T., Wethington, I.A.R., Rhett, J.M., Smith, T., 2002. Populations of the European freshwater pulmonate *Physa acuta* are not reproductively isolated from American *Physa heterostropha* or *Physa integra* 121, 226–234.

Domingues, V., 2016. Toxicity of silver nanoparticles and silver nitrate to the freshwater planarian *Dugesia tigrina*. University of Aveiro.

Ermakov, A., Popov, A., Ermakova, O., Ivanova, O., Baranchikov, A., Kamenskikh, K., Shekunova, T., Shcherbakov, A., Popova, N., Ivanov, V., 2019. The first inorganic mitogens: Cerium oxide and cerium fluoride nanoparticles stimulate planarian regeneration via neoblastic activation. Mater. Sci. Eng. C 104, 109924.

European Commission, 2011. Commission recommendation of 18 October 2011 on the definition of nanomaterial (2011/696/EU). 38–40. https://eur-lex.europa.eu/legal-content/EN/TXT/?uri=CELEX:32011H0696

Ferrari, B.J.D., Faburé, J., 2017. Field assessment of reproduction-related traits of chironomids using a newly developed emergence platform (E-Board). Ecotoxicol. Environ. Saf. 137, 186–193.

Fletcher, N.D., Lieb, H.C., Mullaugh, K.M., 2019. Stability of silver nanoparticle sulfidation products. Sci. Total Environ. 648, 854–860.

Foroozandeh, P., Aziz, A.A., 2018. Insight into Cellular Uptake and Intracellular Trafficking of Nanoparticles. Nanoscale Res. Lett. 13.

Franklin, N.M., Rogers, N.J., Apte, S.C., Batley, G.E., Gadd, G.E., Casey, P.S., 2007. Comparative toxicity of nanoparticulate ZnO, bulk ZnO, and $ZnCl_2$ to a freshwater microalga (*Pseudokirchneriella subcapitata*): The importance of particle solubility. Environ. Sci. Technol. 41, 8484–8490.

García-Alonso, J., Khan, F.R., Misra, S.K., Turmaine, M., Smith, B.D., Rainbow, P.S., Luoma, S.N., Valsami-Jones, E., 2011. Cellular Internalization of Silver Nanoparticles in Gut Epithelia of the Estuarine Polychaete *Nereis diversicolor*. Environ. Sci. Technol. 45, 4630–4636.

Giese, B., Klaessig, F., Park, B., Kaegi, R., Steinfeldt, M., Wigger, H., Von Gleich, A., Gottschalk, F., 2018. Risks, Release and Concentrations of Engineered Nanomaterial in the Environment. Sci. Rep. 8, 1–18.

Gimbert, F., Petitjean, Q., Al-Ashoor, A., Cretenet, C., Aleya, L., 2018. Encaged *Chironomus riparius* larvae in assessment of trace metal bioavailability and transfer in a landfill leachate collection pond. Environ. Sci. Pollut. Res. 25, 11303–11312.

Gomes, T., Pereira, C.G., Cardoso, C., Pinheiro, J.P., Cancio, I., Bebianno, M.J., 2012. Accumulation and toxicity of copper oxide nanoparticles in the digestive gland of *Mytilus galloprovincialis*. Aquat. Toxicol. 118–119, 72–79.

Gommes, C.J., 2019. Ostwald ripening of confined nanoparticles: chemomechanical coupling in nanopores. Nanoscale 11, 7386–7393.

Gomot, A., 1998. Toxic effects of cadmium on reproduction, development, and hatching in the freshwater snail *Lymnaea stagnalis* for water quality monitoring. Ecotoxicol. Environ. Saf. 41, 288–97.

Gonçalves, S.F., D. Pavlaki, M., Lopes, R., Hammes, J., Gallego-Urrea, J.A., Hassellöv, M., Jurkschat, K., Crossley, A., Loureiro, S., 2017. Effects of silver nanoparticles on the freshwater snail *Physa acuta*: The role of test media and snails' life cycle stage. Environ. Toxicol. Chem. 36, 243–253.

Gratton, S.E.A., Ropp, P.A., Pohlhaus, P.D., Luft, J.C., Madden, V.J., Napier, M.E., DeSimone, J.M., 2008. The effect of particle design on cellular internalization pathways. Proc. Natl. Acad. Sci. U. S. A. 105, 11613–11618.

Handy, R.D., Ahtiainen, J., Navas, J.M., Goss, G., Bleeker, E.A.J., Von Der Kammer, F., 2018. Proposal for a tiered dietary bioaccumulation testing strategy for engineered nanomaterials using fish. Environ. Sci. Nano 5, 2030–2046.

Hansen, S.F., Hansen, O.F.H., Nielsen, M.B., 2020. Advances and challenges towards consumerization of nanomaterials. Nat. Nanotechnol. 15, 964–965.

He, D., Garg, S., Wang, Z., Li, L., Rong, H., Ma, X., Li, G., An, T., Waite, T.D., 2019. Silver sulfide nanoparticles in aqueous environments: Formation, transformation and toxicity. Environ. Sci. Nano 6, 1674–1687.

Ilic, M.D., Tubic, B.P., Marinkovic, N.S., Markovic, V.M., Popovic, N.Z., Zoric, K.S., Rakovic, M.J., Paunovic, M.M., 2018. First report on the non-indigenous triclad *Girardia tigrina* (Girard, 1850) (Tricladida, Dugesiidae) in Serbia, with Notes on its Ecology and Distribution. Acta Zool. Bulg. 70, 39–43.

Inshakova, E., Inshakov, O., 2017. World market for nanomaterials: Structure and trends. MATEC Web Conf. 129, 1–5.

ISO, 2008. International Organization for Standardization. Technical specification ISO/TS 27687:2008(E): Nanotechnologies— Terminology and definitions for nano-objects— Nanoparticle, nanofibre and nanoplate.

John, A.C., Küpper, M., Manders-Groot, A.M.M., Debray, B., Lacome, J.M., Kuhlbusch, T.A.J., 2017. Emissions and possible environmental Implication of engineered nanomaterials (ENMs) in the atmosphere. Atmosphere (Basel). 8, 1–29.

Justice, J.R., Bernot, R.J., 2014. Nanosilver Inhibits Freshwater Gastropod (*Physa acuta*) Ability to Assess Predation Risk. Am. Midl. Nat. 171, 340–349.

Kaegi, R., Voegelin, A., Sinnet, B., Zuleeg, S., Siegrist, H., Burkhardt, M., 2015. Transformation of AgCl nanoparticles in a sewer system - A field study. Sci. Total Environ. 535, 20–27.

Kampe, S., Kaegi, R., Schlich, K., Wasmuth, C., Hollert, H., Schlechtriem, C., 2018. Silver nanoparticles in sewage sludge: Bioavailability of sulfidized silver to the terrestrial isopod *Porcellio scaber*. Environ. Toxicol. Chem. 37, 1606–1613.

Kettiger, H., Schipanski, A., Wick, P., Huwyler, J., 2013. Engineered nanomaterial uptake and tissue distribution: From cell to organism. Int. J. Nanomedicine 8, 3255–3269.

Khan, F.R., Laycock, A., Dybowska, A., Larner, F., Smith, B.D., Rainbow, P.S., Luoma,

S.N., Rehkämper, M., Valsami-Jones, E., 2013. Stable isotope tracer to determine uptake and efflux dynamics of ZnO nano- and bulk particles and dissolved Zn to an estuarine snail. Environ. Sci. Technol. 47, 8532–8539.

Khan, F.R., Misra, S.K., Bury, N.R., Smith, B.D., Rainbow, P.S., Luoma, S.N., Valsami-Jones, E., 2015. Inhibition of potential uptake pathways for silver nanoparticles in the estuarine snail *Peringia ulvae*. Nanotoxicology 9, 493–501.

Khan, F.R., Misra, S.K., Garc, J., Smith, B.D., Strekopytov, S., Rainbow, P.S., Luoma, S.N., Valsami-Jones, E., 2012. Bioaccumulation Dynamics and Modeling in an Estuarine Invertebrate Following Aqueous Exposure to Nanosized and Dissolved Silver. Environ. Sci. Technol. 46, 7621–7628.

Khodaparast, Z., van Gestel, C.A.M., Papadiamantis, A.G., Gonçalves, S.F., Lynch, I., Loureiro, S., 2021. Toxicokinetics of Silver Nanoparticles in the Mealworm *Tenebrio molitor* Exposed via Soil or Food. Sci. Total Environ, 777, 146071.

Knakievicz, T., Ferreira, H.B., 2008. Evaluation of copper effects upon *Girardia tigrina* freshwater planarians based on a set of biomarkers. Chemosphere 71, 419–428.

Kuehr, S., Klehm, J., Stehr, C., Menzel, M., Schlechtriem, C., 2020. Unravelling the uptake pathway and accumulation of silver from manufactured silver nanoparticles in the freshwater amphipod *Hyalella azteca* using correlative microscopy. NanoImpact 19, 100239.

Kuehr, S., Kosfeld, V., Schlechtriem, C., 2021a. Bioaccumulation assessment of nanomaterials using freshwater invertebrate species. Environ. Sci. Eur. 33, 1-36.

Kuehr, S., Kaegi, R., Maletzki, D., Schlechtriem, C., 2021b. Testing the bioaccumulation potential of manufactured nanomaterials in the freshwater amphipod *Hyalella azteca*. Chemosphere 263, 127961.

Kühr, S., Schneider, S., Meisterjahn, B., Schlich, K., Hund-Rinke, K., Schlechtriem, C., 2018. Silver nanoparticles in sewage treatment plant effluents: chronic effects and accumulation of silver in the freshwater amphipod *Hyalella azteca*. Environ. Sci. Eur. 30, 1–11.

Lead, J.R., Batley, G.E., Alvarez, P.J.J., Croteau, M.N., Handy, R.D., McLaughlin, M.J., Judy, J.D., Schirmer, K., 2018. Nanomaterials in the environment: Behavior, fate, bioavailability, and effects—An updated review. Environ. Toxicol. Chem. 37, 2029–2063.

Lee, B.G., Griscom, S.B., Lee, J.-S., Choi, H.J., Koh, C.-H., Luoma, S.N., Fisher, N.S., 2000. Influences of dietary uptake and reactive sulfides on metal bioavailability from aquatic sediments. Science. 287, 282–284.

Lee, S.W., Park, S.Y., Kim, Y., Im, H., Choi, J., 2016. Effect of sulfidation and dissolved organic matters on toxicity of silver nanoparticles in sediment dwelling organism, *Chironomus riparius*. Sci. Total Environ. 553, 565–573.

Levard, C., Hotze, E.M., Colman, B.P., Dale, A.L., Truong, L., Yang, X.Y., Bone, A.J., Brown, G.E., Tanguay, R.L., Di Giulio, R.T., Bernhardt, E.S., Meyer, J.N., Wiesner, M.R., Lowry, G. V., 2013. Sulfidation of silver nanoparticles: Natural antidote to their toxicity. Environ. Sci. Technol. 47, 13440–13448.

Leynen, N., Van Belleghem, F.G.A.J., Wouters, A., Bove, H., Ploem, J.P., Thijssen, E., Langie, S.A.S., Carleer, R., Ameloot, M., Artois, T., Smeets, K., 2019. In vivo Toxicity

Assessment of Silver Nanoparticles in Homeostatic versus Regenerating Planarians. Nanotoxicology 13, 476–491.

Li, P., Su, M., Wang, X., Zou, X., Sun, X., Shi, J., Zhang, H., 2020. Environmental fate and behavior of silver nanoparticles in natural estuarine systems. J. Environ. Sci. 88, 248–259.

Liu, J., Hurt, R.H., 2010. Ion release kinetics and particle persistence in aqueous nano-silver colloids. Environ. Sci. Technol. 44, 2169–2175.

Liu, S., Wang, C., Hou, J., Wang, P., Miao, L., Li, T., 2018. Effects of silver sulfide nanoparticles on the microbial community structure and biological activity of freshwater biofilms. Environ. Sci. Nano 5, 2899–2908.

Lopes, R.S., 2015. MSc thesis, University of Aveiro, Ecotoxicological assessment of engineered nanoparticles in *Chironomus riparius* 1–110.

Luo, X., Xu, S., Yang, Y., Li, L., Chen, S., Xu, A., Wu, L., 2016. Insights into the Ecotoxicity of Silver Nanoparticles Transferred from *Escherichia coli* to *Caenorhabditis elegans*. Sci. Rep. 6, 1–12.

Malakar, A., Kanel, S.R., Ray, C., Snow, D.D., Nadagouda, M.N., 2021. Nanomaterials in the environment, human exposure pathway, and health effects: A review. Sci. Total Environ. 759, 143470.

Martínez, G., Merinero, M., Pérez-Aranda, M., Pérez-Soriano, E.M., Ortiz, T., Begines, B., Alcudia, A., 2021. Environmental impact of nanoparticles' application as an emerging technology: A review. Materials. 14, 1–26.

McGillicuddy, E., Murray, I., Kavanagh, S., Morrison, L., Fogarty, A., Cormican, M., Dockery, P., Prendergast, M., Rowan, N., Morris, D., 2017. Silver nanoparticles in the environment: Sources, detection and ecotoxicology. Sci. Total Environ. 575, 231–246.

Mech, A., Wohlleben, W., Ghanem, A., Hodoroaba, V.D., Weigel, S., Babick, F., Brüngel, R., Friedrich, C.M., Rasmussen, K., Rauscher, H., 2020. Nano or Not Nano? A Structured Approach for Identifying Nanomaterials According to the European Commission's Definition. Small 16, 1–16.

Mogren, C.L., Webb, S.M., Walton, W.E., Trumble, J.T., 2013. Micro x-ray absorption spectroscopic analysis of arsenic localization and biotransformation in *Chironomus riparius* Meigen (Diptera: Chironomidae) and *Culex tarsalis* Coquillett (Culicidae). Environ. Pollut. 180, 78–83.

Monikh, F.A., Chupani, L., Karkossa, I., Gardian, Z., Arenas-lago, D., von Bergen, M., Schubert, K., Piackova, V., Zuskova, E., Jiskoot, W., Vijver, M.G., Peijnenburg, W.J.G.M., 2021. An environmental ecocorona influences the formation and evolution of the biological corona on the surface of single-walled carbon nanotubes. NanoImpact 22, 100315.

Montes, M.O., Hanna, S.K., Lenihan, H.S., Keller, A.A., 2012. Uptake, accumulation, and biotransformation of metal oxide nanoparticles by a marine suspension-feeder. J. Hazard. Mater. 225–226, 139–145.

Nair, P.M.G., Choi, J., 2012. Modulation in the mRNA expression of ecdysone receptor gene in aquatic midge, *Chironomus riparius* upon exposure to nonylphenol and silver nanoparticles. Environ. Toxicol. Pharmacol. 33, 98–106.

Nair, P.M.G., Choi, J., 2011. Identification, characterization and expression profiles of

Chironomus riparius glutathione S-transferase (GST) genes in response to cadmium and silver nanoparticles exposure. Aquat. Toxicol. 101, 550–560.

Nair, P.M.G., Park, S.Y., Choi, J., 2013. Evaluation of the effect of silver nanoparticles and silver ions using stress responsive gene expression in *Chironomus riparius*. Chemosphere 92, 592–599.

Nair, P.M.G., Park, S.Y., Lee, S.W., Choi, J., 2011. Differential expression of ribosomal protein gene, gonadotrophin releasing hormone gene and Balbiani ring protein gene in silver nanoparticles exposed *Chironomus riparius*. Aquat. Toxicol. 101, 31–37.

Nasser, F., Lynch, I., 2016. Secreted protein eco-corona mediates uptake and impacts of polystyrene nanoparticles on *Daphnia magna*. J. Proteomics 137, 45–51.

Natarajan, L., Jenifer, M.A., Mukherjee, A., 2021. Eco-corona formation on the nanomaterials in the aquatic systems lessens their toxic impact: A comprehensive review. Environ. Res. 194, 110669.

Noreña, C., Damborenea, C., Brusa, F., 2015. Phylum Platyhelminthes. 181–203.

OECD, 2012. Test No. 305: Bioaccumulation in Fish: Aqueous and Dietary Exposure. OECD Guideline for the Testing of Chemicals.

OECD, 2010. Test No. 233: Sediment-Water Chironomid Life-Cycle Toxicity Test Using Spiked Water or Spiked Sediment. OECD Guideline for the Testing of Chemicals.

OECD, 2004a. Test No. 219: Sediment-Water Chironomid Toxicity Test Using Spiked Water. OECD Guideline for the Testing of Chemicals.

OECD, 2004b. Test No. 218: Sediment-Water Chironomid Toxicity Test Using Spiked Sediment. OECD Guideline for the Testing of Chemicals.

Oomen, A.G., Steinhäuser, K.G., Bleeker, E.A.J., van Broekhuizen, F., Sips, A., Dekkers, S., Wijnhoven, S.W.P., Sayre, P.G., 2018. Risk assessment frameworks for nanomaterials: Scope, link to regulations, applicability, and outline for future directions in view of needed increase in efficiency. NanoImpact 9, 1–13.

Oviedo, N.J., Nicolas, C.L., Adams, D.S., Levin, M., 2008. Establishing and maintaining a colony of planarians. Cold Spring Harb. Protoc. 3, 1–6.

Pachapur, V.L., Dalila Larios, A., Cledón, M., Brar, S.K., Verma, M., Surampalli, R.Y., 2016. Behavior and characterization of titanium dioxide and silver nanoparticles in soils. Sci. Total Environ. 563–564, 933–943.

Palmer, M.A., Covich, A.P., Lake, S., Biro, P., Brooks, J.J., Cole, J., Dahm, C., Gibert, J., Goedkoop, W., Martens, K., Verhoeven, J., Van De Bund, W.J., 2000. Linkages between aquatic sediment biota and life above sediments as potential drivers of biodiversity and ecological processes. Bioscience 50, 1062–1075.

Pang, C., Selck, H., Banta, G.T., Misra, S.K., Berhanu, D., Dybowska, A., Valsami-Jones, E., Forbes, V.E., 2013. Bioaccumulation, toxicokinetics, and effects of copper from sediment spiked with aqueous Cu, nano-CuO, or micro-CuO in the deposit-feeding snail, *Potamopyrgus antipodarum*. Environ. Toxicol. Chem. 32, 1561–1573.

Panzarini, E., Mariano, S., Carata, E., Mura, F., Rossi, M., Dini, L., 2018. Intracellular Transport of Silver and Gold Nanoparticles and Biological Responses : An Update. Int. J. Mol. Sci. 19.

Park, H.G., Kim, J.I., Chang, K.H., Lee, B. Cheun, Eom, I. Chun, Kim, P., Nam, D.H., Yeo, M.K., 2018. Trophic transfer of citrate, PVP coated silver nanomaterials, and silver ions in a paddy microcosm. Environ. Pollut. 235, 435–445.

Park, S.Y., Chung, J., Colman, B.P., Matson, C.W., Kim, Y., Lee, B.C., Kim, P.J., Choi, K., Choi, J., 2015. Ecotoxicity of bare and coated silver nanoparticles in the aquatic midge, *Chironomus riparius*. Environ. Toxicol. Chem. 34, 2023–2032.

Pavlaki, M., 2016. PhD thesis. Bottom-up contamination in marine systems – Model trophic levels to predict cadmium flow in marine organisms. Univ. Aveiro 181.

Pavlaki, M.D., Morgado, R.G., Soares, A.M.V.M., Calado, R., Loureiro, S., 2018. Toxicokinetics of cadmium in *Palaemon varians* postlarvae under waterborne and/or dietary exposure. Environ. Toxicol. Chem. 37, 1614–1622.

Petersen, E.J., Mortimer, M., Burgess, R.M., Handy, R., Hanna, S., Ho, K.T., Johnson, M., Loureiro, S., Selck, H., Scott-Fordsmand, J.J., Spurgeon, D., Unrine, J., Van Den Brink, N.W., Wang, Y., White, J., Holden, P., 2019. Strategies for robust and accurate experimental approaches to quantify nanomaterial bioaccumulation across a broad range of organisms. Environ. Sci. Nano 6, 1619–1656.

Pulido-Reyes, G., Leganes, F., Fernández-Piñas, F., Rosal, R., 2017. Bio-nano interface and environment: A critical review. Environ. Toxicol. Chem. 36, 3181–3193.

Pulit-Prociak, J., Banach, M., 2016. Silver nanoparticles - A material of the future...? Open Chem. 14, 76–91.

Quik, J.T.K., Stuart, M.C., Wouterse, M., Peijnenburg, W., Hendriks, A.J., van de Meent, D., 2012. Natural colloids are the dominant factor in the sedimentation of nanoparticles. Environ. Toxicol. Chem. 31, 1019–1022.

Ramskov, T., Croteau, M.N., Forbes, V.E., Selck, H., 2015. Biokinetics of different-shaped copper oxide nanoparticles in the freshwater gastropod, *Potamopyrgus antipodarum*. Aquat. Toxicol. 163, 71–80.

Rejman, J., Oberle, V., Zuhorn, I.S., Hoekstra, D., 2004. Size-dependent internalization of particles via the pathways of clathrin-and caveolae-mediated endocytosis. Biochem. J. 377, 159–169.

Ribeiro, F., van Gestel, C.A.M., Pavlaki, M.D., Azevedo, S., Soares, A.M.V.M., Loureiro, S., 2017. Bioaccumulation of silver in *Daphnia magna*: Waterborne and dietary exposure to nanoparticles and dissolved silver. Sci. Total Environ. 574, 1633–1639.

Rink, J.C., 2013. Stem cell systems and regeneration in planaria. Dev Genes Evol. 223, 67–84.

Santos-Rasera, J.R., Sant'Anna Neto, A., Rosim Monteiro, R.T., van Gestel, C.A.M., Pereira De Carvalho, H.W., 2019. Toxicity, bioaccumulation and biotransformation of Cu oxide nanoparticles in: *Daphnia magna*. Environ. Sci. Nano 6, 2897–2906.

Saraiva, A.S., Sarmento, R.A., Gravato, C., Rodrigues, A.C.M., Campos, D., Simão, F.C.P., Soares, A.M.V.M., 2020. Strategies of cellular energy allocation to cope with paraquat-induced oxidative stress: Chironomids vs Planarians and the importance of using different species. Sci. Total Environ. 741, 140443.

Scheringer, M., Strempel, S., Ng, C.A., Hungerbühler, K., 2013. Response to comment on screening for PBT chemicals among the "existing" and "new" chemicals of the EU. Environ. Sci. Technol. 47, 6065–6066.

Schultz, C.L., Wamucho, A., Tsyusko, O. V., Unrine, J.M., Crossley, A., Svendsen, C., Spurgeon, D.J., 2016. Multigenerational exposure to silver ions and silver nanoparticles reveals heightened sensitivity and epigenetic memory in *Caenorhabditis elegans*. Proc. R. Soc. B Biol. Sci. 283.

Selck, H., Handy, R.D., Fernandes, T.F., Klaine, S.J., Petersen, E.J., 2016. Nanomaterials in the aquatic environment: A European Union-United States perspective on the status of ecotoxicity testing, research priorities, and challenges ahead. Environ. Toxicol. Chem. 35, 1055–1067.

Simão, F.C.P., Gravato, C., Machado, A.L., Soares, A.M.V.M., Pestana, J.L.T., 2020. Toxicity of different polycyclic aromatic hydrocarbons (PAHs) to the freshwater planarian *Girardia tigrina*. Environ. Pollut. 266.

Spurgeon, D.J., Lahive, E., Schultz, C.L., 2020. Nanomaterial Transformations in the Environment: Effects of Changing Exposure Forms on Bioaccumulation and Toxicity. Small 16, 1–12.

Spyra, A., Cieplok, A., Strzelec, M., Babczyńska, A., 2019. Freshwater alien species *Physella acuta* (Draparnaud, 1805) - A possible model for bioaccumulation of heavy metals. Ecotoxicol. Environ. Saf. 185, 1–10.

Starnes, D.L., Unrine, J.M., Starnes, C.P., Collin, B.E., Oostveen, E.K., Ma, R., Lowry, G. V., Bertsch, P.M., Tsyusko, O. V., 2015. Impact of sulfidation on the bioavailability and toxicity of silver nanoparticles to *Caenorhabditis elegans*. Environ. Pollut. 196, 239–246.

Suhendra, E., Chang, C.H., Hou, W.C., Hsieh, Y.C., 2020. A review on the environmental fate models for predicting the distribution of engineered nanomaterials in surface waters. Int. J. Mol. Sci. 21, 1–19.

Svendsen, C., Walker, L.A., Matzke, M., Lahive, E., Harrison, S., Crossley, A., Park, B., Lofts, S., Lynch, I., Vázquez-Campos, S., Kaegi, R., Gogos, A., Asbach, C., Cornelis, G., von der Kammer, F., van den Brink, N.W., Mays, C., Spurgeon, D.J., 2020. Key principles and operational practices for improved nanotechnology environmental exposure assessment. Nat. Nanotechnol. 15, 731–742.

Tangaa, S.R., Selck, H., Winther-Nielsen, M., Khan, F.R., 2016. Trophic transfer of metal-based nanoparticles in aquatic environments: A review and recommendations for future research focus. Environ. Sci. Nano 3, 966–981.

Thalmann, B., Voegelin, A., Von Gunten, U., Behra, R., Morgenroth, E., Kaegi, R., 2015. Effect of Ozone Treatment on Nano-Sized Silver Sulfide in Wastewater Effluent. Environ. Sci. Technol. 49, 10911–10919.

Timmermans, K.R., Peeters, W., Tonkes, M., 1992. Cadmium, zinc, lead and copper in *Chironomus riparius* (Meigen) larvae (Diptera, Chironomidae): uptake and effects. Hydrobiologia 241, 119–134.

Toro, D.M. Di, Allen, H.E., Bergman, H.L., Meyer, J.S., Paquin, P.R., Santore, R.C., 2001. Biotic Ligand Model of the Acute Toxicity of Metals. 1. Technical Basis. Environ. Toxicol. Chem. 20, 2383–2396.

Tourinho, P.S., van Gestel, C.A.M., Lofts, S., Svendsen, C., Soares, A.M.V.M., Loureiro, S., 2012. Metal-based nanoparticles in soil: Fate, behavior, and effects on soil invertebrates. Environ. Toxicol. Chem. 31, 1679–1692.

Tourinho, P.S., van Gestel, C.A.M., Morgan, A.J., Kille, P., Svendsen, C., Jurkschat, K., Mosselmans, J.F.W., Soares, A.M.V.M., Loureiro, S., 2016. Toxicokinetics of Ag in the terrestrial isopod *Porcellionides pruinosus* exposed to Ag NPs and $AgNO_3$ via soil and food. Ecotoxicology 25, 267–278.

Turan, N.B., Erkan, H.S., Engin, G.O., Bilgili, M.S., 2019. Nanoparticles in the aquatic environment : Usage , properties , transformation and toxicity — A review. Process Saf. Environ. Prot. 130, 238–249.

Uddin, M.N., Desai, F., Asmatulu, E., 2020. Engineered nanomaterials in the environment: bioaccumulation, biomagnification and biotransformation. Environ. Chem. Lett. 18, 1073–1083.

van den Brink, N.W., Jemec Kokalj, A., Silva, P. V., Lahive, E., Norrfors, K., Baccaro, M., Khodaparast, Z., Loureiro, S., Drobne, D., Cornelis, G., Lofts, S., Handy, R.D., Svendsen, C., Spurgeon, D., van Gestel, C.A.M., 2019. Tools and rules for modelling uptake and bioaccumulation of nanomaterials in invertebrate organisms. Environ. Sci. Nano 6, 1985–2001.

van der Zande, M., Jemec Kokalj, A., Spurgeon, D., Loureiro, S., Silva, P. V., Khodaparast, Z., Drobne, D., Clark, N.J., van den Brink, N., Baccaro, M., van Gestel, C.A.M., Bouwmeester, H., Handy, R.D., 2020. The Gut Barrier and the Fate of Engineered Nanomaterials: A View from Comparative Physiology. Environ. Sci. Nano 7, 1874–1898.

van Leeuwen, H.P., Town, R.M., Buffle, J., Cleven, R.F.M.J., Davison, W., Puy, J., Van Riemsdijk, W.H., Sigg, L., 2005. Dynamic speciation analysis and bioavailability of metals in aquatic systems. Environ. Sci. Technol. 39, 8545–8556.

Vijver, M.G., Vink, J.P.M., Jager, T., van Straalen, N.M., Wolterbeek, H.T., van Gestel, C.A.M., 2006. Kinetics of Zn and Cd accumulation in the isopod *Porcellio scaber* exposed to contaminated soil and/or food. Soil Biol. Biochem. 38, 1554–1563

Vijver, M.G., Zhai, Y., Wang, Z., Peijnenburg, W.J.G.M., 2018. Emerging investigator series: the dynamics of particle size distributions need to be accounted for in bioavailability modelling of nanoparticles. Environ. Sci. Nano 5, 2473–2481.

Ward, J.E., Kach, D.J., 2009. Marine aggregates facilitate ingestion of nanoparticles by suspension-feeding bivalves. Mar. Environ. Res. 68, 137–142.

Wigger, H., Kägi, R., Wiesner, M., Nowack, B., 2020. Exposure and Possible Risks of Engineered Nanomaterials in the Environment—Current Knowledge and Directions for the Future. Rev. Geophys. 58, 1–25.

Williams, R.J., Harrison, S., Keller, V., Kuenen, J., Lofts, S., Praetorius, A., Svendsen, C., Vermeulen, L.C., Wijnen, J. Van, 2019. Models for assessing engineered nanomaterial fate and behaviour in the aquatic environment. Curr. Opin. Environ. Sustain. 36, 105–115.

Wu, J.P., Chen, H.C., Li, M.H., 2011. The preferential accumulation of cadmium in the head portion of the freshwater planarian, *Dugesia japonica* (Platyhelminthes: Turbellaria). Metallomics 3, 1368–1375.

Wu, J.P., Li, M.H., 2018. The use of freshwater planarians in environmental toxicology studies: Advantages and potential. Ecotoxicol. Environ. Saf. 161, 45–56.

Xiao, B., Zhang, Y., Wang, X., Chen, M., Sun, B., Zhang, T., Zhu, L., 2019. Occurrence and

trophic transfer of nanoparticulate Ag and Ti in the natural aquatic food web of Taihu Lake, China. Environ. Sci. Nano 6, 3431–3441.

Yoo, H., Lee, J.S., Lee, B.G., Lee, I.T., Schlekat, C.E., Koh, C.H., Luoma, S.N., 2004. Uptake pathway for Ag bioaccumulation in three benthic invertebrates exposed to contaminated sediments. Mar. Ecol. Prog. Ser. 270, 141–152.

Zhao, F., Zhao, Ying, Liu, Y., Chang, X., Chen, C., Zhao, Yuliang, 2011. Cellular uptake, intracellular trafficking, and cytotoxicity of nanomaterials. Small 7, 1322–1337.

Zhao, J., Wang, X., Hoang, S.A., Bolan, N.S., Kirkham, M.B., Liu, J., Xia, X., Li, Y., 2021. Silver nanoparticles in aquatic sediments: Occurrence, chemical transformations, toxicity, and analytical methods. J. Hazard. Mater. 418, 126368.

Chapter 2

Toxicokinetics of pristine and aged silver nanoparticles in *Physa acuta*

Published in Environmental Science: Nano, 2020,7, 3849-3868
doi.org/10.1039/D0EN00946F

Patrícia V. Silva[1], Cornelis A. M. van Gestel[2], Rudo A. Verweij[2], Anastasios G. Papadiamantis[3,4], Sandra F. Gonçalves[1], Iseult Lynch[3], and Susana Loureiro[1]

[1]Department of Biology & CESAM, University of Aveiro, Campus Universitário de Santiago, 3810-193 Aveiro, Portugal
[2]Department of Ecological Science, Faculty of Science, Vrije Universiteit Amsterdam, The Netherlands
[3]School of Geography, Earth and Environmental Sciences, University of Birmingham, Edgbaston, B15 2TT Birmingham, UK
[4]NovaMechanics Ltd., 1065, Nicosia, Cyprus

Toxicokinetics of pristine and aged silver nanoparticles in *Physa acuta*

2.1. Abstract

Aquatic environments, particularly sediments, can be important final sinks for engineered nanoparticles (ENPs), with benthic biota being potentially exposed. There is an increasing need for hazard data to improve the environmental risk assessment of ENPs regarding aquatic systems. The aim of this study was to determine the toxicokinetics of several pristine (as manufactured) Ag NPs, Ag_2S NPs (used to simulate environmental aging of silver nanoparticles) and $AgNO_3$ as the ionic counterpart, in the freshwater snail *Physa acuta*. Snails were exposed through 1) contaminated water (without sediment), 2) contaminated water and clean sediment, and 3) contaminated sediment. Bioavailability of Ag to the snails was greatly influenced by Ag characteristics, as different uptake and elimination kinetics were found for the different Ag forms within the same exposure route. Snails exposed via water revealed, in general, similar uptake kinetics, differing from exposure via contaminated sediment, suggesting that exposure route also had a determining role in Ag bioavailability. The simulated aged form (Ag_2S NPs) revealed fast uptake and depuration in snails from all experiments. When considering uptake from both water and sediment, which provides a more realistic exposure scenario, water was the predominant Ag uptake route. The remarkably low elimination and high stored fraction of Ag in some exposures emphasizes the bioaccumulation ability of *P. acuta* and may raise concerns about possible trophic transfer. Snail shells accumulated low amounts of Ag. The present study highlights the need for a proper examination of the overall exposure scenario of Ag NPs to benthic organisms. Our results contribute to the environmental risk assessment of Ag NPs in benthic environments.

Keywords: freshwater snails, sediment, silver sulfide nanoparticles, exposure route, bioavailability, bioaccumulation.

2.2. Introduction

The increasing demand for nano-containing products has led to the large-scale production and commercialisation of engineered nanoparticles (ENPs), which increases the risk of their release into the environment (Sharma et al., 2019). Over the past two decades impressive progress has been made in understanding the potential hazards ENPs may pose to the environment and consequently to humans. While past studies focused on the ecotoxicity of ENPs in aquatic and terrestrial systems (Jeng and Swanson 2006; Ribeiro et al., 2014; Tourinho et al., 2013; Zeyons et al., 2009), subsequent works invested in studying the fate, kinetics and bioavailability of ENPs (Baccaro et al., 2018; Clark et al., 2019; Domercq et al., 2018; Tourinho et al., 2016). Results suggest that the dynamic nature of ENPs can lead to continuous physicochemical transformations, during their entire life-cycle, which combined with their unique properties can trigger myriad biological and/or ecological responses with transformations continuing even after reaching biological receptors (Schwirn et al., 2020; Wang et al., 2016) .

Extensive research has been conducted on silver nanoparticles (Ag NPs) as these are among the most widely produced ENPs and are applied in a broad variety of consumer products. This means that their discharge into aquatic environments is inevitable, with wastewater effluents being one of the main sources (Azimzada et al., 2017). Studies have reported Ag NP concentrations ranging from 0.3 to 2.5 ng L^{-1} in Dutch surface waters (Peters et al., 2018) and <12 ng L^{-1} in wastewater effluents in Germany (Li et al., 2013). A U.S. study from 1998 detected total silver concentrations between 0.028 to 5.56 µg L^{-1} in wastewater effluent and between 1.78 and 105 µg L^{-1} in wastewater influent (Shafer et al., 1998). Another study measured total Ag concentrations of 0.21 µg L^{-1} in wastewater influent during the summer of 2016 in Upper Austria (Vogt et al., 2019). Once in the aquatic environment, the fate of Ag NPs will be determined by transformation processes. These transformations are driven by the Ag NP characteristics, the chemical properties of the aquatic systems, and the interaction of processes such as dissolution, agglomeration / heteroaggregation and sedimentation (among others) and are also seasonal variable (Azimzada et al., 2017; Ellis et al., 2018; Rearick et al., 2018). Aggregation and consequent sedimentation is a likely pathway for Ag NPs thus, sediments have been suggested as ultimate sinks (Cross et al., 2015; Selck et al., 2016) with predicted concentrations of Ag NPs varying from 2.2 µg kg^{-1} sediment (Gottschalk et al., 2009) to 30.1 µg kg^{-1} sediment (Sun et al., 2016). Incomplete dissolution in natural waters has also been reported, which means that Ag NPs can persist for long periods leading to long-term Ag^{+} release and subsequent mobility (Dobias and Bernier-Latmani 2013; Rearick et al., 2018). In wastewater

treatment plants, Ag NPs are predominantly transformed into silver sulfide NPs (Ag_2S NPs) and effluent discharges constitute entrance routes for this Ag species into surface waters. In aquatic systems, Ag_2S NPs can be formed from Ag NPs or Ag^+ in the presence of naturally occurring sulfides, including metal sulfides (Lowry et al., 2012; Thalmann et al., 2015). These transformations occur mainly at the bottom of the water column or in the sediment, although under certain conditions they can also occur higher in the water column (Zhang et al., 2019). Ag_2S NPs have very low dissolution, leading to long-term exposure to these particles but also to low release of more toxic Ag^+ ions. Due to reduced ion availability, these NPs are expected to be less toxic to organisms. However, these NPs have demonstrated some bioavailability and potential to cause hazardous effects (Kuehr et al., 2020; Kühr et al., 2018; Lee et al., 2016; Liu et al., 2018).

It is fundamental for risk assessment to understand and evaluate the bioavailability and exposure of ENPs to organisms. Therefore, emphasis should be given to the determination of kinetic processes such as uptake, internal distribution and depuration of ENPs. Moreover, studies on the exposure and bioaccumulation in benthic organisms, especially for aged/modified ENPs, are needed (Lead et al., 2018; Selck et al., 2016). Some studies have evaluated the uptake and bioavailability of Ag NPs towards benthic organisms. The results varied according to the nature of the Ag NPs, exposure medium and organism used, highlighting that the interplay of these factors largely determines exposure and bioaccumulation (Bao et al., 2018; Croteau et al., 2011; Khan et al., 2012, 2015; Ramskov et al., 2015a; Stoiber et al., 2015; Tangaa et al., 2018). Benthic ecosystems are essential components of aquatic environments, and benthic organisms may potentially be the biota most affected by ENPs as they can be exposed through both water and sediments. Exposure can potentially happen via ingestion of sediment or food and through direct contact of their body surfaces with both phases (e.g., transdermal uptake) (Cross et al., 2015; Cross et al., 2019; Ma et al., 2017). Addressing the need for kinetic studies to improve the environmental risk assessment of ENPs, the present study aimed at determining the toxicokinetics of Ag NPs in the freshwater snail *Physa acuta*. Several pristine (as manufactured) Ag NPs with different characteristics, Ag_2S NPs (simulating an environmentally aged Ag NP form) and $AgNO_3$ (ionic control) were tested through different exposure routes to *P. acuta*: 1) contaminated water (without sediment), 2) contaminated water and clean sediment, and 3) contaminated sediment (clean water). *P. acuta* is an invasive snail found in lotic (riverine) and lentic (still water) ecosystems, representing a link between primary producers and predators in freshwater food chains, and can be vulnerable to contaminants in both sediment and water phases (Gonçalves et al., 2017). The toxicity

of Ag NPs to *P. acuta* has been previously studied (Bernot and Brandenburg 2013; Gonçalves et al., 2017; Justice and Bernot 2014). Studies often evaluate accumulation only in soft tissues. However, shells can also accumulate contaminants, which can continue over time and possibly lead to accumulation by food-chain transfer (Ramskov et al., 2014; Spyra et al., 2019). Considering this, shell fractions were separately analysed in this study.

2.3. Material and Methods

2.3.1. Test species and breeding

Adult *Physa acuta* were collected from a pond at the Campus of the University of Aveiro, Portugal, and acclimated under laboratory conditions for a month before using egg masses deposited by adult snails to increase the cultures. Cultures were maintained in 6 L glass aquariums filled with 3-L of artificial pond water (APW) medium and with approximately 50 individuals per aquarium. For the APW medium, the following stock solutions were prepared using ultrapure water (UPW): calcium chloride (58.8 g L^{-1} $CaCl_2.2H_2O$), potassium chloride (1.15 g L^{-1} KCl), magnesium sulphate (24.65 g L^{-1} $MgSO_4.7H_2O$) and sodium hydrogen carbonate (12.95 g L^{-1} $NaHCO_3$). Then, 100 mL of each stock solution were added to a 20-L carboy filled with UPW (Naylor et al., 1989). APW medium was fully renewed once a week and partially renewed every other day. Medium pH was kept to basic levels (7.9 ± 0.3) to avoid shell fracturing, and continuous aeration was applied, maintaining levels of dissolved oxygen above 8 mg L^{-1}. Snails were fed *ad libitum* with ground TetraMin® (fish food) every other day and kept under controlled conditions of 20 ± 1 ºC and 16:8h light: dark photoperiod (Gonçalves et al., 2017).

2.3.2. Nanoparticles

NP batches were supplied by partners of the EU H2020 NanoFASE project (http://www.nanofase.eu/). Three pristine Ag NPs with different sizes (nominal sizes of 3-8 nm, 50 nm and 60 nm) and silver sulfide NPs (Ag_2S NPs, nominal size of 20 nm) were tested. The soluble salt silver nitrate ($AgNO_3$; Sigma Aldrich; CAS number 7761-88-8; 99% purity; crystalline powder) was used as the ionic control. Ag NPs of 3-8 nm (alkane coated) and 60 nm (Polyvinylpyrrolidone (PVP)) were supplied by AMEPOX Enterprise (Poland), dispersed in UPW at a concentration of 1000 mg Ag L^{-1}. Dispersed solutions of Ag NPs of 50 nm (5.5 mM sodium citrate, 25 µM tannic acid, 47.3 ± 5.3 nm, 12.3 g Ag L^{-1}) and Ag_2S NPs (PVP; with two stock suspensions of 3.6 g Ag L^{-1} and 6.56 g Ag L^{-1}) were supplied by Applied Nanoparticles (Barcelona, Spain). Ag_2S NPs were used as a simulated aged Ag

NP form, in order to increase the environmental relevance of the exposures and to compare it with the pristine Ag NPs.

2.3.3. Nanoparticle characterization

Size and morphology of the pristine 3-8 nm Ag NPs have been reported in Ribeiro et al. (2014). Details on the TEM data for the 50 nm Ag NPs and Ag_2S NPs have been reported previously in Baccaro et al. (2018). The stability of all NPs was monitored by measuring the hydrodynamic size, Zeta potential and dissolution at different time points matched to the periods between water changes. The hydrodynamic size, polydispersity index (PDI) and Z-potential were measured in UPW (pH: 7.00) and APW (pH: 8.00) suspensions prior to exposure and at 0, 2, 4, 8, 24 and 48 hours post-exposure using a Malvern Zetasizer (Nano ZS) equipped with a LASER of 632.8 nm and a scattering angle of 173°. All measurements were performed at 20 °C following a 2-minute equilibration, using Sarstedt polystyrene (Ref: 67.742, 10 x 4 x 45 mm) cuvettes and Malvern Zetasizer DTS0170 disposable folded capillary cells, respectively. In both cases, the concentration of the suspensions was 1 mg L^{-1}. The operation procedures used the built-in values for the refractive indices (η) and absorption coefficients (α) for Ag and Ag_2S of the Malvern Zetasizer Software (version 7.13). The acquired results are the average of 5 consecutive measurements (14 replicates per measurement).

NP dissolution monitoring was performed using the protocol of Avramescu et al. (2017), based on the European Committee for Standardization (CEN) guidance EN 71-3:2019 on "Safety of toys - Part 3: Migration of certain elements" and is commonly used in metal bioaccessibility assays (Dodd et al., 2013). Ag NP and Ag_2S NP dissolution was measured in 1 mg L^{-1} suspensions of UPW and APW at 0, 2, 4, 8, 24 and 48 hours. At each time point, part of each sample was filtered to separate the dissolved from the particulate material using 0.02 µm pore-diameter syringe filters (Anotop™, Whatman) and directly acidified for analysis using pure ICP-grade HNO_3 (Sigma Aldrich; CAS Number 7697-37-2) to a final concentration of 2% HNO_3. Syringe filtering was chosen over centrifugation, so that the standard 30-minute centrifugation delay needed in the latter case, would not affect the results. The dissolved Ag^+ concentration was measured using an Inductively Coupled Plasma Mass Spectrometer (ICP-MS, PerkinElmer, Nexion 3000). Appropriate calibration curves were created using ICP-grade standards and were considered acceptable when the correlation coefficient was greater than 0.999. All samples were spiked with ^{103}Rh as internal standard for QC purposes. Failed QCs resulted in recalibration and reanalysis of the respective samples. Results were converted and reported as percentage dissolution

(%Diss), determined as the amount of dissolved Ag ([DAg^+]) divided by the original Ag concentration ([Ag^+]) used for the experiment (%Diss=([DAg^+]/[Ag^+])×100%) to correspond with that used in the OECD classification scheme (OECD 2015). The rest of the sample was, simultaneously, analysed to measure the hydrodynamic size and Z-potential as described above.

2.3.4. Experimental set up and sampling procedure

Experiments considering different routes of exposure were performed: 1) contaminated APW medium at a nominal concentration of 10 µg Ag L^{-1} (no sediment), 2) contaminated APW medium at a nominal concentration of 10 µg Ag L^{-1} and clean sediment, 3) contaminated sediment at a nominal concentration of 10 mg Ag kg^{-1} and clean APW medium. The different experiments will be referred to as 1) Ag-spiked water test, 2) Ag-spiked water and clean sediment test, 3) Ag-spiked sediment test. Both tests with spiked water used a low nominal concentration that allowed reliable analytical detection and could still be close to environmentally relevant concentrations of Ag NPs and total Ag. In the Ag-spiked water and clean sediment test, it was found that snails were also exposed to sediment concentrations of environmental relevance (explained in section 2.3.7). Therefore, in the Ag-spiked sediment test a higher concentration was used to increase the Ag availability to the snails in order to better understand the toxicokinetic processes.

All NP stock solutions were prepared according to the OECD guideline 318 (2017). Tests consisted of an uptake phase and an elimination phase. Snails (around 2 months old, shell size between 4-7 mm) were individually exposed to contaminated medium during the uptake phase for 7 days, and then transferred to clean medium for a 7-day elimination phase. Tests were maintained under controlled conditions, at 20 ± 1 ºC and 16:8h light: dark photoperiod. Temperature, dissolved oxygen (DO) concentration and pH were recorded during all experiments to ensure parameter quality, according to the OECD guideline 243 (2016).

2.3.4.1. Ag-spiked water test

Snails were exposed in 6-well microplates, with each well filled with 12.5 mL of test medium. The test medium was renewed every other day in the uptake and elimination phases, therefore no aeration was provided. For spiking, stock solutions/suspensions were prepared in UPW, then diluted in APW medium to the desired concentration and poured into the microplates of the respective treatment. Snails were inspected daily and not fed

during the experiment. At 1, 2, 5, 7, 8, 9, 12 and 14 days, snails from three replicates per treatment were sampled, washed three times in UPW and frozen at -80 ºC to allow dissecting into soft body and shell. Partially thawed snails were dissected (Croteau et al., 2014) under a magnifying glass, with the help of two tweezers, one tweezer carefully held the shell, and the other pulled the soft body. Shell and soft body were oven-dried at 60 ºC for 48h and individually weighted. In addition, water was sampled at day 0 (*n*=3 per treatment) for total Ag analysis.

2.3.4.2. Ag-spiked water and clean sediment test

Snails were exposed in 50 mL glass vials, with a depth ratio of 4:1 of APW:sediment (inorganic fine sediment (<1mm), previously burnt for 4h at 500 ºC), prepared 24h prior to spiking. The spiking of APW was performed with adaptations of the OECD protocol 233 (2010). Briefly, the required amount of the stock solution/suspension (in UPW) was applied to each test vial, below the water surface and then gently stirred with a needle to ensure homogenization while not disturbing the sediment. Each vial was covered with a lid to avoid evaporation. Low aeration was provided 24 h after water spiking by needles connected to an air pump, to avoid disturbing the sediment (OECD 2016). No food was provided to the organisms during the experiment and vials were inspected daily. At 1, 2, 5, 7, 8, 9, 12 and 14 days, snails from three replicates per treatment were sampled and left to depurate in clean APW medium for 24h to empty their gut, since benthic snails can ingest sediment particles (Dillon 2000; Ramskov et al., 2015a). After depuration, the same procedure as described in section 2.3.4.1 was followed. In addition, water and sediment were sampled at days 0, 3 and 7 (*n*=3 per treatment) for total Ag analysis (sediment was stored frozen until analysis).

2.3.4.3. Ag-spiked sediment test

Snails were exposed in 50 mL glass vials, with the APW:sediment ratio as for the previous test (section 2.3.4.2). The spiking of sediment followed adaptations of OECD protocol 218 (2004). Briefly, 10 g of sediment were spiked in the individual test vials with the required amount (volume corresponding to 20% of the sediment amount) of the stock solutions (in UPW) and homogenised by hand, making sure the solution was evenly distributed. Then, APW medium was very carefully added, avoiding disturbance of the sediment as much as possible, and then left to equilibrate for 48h prior to the start of the exposures. Lid covering and low aeration was provided to each vial after 48h of

equilibration, as in section 2.3.4.2. Incubations and sampling (organisms and sediment) were performed as described in section 2.3.4.2.

2.3.5. Ultrafiltration of water samples

In separate experiments, water samples were collected from the same vials (*n*=3 per treatment) during the uptake phase (nominal concentration of 10 µg Ag L^{-1}) of the different Ag exposures at days 0 (meaning at 0h), 1 and 2 of the Ag-spiked water test, and at days 0 (0h), 1, 2 and 7 of the Ag-spiked water and clean sediment test, for ultrafiltration. Additionally, water samples were also collected at day 0 (0h) for both experiments and digested for total Ag determination. For ultrafiltration, 3 mL of water collected directly from the test vials was filtered using a syringe filter with a membrane pore size of 0.02 µm (Anotop^{TM}, Whatman). To prevent losses of Ag to the filter, filters were previously treated with a solution of 0.1 M $CuSO_4$ (Cornelis et al., 2010). Following filtration, samples were immediately acidified with concentrated HNO_3 (65% purity, PanReac AppliChem, trace analysis) to a final acid concentration of 2%.

2.3.6. Sample digestion and total Ag analysis

Water samples were digested following the approach of Ribeiro et al. (2014, 2015). Briefly, samples were placed in Teflon beakers on a hotplate and left to evaporate until 1 mL volume was reached. Then, a 4 mL mixture of concentrated HCl (37%):HNO_3 (65%) (aqua regia) (3:1. v/v, PanReac AppliChem, trace analysis) was added and left to evaporate until approximately 1 mL. Afterwards, samples were diluted to a final volume of 45 mL with a solution of 1% HCl (37% purity, PanReac AppliChem, trace analysis). In each digestion run, three blanks (APW medium) and three recovery controls (with known Ag concentration) were analysed jointly with the samples to evaluate the accuracy and recovery of the procedure. The average recovery of Ag was of 101 ± 29.8 % (mean ± SD; *n*=66).

Snail soft body and shell samples were digested according to Ribeiro et al. (2017). Firstly, 3 mL of concentrated HNO_3 (65% purity, PanReac AppliChem, trace analysis) was added to Teflon beakers and samples were heated on a hotplate with the lids on. After breaking down the tissue, 1 mL of concentrated HCl (37% purity, PanReac AppliChem, trace analysis) was added. Lids were removed after 30 min, and samples were left to evaporate until approximately 1 mL. After evaporation, samples were diluted to a final volume of 45 mL with a solution of 1% HCl (37% purity, PanReac AppliChem, trace analysis). In the individual digestion runs, blanks and reference material were analysed in

triplicate to assess method accuracy and recovery. The certified reference materials DOLT-3 and DOLT-5 (Dogfish liver) were used, giving an average Ag recovery of 102 ± 31.6% (mean ± SD; *n*=30).

Sediment samples were oven dried at 50ºC before digestion. Approximately 130 mg of sediment was digested for 7 h in closed Teflon containers using a 2 mL mixture of concentrated HCl (37%):HNO_3 (65%) (4:1. v/v, J.T. Baker, trace analysis), in an oven (BINDER ED53) at 140 ºC, after which samples were diluted to a final volume of 10 mL with demineralized water. DOLT-4 was used as the certified reference material, giving 103 ± 6.1% (mean ± SD*; n*=2) of Ag recovery.

Total Ag concentrations in soft body, shell, water and sediment samples were measured by Graphite furnace Atomic Absorption Spectrometry (AAS; PinAAcle 900Z, PerkinElmer, Singapore). The limit of detection (LOD) ranged between 0.035-0.198 µg Ag L^{-1} in the different runs.

2.3.7. Toxicokinetic modelling

First order one-compartment models, adapted from van den Brink et al. (2019) were fit to the data to describe the toxicokinetics of the different Ag forms in the snails. These models considered a stored fraction (SF) in which metals are stored and not eliminated from the body during uptake and elimination phases (van den Brink et al., 2019).

Model 1 considers only one exposure route and was used to fit the data of the Ag-spiked water and Ag-spiked sediment tests. Sediment analysis of the Ag-spiked water and clean sediment test revealed Ag background concentrations at day 0. Since Ag concentrations increased over time in the sediment while decreasing in the water (see section 2.4.3), a model including both exposures (model 2) was applied to Ag-spiked water and clean sediment test data. Ag concentration decrease rate constant in water (kd_{water}) and increase rate constant in sediment (ki_{sed}) were calculated using an exponential equation of Ag concentration vs. time. To check whether the kinetics were better explained by single or double exposures, further modelling was performed considering only exposure through water (model 3) and exposure only through sediment (model 4). Since the snails lost weight in all tests (due to lack of feeding), a growth decrease rate constant was calculated and included in all models, by fitting an exponential curve to the individual snail dry weights (dw) during the 14-day test duration.

In model 1, uptake and elimination phases were modelled applying equations 1 and 2, respectively:

$$Q(t) = C_0 + \left(C_{exp} * k1 * SF * t\right) + \left(C_{exp} * \left(\frac{k1}{(k2+k_{growth})}\right) * \left(1 - e^{(-(k2+k_{growth})*t)}\right) * (1 - SF)\right)$$

(1)

$$Q(t) = C_0 + \left(C_{exp} * k1 * SF * t_c\right) + \left(C_{exp} * \left(\frac{k1}{(k2+k_{growth})}\right) * \left(1 - e^{(-(k2+k_{growth})*t_c)}\right) * e^{\left(-(k2+k_{growth})*(t-t_c)\right)} * (1 - SF)\right)$$

(2)

Equations 3 and 4 were used in model 2 to fit the data from the uptake and elimination phases:

$$Q(t) = C_0 + \left(\left(C_{\exp water} * kw + C_{\exp sed} * ks\right) * SF * t\right) + \left(\frac{(C_{\exp water} * kw + C_{\exp sed} * ks)}{(k2+k_{growth} - kd_{water})}\right) * \left(e^{(-kd_{water}*t)} - e^{(-(k2+k_{growth})*t)}\right) * (1 - SF)$$

(3)

$$Q(t) = C_0 + \left((C_{\exp water} * kw + C_{\exp sed} * ks) * SF * t_c\right) + \left(\frac{(C_{\exp water} * kw + C_{\exp sed} * ks)}{(k2+k_{growth} - kd_{water})}\right) * \left(e^{(-kd_{water}*t)} - e^{(-(k2+k_{growth})*t)}\right) * \left(e^{(-(k2+k_{growth})*(t-t_c))}\right) * (1 - SF)$$

(4)

For the individual exposures of the Ag-spiked water and clean sediment test, model 3 (equations 5 and 6) was applied to water exposure and model 4 (equations 7 and 8) to sediment exposure:

$$Q(t) = C_0 + \left(C_{\exp water} * k1 * SF * t\right) + \left(C_{\exp water} * \left(\frac{k1}{(k2+k_{growth} - kd_{water})}\right) * \left(e^{(-kd_{water}*t)} - e^{(-(k2+k_{growth})*t)}\right) * (1 - SF)\right)$$

(5)

$$Q(t) = C_0 + \left(C_{\exp water} * k1 * SF * t_c\right) + \left(C_{\exp water} * \left(\frac{k1}{(k2+k_{growth} - kd_{water})}\right) * \left(e^{(-kd_{water}*t)} - e^{(-(k2+k_{growth})*t)}\right) * \left(e^{(-(k2+k_{growth})*(t-t_c))}\right) * (1 - SF)\right)$$

(6)

$$Q(t) = C_0 + \left(C_{\exp sed} * k1 * SF * t\right) + \left(C_{\exp sed} * \left(\frac{k1}{(k2+k_{growth} - ki_{sed})}\right) * \left(e^{(-ki_{sed}*t)} - e^{(-(k2+k_{growth})*t)}\right) * (1 - SF)\right)$$

(7)

$$Q(t) = C_0 + \left(C_{\exp sed} * k1 * SF * t_c\right) + \left(C_{\exp sed} * \left(\frac{k1}{\left(k2+k_{growth}-ki_{sed}\right)}\right) * \left(e^{(-ki_{sed}*t)} - e^{(-(k2+k_{growth})*t)}\right) * \left(e^{(-(k2+k_{growth})*(t-t_c))}\right) * (1-SF)\right)$$

(8)

Where Q(t) = Ag internal concentration in the snails at time t days (µg Ag $g^{-1}_{organism}$ dw); k1 = uptake rate constant (L_{water} $g^{-1}_{organism}$ day^{-1} or $g_{sediment}$ $g^{-1}_{organism}$ day^{-1}); k2 = elimination rate constant (day^{-1}); C_0 = background internal concentration measured at day 0 (µg Ag $g^{-1}_{organism}$ dw), C_{exp} = Ag exposure concentration in water (µg Ag L^{-1}) or sediment (mg Ag kg^{-1}); t = time in days and t_c = time at which snails were transferred from contaminated to clean medium (day 7); SF= stored fraction (ranging from 0 to 1; unit less); k_{growth} = growth decrease rate constant (day^{-1}); kw = uptake rate constant from water (L_{water} $g^{-1}_{organism}$ day^{-1}); ks = uptake rate constant from sediment ($g_{sediment}$ $g^{-1}_{organism}$ day^{-1}); $C_{exp\ water}$ = Ag exposure concentration in water (µg Ag L^{-1}); $C_{exp\ sed}$ = Ag exposure concentration in sediment (mg Ag kg^{-1}); kd_{water} = Ag water concentration decrease rate constant (day^{-1}); ki_{sed} = Ag sediment concentration increase rate constant (day^{-1}).

For the double exposure, further calculations (equations 9 and 10) were performed in order to determine the relative contribution of each uptake route to the total uptake.

Water uptake route:

$$\left(\frac{(C_{\exp water} * kw)}{(C_{\exp water} * kw + C_{\exp sed} * ks)}\right) * 100$$

(9)

Sediment uptake route:

$$\left(\frac{(C_{\exp sed} * ks)}{(C_{\exp water} * kw + C_{\exp sed} * ks)}\right) * 100$$

(10)

2.3.8. Statistical analysis

The described models were fitted to the data and toxicokinetics parameters were determined by non-linear regression in SPSS (version 25). Several models were used to fit the data (data not shown) and the selection of the best fitting ones was performed by applying the Akaike Information Criteria tests (AIC and AICc). Differences between k1 and k2 of each Ag form were tested using Generalised Likelihood Ratio Tests (GLR) in SPSS. Using the SigmaPlot 12.5 software, one-way analysis of variance (ANOVA) followed by the

Holm-Sidak method ($p<0.05$) was conducted to determine significance of the differences in total and dissolved Ag concentrations between treatments in water, and in total Ag concentrations between treatments in sediments. One-way repeated measures ANOVA followed by the Holm-Sidak method ($p<0.05$) (SigmaPlot 12.5 software) was applied to compare dissolved Ag concentrations between days in each treatment of the Ag-spiked water and Ag-spiked water and clean sediment tests. Two-way ANOVA followed by the Holm-Sidak method ($p<0.05$) (SigmaPlot 12.5 software), with Ag treatment and time as factors, was used to determine significance of the differences in Ag concentrations of water or sediment samples of the Ag-spiked water and clean sediment test, and sediment samples of the Ag-spiked sediment test. Data transformation was performed when ANOVA assumptions were not met.

2.4. Results

2.4.1. Nanoparticle stability

NP stability was evaluated by monitoring the hydrodynamic size, Z-potential and dissolution in UPW and APW at 0, 2, 4, 8, 24 and 48 hours. Detailed results can be found in Tables S2.1 and S2.2 for UPW and APW, respectively. Dissolution results are presented graphically in Figures S2.1 and S2.2. In APW medium, the Z-potential for the 3-8 nm and 50 nm Ag NPs and Ag_2S NPs decreased when compared to UPW (Tables S2.1-S2.2). Strong agglomeration was observed for 3-8 nm Ag NPs in both APW and UPW, being higher in APW with hydrodynamic size ranging from 131-270 nm. While in UPW the hydrodynamic diameter of the 50 nm Ag NPs remained close to their nominal size (~58 nm) (Table S2.1), in APW agglomeration led to a substantial increase of sizes, ranging from 75.6-1840 nm (Table S2.2). The Z-potential of the 60 nm Ag NPs substantially increased in APW (from -16 to -24.8 mV). This affected their hydrodynamic size, which was substantially lower (79.2-174 nm), with respective reductions in the PDI values (Table S2.2). While 60 nm Ag NPs in UPW revealed high dissolution (stable around 27-29%), much lower dissolution was observed for these Ag NPs in APW, and decreasing from 2.3% at 2h to 0.82% at 48h (Table S2.2). This was significantly lower (Holm-Sidak method, $p<0.05$) than dissolution in APW observed for the 3-8 nm and 50 nm Ag NPs and Ag_2S NPs (Table S2.2). The hydrodynamic diameter of Ag_2S NPs was relatively stable over time in APW and minimal dissolution was observed (<0.2 %) (Table S2.2).

2.4.2. Ag-spiked water test

Concentrations of Ag in APW were determined at time 0, and since the medium was renewed every 48h, concentrations in the water column were assumed to be constant during the uptake phase. Still, some adsorption of Ag to the microplate walls could have occurred, contributing to higher exposure to snails, for instance, by adsorption to the foot/shell. Measured Ag concentrations were close to the nominal ones for all Ag forms except Ag_2S NPs, which revealed a value 4 times lower than the nominal 10 µg Ag L^{-1} concentration and significantly lower (Holm-Sidak method, $p<0.001$) than concentrations measured in the other NP treatments (Table 2.1).

Low mortality (<5%) was observed during the experiment (data not shown). Distinct uptake patterns were seen for 60 nm Ag NPs and $AgNO_3$ compared to the remaining NPs (Figure 2.1). On the last day of the uptake phase, mean Ag internal concentrations in snails exposed to 60 nm Ag NPs and $AgNO_3$ were 70.3 and 80.8 µg Ag g^{-1} dw, respectively. For 3-8 nm and 50 nm Ag NPs and Ag_2S NPs body concentrations were 12.0, 19.4 and 7.70 µg Ag g^{-1} dw, respectively. Although the uptake curves were very similar for 60 nm Ag NPs and $AgNO_3$, the elimination curves differed (Figure 2.1).

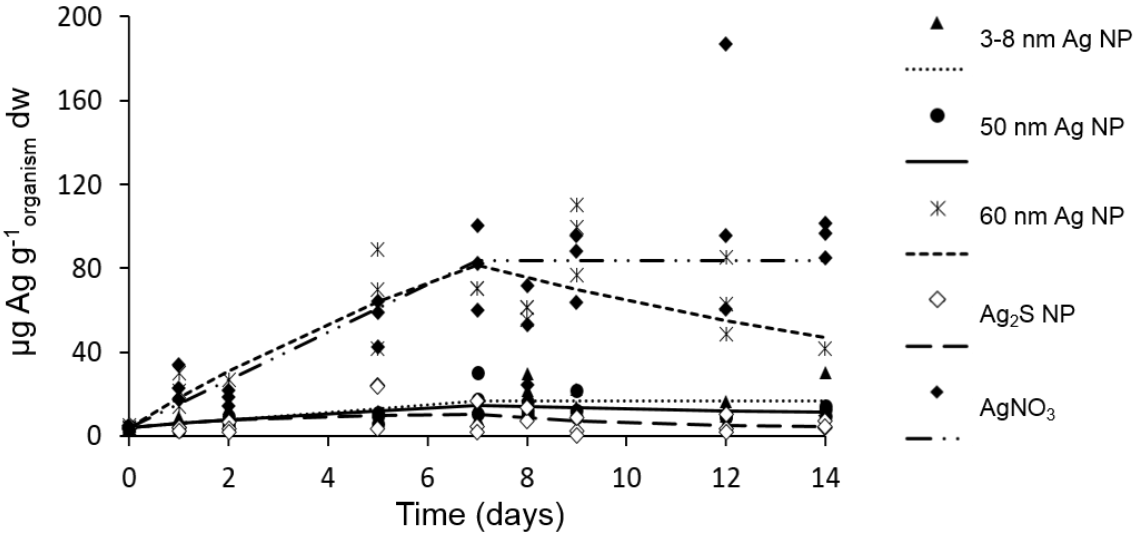

Figure 2.1. Uptake and elimination kinetics of 3-8 nm, 50 nm and 60 nm Ag NPs, Ag_2S NPs and $AgNO_3$ in the freshwater snail *Physa acuta* exposed for 7 days to water spiked at a nominal concentration of 10 µg Ag L^{-1} and then transferred to clean water for 7 days, in the Ag-spiked water test. Lines represent the fit of a one-compartment model to the data, which represent Ag concentrations measured in individual snail soft bodies.

The Ag toxicokinetic parameters are shown in Table 2.1. Values of k1 were lowest for snails exposed to 3-8 nm (0.18 L_{water} $g^{-1}_{organism}$ day^{-1}) and 50 nm (0.22 L_{water} $g^{-1}_{organism}$ day^{-1}) Ag NPs and did not significantly differ ($X^2_{(1)}<3.84$; $p>0.05$). The k1 values of 3-8 nm Ag NPs

were significantly lower ($X^2_{(1)}$>3.84; p<0.05) compared to 60 nm Ag NPs, Ag_2S NPs and $AgNO_3$, and k1 values of 50 nm Ag NPs significantly differed ($X^2_{(1)}$>3.84; p<0.05) from 60 nm Ag NPs and Ag_2S NPs. No significant differences ($X^2_{(1)}$<3.84; p>0.05) in k2 values were found. Low k2 values were registered for 3-8 nm Ag NPs (0.03 day^{-1}) and $AgNO_3$ (0.02 day^{-1}), with SF=1 for both suggesting limited elimination. The remaining Ag NPs revealed higher k2 values and SF of 0, with curves indicating slow elimination. Ag_2S NPs showed the highest k2 (0.44 day^{-1}) and a steeper elimination curve (Figure 2.1, Table 2.1).

Table 2.1. Measured concentrations (µg Ag L^{-1}) given as mean and standard deviation (mean ± SD; *n*=3) and toxicokinetic parameters for 3-8 nm, 50 nm and 60 nm Ag NPs, Ag_2S NPs and $AgNO_3$ in *Physa acuta* exposed to water spiked at a nominal concentration of 10 µg Ag L^{-1}, in the Ag-spiked water test. k1 is the uptake rate constant, k2 the elimination rate constant, kg the growth rate constant and SF the stored fraction. 95% confidence intervals (CI) are given in brackets. Different capital letters in bold within a column indicate statistically significant differences ($X^2_{(1)}$>3.84; p<0.05). Different small letters in italics within a column indicate statistically significant differences (one-way ANOVA followed by Holm-Sidak Method, p<0.05).

Exposure route	Ag form	Measured concentration (µg Ag L^{-1})	k1 (L_{water} $g^{-1}_{organism}$ day^{-1})	k2 (day^{-1})	SF	kg (day^{-1})
Water	3-8 nm	9.85 ± 0.40 *a*	0.18 (0.08-0.29) **A**	0.03 (n.d.)	1 (-)	-0.03
	50 nm	8.32 ± 0.30 *b*	0.22 (-0.04-0.48) **A,C**	0.12 (-1.35-1.58) **A**	0 (-)	-0.06
	60 nm	10.3 ± 0.26 *a*	1.43 (0.32-2.54) **B**	0.11 (-0.63-0.85) **A**	0 (-5.22-5.22)	-0.03
	Ag_2S NPs	2.46 ± 0.48 *c*	1.07 (-0.97-3.10) **B**	0.44 (-0.79-1.67) **A**	0 (-0.52-0.52)	-0.07
	$AgNO_3$	9.46 ± 0.59* *a*	1.20 (0.69-1.70) **B,C**	0.02 (n.d.)	1 (-)	-0.02

(-) very wide 95% confidence intervals.
(n.d.) not possible to determine 95% confidence intervals.
* *n*=2

Table 2.1 also displays the constants (kg) for snail growth rate of each treatment. Snails showed some weight loss during all tests. Total and dissolved Ag concentrations measured in samples collected for ultrafiltration from all exposures are shown in Table S2.3. Since the filters used for ultrafiltration had a pore size of 0.02 µm, possibly other Ag forms (< 20 nm) were measured besides ionic Ag. Mean % of dissolved Ag compared with the total Ag determined was 1.87 ± 0.69 %, 2.52 ± 1.87 %, 33.8 ± 2.04 %, 0.59 ± 0.4 % and 34.7 ± 4.47 % for 3-8 nm, 50 nm, 60 nm Ag NPs, Ag_2S NPs and $AgNO_3$, respectively (data not shown). Dissolved Ag concentrations were significantly higher (Holm-Sidak method, p<0.001) for 60 nm Ag NPs and $AgNO_3$ compared to the remaining Ag forms from day 0 to day 2, and only differed significantly (Holm-Sidak method, p<0.05) between sampling days for $AgNO_3$ (Table S2.3).

2.4.3. Ag-spiked water and clean sediment test

Measured Ag concentrations in water and sediment are displayed in Table S2.4. A low background Ag concentration of 10.1 ± 2.95 µg Ag kg^{-1} was measured in sediments sampled

at day 0 from the initial batch used in all treatments, therefore the snails were exposed to Ag through water and sediment from the beginning of the exposures. Concentrations of Ag in water at day 0 were close to the nominal 10 µg Ag L^{-1}, and showed a steep decrease in the first three days of the uptake phase, which was significant (two-way ANOVA, Holm-Sidak method, $p<0.001$) for all treatments. Concentrations of Ag in the water samples were influenced by Ag treatment and time, and interaction was significant (two-way ANOVA, Holm-Sidak method, $p<0.05$). At day 0, Ag concentrations of the Ag_2S NP treatments were significantly higher (two-way ANOVA, Holm-Sidak method, $p<0.05$) than the other treatments. Ag concentrations in the $AgNO_3$ treatment were significantly lower than for the Ag_2S NPs at day 3, while at day 7 concentrations of the 3-8 nm Ag NP treatment were significantly higher than in the 50 nm Ag NP and ionic exposures (two-way ANOVA, Holm-Sidak method, $p<0.05$). Values of kd_{water} and ki_{sed} were lower for 3-8 nm and 50 nm Ag NPs (Table S2.4). The increase in Ag concentration in sediments from day 0 to 7 was not significant (two-way ANOVA, Holm-Sidak method, $p>0.05$) only for the 3-8 nm Ag NPs. Concentrations between treatments did not differ during time (two-way ANOVA, Holm-Sidak method, $p>0.05$) (Table S2.4). Concentrations in sediments are presented in µg Ag kg^{-1} in Table S2.4, but were converted to mg kg^{-1} to present uniformed units of k1 (in $g_{sediment}$ $g^{-1}_{organism}$ day^{-1}) from uptake through sediment in models 2 and 4.

Total and dissolved Ag concentrations measured in water samples collected for ultrafiltration from all exposures are presented in Table S2.5. Mean % of dissolved Ag compared with the total Ag determined was 0.72 ± 0.6 %, 1.61 ± 1.86 %, 4.23 ± 5.14 %, 0.2 ± 0.22 % and 3.6 ± 4.24 % for 3-8 nm, 50 nm, 60 nm Ag NPs, Ag_2S NPs and $AgNO_3$, respectively (data not shown). No dissolved Ag was detected at day 0 in any exposure, including $AgNO_3$. However, an increase in dissolved Ag was seen from day 0 to day 1. The 60 nm Ag NPs and $AgNO_3$ had higher dissolved Ag concentrations at days 1 and 2, but only at day 2 significant differences (Holm-Sidak method, $p<0.05$) were detected between treatments. From day 1, a decrease in concentration was visible, except for 50 nm Ag NPs which showed a low increase (not significant, Holm-Sidak method, $p>0.05$). From days 2 to 7, Ag concentrations generally decreased to zero, which was significant for Ag_2S NPs (Holm-Sidak method, $p<0.05$) (Table S2.5).

No mortality was observed (data not shown). Uptake and elimination curves and kinetics parameters are presented in Figure 2.2 and Table 2.2, respectively. Higher internal Ag concentrations were measured after 7 days in snails exposed to 60 nm Ag NPs (31.3 µg Ag g^{-1} dw) and $AgNO_3$ (53.6 µg Ag g^{-1} dw) than in snails exposed to 3-8 nm (15.6 µg Ag g^{-1} dw) and 50 nm (9.22 µg Ag g^{-1} dw) Ag NPs and Ag_2S NPs (2.98 µg Ag g^{-1} dw). Highest uptake

rates were determined for 60 nm Ag NPs and $AgNO_3$ (Figure 2.2). Ag body concentrations for snails exposed to Ag_2S NPs reached a peak at day 2, followed by a considerable decrease afterwards. The kinetic curve follows this pattern, with a fast increase of the uptake rate during the first day, and a steep decline after day 2 (Figure 2.2).

Highest kw (uptake from water) values were calculated upon exposure to Ag_2S NPs (3.15 $L_{water}\ g^{-1}_{organism}\ day^{-1}$) and 60 nm Ag NPs (2.19 $L_{water}\ g^{-1}_{organism}\ day^{-1}$) followed by $AgNO_3$ (1.88 $L_{water}\ g^{-1}_{organism}\ day^{-1}$). For uptake from sediment, Ag_2S NPs presented the highest ks value, of 1.91 $g_{sediment}\ g^{-1}_{organism}\ day^{-1}$. It was not possible to evaluate differences between kw or ks of the different Ag forms as no 95% CI could be determined (Table 2.2).

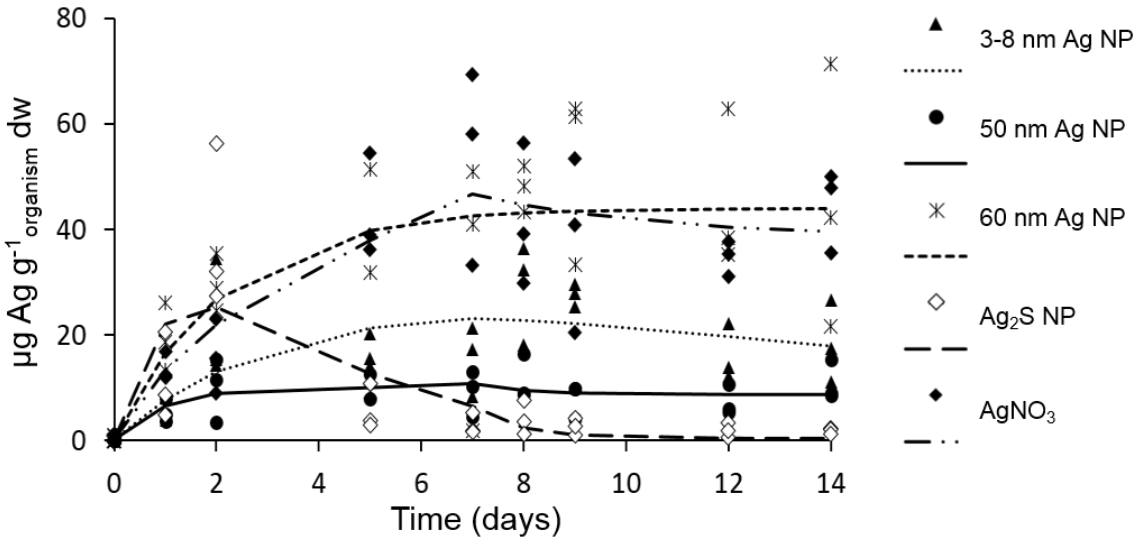

Figure 2.2. Uptake and elimination kinetics of 3-8 nm, 50 nm and 60 nm Ag NPs, Ag_2S NPs and $AgNO_3$ in the freshwater snail *Physa acuta* exposed for 7 days to water spiked at a nominal concentration of 10 µg Ag L^{-1} and then transferred to clean water for 7 days, in the Ag-spiked water and clean sediment test. Lines represent the fit of a one-compartment model to the data, which represent Ag concentrations measured in individual snail soft bodies.

Snails exposed to 60 nm Ag NPs did not eliminate Ag during the 7-day elimination period, showing a steady curve and a k2 of 0 day^{-1}, while snails exposed to Ag_2S NP presented the highest k2 value (0.74 day^{-1}). This k2 value was significantly different ($X^2_{(1)}$>3.84; p<0.05) from all treatments, except for 50 nm Ag NPs. In general, very low SF were calculated, with the highest value of 0.33 determined for $AgNO_3$ (Table 2.2).

Table 2.2. Toxicokinetic parameters for 3-8 nm, 50 nm and 60 nm Ag NPs, Ag_2S NPs and $AgNO_3$ in *Physa acuta* exposed to water spiked at nominal concentration of 10 µg Ag L^{-1}, in the Ag-spiked water and clean sediment test. k1 is the uptake rate constant, k2 the elimination rate constant, kw the uptake rate constant from water, ks the uptake rate constant from sediment, kg the growth rate constant and SF the stored fraction. 95% confidence intervals (CI) are given in brackets. Different letters within a column indicate statistically significant differences ($X^2_{(1)}$>3.84; p<0.05).

Exposure route	Ag form	kw (L_{water} $g^{-1}_{organism}$ day^{-1})	ks ($g_{sediment}$ $g^{-1}_{organism}$ day^{-1})	k1 (L_{water} $g^{-1}_{organism}$ day^{-1}; $g_{sediment}$ $g^{-1}_{organism}$ day^{-1})	k2 (day^{-1})	SF	k_{growth} (day^{-1})
Water and sediment (model 2)	3-8 nm	0.88 (n.d.)	0.25 (n.d.)		0.05 (-0.02-0.12) **A**	0 (-0.61-0.61)	-0.02
	50 nm	1.11 (n.d.)	0.30 (n.d.)		0.65 (-0.51-1.80) **A,B,C**	0.13 (-0.03-0.28)	-0.01
	60 nm	2.19 (n.d.)	0.50 (n.d.)		0 (-0.03-0.03) **B**	0.01 (-0.33-0.35)	0
	Ag_2S NPs	3.15 (n.d.)	1.91 (n.d.)		0.74 (0.02-1.46) **C**	0.001 (-0.02-0.02)	0
	$AgNO_3$	1.88 (n.d.)	0.40 (n.d.)		0.16 (-0.45-0.78) **A,B**	0.33 (0.13-0.53)	-0.01
Water (model 3)	3-8 nm			0.88 (0.35-1.40) **A**	0.05 (-0.02-0.11) **A**	0 (-0.57-0.57)	
	50 nm			1.11 (0.27-1.95) **A**	0.65 (-0.22-1.51) **A,B,C**	0.13 (0.04-0.21)	
	60 nm			2.19 (0.79-3.36) **B,C**	0 (-0.03-0.02) **B**	0.01 (-0.32-0.32)	
	Ag_2S NPs			3.16 (1.36-4.95) **B**	0.74 (0.12-1.36) **C**	0.001 (-0.02-0.02)	
	$AgNO_3$			1.88 (0.59-3.17) **C**	0.16 (-0.41-0.73) **A,B**	0.33 (0.14-0.53)	
Sediment (model 4)	3-8 nm			416 (279-560) **A**	0.18 (-0.17-0.52) **A**	0 (-5.24-5.24)	
	50 nm			607 (-625-1848) **A,B**	1.76 (-3.27-6.80) **A,B**	0.19 (-0.17-0.56)	
	60 nm			642 (302-993) **A,B**	0.16 (n.d.)	1 (-4.10-6.10)	
	Ag_2S NPs			1882 (-6013-9777) **B,C**	2.67 (-9.59-14.9) **B**	0 (-0.06-0.06)	
	$AgNO_3$			2046 (-1535-5661) **C**	2.18 (-3.65-8.00) **B**	0.27 (-0.18-0.72)	

(n.d.) not possible to determine 95% confidence intervals.

The percentage of the relative contribution of each uptake route was calculated. For all Ag forms nearly 100% of the Ag in the animals was from the water, with less than 0.1% coming from the sediment. Highest contribution of sediment uptake to total uptake was seen for the Ag_2S NPs, with 0.07%, for all other Ag forms it was around 0.04%. When considering a single exposure route (models 3 and 4), it was possible to determine 95% CI for the kinetic parameters (Table 2.2). When accounting only for water exposure (model 3), identical values to those determined by model 2 (kw, k2 and SF) were calculated, with the same significant differences between k2 values. Statistically significant differences ($X^2_{(1)}>3.84$; $p<0.05$) were found for k1 values of 3-8 nm and 50 nm Ag NPs in comparison with 60 nm Ag NPs, Ag_2S NPs and $AgNO_3$, and also between Ag_2S NPs and $AgNO_3$ (Table 2.2).

Considering sediment as single exposure route (model 4), Ag_2S NPs and $AgNO_3$ presented the highest k1 (1882 $g_{sediment}\ g^{-1}_{organism}\ day^{-1}$ and 2046 $g_{sediment}\ g^{-1}_{organism}\ day^{-1}$, respectively) and k2 values (2.68 day^{-1} and 2.18 day^{-1}, respectively) (Table 2.2), probably explained by the fast drop of the curve from day 7 to 8 (Figure S2.3). A SF of zero was determined for all treatments, except for 60 nm Ag NPs, which presented a SF of 1. This SF contrasts with the values very close to zero determined for this Ag form by models 2 and 3 (Table 2.2). Although the general patterns of the curves share similarities, some differences were observed between kinetic curves determined by model 2 and model 4 (Figures 2.2 and S2.3). This is especially notable for the Ag_2S NP uptake curve, which increases gradually after the first day of the uptake phase (Figure S2.3). Kinetic curves determined by model 3 are the same as those observed in Figure 2.2.

2.4.4. Ag-spiked sediment test

Kinetics curves determined for snails exposed to Ag-spiked sediment are presented in Figure 2.3, and corresponding kinetic parameters are given in Table 2.3. Total Ag concentrations in sediment were similar to the nominal 10 mg Ag kg^{-1} (Tables 2.3 and S2.6). Concentrations of Ag from the 3-8 nm exposure were significantly higher among treatments at day 0 (two-way ANOVA, Holm-Sidak method, $p<0.05$). At day 7, samples from the 60 nm Ag NP and Ag_2S NP treatments showed the highest Ag concentration in sediments (two-way ANOVA, Holm-Sidak method, $p<0.05$). Concentrations remained relatively stable in time, showing a significant decrease from day 0 to 3 in the 3-8 nm Ag NP exposure (two-way ANOVA, Holm-Sidak method, $p<0.001$), and a significant increase from day 3 to 7 in the 60 nm Ag NP treatment (two-way ANOVA, Holm-Sidak method, $p<0.05$) (Table S2.6). Nevertheless, concentrations were very similar and for the sake of comparison between Ag forms, the mean Ag concentration at days 0, 3 and 7 were used as the exposure

concentration for each treatment, instead of calculating rate constants for concentration changes (Table 2.3). Very low mortality (3%) occurred (data not shown) although much higher internal Ag concentrations were measured in the snails at the end of the uptake phase, increasing in the order: 50 nm Ag NPs (111 µg Ag g^{-1} dw), 60 nm Ag NPs (133 µg Ag g^{-1} dw), $AgNO_3$ (135 µg Ag g^{-1} dw), Ag_2S NPs (153 µg Ag g^{-1} dw) and 3-8 nm Ag NPs (176 µg Ag g^{-1} dw).

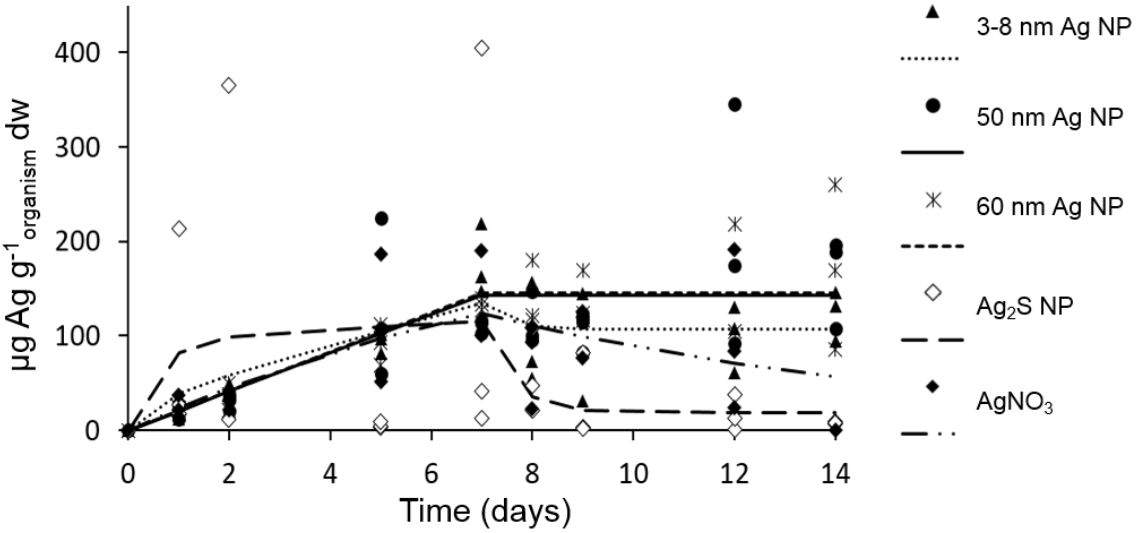

Figure 2.3. Uptake and elimination kinetics of 3-8 nm, 50 nm and 60 nm Ag NPs, Ag_2S NPs and $AgNO_3$ in the freshwater snail *Physa acuta* exposed for 7 days to sediment spiked at a nominal concentration of 10 mg Ag kg^{-1} and then transferred to clean sediment for 7 days, in the Ag-spiked sediment test. Lines represent the fit of a one-compartment model to the data, which represent Ag concentrations measured in individual snail soft bodies.

Uptake curves were similar between Ag forms except for Ag_2S NPs (Figure 2.3). The k1 value was highest for Ag_2S NPs (16.5 $g_{sediment}$ $g^{-1}_{organism}$ day^{-1}) followed by 3-8 nm Ag NPs (7.24 $g_{sediment}$ $g^{-1}_{organism}$ day^{-1}) (Table 2.3). Values of k2 were also higher for Ag_2S NPs and especially for 3-8 nm Ag NPs. Although 3-8 nm Ag NPs presented a SF of 0.22 and the elimination curve remained relatively constant, this k2 value may be explained by the decrease in Ag body mean concentrations at the first day of elimination (95.1 µg Ag g^{-1} dw) and consequently forming the slope in the curve during the beginning of the elimination phase.

Table 2.3. Measured concentrations (mg Ag kg^{-1}) given as mean and standard deviation (mean ± SD; *n*=3) and toxicokinetic parameters for 3-8 nm, 50 nm and 60 nm Ag NPs, Ag_2S NPs and $AgNO_3$ in *Physa acuta* exposed to sediment spiked at a nominal concentration of 10 mg Ag kg^{-1}, in the Ag-spiked sediment test. k1 is the uptake rate constant, k2 the elimination rate constant, kg the growth rate constant and SF the stored fraction. 95% confidence intervals (CI) are given in brackets. Different letters within a column indicate statistically significant differences ($X^2_{(1)}$>3.84; p<0.05).

Exposure route	Ag form	Measured concentration (mg Ag kg^{-1})*	k1 ($g_{sediment}$ $g^{-1}_{organism}$ day^{-1})	k2 (day^{-1})	SF	kg (day^{-1})
Sediment	3-8 nm	9.83 ± 1.89	7.24 (-)	2.02 (-8.62-12.7) **A,B,C**	0.22 (-0.55-0.99)	-0.01
	50 nm	7.99 ± 0.94	2.56 (n.d.)	0.01 (n.d.)	1 (n.d.)	-0.01
	60 nm	10.2 ± 1.63	2.03 (1.38-2.68) **A**	0.001 (n.d.)	1 (-)	0
	Ag_2S NPs	10.2 ± 0.82	16.5 (-)	1.71 (-4.89-8.31) **B**	0.02 (-0.05-0.08)	-0.01
	$AgNO_3$	8.58 ± 0.71	2.98 (-0.18-6.13) **A**	0.14 (-0.82-1.09) **C**	0 (-4.56-4.56)	-0.02

(-) very wide 95% confidence intervals.
(n.d.) not possible to determine 95% confidence intervals.
* mean concentrations measured at days 0, 3 and 7 for each treatment, used as exposure concentrations for the kinetic model.

SF was 1 for 50 nm and 60 nm Ag NPs and SF=0 for $AgNO_3$, while Ag_2S NPs had a SF of almost 0. No statistically significant differences ($X^2_{(1)}$<3.84; p>0.05) were found between k1 values which can be due to very wide 95% CI. k2 values differed significantly ($X^2_{(1)}$>3.84; p<0.05) between Ag_2S NPs and $AgNO_3$ (Table 2.3).

2.4.5. Ag concentrations in shells

Total Ag concentrations in the shells were much lower than in the soft body samples, at around 25% or less of the concentration measured in the soft body fractions on the last day of the uptake phase (Table 2.4). In general, shells of snails exposed to Ag-spiked water and clean sediment had lower concentrations that remained relatively constant during the experiment (Figure S2.4). Higher shell Ag concentrations were obtained for snails exposed to Ag-spiked sediment, especially those exposed to 60 nm Ag NPs, which may be related to the much higher exposure concentrations (Table 2.4, Figure S2.4). In general, Ag concentrations in shells did not tend to increase or decrease in any phase of the three experiments and varied throughout the test period for some exposures (Figure S2.4).

Table 2.4. Ag concentrations (µg Ag g^{-1} dw) (mean ± SD) and Ag % in shells at the end of the uptake phase (day 7) and at the end of the elimination phase (day 14), in *Physa acuta* exposed to 3-8 nm, 50 nm and 60 nm Ag NPs, Ag_2S NPs and $AgNO_3$ in all tests. Ag % in shells are given in relation to the Ag concentration measured in soft bodies at days 7 and 14.

Ag form	Ag-spiked water test				Ag-spiked water and clean sediment test				Ag-spiked sediment test			
	Day 7	Day 14	Ag % at day 7	Ag % at day 14	Day 7	Day 14	Ag % at day 7	Ag % at day 14	Day 7	Day 14	Ag % at day 7	Ag % at day 14
3-8 nm	1.4 ± 0.7	1.6 ± 0.1	12	5.4	4 ± 3.6	5.2 ± 2.9	25.5	28.5	14.5 ± 5.8	7.1 ± 3	8.2	5.7
50 nm	2.5 ± 1.1	6.3 ± 2.2	12.9	51.2	1 ± 1.6	1 ± 0.5	10.8	9.4	7.3 ± 4.3	2.7 ± 0.7	6.6	1.6
60 nm	3.3 ± 1.6	1.8 ± 2	4.7	7.7	3.9 ± 3.9	1.8 ± 1.6	12.5	4	17.6 ± 3.7	18.5 ± 4.2	13.2	10.8
Ag_2S NPs	1.3 ± 0.3	7.8 ± 2.8	17.2	153	0.1 ± 0.1	0.4 ± 0.7	2.5	23.3	9.5 ± 11.7	3.9 ± 3	6.2	47.9
$AgNO_3$	6.1 ± 4.4	3.5 ± 0.8	7.5	3.7	1.7 ± 2	1.7 ± 0.9	3.2	3.8	18.5 ± 3.7	10.4 ± 0.3	13.7	2852

The three experiments revealed for some exposures an increase of Ag % in the shell compared to the Ag concentration measured in the soft body at day 14 (Table 2.4). Snails exposed to Ag_2S NPs in the Ag-spiked water and Ag-spiked water and clean sediment tests had increased Ag % in shells at day 14, due to the increase of Ag concentrations in the shell and the decrease in the soft body due to elimination. For $AgNO_3$ in the Ag-spiked sediment test, Ag concentrations in the shell were 2852% at day 14 (Table 2.4), but this is related to the fact that only one replicate (soft body) was available with a very low Ag concentration (0.37 µg Ag g^{-1} dw).

2.5. Discussion

2.5.1. Nanoparticle stability

Data on NP stability revealed dissolved material of approximately 29% for 60 nm Ag NPs in UPW for all timepoints (Table S2.1), which could suggest the presence of some free ionic Ag in the received solutions as a result of dissolution during storage (Izak-Nau et al., 2015). However, in APW a lower dissolution of the 60 nm Ag NPs was observed when compared to the 3-8 nm and 50 nm Ag NPs (Figure S2.2 and Table S2.2). This could mean either higher NP stability or faster precipitation of other larger Ag particles due to Ostwald ripening or formation of other Ag phases (e.g., AgCl, Ag_2S) in APW (Wan et al., 2018; Wimmer et al., 2018). This is further supported by the observed decrease in dissolution of the 60 nm Ag NPs in APW (Table S2.2). On the other hand, the 3-8 nm and 50 nm Ag NPs presented in both cases (UPW and APW) a gradual increase in dissolution over time. While in UPW the behaviour between the two was similar, in APW faster dissolution was observed for the 3-8 nm Ag NPs than for the 50 nm Ag NPs. This is probably due to the free ions present in the APW and their interaction with the surface of these NPs. Alkane coated 3-8 nm Ag NPs are least reactive in APW since alkane (paraffin), as a saturated hydrocarbon, is less susceptible to van der Waals forces (Drummond et al., 1996) compared to the negatively charged citrate used in 50 nm Ag NPs. The effects of the different medium were apparent in the Z-potential changes for all Ag NPs, as the presence of free ions in the APW solutions affected the Stern layer of ions formed around the NPs, regulating the observed Z-potentials (Lowry et al., 2016). In fact, this was also apparent in the changes in hydrodynamic sizes, which (compared to UPW) increased for 3-8 nm and 50 nm Ag NPs while their Z-potentials decreased thus reducing the ability of the NPs to repel each other. The opposite was observed for the 60 nm Ag NPs, i.e. decreased hydrodynamic size and increased Z-potential. The effect of the ionic strength of APW was visible in the Z-potential

changes of the Ag_2S NPs, the stability of which was apparent through the low dissolution rates in both UPW and APW.

2.5.2. Dissolved Ag concentrations

No dissolved Ag was detected in the water at day 0 in any of the Ag-spiked water and clean sediment test, although detection was possible for Ag-spiked water test samples (Tables S2.3 and S2.5). Some explanations could be: 1) an analytical error at day 0; 2) perhaps the different water spiking methods applied may have influenced the results; 3) the presence of sediment may have accelerated complexation; 4) formation of AgCl precipitates during sample digestion. Nevertheless, dissolved Ag concentrations measured in both Ag-spiked water and Ag-spiked water and clean sediment tests may have been underestimated. Some Ag loss may have occurred, by adsorption to the container walls, especially in the case of glass containers such as those used in the Ag-spiked water and clean sediment test (Sekine et al., 2015). Additionally, complexation of Ag^+ with Cl^- may have promoted faster sedimentation and decreasing Ag concentrations in the water column (Gonçalves et al., 2017). In addition, chloride can form a $AgCl_{(s)}^0$ shell on NP surfaces reducing or even inhibiting dissolution (Radwan et al., 2019).

Ag NPs with similar nominal sizes were tested however, differences in their behaviour and consequent bioavailability were observed. The PVP-coated 60 nm Ag NPs presented higher concentrations of dissolved Ag in both experiments than the citrate-coated 50 nm Ag NPs, hence, these differences may be attributed to the coating type. However, sterically stabilized PVP-coated Ag NPs are considered to be more stable than charge stabilized citrate-coated Ag NPs. The PVP polymer is strongly bound to the NP surface while citrate stabilizes by electrostatic repulsion and is weakly bound to the NP surface. Studies have reported lower dissolution of citrate-coated Ag NPs than PVP-coated Ag NPs in UPW (Kittler et al., 2010) and lake/river waters (Dobias and Bernier-Latmani 2013), probably because citrate may reduce the oxide layer at the surface to zero-valent Ag, decreasing ion release. However, other studies have also determined higher dissolution of citrate-coated Ag NPs than PVP-coated Ag NPs in *Daphnia* test medium (Hou et al., 2017) and in freshwater and seawater (Angel et al., 2013).

As mentioned above, results on NP stability showed a gradual increase in dissolution of the 50 nm Ag NPs in APW (Table S2.2) but very low dissolved Ag concentrations were detected in water samples from Ag-spiked water and Ag-spiked water and clean sediment tests (Tables S2.3 and S2.5). It can be hypothesized that fast complexation of the available Ag ions may have occurred in APW leading to a faster precipitation, explaining the lower

dissolved Ag concentrations measured. On the other hand, 60 nm Ag NPs revealed very low % dissolution in APW samples from the NP dissolution tests (Table S2.2), which is the opposite of what was observed in water samples from the Ag-spiked water and Ag-spiked water and clean sediment tests (Tables S2.3 and S2.5). Nonetheless, it should be kept in mind that the exposure concentration was much lower (10 µg Ag L^{-1}) than the concentration used in the NP dissolution tests (1 mg Ag L^{-1}) and thus the behaviour could have been different (Croteau et al., 2014). It is possible that at the snail's exposure Ag concentration, the 60 nm Ag NPs may have had the highest dispersion stability in APW, thus being more susceptible to dissolution (Stoiber et al., 2015). Comparable low dissolved Ag concentrations were also measured in water samples spiked with similar concentrations of the same 3-8 nm Ag NPs as used in this study (Gonçalves et al*.,* 2017). As expected, very low dissolution was measured for Ag_2S NPs in both spiking and dissolution tests (Tables S2.3 and S2.5).

2.5.3. Ag-spiked water test

Similarities between internal Ag concentrations in the snails, uptake curves and k1 values of 60 nm Ag NPs and $AgNO_3$ suggest that uptake was mainly from dissolved Ag (Figure 2.1, Table 2.1). The higher dissolved Ag concentrations determined for these exposures confirmed that snails were more exposed to dissolved Ag with the 60 nm Ag NPs than with other nanoforms (Table S2.3). However, differences in elimination kinetics suggest that uptake of NPs also occurred upon exposure to 60 nm Ag NPs and thus the snails dealt in a different way with particulate and dissolved Ag. Probably, dissolved Ag was not eliminated from the body at least during the 7-day elimination period (explaining the k2 close to zero and SF of 1 for $AgNO_3$ exposure) and the gradual elimination observed in snails exposed to 60 nm Ag NPs was presumably of the nanoparticulate form (Figure 2.1, Table 2.1). Other studies have also reported uptake of the nanoparticulate form, which in some cases was dominant when compared to dissolved Ag uptake. *Lymnaea stagnalis* exposed to waterborne Ag also revealed comparable uptake rate constants for $AgNO_3$ and humic acid-coated Ag NPs, which were clearly higher than for citrate-coated Ag NPs (Croteau et al., 2011). Elimination of Ag from $AgNO_3$ exposure was very slow while from NP exposures it was relatively fast, further suggesting that uptake of nanoparticulate Ag may also have occurred (Croteau et al*.,* 2011). Uptake of Ag from PVP Ag NPs in *L. stagnalis* was slower than for $AgNO_3$ when considering total Ag exposure concentrations, but higher when accounting only for ionic Ag concentrations (Stoiber et al., 2015). This “excess” uptake in Ag NP exposures was attributed to particulate Ag as the main uptake

driver, likely because NP concentrations exceeded dissolved Ag concentrations (Stoiber et al., 2015), which was also the case in the present work. When comparing the relative contribution of each Ag form, Croteau et al. (2014) predicted that around 80% of the bioaccumulation of citrate-coated Ag NPs by *L. stagnalis* was driven by uptake of particulate Ag, at concentrations close to those used in this work.

The lowest uptake rate and internal Ag concentrations were obtained for Ag_2S NPs, although it can also be related to the lower Ag concentration measured in the test medium (Figure 2.1, Table 2.1). Nevertheless, this Ag form presented one of the highest k1, very close to the k1 values of $AgNO_3$ and 60 nm Ag NPs and not differing significantly ($X^2_{(1)}<3.84$; $p>0.05$) (Table 2.1). Therefore, considering their very low dissolution (Table S2.3), Ag_2S NPs seemed available for uptake by the snails as particles. The 3-8 nm and 50 nm Ag NPs presented similar k1 values, uptake rate curves and also very low dissolution. However, 3-8 nm Ag NPs and $AgNO_3$ showed the same elimination patterns, k2 and SF values, which may suggest the uptake was from dissolved Ag in spite of the very low dissolution of these Ag NPs (Figure 2.1, Tables 2.1 and S2.3). Gonçalves et al. (2017) attributed the toxicity of 3-8 nm Ag NPs to *P. acuta* mainly to NP properties rather than to Ag^+. Uptake rates constants of Ag in the oligochaete *Tubifex tubifex* exposed to waterborne $AgNO_3$ were nearly 25-times higher than for Ag NPs (the same type as the 3-8 nm Ag NPs as used in the present work) and no significant loss was detected after 20 days depuration of either Ag form, as also observed in this work (Tangaa et al., 2018). Although cellular uptake and internalization pathways may differ between Ag^+ and Ag NPs, once within the cells these forms might experience the same processes, which can explain the similar elimination patterns observed for $AgNO_3$ and 3-8 nm Ag NPs in the present work (Cross 2017; Novo et al., 2015). For 50 and 60 nm Ag NPs and Ag_2S NP, SF was 0, which can indicate that snails handled Ag differently than in the other exposures (Table 2.1).

The uptake mechanism of Ag^+ is mainly via ion transport channels, such as the proton-coupled Na^+ channels, while for Ag NPs uptake might be via endocytosis (Ribeiro et al., 2017). Khan et al. (2015) demonstrated that uptake pathway is determinant of the intracellular fate and toxicity of the Ag NPs in the estuarine mudsnail *Peringia ulvae*. They combined these results with those of Khan et al. (2012), suggesting a "Trojan horse" elimination mechanism for Ag NPs, whereby a fast Ag efflux followed by a slow elimination were observed: Ag NPs internalized through a caveolae-mediated endocytosis pathway and micropinocytosis were not directed to lysosomes and could have been responsible for the fast efflux. Ag NPs taken up via clathrin-mediated endocytosis were directed towards lysosomal degradation, promoting ion release. The intracellular released Ag^+, jointly with

Ag^+ uptake from Ag NP dissolution in the medium, could have been eliminated slowly from the snails (Khan et al., 2015). These processes are dependent on the NP properties, such as size (50 nm seemed optimal for NP uptake via clathrin-mediated processes (Cross et al., 2019) and 50-100 nm for caveolae-mediated pathways) and charge, since positively charged NPs are preferentially internalized by clathrin-mediated endocytosis (Dai et al., 2013), and their interactions with the media (Khan et al., 2015). Considering this, it is fair to suggest that multiple possible uptake pathways for Ag NPs along with the intrinsic and extrinsic NP properties and interactions with the test medium may have contributed to the differences in uptake and elimination kinetics observed in the present study.

Interestingly, in this test, Ag_2S NPs presented higher k1 values, similar to 60 nm Ag NPs and $AgNO_3$, (Table 2.1) but similar uptake rates with 3-8 nm and 50 nm Ag NPs (Figure 2.1) which could be related with the lower total Ag concentration of Ag_2S NPs in the medium, as mentioned above. Additionally, different sizes of NP agglomerates could have contributed to differences in their uptake by the snails. However, Ag_2S NPs also showed higher k2 values than the other pristine Ag NPs (Table 2.1). One hypothesis is dissolution. Even though the low dissolution observed for 3-8 nm and 50 nm Ag NPs, some ionic Ag seemed to be taken up, which could have led to higher internalization, explaining the lower elimination compared to Ag_2S NPs. Furthermore, the NPs/agglomerates taken up by the snails could have determined their size- and charge-dependent internalization pathways (e.g., clathrin- or caveolae-mediated endocytosis) and consequently their elimination. It can be further hypothesized that intracellular dissolution of NPs occurred leading to additional Ag^+ that was slowly eliminated, and that dissolution only occurred or was higher for pristine NPs than for Ag_2S NPs. Nevertheless, the lack of information on these factors (e.g., complete characterization of the NPs in the test medium at the concentration used, internal distribution of Ag) limited deeper analyses.

2.5.4. Ag-spiked water and clean sediment test

Higher Ag body concentrations and higher uptake rates were observed in snails exposed to 60 nm Ag NPs and $AgNO_3$, which can be related once again with the higher dissolution of the 60 nm Ag NPs (Figure 2.2, Tables 2.2 and S2.5). The high uptake rate obtained for Ag_2S NPs may be explained by the rapid uptake in the first day, indicating that these NPs were easily available. After day 2, the uptake curve declined following the body concentration pattern. This can be due to the higher k2 values observed for this Ag form, indicating that probably elimination overcame uptake after day 2, and therefore this Ag form was easily eliminated from the body (Figure 2.2, Table 2.2). Moreover, since water revealed

much higher contribution to Ag uptake, the decrease in water Ag concentrations observed at day 3 may have resulted in lower uptake of Ag_2S NPs by the snails (Table S2.4). Body Ag concentrations from exposures to 60 nm Ag NPs and $AgNO_3$ were in general lower in this experiment when compared with the Ag-spiked water test, which can be related with the lower dissolution of these Ag forms in this test, possibly as a result of heteroaggregation with sediment particles (Table S2.5). Furthermore, the medium was not renewed in this experiment, unlike in the Ag-spiked water test. Ag NPs are likely to agglomerate and deposit into sediments, which combined with the low dissolution indicates that Ag was likely associated with sediment but probably still available to the snails. Citrate-coated 50 nm Ag NPs are expected to rapidly agglomerate and to sedimentate (Ellis et al., 2016, 2018). The very low dissolution may have led to lower body concentrations in the snails at least during the first 2 days for the 50 nm and 3-8 nm Ag NPs. The decrease in Ag concentrations in water and increase in sediments suggests that Ag was settling into the sediment phase in the present test (Table S2.4). The movement of snails on the sediment surface may have promoted exchange of Ag to the water at the interface with the sediment, facilitating uptake by water ingestion or by direct contact with the skin and adsorption to the foot. Still, some accidental ingestion of sediment particles cannot be ruled out as having some contribution, albeit minor, for Ag uptake. In contrast to what was observed in the Ag-spiked water test, snails exposed to 60 nm Ag NPs were not able to eliminate Ag, at least during the 7-day elimination period, while snails exposed to 50 nm Ag NP and $AgNO_3$ revealed higher Ag elimination (Figure 2.2, Table 2.2). Using the double exposure model (model 2) could bring a more realistic approach to the exposure scenario, considering that in the environment NPs may deposit from the water column to the sediment and benthic organisms can simultaneously be exposed to both exposure routes (Cross et al., 2015). However, the lack of 95% CI for all kw and ks values may raise uncertainties about this model (Table 2.2). Looking at the results from single exposures, some differences are observed between the kinetic curves. There is a clear difference in the uptake curves obtained for Ag_2S NPs when modelling sediment as single exposure route (model 4) (Figure S2.3). There is a relatively fast increase of Ag body concentrations during day 1 and then a gradual increase until day 7, followed by a sharp decrease on the first day of the elimination phase. This sharp decrease was also observed in snails exposed to $AgNO_3$, showing a fast decline of their body concentrations during the first day and stabilising from day 9 onwards (Figure S2.3). *Lumbriculus variegatus* exposed to $AgNO_3$ also demonstrated a biphasic elimination, with rapid loss of the majority of Ag during the first 6 h of depuration, followed by very slow elimination over 6 days (Cross 2017). Elimination may have been more efficient with

ingestion of clean sediment by *L. variegatus* during the depuration phase, since clean sediment passing through the gut may assist in the removal of Ag (Cross 2017). Therefore, if any ingestion of sediment by snails occurred in the present work, the fast drop can be a result of an efflux of Ag associated with sediment particles and the "stable" phase may be Ag^+ that is not eliminated, probably mostly taken up as dissolved Ag not associated with sediment particles. Background concentrations in sediments were probably maintained during the depuration phase, so it should not be disregarded as having some influence on elimination. However, considering the remarkably high k1 values from sediment, especially when compared with the Ag-spiked sediment test, it can be considered that Ag concentrations in the sediment of the present test were too low to explain Ag uptake by snails (Tables 2.2 and 2.3).

The estuarine polychaete *Nereis diversicolor* revealed Ag uptake by the gut epithelium after ingestion of sediments spiked with citrate-capped Ag NPs and $AgNO_3$ (García-Alonso et al., 2011). In this organism, the Ag accumulation process from Ag NPs was mainly associated with organelles, inorganic granules and heat denatured proteins, and accumulation of dissolved Ag was predominantly in the metallothionein fraction (García-Alonso et al., 2011). Metallothioneins (MTs) are metal binding proteins playing an important role in the detoxification and storage of metals present in many species (Amiard et al., 2006), including freshwater snails (Gnatyshyna et al., 2011). Moreover, the sequestration of Ag^+ by MTs has been previously demonstrated (Amiard et al., 2006; Kuehr et al., 2021; Wang and Rainbow, 2010). The much higher BCF in the freshwater amphipod *Hyalella azteca* exposed to $AgNO_3$, and the delayed/incomplete Ag elimination observed in $AgNO_3$ and Ag NP exposures was explained by Ag^+ association with metal-binding proteins, such as MTs (Kuehr et al., 2021). It is possible that Ag^+ accumulation in *P. acuta* could be associated with MTs, leading to a slower elimination of this form. Therefore, it can also be hypothesised that the slow elimination observed for some Ag NPs could be of ionic Ag (from NP dissolution in exposure medium or intracellular dissolution) sequestered by MTs, while particulate Ag forms were eliminated faster. This highlights the role of ions, possibly contributing to higher Ag accumulation in nanoparticulate exposures. Moreover, the fast elimination observed in snails from Ag_2S NP exposures suggests that the nanoparticulate form is probably not internalized in tissues and rapidly eliminated. The possible low gut residence time could have limited internalization into the gut epithelium. However, comparing elimination rates between Ag NP and $AgNO_3$ exposures of the present study showed that, in some cases, the elimination of Ag from the snails in nanoparticulate exposures was slower than for $AgNO_3$ (e.g., 3-8 nm and 60 nm Ag NPs). This could be an

indication of potential slow elimination of Ag NPs. For instance, NPs could be taken up via clathrin-mediated endocytosis and directed towards lysosomal degradation, slowing down their elimination, as seen for the mudsnail *P. ulvae* (Khan et al., 2015). In turn, lysosomal degradation can lead to ion release and possibly to further Ag^+ association with MTs.

Tangaa et al. (2018), determining the relative importance of Ag uptake via water and sediment to *T. tubifex,* showed that sediment was the most relevant exposure route for both Ag NPs and $AgNO_3$, based on the $k_d = 10^5$ (sediment:water distribution coefficient) for Ag in freshwater ecosystems. The present study revealed that water contributed almost to 100% of Ag uptake in *P. acuta* for all Ag forms. Looking at the similarities of the uptake patterns between Ag-spiked water and Ag-spiked water and clean sediment tests, it may be assumed that the water determined uptake, although at a certain point Ag is expected to be predominantly in the sediment.

2.5.5. Ag-spiked sediment test

Sediment Ag concentrations were relatively constant throughout the experiment (Table S2.6). Although the overlying water was not analysed, the Ag concentration available for uptake in water was assumed to be negligible when compared to the sediment. Ramskov et al. (2015a) detected >98% of Ag in the sediment phase from citrate-coated Ag NP and $AgNO_3$ treatments, and levels were mostly below the detection limit in the water. Bao et al. (2018) detected <0.6% of Ag (by mass) lost from the sediment to the overlaying water. Although not analysed in this work, Ag NP behaviour and speciation may undergo alterations after sediment spiking. The 3-8 nm Ag NPs showed an opposite trend to the water-exposure tests, presenting higher k1 and k2 values. In the Ag-spiked sediment test, $AgNO_3$ and 50 nm and 60 nm Ag NPs had similar uptake curves and k1 values. The 50 nm and 60 nm Ag NPs also presented similar elimination rates, k2 and SF (Figure 2.3, Table 2.3). This suggests that dissolution of $AgNO_3$ or Ag NPs in the sediment-spiked test may have had less influence than in the water-spiked tests, thus Ag uptake could have been mainly associated with ingestion of sediment particles, or transdermal uptake during the movement of snails on the sediment surface. Thus, it seems that the behaviour (e.g., dissolution, agglomeration) of the pristine Ag NPs and $AgNO_3$ changed in spiked sediment when compared with the water exposures, indicating that sediment had a large influence. In addition, the very different concentration range should also be considered. On the last day of the uptake phase, internal Ag concentrations in snails exposed to Ag_2S NPs in sediment were 50 times higher when compared with those in snails exposed to the Ag-spiked water and clean sediment test, while for 3-8 nm and 50 nm Ag NPs internal

concentrations were around 11 to 12 times higher, respectively, and for 60 nm Ag NPs and $AgNO_3$ 2.5 to 4 times higher, respectively (data not shown). Therefore, despite the higher body Ag concentrations determined in this experiment, much higher body Ag concentrations would be expected considering the 1000 times higher sediment concentrations than those measured in the tests with Ag-spiked water and clean sediment (Tables S2.4 and S2.6). This suggests that ingestion of sediment had low contribution for Ag uptake in the Ag-spiked sediment test. Bioavailability of Ag^+ is expected to decrease in sediment due to complexation with inorganic ligands such as chlorides and sulfides, which can also modify Ag NP speciation and dissolution (Bao et al., 2018; Lowry et al., 2012). Instead, it is likely that Ag NP dissolution products may persist as complexes and soluble species (Cross 2017). Since the sediment was burnt in the present experiment prior to the exposure, sorption of Ag to organic matter was not possible, leading to higher bioavailability than would be typical in the environment. This may have facilitated exchange of Ag to water/pore water, mainly at the sediment-water interface, contributing to uptake through the dermis or water ingestion, which could have been higher for Ag_2S NPs due to their higher stability. This may explain the difference between Ag uptake from the Ag_2S NPs compared to the other Ag forms. In the present test, the analogous uptake rates observed for pristine Ag NPs and $AgNO_3$ may imply similar Ag bioavailability. Similar bioavailability for both aqueous and particulate Cu to *Potamopyrgus antipodarum* in sediments has also been reported (Ramskov et al., 2015b). Despite the comparable bioavailabilities, the dissimilarities observed in elimination rate constants between treatments suggest that different Ag forms were taken up and processed differently by snails. Notably, pristine Ag NPs in this study showed steady elimination, whilst the $AgNO_3$ elimination rate decreased considerably (Figure 2.3). The differences in uptake and elimination of $AgNO_3$ in snails exposed to the spiked sediment compared with the water exposures suggests that some ingestion of sediment particles possibly occurred in the Ag-spiked sediment test, and that Ag from the $AgNO_3$ exposure could have been eliminated faster associated with sediment particles. Elimination of 3-8 nm Ag NPs had a fast decline on the first day of elimination and remained constant thereafter (Figure 2.3). In Khan et al. (2012), when accounting for a two-component efflux rate in *P. ulvae* exposed to Ag NPs, fast loss was higher and probably shorter for Ag NPs than for $AgNO_3$, but the slow efflux was almost identical for both Ag forms. The authors suggested that for snails exposed to Ag NPs, fast elimination corresponds to the particulate form and slower loss to dissolved Ag from Ag NP dissolution *in vivo*, supporting the "Trojan Horse" concept (Khan et al., 2012).

Citrate- and PEG-coated Ag NPs and $AgNO_3$ experienced similar dissolution in sediments spiked at a nominal concentration of 2.5 mg kg^{-1} (Cross 2017). Transdermal uptake of dissolution products in sediment pore water was found to be predominantly responsible for Ag accumulation in the oligochaete *L. variegatus* exposed to citrate-coated Ag NPs and $AgNO_3$. However, in another experiment, PVP-coated Ag NPs and Ag_2S NPs at a nominal concentration of 2.5 mg kg^{-1} did not dissolve within sediments and no Ag was accumulated by *L. variegatus*, while the opposite was found upon $AgNO_3$ exposure (Cross 2017). Other studies reported higher Ag accumulation in benthic organisms exposed to the ionic counterpart than to the particulate form in sediments (Bao et al., 2018; Dai et al., 2013). Ramskov et al. (2015a) however, reported higher Ag accumulation in *P. antipodarum* clone A only from $AgNO_3$ exposures and significantly higher particulate Ag accumulation in *P. antipodarum* clone B from citrate-coated Ag NP exposures. Others reported higher accumulation of NPs that the ionic counterpart (Pang et al., 2012). Pang et al. (2012) further indicated that particle selection by deposit feeders may determine NP bioavailability. Freshwater pulmonated snails exhibit structures and particle-related processes in the gut that can act as barriers to NPs, such as sorting mechanisms in their digestive tract (Pang et al., 2013). Briefly, ingested particles are ground and sorted in the gizzard. Particle-size selection occurs in the ciliated passages system of the pylorus, where only particles ≤ 4 µm pass into the digestive gland for extracellular/intracellular digestion, and larger particles pass into the intestine for excretion (Dillon 2000; Pang et al., 2012, 2013; van der Zande et al., 2020). In the present experiment, there was no indication of size-dependent uptake, however, looking at the elimination kinetics it is possible that some particle/form selection may have occurred in the snails. In addition, cuticle (gastric shield) and mucus secreting cells in the stomach (and associated glycoproteins) also act as barriers to NP translocation across the epithelium in snails (van der Zande et al., 2020). The high internal Ag concentrations determined for *P. acuta* and the very low mortality observed reflect the high tolerance to metals of these organisms. Detoxification strategies such MTs, phytochelatins, or storing metals in insoluble granules to prevent biochemical reactions are also part of the barrier that freshwater snails, among other invertebrates, developed to deal with high metal accumulation (Gonçalves et al., 2016; van der Zande et al., 2020). The digestive gland of gastropod molluscs is the main location of accumulation and biotransformation of xenobiotics (Desouky 2006). The digestive gland was the major target tissue for Ag accumulation in the freshwater snail *Bellamya aeruginosa* exposed to sediment-associated Ag nanoparticles (Bao et al., 2018). *P. acuta* is considered an invasive species that can survive in sewage treatment plants and drains, therefore, this species may likely have

developed strategies to cope with metal contaminated environments (Spyra et al., 2019). This high ability further suggests that although Ag^{+} and Ag NPs were probably bioavailable for uptake and internalization, they were sequestered and inactive thus no toxicity was observed in the Ag-spiked sediment test.

2.5.6. Ag concentrations in shells

At the last day of the uptake phase, Ag concentrations in shells were up to 25% of the amount measured in the soft bodies (Table 2.4). Spyra et al. (2019) detected less than 20% of the metals Cd, Cu and Pb concentrations in shells when compared to the soft body in *P. acuta*. In the present study, no clear tendency of Ag concentrations to increase or decrease was observed in shells during uptake or elimination phases (Table 2.4, Figure S2.4). Although the proportion of Ag in shells was higher in comparison to soft bodies at day 14 in some exposures, this can be due to higher Ag concentrations detected in shell samples of the elimination phase and/or to the decrease of concentrations in the respective soft bodies. As an example, Ag concentration in shells exposed to 60 nm Ag NPs in the Ag-spiked water test decreased from 3.3 to 1.8 µg Ag g^{-1} dw, while the proportion of Ag increased from 4.7 to 7.7% (Table 2.4). Soft body Ag concentrations decreased from 70.3 to 23.9 µg Ag g^{-1} dw at days 7 and 14, respectively (data not shown). It should not be disregarded, however, that dissecting the soft body and shell is prone to human error. Concentrations increased in shells of *Lymnaea peregra* exposed to Pb contaminated sediment but reduced loss occurred in clean medium for 28 days, suggesting that shells may act as a sink for Pb (Everard and Denny 1984). Ramskov et al. (2014) detected higher amounts of accumulated Cu in shells instead of soft body, in CuO NPs and $CuCl_2$ treatments. In another study, *P. antipodarum* snails revealed higher Cu concentrations in the shell after 2 weeks exposure to $CuCl_2$ and CuO NPs (6 nm) but, in contrast, during the elimination phase Cu concentrations were higher in soft body and reduced rapidly in the shells (Pang et al., 2013). It has been suggested that CuO NPs were loosely sorbed onto the shell and were subsequently lost due to snail movement in clean sediment (Ramskov et al., 2015b).

Everard and Denny (1984) suggested that since empty shells exposed to Pb did not absorb the metal, it can be assumed that metals are incorporated into the shells during their formation and cannot be eliminated. This means that Pb could be incorporated into the shell during growth and not be removed. Since in most cases snails decreased in weight (probably due to not being fed during the entire exposure period), it is unlikely that Ag incorporation into the shells of *P. acuta* occurred in our experiments. Differences in metal assimilation between soft body and shell were suggested to be related to different uptake

modes, as the soft body presents strategies such as formation of granules in different organs that can be excreted, while shells lack specific binding sites and may accumulate metal over time (Beeby and Richmond 1989).

Although the empty shells exposed by Everard and Denny (1984) did not absorb Pb, the high adsorption tendency of metals to mollusc shells is extensively studied and so is its use for biomonitoring and remediation of metal contaminated waters (Hossain and Aditya 2013; Pourang et al., 2019). Pb concentrations in shells of the terrestrial snail *Helix aspersa* fed on Pb-dosed diets decreased when concentrations in the soft body also fell, suggesting that shells could be storage sites for Pb when ingested levels are high, being part of the detoxification strategies of the snails (Beeby and Richmond 1989). Ag NPs (PAAm coated) and ionic Ag were transported at similar levels from soft body to the extrapallial fluid of the mussel *Mytilus edulis*. It is known that metals transported to the extrapallial fluid can be incorporated into the interior shell surface of the bivalves (Zuykov et al., 2011).

In the present work, no direct and clear correlation between Ag concentrations in these two fractions was observed, and there is no evidence to support the theory of Ag redistribution between soft body and shell (Table 2.4, Figure S2.4). Considering also the decrease in snail weight, it is more plausible that the Ag detected was, at least in its majority, adsorbed to shells from the contaminated medium.

2.6. Conclusions

In the present work, uptake and elimination kinetics of pristine and simulated aged Ag NPs and its ionic form were evaluated in the snail *P. acuta*, exposed through different routes. The results suggest that Ag NP characteristics largely influenced their bioavailability, leading to different uptake and elimination patterns in snails exposed to different Ag forms within the same exposure route. Snails from tests with Ag-spiked water with and without clean sediment had, in general, more similar uptake kinetics that differed from those of snails exposed to Ag-spiked sediment. This suggests that exposure route had a determining role in the bioavailability of the tested Ag forms. The different elimination kinetics of the same Ag forms in Ag-spiked water with and without clean sediment suggest possible interactions with sediment that changed the Ag form taken up by the snails. This emphasizes the need to properly evaluate NP form in the exposure medium as well as internally. The similar uptake curves observed for all Ag forms (except for Ag_2S NPs) in the Ag-spiked sediment indicate that sediment greatly influenced Ag behaviour and the form taken up by snails. When accounting for exposure via both water and sediment, water

contributed nearly 100% for the total uptake. Moreover, The Ag_2S NPs were not only highly available to snails but were also easily depurated.

The remarkably low elimination and high stored fraction observed in some exposures highlights the bioaccumulation ability of *P. acuta* and may raise concerns about possible adverse consequences in terms of chronic exposure and trophic transfer, especially in scenarios of continued Ag NP exposure. The shell fraction accumulated lower Ag amounts, which can contribute to transfer to predators that ingest the whole snail. This work highlights the need for additional examination of the overall exposure scenario, such as the factors controlling bioavailability, internalization, and elimination in different scenarios with full speciation analysis and mass-balance accounting. The results also contribute important hazard data for the environmental risk assessment of Ag NPs to benthic biota.

2.7. References

Amiard, J.C., Amiard-Triquet, C., Barka, S., Pellerin, J., Rainbow, P.S., 2006. Metallothioneins in aquatic invertebrates: Their role in metal detoxification and their use as biomarkers. Aquat. Toxicol. 76, 160–202.

Angel, B.M., Batley, G.E., Jarolimek, C. V., Rogers, N.J., 2013. The impact of size on the fate and toxicity of nanoparticulate silver in aquatic systems. Chemosphere 93, 359–365.

Avramescu, M.L., Rasmussen, P.E., Chénier, M., Gardner, H.D., 2017. Influence of pH, particle size and crystal form on dissolution behaviour of engineered nanomaterials. Environ. Sci. Pollut. Res. 24, 1553–1564.

Azimzada, A., Tufenkji, N., Wilkinson, K.J., 2017. Transformations of silver nanoparticles in wastewater effluents: links to Ag bioavailability. Environ. Sci. Nano 4, 1339–1349.

Baccaro, M., Undas, A.K., De Vriendt, J., Van Den Berg, J.H.J., Peters, R.J.B., van den Brink, N.W., 2018. Ageing, dissolution and biogenic formation of nanoparticles: How do these factors affect the uptake kinetics of silver nanoparticles in earthworms? Environ. Sci. Nano 5, 1107–1116.

Bao, S., Huang, J., Liu, X., Tang, W., Fang, T., 2018. Tissue distribution of Ag and oxidative stress responses in the freshwater snail *Bellamya aeruginosa* exposed to sediment-associated Ag nanoparticles. Sci. Total Environ. 644, 736–746.

Beeby, A., Richmond, L., 1989. The Shell as a Site of Lead Deposition in *Helix aspersa*. Arch. Environ. Contam. Toxicol. 18, 623–628.

Bernot, R.J., Brandenburg, M., 2013. Freshwater snail vital rates affected by non-lethal concentrations of silver nanoparticles. Hydrobiologia 714, 25–34.

Clark, N.J., Boyle, D., Eynon, B.P., Handy, R.D., 2019. Dietary exposure to silver nitrate compared to two forms of silver nanoparticles in rainbow trout: Bioaccumulation potential with minimal physiological effects. Environ. Sci. Nano 6, 1393–1405.

Cornelis, G., Kirby, J.K., Beak, D., Chittleborough, D., McLaughlin, M.J., 2010. A method

for determination of retention of silver and cerium oxide manufactured nanoparticles in soils. Environ. Chem. 7, 298–308.

Cross, R.K., 2017. The fate of engineered nanomaterials in sediments and their route to bioaccumulation. PhD Thesis, University of Exeter. 210 p.

Cross, R.K., Tyler, C.R., Galloway, T.S., 2019. The fate of cerium oxide nanoparticles in sediments and their routes of uptake in a freshwater worm. Nanotoxicology 13, 894–908.

Cross, R.K., Tyler, C.R., Galloway, T.S., 2015. Transformations that affect fate, form and bioavailability of inorganic nanoparticles in aquatic sediments. Environ. Chem. 12, 627–642.

Croteau, M.N., Dybowska, A.D., Luoma, S.N., Misra, S.K., Valsami-Jones, E., 2014. Isotopically modified silver nanoparticles to assess nanosilver bioavailability and toxicity at environmentally relevant exposures. Environ. Chem. 11, 247–256.

Croteau, M.N., Misra, S.K., Luoma, S.N., Valsami-Jones, E., 2011. Silver bioaccumulation dynamics in a freshwater invertebrate after aqueous and dietary exposures to nanosized and ionic Ag. Environ. Sci. Technol. 45, 6600–6607.

Dai, L., Syberg, K., Banta, G.T., Selck, H., Forbes, V.E., 2013. Effects, Uptake, and Depuration Kinetics of Silver Oxide and Copper Nanoparticles in a Marine Deposit Feeder, *Macoma balthica*. ACS Sustain. Chem. Eng. 1, 760−767.

Desouky, M.M.A., 2006. Tissue distribution and subcellular localization of trace metals in the pond snail *Lymnaea stagnalis* with special reference to the role of lysosomal granules in metal sequestration. Aquat. Toxicol. 77, 143–152.

Dillon, R.T.J., 2000. The ecology of freshwater molluscs. Cambridge Univ. Press, 524 p.

Dobias, J., Bernier-Latmani, R., 2013. Silver release from silver nanoparticles in natural waters. Environ. Sci. Technol. 47, 4140–4146.

Dodd, M., Rasmussen, P.E., Chénier, M., 2013. Comparison of Two In Vitro Extraction Protocols for Assessing Metals' Bioaccessibility Using Dust and Soil Reference Materials. Hum. Ecol. Risk Assess. 19, 1014–1027.

Domercq, P., Praetorius, A., Boxall, A.B.A., 2018. Emission and fate modelling framework for engineered nanoparticles in urban aquatic systems at high spatial and temporal resolution. Environ. Sci. Nano 5, 533–543.

Drummond, C.J., Georgaklis, G., Chan, D.Y.C., 1996. Fluorocarbons: Surface free energies and van der Waals interaction. Langmuir 12, 2617–2621.

Ellis, L.J.A., Baalousha, M., Valsami-Jones, E., Lead, J.R., 2018. Seasonal variability of natural water chemistry affects the fate and behaviour of silver nanoparticles. Chemosphere 191, 616–625.

Ellis, L.J.A., Valsami-Jones, E., Lead, J.R., Baalousha, M., 2016. Impact of surface coating and environmental conditions on the fate and transport of silver nanoparticles in the aquatic environment. Sci. Total Environ. 568, 95–106.

European's Committee for Standardisation (CEN), 2019. CEN/TC 52. Safety of toys - Part 3: Migration of certain elements. guidance EN 71-3:2019.

Everard, M., Denny, P., 1984. The transfer of lead by freshwater snails in Ullswater,

Cumbria. Environ. Pollution. Ser. A, Ecol. Biol. 35, 299–314.

García-Alonso, J., Khan, F.R., Misra, S.K., Turmaine, M., Smith, B.D., Rainbow, P.S., Luoma, S.N., Valsami-Jones, E., 2011. Cellular Internalization of Silver Nanoparticles in Gut Epithelia of the Estuarine Polychaete *Nereis diversicolor*. Environ. Sci. Technol. 45, 4630–4636.

Gnatyshyna, L.L., Fal'fushynska, G.I., Golubev, O.P., Dallinger, R., Stoliar, O.B., 2011. Role of metallothioneins in adaptation of *Lymnaea stagnalis* (Mollusca: Pulmonata) to environment pollution. Hydrobiol. J. 47, 56–66.

Gonçalves, S.F., Pavlaki, M.D., Lopes, R., Hammes, J., Gallego-Urrea, J.A., Hassellöv, M., Jurkschat, K., Crossley, A., Loureiro, S., 2017. Effects of silver nanoparticles on the freshwater snail *Physa acuta*: The role of test media and snails' life cycle stage. Environ. Toxicol. Chem. 36, 243–253.

Gonçalves, S.F., Davies, S.K., Bennett, M., Raab, A., Feldmann, J., Kille, P., Loureiro, S., Spurgeon, D.J., Bundy, J.G., 2016. Sub-lethal cadmium exposure increases phytochelatin concentrations in the aquatic snail *Lymnaea stagnalis*. Sci. Total Environ. 568, 1054–1058.

Gottschalk, F., Sondere, T., Schols, R., Nowack, B., 2009. Modeled Environmental Concentrations of Engineered Nanomaterials (TiO_2, ZnO, Ag, CNT, Fullerenes) for for Different Regions. Environ. Sci. Technol. 43, 9216–9222.

Hossain, A., Aditya, G., 2013. Cadmium biosorption potential of shell dust of the fresh water invasive snail *Physa acuta*. J. Environ. Chem. Eng. 1, 574–580.

Hou, J., Zhou, Y., Wang, C., Li, S., Wang, X., 2017. Toxic Effects and Molecular Mechanism of Different Types of Silver Nanoparticles to the Aquatic Crustacean *Daphnia magna*. Environ. Sci. Technol. 51, 12868–12878.

Izak-Nau, E., Huk, A., Reidy, B., Uggerud, H., Vadset, M., Eiden, S., Voetz, M., Himly, M., Duschl, A., Dusinska, M., Lynch, I., 2015. Impact of storage conditions and storage time on silver nanoparticles' physicochemical properties and implications for their biological effects. RSC Adv. 5, 84172–84185.

Jeng, H.A., Swanson, J., 2006. Toxicity of metal oxide nanoparticles in mammalian cells. J. Environ. Sci. Heal. - Part A 41, 2699–2711.

Justice, J.R., Bernot, R.J., 2014. Nanosilver Inhibits Freshwater Gastropod (*Physa acuta*) Ability to Assess Predation Risk. Am. Midl. Nat. 171, 340–349.

Khan, F.R., Misra, S.K., Bury, N.R., Smith, B.D., Rainbow, P.S., Luoma, S.N., Valsami-Jones, E., 2015. Inhibition of potential uptake pathways for silver nanoparticles in the estuarine snail *Peringia ulvae*. Nanotoxicology 9, 493–501.

Khan, F.R., Misra, S.K., García-Alonso, J., Smith, B.D., Strekopytov, S., Rainbow, P.S., Luoma, S.N., Valsami-Jones, E., 2012. Bioaccumulation Dynamics and Modeling in an Estuarine Invertebrate Following Aqueous Exposure to Nanosized and Dissolved Silver. Environ. Sci. Technol. 46, 7621–7628.

Kittler, S., Greulich, C., Diendorf, J., Köller, M., Epple, M., 2010. Toxicity of silver nanoparticles increases during storage because of slow dissolution under release of silver ions. Chem. Mater. 22, 4548–4554.

Kuehr, S., Kaegi, R., Maletzki, D., Schlechtriem, C., 2021. Testing the bioaccumulation potential of manufactured nanomaterials in the freshwater amphipod *Hyalella azteca*.

Chemosphere 263, 127961.

Kuehr, S., Klehm, J., Stehr, C., Menzel, M., Schlechtriem, C., 2020. Unravelling the uptake pathway and accumulation of silver from manufactured silver nanoparticles in the freshwater amphipod *Hyalella azteca* using correlative microscopy. NanoImpact 19, 100239.

Kühr, S., Schneider, S., Meisterjahn, B., Schlich, K., Hund-Rinke, K., Schlechtriem, C., 2018. Silver nanoparticles in sewage treatment plant effluents: chronic effects and accumulation of silver in the freshwater amphipod *Hyalella azteca*. Environ. Sci. Eur. 30, 1–11.

Lead, J.R., Batley, G.E., Alvarez, P.J.J., Croteau, M.N., Handy, R.D., McLaughlin, M.J., Judy, J.D., Schirmer, K., 2018. Nanomaterials in the environment: Behavior, fate, bioavailability, and effects—An updated review. Environ. Toxicol. Chem. 37, 2029–2063.

Lee, S.W., Park, S.Y., Kim, Y., Im, H., Choi, J., 2016. Effect of sulfidation and dissolved organic matters on toxicity of silver nanoparticles in sediment dwelling organism, *Chironomus riparius*. Sci. Total Environ. 553, 565–573.

Li, L., Hartmann, G., Döblinger, M., Schuster, M., 2013. Quantification of nanoscale silver particles removal and release from municipal wastewater treatment plants in Germany. Environ. Sci. Technol. 47, 7317–7323.

Liu, S., Wang, C., Hou, J., Wang, P., Miao, L., Li, T., 2018. Effects of silver sulfide nanoparticles on the microbial community structure and biological activity of freshwater biofilms. Environ. Sci. Nano 5, 2899–2908.

Lowry, G. V., Hill, R.J., Harper, S., Rawle, A.F., Hendren, C.O., Klaessig, F., Nobbmann, U., Sayre, P., Rumble, J., 2016. Guidance to improve the scientific value of zeta-potential measurements in nanoEHS. Environ. Sci. Nano 3, 953–965.

Lowry, G. V, Espinasse, B.P., Badireddy, A.R., Richardson, C.J., Reinsch, B.C., Bryant, L.D., Bone, A.J., Deonarine, A., Chae, S., Therezien, M., Colman, B.P., Hsu-kim, H., Bernhardt, E.S., Matson, C.W., Wiesner, M.R., 2012. Long-Term Transformation and Fate of Manufactured Ag Nanoparticles in a Simulated Large Scale Freshwater Emergent Wetland. Environ. Sci. Technol. 46, 7027−7036.

Ma, T., Gong, S., Tian, B., 2017. Effects of sediment-associated CuO nanoparticles on Cu bioaccumulation and oxidative stress responses in freshwater snail *Bellamya aeruginosa*. Sci. Total Environ. 580, 797–804.

Naylor, C., Maltby, L., Calow, P., 1989. Scope for growth in *Gammarus pulex*, a freshwater benthic detritivore. Hydrobiologia 188/189, 517–523.

Novo, M., Lahive, E., Díez-Ortiz, M., Matzke, M., Morgan, A.J., Spurgeon, D.J., Svendsen, C., Kille, P., 2015. Different routes, same pathways: Molecular mechanisms under silver ion and nanoparticle exposures in the soil sentinel *Eisenia fetida*. Environ. Pollut. 205, 385–393.

OECD, 2017. Test No. 318: Dispersion Stability of Nanomaterials in Simulated Environmental Media. OECD Guideline for the Testing of Chemicals.

OECD, 2010. Test No. 233: Sediment-Water Chironomid Life-Cycle Toxicity Test Using Spiked Water or Spiked Sediment. OECD Guideline for the Testing of Chemicals.

OECD, 2004. Test No. 218: Sediment-Water Chironomid Toxicity Test Using Spiked

Sediment. OECD Guideline for the Testing of Chemicals.

OECD, 2015. Test No. 62: Series on the Safety of Manufactured Nanomaterials. Organisation for Economic Co-Operation and Development. Considerations for Using Dissolution As a Function of Surface Chemistry To Evaluate Environmental Behaviour of Nanomaterials in Risk Assessments. WPMN ENV/JM/MONO(2015)44.

OECD, 2016. Test No. 243: *Lymnaea stagnalis* Reproduction Test. OECD Guideline for the Testing of Chemicals.

Pang, C., Selck, H., Banta, G.T., Misra, S.K., Berhanu, D., Dybowska, A., Valsami-Jones, E., Forbes, V.E., 2013. Bioaccumulation, toxicokinetics, and effects of copper from sediment spiked with aqueous Cu, nano-CuO, or micro-CuO in the deposit-feeding snail, *Potamopyrgus antipodarum*. Environ. Toxicol. Chem. 32, 1561–1573.

Pang, C., Selck, H., Misra, S.K., Berhanu, D., Dybowska, A., Valsami-Jones, E., Forbes, V.E., 2012. Effects of sediment-associated copper to the deposit-feeding snail, *Potamopyrgus antipodarum*: A comparison of Cu added in aqueous form or as nano- and micro-CuO particles. Aquat. Toxicol. 106–107, 114–122.

Peters, R.J.B., van Bemmel, G., Milani, N.B.L., den Hertog, G.C.T., Undas, A.K., van der Lee, M., Bouwmeester, H., 2018. Detection of nanoparticles in Dutch surface waters. Sci. Total Environ. 621, 210–218.

Pourang, N., Bahrami, A., Nasrolahzadeh Saravi, H., 2019. Shells of *Bufonaria echinata* as biomonitoring materials of heavy metals (Cd, Ni and Pb) pollution in the Persian Gulf: With emphasis on the annual growth sections. Iran. J. Fish. Sci. 18, 256–271.

Radwan, I.M., Gitipour, A., Potter, P.M., Dionysiou, D.D., Al-Abed, S.R., 2019. Dissolution of silver nanoparticles in colloidal consumer products: effects of particle size and capping agent. J. Nanoparticle Res. 21: 155, 1–13.

Ramskov, T., Forbes, V.E., Gilliland, D., Selck, H., 2015a. Accumulation and effects of sediment-associated silver nanoparticles to sediment-dwelling invertebrates. Aquat. Toxicol. 166, 96–105.

Ramskov, T., Croteau, M.N., Forbes, V.E., Selck, H., 2015b. Biokinetics of different-shaped copper oxide nanoparticles in the freshwater gastropod, *Potamopyrgus antipodarum*. Aquat. Toxicol. 163, 71–80.

Ramskov, T., Selck, H., Banta, G., Misra, S.K., Berhanu, D., Valsami-Jones, E., Forbes, V.E., 2014. Bioaccumulation and effects of different-shaped copper oxide nanoparticles in the deposit-feeding snail *Potamopyrgus antipodarum*. Environ. Toxicol. Chem. 33, 1976–1987.

Rearick, D.C., Telgmann, L., Hintelmann, H., Frost, P.C., Xenopoulos, M.A., 2018. Spatial and temporal trends in the fate of silver nanoparticles in a whole-lake addition study. PLoS One 13, 1–18.

Ribeiro, F., Gallego-Urrea, J.A., Goodhead, R.M., van Gestel, C.A.M., Moger, J., Soares, A.M.V.M., Loureiro, S., 2015. Uptake and elimination kinetics of silver nanoparticles and silver nitrate by *Raphidocelis subcapitata*: The influence of silver behaviour in solution. Nanotoxicology 9, 686–695.

Ribeiro, F., Gallego-Urrea, J.A., Jurkschat, K., Crossley, A., Hassellöv, M., Taylor, C., Soares, A.M.V.M., Loureiro, S., 2014. Silver nanoparticles and silver nitrate induce high toxicity to *Pseudokirchneriella subcapitata*, *Daphnia magna* and *Danio rerio*. Sci.

Total Environ. 466–467, 232–241.

Ribeiro, F., van Gestel, C.A.M., Pavlaki, M.D., Azevedo, S., Soares, A.M.V.M., Loureiro, S., 2017. Bioaccumulation of silver in *Daphnia magna*: Waterborne and dietary exposure to nanoparticles and dissolved silver. Sci. Total Environ. 574, 1633–1639.

Schwirn, K., Voelker, D., Galert, W., Quik, J., Tietjen, L., 2020. Environmental Risk Assessment of Nanomaterials in the light of new obligations under the REACH regulation - Which challenges remain and how to approach them? Integr. Environ. Assess. Manag. 16, 706–717.

Sekine, R., Khurana, K., Vasilev, K., Lombi, E., Donner, E., 2015. Quantifying the adsorption of ionic silver and functionalized nanoparticles during ecotoxicity testing: Test container effects and recommendations. Nanotoxicology 9, 1005–1012.

Selck, H., Handy, R.D., Fernandes, T.F., Klaine, S.J., Petersen, E.J., 2016. Nanomaterials in the aquatic environment: A European Union-United States perspective on the status of ecotoxicity testing, research priorities, and challenges ahead. Environ. Toxicol. Chem. 35, 1055–1067.

Shafer, M.M., Overdier, J.T., Armstong, D.E., 1998. Removal, partitioning, and fate of silver and other metals in wastewater treatment plants and effluent-receiving streams. Environ. Toxicol. Chem. 17, 630–641.

Sharma, V.K., Sayes, C.M., Guo, B., Pillai, S., Parsons, J.G., Wang, C., Yan, B., Ma, X., 2019. Interactions between silver nanoparticles and other metal nanoparticles under environmentally relevant conditions: A review. Sci. Total Environ. 653, 1042–1051.

Spyra, A., Cieplok, A., Strzelec, M., Babczyńska, A., 2019. Freshwater alien species *Physella acuta* (Draparnaud, 1805) - A possible model for bioaccumulation of heavy metals. Ecotoxicol. Environ. Saf. 185, 109703.

Stoiber, T., Croteau, M.N., Romer, I., Tejamaya, M., Lead J.R., Luoma, S.N., 2015. Influence of hardness on the bioavailability of silver to a freshwater snail after waterborne exposure to silver nitrate and silver nanoparticles. Nanotoxicology 9, 918–927.

Sun, T.Y., Bornhöft, N.A., Hungerbühler, K., Nowack, B., 2016. Dynamic Probabilistic Modeling of Environmental Emissions of Engineered Nanomaterials. Environ. Sci. Technol. 50, 4701–4711.

Tangaa, S.R., Selck, H., Winther-Nielsen, M., Croteau, M.N., 2018. A biodynamic understanding of dietborne and waterborne Ag uptake from Ag NPs in the sediment-dwelling oligochaete, *Tubifex tubifex*. NanoImpact 11, 33–41.

Thalmann, B., Voegelin, A., Von Gunten, U., Behra, R., Morgenroth, E., Kaegi, R., 2015. Effect of Ozone Treatment on Nano-Sized Silver Sulfide in Wastewater Effluent. Environ. Sci. Technol. 49, 10911–10919.

Tourinho, P.S., van Gestel, C.A.M., Lofts, S., Soares, A.M.V.M., Loureiro, S., 2013. Influence of soil pH on the toxicity of zinc oxide nanoparticles to the terrestrial isopod *Porcellionides pruinosus*. Environ. Toxicol. Chem. 32, 2808–2815.

Tourinho, P.S., van Gestel, C.A.M., Morgan, A.J., Kille, P., Svendsen, C., Jurkschat, K., Mosselmans, J.F.W., Soares, A.M.V.M., Loureiro, S., 2016. Toxicokinetics of Ag in the terrestrial isopod *Porcellionides pruinosus* exposed to Ag NPs and $AgNO_3$ via soil and food. Ecotoxicology 25, 267–278.

van den Brink, N.W., Kokalj, A.J., Silva, P.V., Lahive, E., Norrfors, K., Baccaro, M., Khodaparast, Z., Loureiro, S., Drobne, D., Cornelis, G., Lofts, S., Handy, R.D., Svendsen, C., Spurgeon, D., van Gestel, C.A.M., 2019. Tools and rules for modelling uptake and bioaccumulation of nanomaterials in invertebrate organisms. Environ. Sci. Nano 6, 1985–2001.

van der Zande, M., Kokalj, A.J., Spurgeon, D., Loureiro, S., Silva, P. V., Khodaparast, Z., Drobne, D., Clark, N.J., van den Brink, N., Baccaro, M., van Gestel, C.A.M., Bouwmeester, H., Handy, R.D., 2020. The Gut Barrier and the Fate of Engineered Nanomaterials: A View from Comparative Physiology. Environ. Sci. Nano 7, 1874–1898.

Vogt, R., Mozhayeva, D., Steinhoff, B., Schardt, A., Spelz, B.T.F., Philippe, A., Kurtz, S., Schaumann, G.E., Engelhard, C., Schönherr, H., Lamatsch, D.K., Wanzenböck, J., 2019. Spatiotemporal distribution of silver and silver-containing nanoparticles in a prealpine lake in relation to the discharge from a wastewater treatment plant. Sci. Total Environ. 696, 134034.

Wan, M., Tao, J., Jia, D., Chu, X., Li, S., Ji, S., Ye, C., 2018. High-purity very thin silver nanowires obtained by Ostwald ripening-driven coarsening and sedimentation of nanoparticles. CrystEngComm 20, 2834–2840.

Wang, S., Lv, J., Ma, J., Zhang, S., 2016. Cellular Internalization and Intracellular Biotransformation of Silver Nanoparticles in *Chlamydomonas Reinhardtii*. Nanotoxicology 10, 1129–1135.

Wang, W.X., Rainbow, P.S., 2010. Significance of metallothioneins in metal accumulation kinetics in marine animals. Comp. Biochem. Physiol. - Part C, 152, 1–8.

Wimmer, A., Kalinnik, A., Schuster, M., 2018. New insights into the formation of silver-based nanoparticles under natural and semi-natural conditions. Water Res. 141, 227–234.

Zeyons, O., Thill, A., Chauvat, F., Menguy, N., Cassier-Chauvat, C., Oréar, C., Daraspe, J., Auffan, M., Rose, J., Spalla, O., 2009. Direct and indirect CeO_2 nanoparticles toxicity for *Escherichia col*i and *Synechocystis*. Nanotoxicology 3, 284–295.

Zhang, W., Ke, S., Sun, C., Xu, X., Chen, J., Yao, L., 2019. Fate and toxicity of silver nanoparticles in freshwater from laboratory to realistic environments: a review. Environ. Sci. Pollut. Res. 26, 7390–7404.

Zuykov, M., Pelletier, E., Demers, S., 2011. Colloidal complexed silver and silver nanoparticles in extrapallial fluid of *Mytilus edulis*. Mar. Environ. Res. 71, 17–21.

2.8. Supplementary information

Table S2.1. Characteristics of the Ag NPs dispersed in ultrapure water (UPW). Shown are Z-potential values (mV), polydispersity Index (PDI) and mean hydrodynamic diameter (nm) measured by Dynamic Light Scattering (DLS); Dissolved Ag concentration (µg L^{-1}) and percentage of dissolution measured by ICP-MS of 3-8 nm, 50 nm and 60 nm Ag NPs and Ag_2S NPs measured in UPW stock solutions at a nominal concentration of 1 mg Ag L^{-1}. All values are given as mean and standard deviation (mean ± SD; *n*=3).

Nanoparticle	Timepoint (h)	Z-potential (mV)	DLS (nm)	PDI	Dissolved Ag concentration (µg L^{-1})	% Dissolution
3-8 nm Ag NP	0	0.03 ± 0.52	144 ± 19.4	0.29 ± 0.04	65 ± 7.06	6.50 ± 0.71
	2	0.20 ± 0.55	115 ± 4.64	0.23 ± 0.04	76.6 ± 5.17	7.66 ± 0.52
	4	-45.7 ± 2.93	121 ± 3.74	0.26 ± 0.02	91.9 ± 5.04	9.19 ± 0.50
	8	-41 ± 5.9	112 ± 1.92	0.20 ± 0.03	109 ± 17.8	10.9 ± 1.78
	24	-43.1 ± 6.33	116 ± 5.79	0.21 ± 0.04	187 ± 25.2	18.7 ± 2.52
	48	-34.1 ± 12.3	125 ± 20	0.17 ± 0.05	210 ± 40.4	21.1 ± 4.04
50 nm Ag NP	0	-35.6 ± 11.2	59 ± 1.19	0.22 ± 0.01	52.7 ± 3.51	5.27 ± 0.35
	2	-54.9 ± 1.34	58.1 ± 1.48	0.23 ± 0.01	86.1 ± 16.4	8.61 ± 1.64
	4	-42.6 ± 6.67	58.1 ± 1.75	0.23 ± 0.01	108 ± 31	10.8 ± 3.10
	8	-38.7 ± 18.1	58.7 ± 1.69	0.23 ± 0.01	166 ± 41.8	16.6 ± 4.18
	24	-32 ± 19.6	56 ± 1.61	0.23 ± 0.02	162 ± 57.6	16.2 ± 5.76
	48	-25.1 ± 6.78	54.8 ± 1.34	0.23 ± 0.03	261 ± 60.2	26.1 ± 6.02
60 nm Ag NP	0	1.02 ± 43.3	n.a.	n.a.	n.a.	n.a.
	2	-20.6 ± 29.7	996 ± 635	0.91	1.97 ± 0.01	28.2 ± 0.11
	4	-6.11 ± 53.7	1265 ± 673	1	2.05 ± 0.03	29.2 ± 0.33
	8	n.a.	n.a.	n.a.	n.a.	n.a.
	24	-3.86 ± 38.5	1406 ± 778	0.83	1.90 ± 0.08	27.2 ± 0.94
	48	-24.8 ± 21.6	1800 ± 1497	0.93	2.05 ± 0.06	29.3 ± 0.73
Ag_2S NP	0	-33.9 ± 0.74	215 ± 9.76	0.34	n.a.	n.a.
	2	-33.1 ± 14	206 ± 22.3	0.41	0.13 ± 0.05	0.04 ± 0.02
	4	-36.2 ± 5.64	206 ± 23.1	0.38	0.03 ± 0.01	0.01 ± 0.002
	8	n.a.	n.a.	n.a.	n.a.	n.a.
	24	-44.4 ± 3.36	207 ± 32.9	0.4	0.02 ± 0.005	0.01 ± 0.001
	48	-42.1 ± 4.37	212 ± 18.2	0.37	0.05 ± 0.01	0.01 ± 0.003

n.a. not analysed at that time point.

Table S2.2. Characteristics of the Ag NPs dispersed in APW medium. Shown are Z-potential values (mV), PDI and mean hydrodynamic diameter (nm) measured by DLS; Dissolved Ag concentration (µg L^{-1}) and percentage of dissolution measured by ICP-MS of 3-8 nm, 50 nm and 60 nm Ag NPs and Ag_2S NPs measured in APW medium at a nominal concentration of 1 mg Ag L^{-1}. All values are given as mean and standard deviation (mean ± SD; *n*=3).

Nanoparticle	Timepoint (h)	Z-potential (mV)	DLS	PDI	Dissolved Ag concentration (µg L^{-1})	% Dissolution
3-8 nm Ag NP	0	-25.4 ± 2.41	131 ± 8.77	0.30 ± 0.04	80 ± 0.28	8 ± 0.03
	2	-0.14 ± 0.27	137 ± 2.57	0.20 ± 0.02	121 ± 15.1	12.1 ± 1.51
	4	-23.6 ± 0.99	153 ± 5.33	0.22 ± 0.01	123 ± 11.1	12.3 ± 1.11
	8	-21.7 ± 0.76	162 ± 2.77	0.23 ± 0.01	136 ± 8.20	13.6 ± 0.82
	24	-24.4 ± 1.12	242 ± 10.5	0.36 ± 0.03	209 ± 15.2	20.9 ± 1.52
	48	-22.3 ± 2.02	270 ± 5.61	0.40 ± 0.03	209 ± 15.2	20.9 ± 1.52
50 nm Ag NP	0	-15.8 ± 0.79	75.6 ± 1.52	0.27 ± 0.01	78.9 ±14	7.89 ± 1.40
	2	-6.07 ± 8.81	187 ± 9.09	0.31 ± 0.03	68.9 ± 24.2	6.89 ± 2.42
	4	-18.2 ± 1.07	236 ± 5.29	0.36 ± 0.05	71.8 ± 27.7	7.18 ± 2.76
	8	-18.4 ± 0.63	254 ± 8.36	0.42 ± 0.02	83.9 ± 31.4	8.39 ± 3.14
	24	-19.8 ± 0.89	1133 ± 168	0.1 ± 0.01	107 ± 34.5	10.7 ± 3.45
	48	-19.7 ± 1.27	1840 ± 503	1 ± 0	140 ± 21.5	14 ± 2.15
60 nm Ag NP	0	-20.7 ± 4.2	79.22	0.31	n.a.	n.a.
	2	-16 ± 2.59	154 ± 34.7	0.30	0.16 ± 0.04	2.3 ± 0.60
	4	-18.4 ± 3.71	174 ± 48	0.32	0.12 ± 0.01	1.65 ± 0.08
	8	n.a.	n.a.	n.a.	n.a.	n.a.
	24	-22.4 ± 2.15	132 ± 14	0.24	0.08 ± 0.01	1.12 ± 0.18
	48	-24.8 ± 1.44	134 ± 9.41	0.24	0.06 ± 0.003	0.82 ± 0.05
Ag_2S NP	0	-9.55 ± 0.66	191 ± 6.55	0.33	n.a.	n.a.
	2	-9.31 ± 2.51	213 ± 30.6	0.4	0.71 ± 0.06	0.2 ± 0.02
	4	-8.93 ± 0.49	206 ± 16.8	0.41	0.15 ± 0.16	0.04 ± 0.05
	8	n.a.	n.a.	n.a.	n.a.	n.a.
	24	-8.35 ± 2.18	183 ± 20.6	0.37	0.12 ± 0.17	0.03 ± 0.05
	48	-7.97 ± 3.68	159 ± 13.5	0.35	0.01 ± 0.002	0.002 ± 0 .0005

n.a. not analysed at that time point.

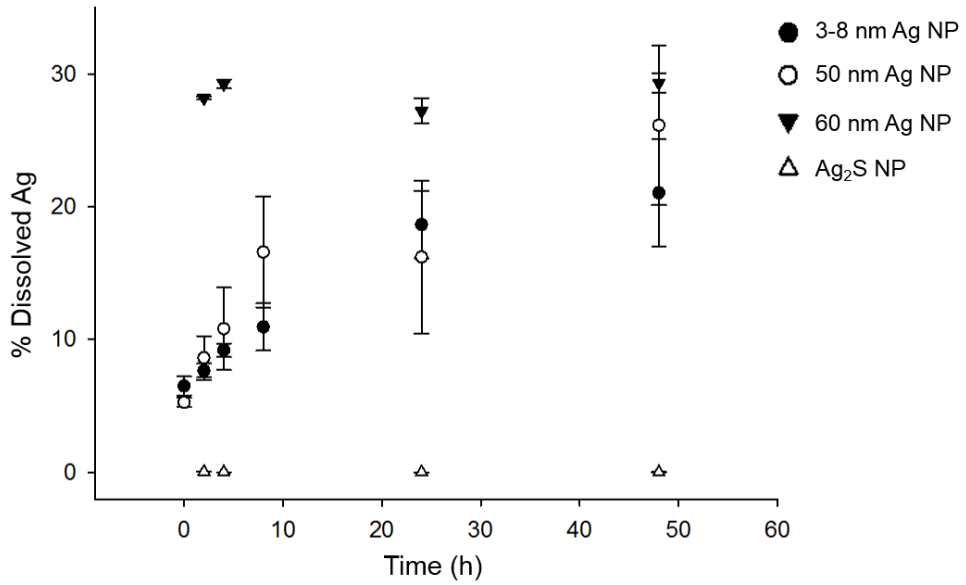

Figure S2.1. Percentage of dissolved Ag at 0, 2, 4, 8, 24 and 48 hours from 3-8 nm and 50 nm Ag NPs and at 2, 4, 24 and 48 hours from 60 nm Ag NPs and Ag_2S NPs, measured by ICP-MS in ultrapure water (UPW) stock solutions of 1 mg Ag L^{-1}. Error bars indicate the standard deviation.

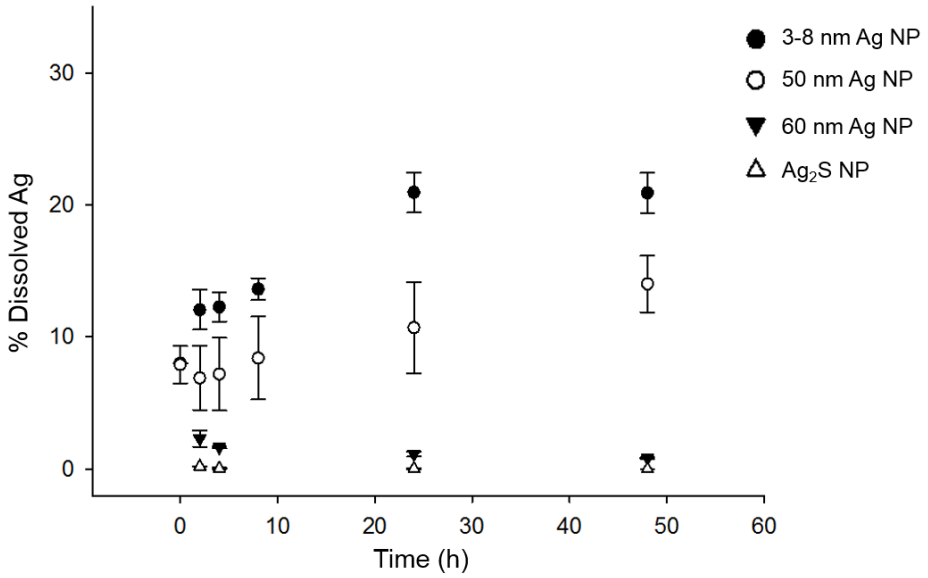

Figure S2.2. Percentage of dissolved Ag at 0, 2, 4, 8, 24 and 48 hours from 3-8 nm and 50 nm Ag NPs and at 2, 4, 24 and 48 hours from 60 nm Ag NPs and Ag_2S NPs, measured by ICP-MS in APW medium solutions at a nominal concentration of 1 mg Ag L^{-1}. Error bars indicate the standard deviation.

Table S2.3. Total Ag concentrations determined at day 0 and dissolved Ag concentrations (µg Ag L^{-1}) determined at days 0, 1 and 2 in water samples of all exposures of the Ag-spiked water test. Values are given as mean and standard deviation (mean ± SD; *n*=3). Different small letters within a row indicate statistically significant differences (one-way repeated measures ANOVA followed by Holm-Sidak Method, p<0.05); different capital letters in bold within a column indicate statistically significant differences (one-way ANOVA followed by Holm-Sidak Method, p<0.05).

Ag form	**Total Ag concentrations** (µg Ag L^{-1})	**Dissolved Ag concentrations** (µg Ag L^{-1})		
	Day 0	**Day 0**	**Day 1**	**Day 2**
3-8 nm Ag NP	11.1 ± 0.62 **A**	0.12 ± 0.04 **A** / *a*	0.26 ± 0.14 **A** / *a*	0.25 ± 0.14 **A** / *a*
50 nm Ag NP	8.28 ± 0.30 **B**	0.03 ± 0.02 **A** / *a*	0.27 ± 0.16 **A** / *a*	0.32 ± 0.29 **A** / *a*
60 nm Ag NP	10.3 ± 0.42 **A**	3.25 ± 0.48 **B** / *a*	3.57 ± 0.62 **B** / *a*	3.64 ± 0.06 **B** / *a*
Ag_2S NPs	16.8 ± 0.72 **C**	0.08 ± 0.1 **A** / *a*	0.17 ± 0.09 **A** / *a*	0.05 ± 0.08 **A** / *a*
$AgNO_3$	7.51 ± 0.26 **B**	2.35 ± 0.2 **B** / *a*	2.49 ± 0.16 **C** / *a,b*	2.99 ± 0.12 **C** / *b*

Table S2.4. Measured concentrations given as mean and standard deviation (mean ± SD; *n*=3) in water spiked at a nominal concentration of 10 µg Ag L^{-1} and non-spiked sediment at days 0, 3 and 7 of the uptake phase of all exposures of the Ag-spiked water and clean sediment test. Measured concentrations in water are expressed in µg Ag L^{-1} and in the sediment are in µg Ag kg^{-1}. kd_{water} and ki_{sed} (day^{-1}) are the Ag concentration decrease rate constant in water and Ag concentration increase rate constant in sediment, respectively. Different capital letters in bold within a column and different small letters in italics within a row indicate statistically significant differences between Ag treatments and sampling times, respectively (two-way ANOVA followed by Holm-Sidak Method, p<0.05).

Exposure route	Ag form	Measured concentration at day 0 (µg Ag L^{-1} and µg Ag kg^{-1})*	Measured concentration at day 3 (µg Ag L^{-1} and µg Ag kg^{-1})	Measured concentration at day 7 (µg Ag L^{-1} and µg Ag kg^{-1})	kd_{water} or ki_{sed} (day^{-1})
Water	3-8 nm	10 ± 0.08 **A** / *a*	3.31 ± 1.46 **A,B** / *b*	2.47 ± 0.04 **A** / *b*	-0.29
	50 nm	8.82 ± 0.43 **A** / *a*	3.17 ± 1.01 **A,B** / *b*	0.35 ± 0.26 **B** / *c*	-0.36
	60 nm	9.43 ± 0.23 **A** / *a*	1.91 ± 0.39** **A,B** / *b*	0.9 ± 1.25 **A,B** / *b*	-0.49
	Ag_2S NPs	12.2 ± 0.74 **B** / *a*	3.58 ± 1.66 **A** / *b*	0.75 ± 0.39 **A,B** / *c*	-0.41
	$AgNO_3$	8.84 ± 0.58 **A** / *a*	1.42 ± 0.16 **B** / *b*	0.31 ± 0.13 **B** / *b*	-0.60
Sediment	3-8 nm	10.1 ± 2.95 *a*	15.3 ± 2.32 **A** / *a*	16.9 ± 4.08 **A** / *a*	0.08
	50 nm	10.1 ± 2.95 *a*	12.8 ± 1.38 **A** / *a,b*	18.3 ± 1.40 **A** / *b*	0.09
	60 nm	10.1 ± 2.95 *a*	22.2 ± 5.17 **A**/ *b*	25.6 ± 4.40 **A** / *b*	0.14
	Ag_2S NPs	10.1 ± 2.95 *a*	24.3 ± 2.93 **A** / *b*	20.8 ± 1.02 **A** / *b*	0.12
	$AgNO_3$	10.1 ± 2.95 *a*	32.8 ± 20.7 **A** / *b*	18.5 ± 1.92 **A** / *c*	0.12

* background concentration in sediments, therefore, was considered the same concentration at day 0 for sediments of all treatments.
** *n*=2

Table S2.5. Total Ag concentrations determined at day 0 and dissolved Ag concentrations (µg Ag L^{-1}) determined at days 0, 1, 2 and 7 in water samples of all exposures of the Ag-spiked water and clean sediment test. Values are given as mean and standard deviation (mean ± SD; *n*=3). Different small letters within a row indicate statistically significant differences (one-way repeated measures ANOVA followed by Holm-Sidak Method, p<0.05); different capital letters in bold within a column indicate statistically significant differences (one-way ANOVA followed by Holm-Sidak Method, p<0.05).

Ag form	Total Ag concentrations (µg Ag L^{-1})	Dissolved Ag concentrations (µg Ag L^{-1})			
	Day 0	Day 0	Day 1	Day 2	Day 7
3-8 nm	11.9 ± 0.31*** **A, B**	0 ± 0 **A** / *a*	0.15 ± 0.11 **A** / *a*	0.14 ± 0.07 **A**/ *a*	0.05 ± 0.01 **A** / *a*
50 nm	11.2 ± 2.48 **A**	0 ± 0 **A** / *a*	0.34 ± 0.33 **A** / *a*	0.38 ± 0.13 **B** / *a*	0 ± 0 **A** / *a*
60 nm*	11.1** **A**	0.02 ± 0.02 **A** / *a*	1.19 ± 0.82 **A** / *b*	0.66 ± 0.11 **C** / *a,b*	0 ± 0 **A** / *a*
Ag_2S NPs	16.8 ± 1.41 **B**	0 ± 0 **A** / *a*	0.06 ± 0.03 **A** / *b*	0.07 ± 0.03 **A** / *b*	0 ± 0 **A** / *a*
$AgNO_3$*	9.35 ± 0.13*** **A**	0 ± 0 **A** / *a*	0.79 ± 0.61 **A** / *b*	0.54 ± 0.03 **B, C** / *a,b*	0.01 ± 0.01 **A** / *a*

* one-way repeated measures ANOVA followed by Fisher LSD Method (p<0.05).
** denotes a single measurement.
*** denotes two measurements.

Table S2.6. Measured concentrations (mg Ag kg^{-1}) given as mean and standard deviation (mean ± SD, *n*=3) in sediment spiked at a nominal concentration of 10 mg Ag kg^{-1} at days 0, 3 and 7 of the uptake phase of all exposures of the Ag-spiked sediment test. Different capital letters in bold within a column and different small letters in italics within a row indicate statistically significant differences between Ag treatments and sampling times, respectively (two-way ANOVA followed by Holm-Sidak Method, p<0.05).

	Ag form	Measured concentration at day 0 (mg Ag kg^{-1})	Measured concentration at day 3 (mg Ag kg^{-1})	Measured concentration at day 7 (mg Ag kg^{-1})
Sediment	3-8 nm	12.2 ± 1.07 **A** / *a*	8.30 ± 0.13 **A,B** / *b*	8.99 ± 0.43 **A** / *b*
	50 nm	8.13 ± 1.25 **B** / *a*	7.20 ± 0.20 **A** / *a*	8.65 ± 0.57 **A** / *a*
	60 nm	9.55 ± 0.82 **B** / *a*	9.42 ± 0.92 **B** / *a*	11.7 ± 2.04 **B** / *b*
	Ag_2S NPs	9.89 ± 0.21 **B** / *a*	9.52 ± 0.54 **B** / *a*	11 ± 0.72 **B** / *a*
	$AgNO_3$	8.26 ± 1.05 **B** / *a*	8.51 ± 0.67 **A,B** / *a*	8.97 ± 0.23 **A** / *a*

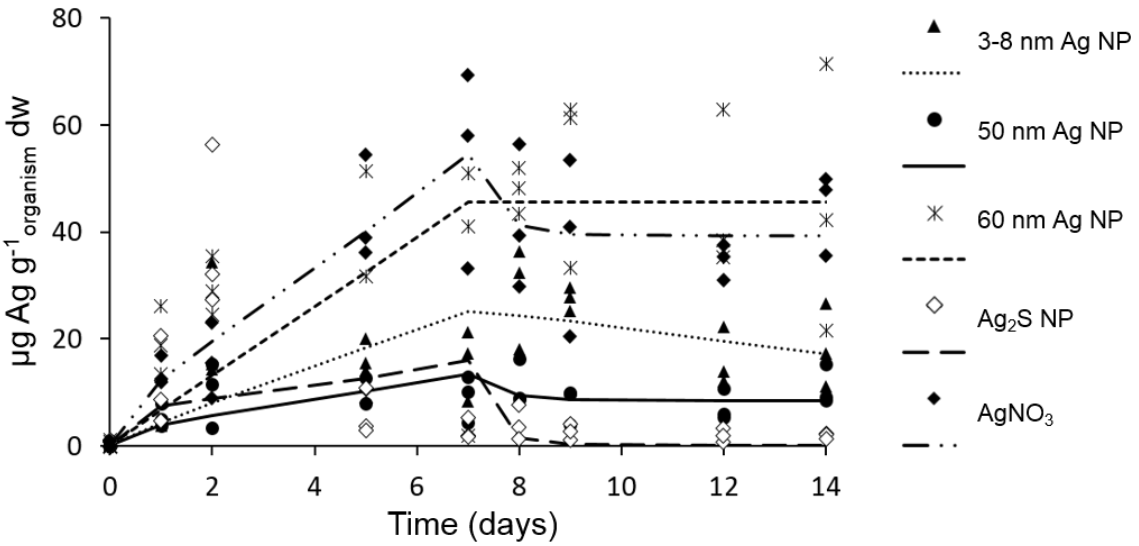

Figure S2.3. Uptake and elimination kinetics of 3-8 nm, 50 nm and 60 nm Ag NPs, Ag_2S NPs and $AgNO_3$ in the freshwater snail *Physa acuta* exposed for 7 days to water spiked at a nominal concentration of 10 µg Ag L^{-1} and then transferred to clean water for 7 days, in the Ag-spiked water and clean sediment test. Lines represent the fit of a one-compartment model to the data, which represent Ag concentrations measured in individual snail soft bodies. Data was modelled considering the sediment as the single exposure route.

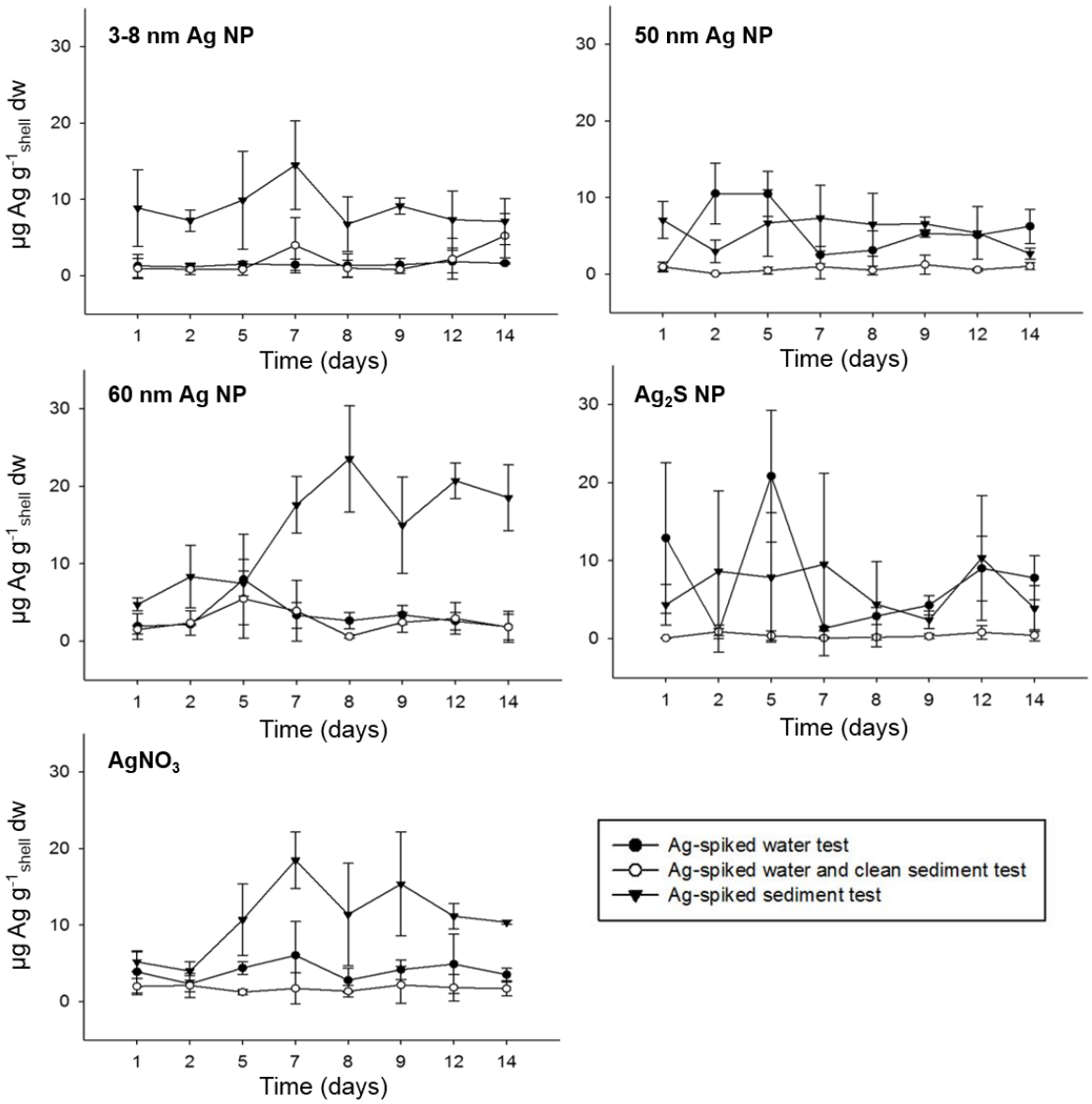

Figure S2.4. Silver concentrations (µg Ag g^{-1} dw) given as mean and standard deviation (mean ± SD, *n*=3) measured in the shell of *Physa acuta* exposed to 3-8 nm, 50 nm and 60 nm Ag NPs, Ag_2S NPs and $AgNO_3$ during the uptake and elimination phases of the Ag-spiked water test, Ag-spiked water and clean sediment test and Ag-spiked sediment test. Error bars indicate standard deviation.

Chapter 3

Toxicokinetics of silver and silver sulfide nanoparticles in *Chironomus riparius* under different exposure routes

To be submitted

Patrícia V. Silva[1], Cátia S. A. Santos[1], Anastasios G. Papadiamantis[3,4], Sandra F. Gonçalves[1], Marija Prodana[1], Rudo A. Verweij[2], Iseult Lynch[3], Cornelis A. M. van Gestel[2] and Susana Loureiro[1]

[1]CESAM-Centre for Environmental and Marine Studies & Department of Biology, University of Aveiro, Campus Universitário de Santiago, 3810-193 Aveiro, Portugal
[2]Department of Ecological Science, Faculty of Science, Vrije Universiteit Amsterdam, The Netherlands
[3]School of Geography, Earth and Environmental Sciences, University of Birmingham, Edgbaston, B15 2TT Birmingham, UK
[4]NovaMechanics Ltd., 1065, Nicosia, Cyprus

Toxicokinetics of silver and silver sulfide nanoparticles in *Chironomus riparius* under different exposures routes

3.1. Abstract

Engineered nanoparticles released into aquatic systems may accumulate in sediments, potentially threatening benthic organisms. This study determined the toxicokinetics of pristine silver nanoparticles (Ag NPs), a simulating aged Ag NP form (Ag_2S NPs) and $AgNO_3$ in *Chironomus riparius*. Chironomid larvae were exposed to the different Ag forms through water, sediment, or food. The potential transfer of Ag from larvae to adult midges was also evaluated. Results revealed higher Ag uptake by *C. riparius* upon exposure to Ag_2S NPs, while larvae exposed to pristine Ag NPs and $AgNO_3$ generally presented similar kinetics. Uptake patterns of the different Ag forms were generally similar in the tests with water or sediment exposures, suggesting similar uptake routes. In both water and sediment tests, Ag uptake in the chironomid larvae seemed better explained by exposure to water than from the ingestion of sediment particles. Ag uptake via food exposure was only significant for Ag_2S NPs. Ag transfer to the terrestrial compartment seems to be low, although some concerns can be raised for ionic Ag. In the environmentally relevant scenario chironomid larvae accumulated relatively high Ag concentrations and elimination was extremely low in some cases. This suggests potential bioaccumulation of Ag in its nanoparticulate and/or ionic form, which may raise concerns regarding chronic exposure and trophic transfer.

Keywords: uptake route, nanomaterials, bioaccumulation, bioavailability, benthic organisms.

3.2. Introduction

Due to the immense growth of the nanotechnology industry, it is imperative to develop adequate knowledge on the fate and effects of engineered nanoparticles (NP) for a robust environmental risk assessment (Selck et al., 2016). Although many interdisciplinary studies have contributed to the environmental risk assessment of NPs, they have also identified the challenges ahead (Lead et al., 2018). For instance, a key challenge is to predict the interactions and subsequent transformations of NPs during their life-cycle (Selck et al.,

2016). The highly dynamic nature of NPs following release into the environment leads to many uncertainties about the actual NP forms and the environmental concentrations to which organisms are exposed (van den Brink et al., 2019). A sizable body of research has been conducted on silver nanoparticles (Ag NPs) because they are widely incorporated into commercial and industrial products, with global Ag NP consumption estimated to be 450 ton/year (Lazareva and Keller, 2014). Wastewater treatment plants (WWTP) are major sources of Ag NPs into the environment and a crucial point for Ag NP transformations (McGillicuddy et al., 2017). A field study reported that silver chloride (AgCl NPs) and silver sulfide NPs (Ag_2S NPs) were the dominant Ag forms in industrial laundry effluents discharged to the sewer system. During transportation from the sewer to the WWTP, AgCl NPs were transformed into Ag_2S NPs, which remained the dominant Ag species during subsequent WWT processes (Kaegi et al., 2015). Contrary to Ag NPs, Ag_2S NPs present high chemical stability and very limited dissolution (Peixoto et al., 2020). This is an important aspect as it makes Ag_2S NPs more persistent and the main Ag nanoform released into the aquatic environment (Clark et al., 2019). Ag NP concentrations in influent, effluent, reclaimed and backwash waters of a WWTP in Santa Barbara, California, were 13.5, 3.2, 0.5 and 9.8 ng L^{-1}, respectively (Cervantes-Avilés et al., 2019).

In surface water, sediments are considered the final sink due to the settling tendency of Ag NPs from the water column (Niemuth et al., 2019). The predicted environmental concentrations of Ag nanomaterials in freshwater sediments range between 1.85 and 29.6 µg kg^{-1} (Giese et al., 2018). The ongoing introduction of Ag NPs in aquatic systems can lead to an increasing accumulation in sediments over time and thus benthic biota might be at risk, especially deposit feeders (Niemuth et al., 2019). Potential exposure of benthic biota to NPs includes ingestion of contaminated sediments/food and suspended particles, and exposure to pore water or overlying water, either by ingestion or contact with epithelial surfaces (Gallego-Gallegos et al., 2013; Gimbert et al., 2018; Yoo et al., 2004).

The ecologically relevant species *Chironomus riparius* (non-biting midge) was chosen as the test organism for this study, as this species offers several advantages. *C. riparius* belongs to the most abundant insect group found in freshwater ecosystems and are considered relevant indicators of metal bioaccumulation (Dabrin et al., 2012; Nair et al., 2011). They are deposit-feeding organisms that can potentially be exposed to contaminants through water and through sediment (Lee et al., 2016). *C. riparius* undergoes full metamorphosis, with the larval stages dwelling in the sediment (Ferrari and Faburé, 2017), and is an important food source for many organisms living in the sediment or in the water column. Therefore, larvae may contribute to the re-transfer of NPs to the water phase after

sedimentation (Bour et al., 2017). NPs have been reported to be packed into the gut of chironomid larvae (Bour et al., 2015; Lorenz et al., 2017). Furthermore, adult stages can be potential vectors for NP trophic transfer to terrestrial predators, such as birds, amphibians or other insects (Ferrari and Faburé, 2017). In addition, several studies have evaluated the toxicity of Ag NPs to *C. riparius* larvae, including effects at the gene level (Lee et al., 2016; Nair et al., 2013, 2011; Nair and Choi, 2012, 2011; Park et al., 2015). Although assessing the potential toxicity of NPs is of great importance for risk assessment, understanding their bioaccumulation potential has been the focus of regulatory decision making. Toxicokinetic studies are suggested as key tools to evaluate the uptake and elimination of NPs and to help generate complete understanding of their behaviour and potential risks (Petersen et al., 2019). Thus, bioaccumulation studies of NPs in invertebrates are required, and particular interest has been given to benthic species (Kuehr et al., 2021; Petersen et al., 2019; Selck et al., 2016).

This study aimed at evaluating the toxicokinetics of different pristine (unmodified) Ag NPs, Ag_2S NPs (a synthetized Ag form which simulates an environmentally aged particle) and the ionic counterpart ($AgNO_3$), exposing *C. riparius* larvae through different routes: water, sediment, and food. Different exposure routes were studied in order to understand the uptake and bioavailability of particulate and ionic Ag to the larvae through the separate sources. Using pristine Ag NPs allows assessment of the uptake of both nanoparticles and associated ionic Ag. Using Ag_2S NPs enables understanding the uptake of the most environmentally relevant nanoparticulate Ag form (Baccaro et al., 2018). The potential transfer of Ag to the adult stage was also assessed in this study. This is the first study determining the toxicokinetics of nanoparticles in *Chironomus*.

3.3. Material and Methods

3.3.1. Test species and breeding

Cultures of *Chironomus riparius* were established at the University of Aveiro, Portugal. *C. riparius* larvae were maintained in plastic containers with a 1:4 depth ratio of inorganic sediment (particle size <1 mm, which had been previously burned at 500 °C for 4h) and American Society for Testing Materials hard water (ASTM; details in the Supplementary Information (SI)) (ASTM, 1980). Sediment was fully renewed monthly, and ASTM medium was fully renewed biweekly. The containers were kept inside an acrylic cage to prevent adult *C. riparius* from escaping. Cultures were maintained with continuous aeration of the ASTM medium and at controlled conditions of 20 ± 1 ºC and 16:8h light: dark photoperiod.

Larvae were fed *ad libitum* three times a week with a suspension of ground fish food (TetraMin®). For the experiments, egg ropes were separated from the cultures. After hatching, larvae grew under the same conditions as the cultures and were fed every other day until they reached the 4th instar (12-days old).

3.3.2. Nanoparticles

Four different types of silver nanoparticles (Ag NPs) were tested: three pristine Ag NPs with nominal sizes of 3-8 nm, 50 nm, and 60 nm, and silver sulfide NPs (Ag_2S NP) with a nominal size of 20 nm. Silver nitrate ($AgNO_3$) was used as the ionic control (Sigma Aldrich; CAS number 7761-88-8; 99% purity; crystalline powder). All NPs were supplied as dispersed solutions by partners of the EU Horizon 2020 (H2020) NanoFASE project (http://www.nanofase.eu/). Ag NPs of 3-8 nm (alkane; 1,000 mg Ag L^{-1}) and of 60 nm (Polyvinylpyrrolidone (PVP); 1,000 mg Ag L^{-1}) were supplied by AMEPOX Enterprise (Poland). Ag NPs of 50 nm (5.5 mM sodium citrate, 25 µM tannic acid, 47.3 ± 5.3 nm, 12.3 g Ag L^{-1}) and Ag_2S NPs (PVP; 6.56 g Ag L^{-1}) were supplied by Applied Nanoparticles (Barcelona, Spain). Ag_2S NPs were produced *ab initio* as Ag_2S to simulate an environmentally aged Ag NPs, allowing the comparison between the most relevant Ag form in the environment with the pristine forms.

3.3.3. Ag NP characterization

The stability in ASTM medium of the 3-8 nm, 50 nm, 60 nm Ag NPs and Ag_2S NPs was assessed by monitoring dissolution, zeta potential and hydrodynamic size at different time points, following the methodology described by Silva et al. (2020). Results can be found in Table S3.1 in the SI. The stability in ultra-pure water (UPW) of the same NPs has also been described in Silva et al. (2020). TEM data has been previously reported (different batches) for the 3-8 nm Ag NPs by Ribeiro et al. (2014) and for the 50 nm Ag NPs and Ag_2S NPs by Baccaro et al. (2018).

3.3.4. Experimental design

3.3.4.1. Water exposure bioaccumulation test

The experimental design of all tests consisted of an uptake phase and an elimination phase. In the uptake phase, larvae were exposed for 48 hours to ASTM medium spiked with a nominal concentration of 10 µg Ag L^{-1}. After this period, the larvae were transferred

to clean ASTM medium for the 48-hour elimination phase. The exposure concentration was chosen to be environmentally relevant, while allowing reliable detection of Ag in the test media and test organisms. The water was spiked to simulate a realistic scenario, where Ag NPs are emitted through the water phase and reach sediments after settlement from the water column.

NP stock suspensions were prepared in ultrapure water (UPW), following the OECD guideline 318 (2017). Glass vials of 150 mL were filled with inorganic sediment (<1mm, previously burned for 4h at 500 ºC) and ASTM medium and at a depth ratio of 1:4, respectively, and left to settle for 24h. Subsequently, 10 larvae (4^{th} instar) were placed in each replicate. ASTM medium was spiked following the OECD guideline 233 (2010), in which the desired volume of the NP/$AgNO_3$ stock suspensions/solutions was added below the water surface of each vial and homogenized by stirring with a needle, avoiding sediment disturbances. Each replicate was covered with a lid to avoid evaporation, and needles connected to an air pump provided low aeration to the ASTM medium (24h after spiking). Test conditions were monitored by measuring dissolved oxygen, temperature and pH, and the experiment was run at 20 ± 1 ºC and 16:8 h light: dark photoperiod (OECD, 2010). Vial inspection was performed daily, and larvae were not fed during the test. Three replicates per treatment were sampled at 12h, 24h, 36h, 48h, 60h, 72h, 84h and 96h and the animals were left to depurate for 4h in clean ASTM medium (no sediment). Following depuration, the larvae were rinsed in UPW, immediately blotted dry on filter paper, oven dried at 60 ºC for 48h and then weighted. Water and sediment were sampled (n = 3 per treatment) at 0h, 24h and 48h for total Ag analysis. Water was digested immediately after sampling and sediment samples were stored at -20 ºC until digestion.

A separate experiment was conducted, in which vials without organisms were assembled and kept at the same conditions as the test, to collect water samples (n = 3 per treatment) at day 0 (0h) for total Ag analysis. At 0h, 24h and 48h of the uptake phase water samples (n=3 per treatment) were collected from the same vials in each treatment, for ultrafiltration and posterior dissolved Ag determination. For ultrafiltration, 3 mL of water were directly sampled from the vials and filtered through a syringe filter (0.02 µm; Anotop™, Whatman), previously soaked with a solution of 0.1 M $CuSO_4$ to prevent loss of Ag to the filter (Cornelis et al., 2010). Samples were immediately acidified after filtration to a final acid concentration of 2% using concentrated HNO_3 (65% purity, PanReac AppliChem, trace analysis).

3.3.4.2. Sediment exposure bioaccumulation test

The experimental design followed the methodology described in section 3.3.4.1, with the difference that the sediment was spiked. Nominal concentrations in sediments assumed a more extreme exposure scenario, to compare the kinetics with the lower exposure concentrations in sediments from the previous test (see section 3.4.2). Sediment was spiked at a nominal concentration of 1 mg Ag kg^{-1}, following the OECD guideline 218 (2004). Sediment was homogenised by hand in the individual glass vials with a volume of the NP/$AgNO_3$ stock suspensions/solutions (in UPW) corresponding to 20% of the sediment mass. ASTM medium was then gently added to each vial to avoid disturbing the sediment and left to equilibrate for 48h. After this period, 10 larvae (4^{th} instar) were added to each replicate, all vials were covered, and aeration was provided to the ASTM medium. Test conditions, monitoring, larvae sampling and depuration followed the procedure described in section 3.3.4.1. Extra vials (*n* = 3) from the 3-8 nm Ag NP, Ag_2S NP and $AgNO_3$ treatments were kept in sediment-spiked medium (no elimination phase) until emergence of the larvae to sample the pupal exuviae (shed skin) and adult *C. riparius* (imagines).

Sediment was sampled for total Ag analysis and for pore water extraction at day 0 (*n* = 3 per treatment). For pore water extraction, sediment was centrifuged through a 70 µm nylon filter (previously soaked in 0.1 M $CuSO_4$) for 15 min at 2000 rcf g^{-1}, at 4 ºC. Following filtration, the sediment pore water was immediately acidified with concentrated HCl (37%, PanReac AppliChem, trace analysis) to a final concentration of 3% and stored at 4 ºC until total Ag analysis.

3.3.4.3. Food exposure bioaccumulation test

The bioaccumulation test followed the same design as described in sections 3.3.4.1 and 3.3.4.2, with the difference that the chironomid larvae were exposed to spiked food (leaves) in clean water and sediment. Leaves were soaked in solutions with the same environmentally relevant concentration as used in water (nominal concentration of 10 µg Ag L^{-1}), considering that in rivers leaves and other detritus are likely contaminated with NPs from the water phase. Alder leaves (*Alnus glutinosa*) were cut into disks (ø 10 mm) and spiked following the methodology described in Tourinho et al. (2016). Briefly, the leaves were separated into groups by dry weight (dw) and each group was soaked in the respective NP/$AgNO_3$ stock suspension/solution (in UPW) and shaken at 150 rpm for 4 days. After adding 10 larvae (4^{th} instar) to each test vial previously assembled with ASTM medium and sediment (as per section 3.3.4.1), three leaf disks were added to each replicate. After the

48-hour uptake phase, Ag-dosed leaves were replaced by clean (untreated) leaves for the elimination phase. At day 0, alder leaves (*n* = 3 per treatment) were sampled, oven dried at 60 ºC for 3 days, and digested for total Ag determination. Test conditions, aeration, monitoring, and organism sampling/depuration were performed as described in section 3.3.4.1.

3.3.5. Sample digestion and total Ag analysis

Organisms were digested following the methodology described in Ribeiro et al. (2017) with small adaptations. Briefly, each sample of 10 chironomid larvae was digested on a hotplate in Teflon beakers with 3 mL of concentrated HNO_3 (65%, PanReac AppliChem, trace analysis). After tissue digestion, 1 mL of concentrated HCl (37%, PanReac AppliChem, trace analysis) was added, and samples evaporated to approximately 1 mL. Then, the digests were diluted to a final volume of 5 mL with 1% HCl (37%, PanReac AppliChem, trace analysis). To evaluate method accuracy and recovery, blanks and the certified reference material DOLT-5 (Dogfish liver) were analysed in triplicate jointly with the samples in each digestion run, giving an average recovery of 86.6 ± 12.5% (mean ± SD; *n* = 27).

Water digestion followed the methodology described in Ribeiro et al. (2014). Samples (5 mL) were digested in Teflon beakers with a 4 mL mixture of concentrated HCl (37%) : HNO_3 (65%) (3 : 1. v/v, PanReac AppliChem, trace analysis) and heated on a hotplate for evaporation to approximately 1 mL. Samples were then diluted with 1% HCl (37%, PanReac AppliChem, trace analysis) to a final volume of 5 mL. Blanks (ASTM medium) and recovery controls (with known Ag concentration) were also analysed in triplicate in each digestion run. The average recovery of Ag was 109 ± 38.5 % (mean ± SD; *n* = 36).

Sediment samples were oven dried at 50 ºC prior to digestion. Sediments (~130 mg) were digested for 7h at 140 ºC in an oven (BINDER ED53), in closed Teflon containers with a 2 mL mixture of concentrated HCl (37%) : HNO_3 (65%) (4 : 1. v/v, J.T. Baker, trace analysis). The digests were diluted with demineralized water up to a volume of 10 mL. Blanks (*n* = 3) and the certified reference material sewage sludge LGC6181 were included and the average Ag recovery was 88.7 ± 0.02% (mean ± SD*; n* = 2). Leaves (~15 mg) were digested with a 2 mL mixture of concentrated HCl (37%) : HNO_3 (65%) (4 : 1. v/v, PanReac AppliChem, trace analysis) in a microwave (Berghof speed wave). Digestion was performed in three steps, first applying a temperature ramp of 10 ºC up to 180 °C (25 min), held at 180 °C (25 min) and then a ramp from 5 ºC to 100 °C (10 min). This process was performed twice to assure the total digestion of the samples. Next, samples were transferred to Teflon

beakers and left to evaporate on a hotplate until reaching approximately 1 mL and were then diluted to a final volume of 3 mL with 1% HCl (37%, PanReac AppliChem, trace analysis). Blanks (*n* = 3) and reference material DOLT-5 were digested with the samples; the average recovery was 82.4 ± 30.3% (mean ± SD*; n* = 3).

All samples were analysed for total Ag concentration by Graphite furnace Atomic Absorption Spectrometry (GF-AAS; PinAAcle 900Z, PerkinElmer, Singapore). The limit of detection (LOD) ranged between 0.018 and 0.16 µg Ag L^{-1} in the different runs.

3.3.6. Toxicokinetic modelling

A simple commonly used one-compartment model was used to describe the Ag toxicokinetics in the *C. riparius* larvae (Ardestani et al., 2014).

$$Q(t) = \left(\frac{k1}{k2}\right) * C_{exp} * \left(1 - e^{(-k2*t)}\right) \quad (1)$$

$$Q(t) = \left(\frac{k1}{k2}\right) * C_{exp} * \left(e^{(-k2*(t-t_c))} - e^{(-k2*t)}\right) \quad (2)$$

Where Q(t) is the Ag concentration in the larvae at time t (µg Ag $g^{-1}_{organism}$ dw); k1 is the uptake rate constant from water, sediment or food (L $g^{-1}_{organism}$ $hour^{-1}$, $g_{sediment}$ $g^{-1}_{organism}$ $hour^{-1}$, or g_{food} $g^{-1}_{organism}$ $hour^{-1}$); k2 is the elimination rate constant ($hour^{-1}$); C_{exp} is the Ag exposure concentration in water (µg Ag L^{-1}), sediment (mg Ag kg^{-1}) or food (mg Ag kg^{-1}); t is the time in hours; t_c is the time at which larvae were transferred from contaminated to clean media (48 h).

For the water exposure bioaccumulation test, kinetic bioconcentration factors (BCF_ks) were derived as the ratio between the uptake and elimination rate constants ($\frac{k1}{k2}$) determined for water exposure and expressed in L g^{-1}. For the sediment exposure bioaccumulation test, kinetic biota-to-sediment accumulation factors ($BSAF_{ksed}$s) were calculated as the ratio between uptake and elimination rate constants derived from sediment exposure (with the unit g g^{-1}), and pore water BCF_{kspw}s to relate uptake to sediment pore water exposure (unit L g^{-1}).

3.3.7. Statistical analysis

Non-linear regressions in SPSS Statistics 25 were used to fit the toxicokinetics model to the data and determine the kinetic parameters. The best fitting model was identified by applying Akaike Information Criteria tests (AIC and AICc) (data not shown). Generalised Likelihood Ratio tests (GLR) in SPSS were applied to determine statistically significant differences between k1 and k2 for each Ag form. One-way analysis of variance (ANOVA) followed by the Holm-Sidak method ($p<0.05$) was used to determine significant differences in Ag concentrations between treatments. Two-way ANOVA followed by the Holm-Sidak method ($p<0.05$) was applied to determined differences in Ag concentrations in water or sediment samples of the water exposure bioaccumulation test, considering Ag treatment and time as factors (SigmaPlot 12.5 software). Differences between Ag concentrations in exuviae and the respective imagines (adults) from each treatment were determined by applying Student's *t*-tests. One-way repeated measures were used to compare dissolved Ag concentrations between sampling times from the same treatment. Data transformation was performed when ANOVA assumptions were not fulfilled. In cases where data did not follow a normal distribution after transformation, the Kruskal-Wallis test ($p<0.05$) was applied.

The stability of Ag NPs was analysed using one-way ANOVA, followed by Holm-Sidak method ($p<0.05$) (Sigmaplot 12.5). The time represented the independent variable, the measured physicochemical characteristic (Z-potential, hydrodynamic diameter and % dissolution) the dependent one. When the assumption of normality was not fulfilled, the non-parametric Kruskal-Wallis test was run, followed by Dunn's post-hoc method ($p<0.05$).

3.4. Results

3.4.1. Nanoparticle stability

Results on NP stability in ASTM medium are presented in Table S3.1 and Figure S3.1. In general, less negative zeta-potentials were obtained for 3-8 nm and 50 nm Ag NPs compared to the 60 nm Ag NPs and Ag_2S NPs despite the latter being PVP-coated (Table S3.1). Statistically significant differences were found in the pairwise comparisons of 8h versus 24h for 3-8 nm, and 0h versus 8h for 50nm (Kruskal-Wallis test, $p<0.05$). Zeta potential significantly changed in time for 60nm NPs, denoting specific statistically significant differences upon pairwise comparisons of 48h versus 0, 2, 4, and 24h (one-way ANOVA, Holm-Sidak method, $p<0.05$). The only statistically significant difference for Ag_2S

NPs was denoted for 0h versus 24h (Kruskal-Wallis test, $p<0.05$). Strong agglomeration, compared to their nominal sizes, was observed, for the 3-8 nm Ag NPs and Ag_2S NPs, with hydrodynamic diameters remaining relatively stable from 0h to 48h at 132-153 nm and 264-302 nm, respectively (Table S3.1). In the case of 3-8 nm Ag NPs significant differences were observed between 0h and 2, 4, 8, 24, 48h, including 2h versus 48h (one-way ANOVA, Holm-Sidak method, $p<0.05$). For the 50 nm Ag NPs, the hydrodynamic size was relatively close to the nominal size at 0h and agglomerated over time, ranging from 62.7 nm (0h) to 87.9 nm (48h) (Table S3.1). The differences were statistically significant for 0h versus 2, 4, 8, 24 and 48h, and also for 48h versus 4h and 8h (one-way ANOVA, Holm-Sidak method, $p<0.05$). Hydrodynamic size of 60 nm Ag NPs was different for the time 2h versus 4, 24 and 48h (one-way ANOVA, Holm-Sidak method, $p<0.05$). No differences were obtained for the hydrodynamic size of Ag_2S NPs (one-way ANOVA, $p>0.05$).

Dissolution was low for all NPs, especially for the 60 nm Ag NPs (decreasing from 2.30% (2h) to 0.82% (48h)), and for Ag_2S NPs (decreasing from 0.32% (2h) to 0.01% (from 4h until 48h)). For the 3-8 nm Ag NPs, dissolution increased during the 48h, from 4.40% at 0h to 7.37% at 48h (Figure S3.1, Table S3.1), whereas statistically significant differences were found for all the pairwise comparisons (one-way ANOVA, Holm-Sidak method, $p<0.05$), with the exception for 0h versus 4h, 2h versus 8h, and 24h versus 48h (one-way ANOVA, Holm-Sidak method, $p>0.05$). As for the 60 nm Ag NPs dissolution changed in time in a statistically significant manner, with significant differences between 2h versus 24h, 2h versus 48h, and 4h versus 48h (one-way ANOVA, Holm-Sidak method, $p<0.05$). Dissolution did not differ in time for 50 nm Ag NPs and for Ag_2S NPs (Kruskal-Wallis test, $p>0.05$).

3.4.2. Water exposure bioaccumulation test

Very low mortality (<3%) was observed in this experiment. Total and dissolved Ag concentrations in collected water samples following ultrafiltration are displayed in Table S3.2. Total Ag concentrations in water were close to the nominal value of 10 µg Ag L^{-1}, except for the Ag_2S NPs, where the Ag concentration was twice the nominal value (Table S3.2). No significant differences (Kruskall-Wallis test, $p>0.05$) were found between the Ag forms tested. Very low to no dissolved Ag was measured at day 0, but an increase was observed in all exposures at day 1, which was significant (Holm-Sidak method, $p<0.05$) for 3-8 nm Ag NPs and $AgNO_3$ (Table S3.2). Higher dissolved Ag concentrations were found for 60 nm Ag NPs and $AgNO_3$ exposures. Significant differences between Ag forms (one-way ANOVA, Holm-Sidak method, $p<0.05$) were only reported at day 2 (Table S3.2). At day 2, Ag_2S NPs presented the lowest Ag dissolution (0.41 ± 0.04%), followed by 3-8 nm (0.58

± 0.11%), 50 nm (0.63 ± 0.05%) and 60 nm (3.78 ± 0.71%) Ag NPs, with the highest free ionic Ag^+ concentration measured for $AgNO_3$ (5.87 ± 1.81%).

Table S3.3 presents the total Ag concentrations in water and sediment samples from day 0 to day 2. Concentrations in water at day 0 were close to nominal (10 µg Ag L^{-1}) for all Ag forms. The Ag treatment and time influenced the Ag concentrations measured in water samples, and a significant interaction was found between both factors (two-way ANOVA, Holm-Sidak method, $p<0.05$). At day 0, water concentrations were significantly higher (two-way ANOVA, Holm-Sidak method, $p<0.05$) in the Ag_2S NP treatment. At day 1, significant decreases (two-way ANOVA, Holm-Sidak method, $p<0.05$) in Ag concentrations occurred for 60 nm Ag NPs, Ag_2S NPs and $AgNO_3$ (Table S3.3). Concentrations in water were significantly reduced at day 2 (two-way ANOVA, Holm-Sidak method, $p<0.05$) in all Ag treatments and did not differ (two-way ANOVA, Holm-Sidak method, $p>0.05$) between treatments (Table S3.3). A background concentration of 1.54 ± 1.40 µg Ag kg^{-1} was measured in samples from the initial sediment batch and this value was used as the initial exposure level in all treatments. Concentrations of Ag in sediment were influenced by time and Ag treatment, with an increase in sediment Ag concentrations generally observed from day 0 to 2, which was significant for the 60 nm Ag NPs, Ag_2S NPs and $AgNO_3$ treatments (two-way ANOVA, Holm-Sidak method, $p<0.05$) (Table S3.3). Concentrations at days 1 and 2 were generally lower for the 3-8 nm and 50 nm Ag NPs when compared to the other Ag forms. The factors showed a significant interaction (two-way ANOVA, Holm-Sidak method, $p<0.05$) (Table S3.3).

Uptake and elimination kinetics and rate constants for Ag bioaccumulation in the chironomids are shown in Figure 3.1 and Table 3.1, respectively. Table 3.1 also presents the average values for concentrations measured in water and sediment (see Table S3.3), which were used as C_{exp} in the model. Sediment concentrations were converted to mg kg^{-1} to present uniformed units of k1 (in $g_{sediment}\ g^{-1}_{organism}\ hour^{-1}$) from uptake through sediment (Table 3.1).

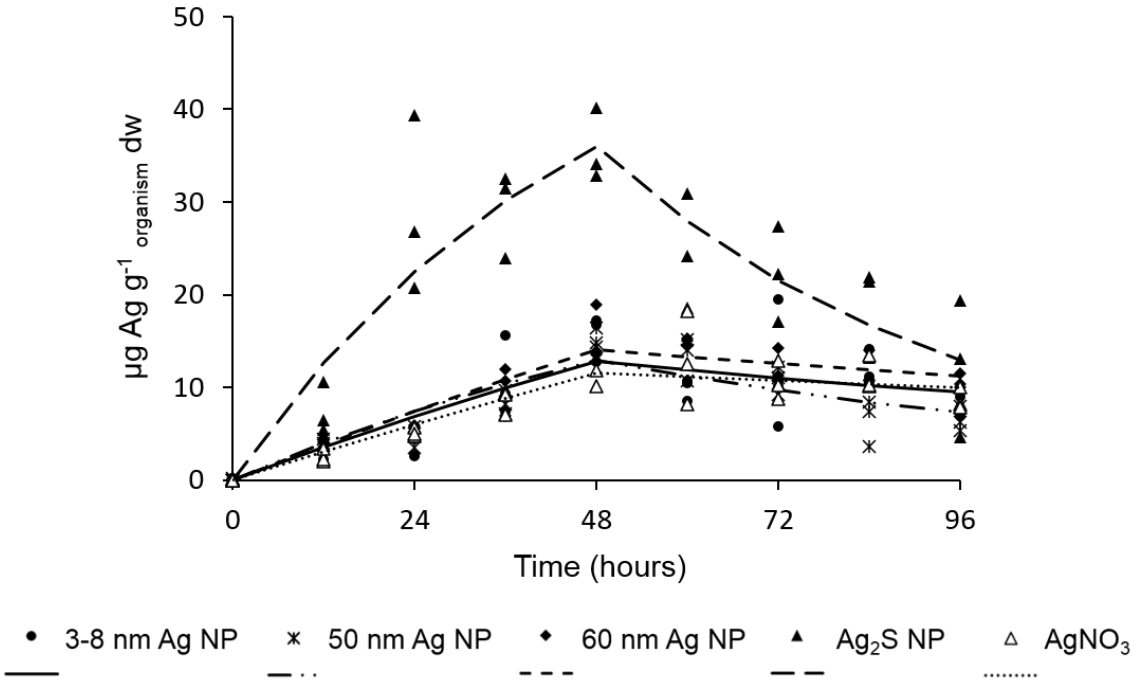

Figure 3.1. Uptake and elimination of Ag in *Chironomus riparius* larvae exposed to 3-8 nm, 50 nm and 60 nm Ag NPs, Ag_2S NPs and $AgNO_3$. Larvae were exposed for 48 hours in water spiked at a nominal concentration of 10 µg Ag L^{-1} and then transferred to clean water for 48 hours. Data points represent Ag concentrations measured in larvae and lines represent the fit of a one-compartment model. See Table 3.1 for the corresponding kinetic parameters.

Significantly higher internal Ag concentrations (one-way ANOVA, Holm-Sidak method, $p<0.05$) were measured in larvae from Ag_2S NP exposure compared to the other Ag treatments. At the last sampling time of the uptake phase (48h), concentrations in larvae were higher for Ag_2S NPs (35.7 µg Ag g^{-1} dw), followed by 3-8 nm (15.6 µg Ag g^{-1} dw), 60 nm (15.5 µg Ag g^{-1} dw), and 50 nm (15.2 µg Ag g^{-1} dw) Ag NPs, and the lowest for $AgNO_3$ exposure (11 µg Ag g^{-1} dw). Higher Ag uptake rates were found for chironomid larvae exposed to Ag_2S NPs. The uptake curves of all the other Ag forms were similar. Organisms exposed to Ag_2S NPs also revealed faster elimination, followed by 50 nm Ag NPs (Figure 3.1). Low k1 values were generally found for all treatments considering water as exposure route (Table 3.1). For water exposure, highest k1 values were found upon Ag_2S NP exposure and lowest for 3-8 nm Ag NPs. No significant differences ($X^2_{(1)}<3.84$; $p>0.05$) were detected between 3-8 nm, 60 nm Ag NPs and $AgNO_3$ exposures (Table 3.1). BCF_ks were highest for larvae exposed to $AgNO_3$, but differed only by a factor of three from the lowest BCF_k value, determined for 50 nm Ag NPs (Table 3.1).

Considering exposure through sediment, the highest k1 value was found for larvae exposed to 3-8 nm Ag NPs, followed by Ag_2S NPs and 50 nm Ag NPs, with values not differing significantly ($X^2_{(1)}<3.84$; $p>0.05$). The highest k2 value was calculated for the Ag_2S

NPs and the lowest for $AgNO_3$, the latter not differing ($X^2_{(1)}$<3.84; p>0.05) from the k2 values for 3-8 nm and 60 nm Ag NPs. The chironomid larvae showed similar internal Ag concentrations for all Ag forms at the end of the elimination phase, with values in the increasing order of 6.51 µg Ag g^{-1} dw for 50 Ag NPs, 7.71 µg Ag g^{-1} dw for 3-8 nm Ag NPs, 8.68 µg Ag g^{-1} dw for $AgNO_3$, 10.6 µg Ag g^{-1} dw for 60 Ag NPs, and 12.4 µg Ag g^{-1} dw for Ag_2S NPs.

3.4.3. Sediment exposure bioaccumulation test

Mortality was below 3% in this test. Table 3.2 displays the measured Ag concentrations in sediment and sediment pore water. Concentrations measured in sediments were close to nominal (1 mg Ag kg^{-1}) for all Ag forms, being significantly higher (Holm-Sidak method, p<0.05) for the Ag_2S NP exposure, at 1.27 mg Ag kg^{-1} (Table 3.2). Silver concentrations measured in sediment pore water were in the same range as in the experiments with water exposure (Tables 3.1 and 3.2). Sediment pore water concentration for the 3-8 nm Ag NPs was highest, and significantly higher (Holm-Sidak method, p<0.05) than the lowest value measured for $AgNO_3$ (Table 3.2). Highest internal Ag concentrations were determined for chironomid larvae exposed to Ag_2S NPs (144 µg Ag g^{-1} dw), followed by 3-8 nm Ag NPs (58.1 µg Ag g^{-1} dw), 60 nm Ag NPs (36.7 µg Ag g^{-1} dw), $AgNO_3$ (30 µg Ag g^{-1} dw) and 50 nm Ag NPs (17.3 µg Ag g^{-1} dw). Uptake rates were higher for larvae exposed to Ag_2S NPs although the elimination rate was slower (Figure 3.2, Table 3.2). Larvae exposed to the 50 nm Ag NPs revealed the slowest uptake rate and a very slow elimination rate. Elimination was also slow for the 60 nm Ag NPs and $AgNO_3$, while organisms exposed to 3-8 nm Ag NPs eliminated Ag at a faster rate (Figure 3.2).

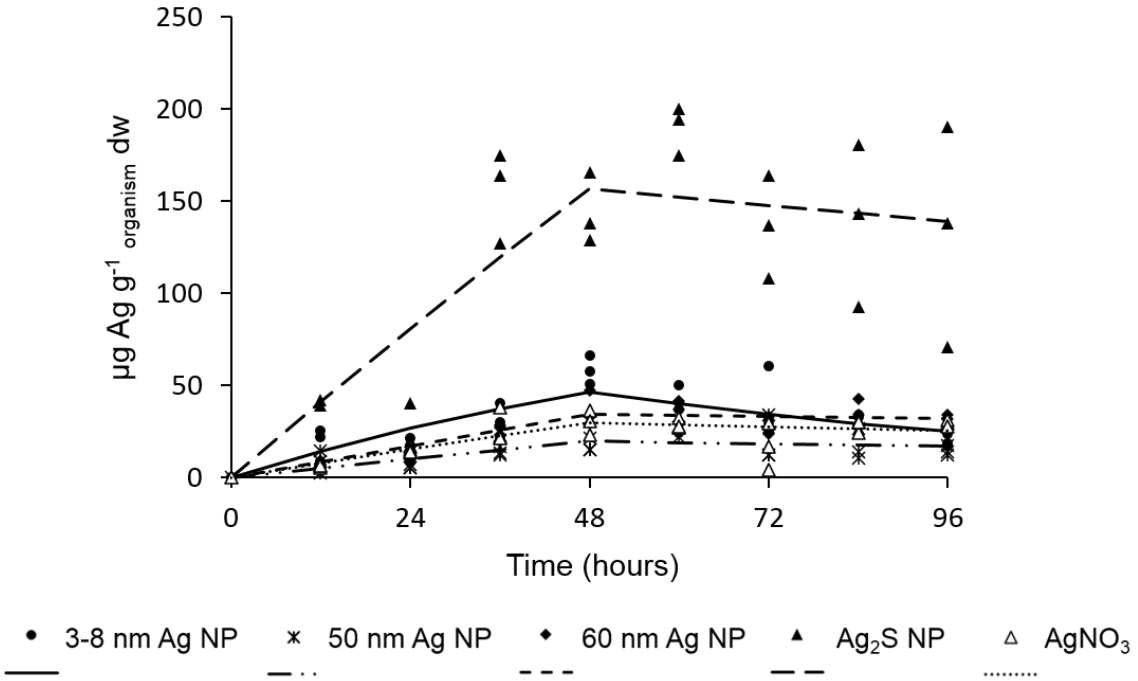

Figure 3.2. Uptake and elimination of Ag in *Chironomus riparius* larvae exposed to 3-8 nm, 50 nm and 60 nm Ag NPs, Ag_2S NPs and $AgNO_3$. Larvae were exposed for 48 hours in sediment spiked at a nominal concentration of 1 mg Ag kg^{-1} and then transferred to clean sediment for 48 hours. Data points represent Ag concentrations measured in larvae and lines represent the fit of a one-compartment model. See Table 3.2 for the corresponding kinetic parameters.

For both sediment and pore water exposure routes, the highest k1 value was found for chironomid larvae upon Ag_2S NP exposure and the lowest for 50 nm Ag NPs (Table 3.2). For sediment exposure, k1 values for Ag_2S NPs and 3-8 nm Ag NPs differed significantly ($X^2_{(1)}$>3.84; p<0.05) from each other and from the other Ag forms, while for the pore water exposure the same relationship was observed between k1 values for Ag_2S NPs and 50 nm Ag NPs (Table 3.2). Very low k2 values were found, with the highest one reported for the 3-8 nm Ag NPs and the lowest for the 60 nm Ag NPs (Table 3.2). Larvae exposed to the Ag_2S NPs showed the higher $BSAF_{ksed}$ and BCF_{kspw} values, while individuals exposed to the 3-8 nm Ag NPs revealed the lowest $BSAF_{ksed}$ and BCF_{kspw} (Table 3.2).

Table 3.1. Uptake (k1) and elimination (k2) rate constants (± 95% confidence intervals (CI)) for Ag uptake in *Chironomus riparius* larvae exposed to water spiked at a nominal concentration of 10 µg Ag L^{-1} with 3-8 nm, 50 nm and 60 nm Ag NPs, Ag_2S NPs and $AgNO_3$. Also shown are mean values of the measured Ag exposure concentrations in water and sediment as reported in Table S3.3 (µg Ag L^{-1} or mg Ag kg^{-1} dry sediment; mean ± standard deviation SD; *n*=3), which were used as C_{exp} in the kinetics modelling; bioconcentration factor (BCF_k) of Ag in *C. riparius* exposed through water. Different capital letters within a column indicate statistically significant differences between k1 or k2 for different Ag forms ($X^2_{(1)}$>3.84; p<0.05).

Ag form	Mean measured concentration in water (µg Ag L^{-1})	Mean measured concentration in sediment (mg Ag kg^{-1})	k1 from water (L_{water} $g^{-1}_{organism}$ $hour^{-1}$)	k1 from sediment ($g_{sediment}$ $g^{-1}_{organism}$ $hour^{-1}$)*	k2 ($hour^{-1}$)	BCF_k (L g^{-1})
3-8 nm	7.45 ± 3.83	0.002 ± 0.003	0.041 (0.030-0.053) **A**	137 (112-197) **A**	0.0062 (0-0.013) **A,B**	6.6
50 nm	5.91 ± 3.44	0.003 ± 0.004	0.060 (0.049-0.071) **B**	113 (96-141) **A**	0.012 (0.0070-0.017) **A,C**	5.0
60 nm	6.82 ± 3.20	0.01 ± 0.001	0.048 (0.042-0.055) **A**	41.6 (35-47) **B**	0.0048 (0.0016-0.0079) **B**	10
Ag_2S NPs	7.90 ± 4.99	0.01 ± 0.01	0.15 (0.12-0.18) **C**	116 (98-142) **A**	0.021 (0.015-0.027) **C**	7.1
$AgNO_3$	5.60 ± 3.32	0.01 ± 0.01	0.046 (0.037-0.056) **A**	34.8 (30-45) **B**	0.0031 (-0.0013-0.0074) **B**	15

Table 3.2. Uptake (k1) and elimination (k2) rate constants (value ± 95% confidence intervals (CI)) for Ag uptake in *Chironomus riparius* larvae exposed to sediment spiked at a nominal concentration of 1 mg Ag kg^{-1} with 3-8 nm, 50 nm and 60 nm Ag NPs, Ag_2S NPs and $AgNO_3$. Also shown are the measured concentrations in sediment and sediment pore water (mg Ag kg^{-1} or µg Ag L^{-1}; mean ± standard deviation SD; *n*=3); biota-to-sediment accumulation factors for sediment exposure ($BSAF_{ksed}$) and bioconcentration factors for sediment pore water exposure (BCF_{kspw}) of Ag in *C. riparius* exposed through sediment and pore water, respectively. Different capital letters within a column indicate statistically significant differences in k1 or k2 values between Ag forms ($X^2_{(1)}$>3.84; p<0.05). Different small letters within a column indicate statistically significant differences in concentrations between Ag forms (one-way ANOVA followed by Holm-Sidak Method, p<0.05).

Ag form	Mean measured concentrations in sediment (mg Ag kg^{-1})	Mean measured concentrations in sediment pore water (µg Ag Lg^{-1})	k1 from sediment ($g_{sediment}$ $g^{-1}_{organism}$ $hour^{-1}$)	k1 from sediment pore water (L_{water} $g^{-1}_{organism}$ $hour^{-1}$)	k2 ($hour^{-1}$)	$BSAF_{ksed}$ (g g^{-1})	BCF_{kspw} (L g^{-1})
3-8 nm	0.93 ± 0.02 **a**	11.5 ± 1.08 **a**	1.39 (0.99-1.80) **A**	0.11 (0.080-0.15) **A**	0.013 (0.0047-0.021) **A**	109	8.9
50 nm	0.70 ± 0.05 **b**	8.92 ± 1.03 **a,b**	0.64 (0.40-0.87) **B**	0.050 (0.031-0.069) **B**	0.0032 (-0.0051-0.012) **A,B**	199	16
60 nm	1.00 ± 0.09 **a**	5.94 ± 1.36 **a,b**	0.74 (0.58-0.89) **B**	0.12 (0.098-0.15) **A**	0.0013 (-0.0032-0.0058) **B**	577	97
Ag_2S NPs	1.27 ± 0.13 **c**	4.27 ± 6.23 **a,b**	2.74 (1.93-3.55) **C**	0.81 (0.57-1.05) **C**	0.0025 (-0.0040-0.0091) **A,B**	1078	321
$AgNO_3$	0.89 ± 0.01 **a**	4.07 ± 1.05 **b**	0.75 (0.54-0.96) **B**	0.16 (0.12-0.21) **A**	0.0032 (-0.0031-0.0096) **A,B**	232	50

Exuviae from larvae exposed to Ag_2S NPs revealed the highest Ag concentration while the respective imagines (adults) showed the lowest internal Ag concentration (Table 3.3). For the 3-8 nm Ag NP exposure, the imagines had higher Ag concentrations than the respective exuviae. Both exuviae and imagines of the $AgNO_3$ treatment had higher Ag % relative to internal Ag concentrations in the larvae sampled at 48h. Concentrations were significantly higher (*t-test*, $p<0.05$) in exuviae than in imagines from the Ag_2S NPs treatment (Table 3.3).

Table 3.3. Internal Ag concentrations (µg Ag g^{-1} dw; mean ± standard deviation SD; *n*=3) of exuviae and imagines emerged from *Chironomus riparius* larvae exposed to sediment spiked at a nominal concentration of 1 mg Ag kg^{-1} with 3-8 nm Ag NP, Ag_2S NP and $AgNO_3$. The Ag level (%) in exuviae and in imagines is given relative to the Ag concentrations measured in larvae sampled at 48h. Common capital letters within a column indicate no statistically significant differences between Ag forms (one-way ANOVA, $p>0.05$). Different small letters within a row indicate statistically significant differences between life stages (*t-test*, $p<0.05$).

Ag form	Exuviae	Ag % exuviae	Imagines	Ag % imagines
3-8 nm	4.24 ± 3.36 **A** / *a*	7.30	6.58 ± 3.19 **A** / *a*	11.3
Ag_2S NPs	14.5 ± 6.92 **A** / *a*	10.0	1.60 ± 2.71 **A** / *b*	1.11
$AgNO_3$	7.26 ± 4.13 **A** / *a*	24.2	6.26 ± 2.04 **A** / *a*	20.9

3.4.4. Food exposure bioaccumulation test

No mortality was observed in this test. Uptake and elimination rate curves are show in Figure 3.3, and toxicokinetic parameters and Ag concentration measured in food are presented in Table 3.4. Ag concentrations were significantly higher (one-way ANOVA, Holm-Sidak method, $p<0.05$) in alder leaves spiked with the 60 nm Ag NPs (21.2 mg Ag kg^{-1} dw) and $AgNO_3$ (13.5 mg Ag kg^{-1} dw) than the other Ag forms, and lowest for the 50 nm Ag NPs (1.96 mg Ag kg^{-1} dw) (Table 3.4). The chironomid larvae contained very low internal Ag concentrations in all food treatments, which for 3-8 nm, 50 nm and 60 nm Ag NPs and $AgNO_3$ did not differ from the control (data not shown), so no significant uptake occurred (two-way ANOVA, Holm-Sidak method, $p>0.05$). Only the larvae exposed to Ag_2S NPs revealed a significant Ag uptake rate (two-way ANOVA, Holm-Sidak method, $p<0.05$) (Figure 3.3).

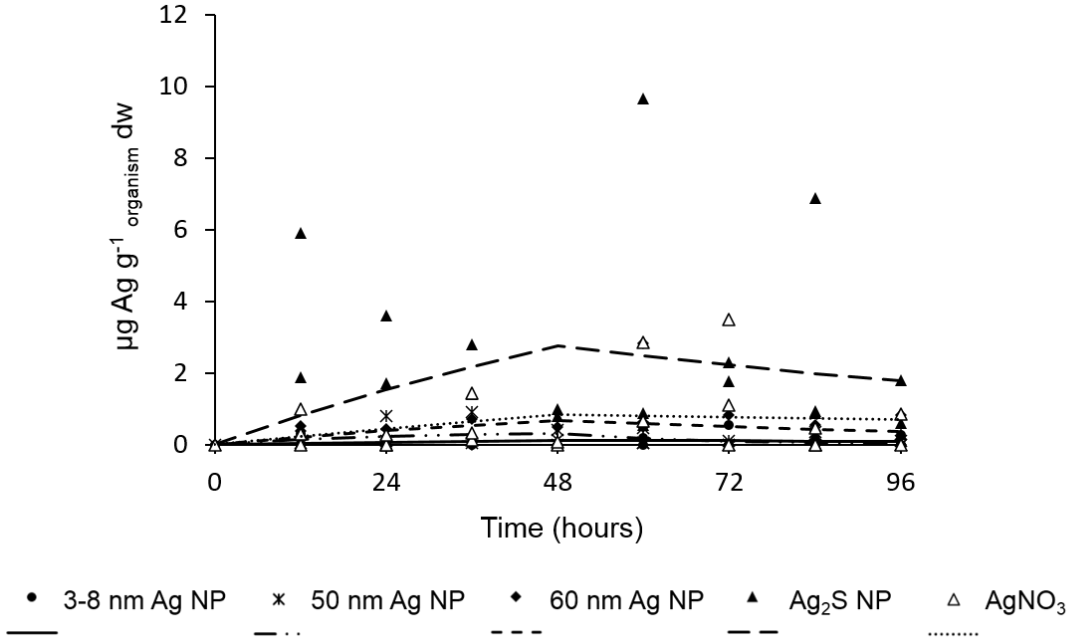

Figure 3.3. Uptake and elimination of Ag in *Chironomus riparius* larvae exposed to 3-8 nm, 50 nm and 60 nm Ag NPs, Ag_2S NPs and $AgNO_3$. Larvae were exposed for 48 hours to spiked food (alder leaves) and then exposed to clean food for 48 hours. Data points represent Ag concentration measured in larvae and lines represent the fit of a one-compartment model. See Table 3.4 for the corresponding kinetic parameters.

Larvae exposed to Ag_2S NPs had the highest k1 (0.02 g_{food} $g^{-1}_{organism}$ $hour^{-1}$) and k2 (0.01 $hour^{-1}$) values but due to the scatter in the data these values were not significantly higher ($X^2_{(1)}$<3.84; p>0.05) than the values for the other Ag forms (Table 3.4).

Table 3.4. Uptake (k1) and elimination (k2) rate constants (value ± 95% confidence intervals (CI)) for Ag uptake by *Chironomus riparius* larvae exposed to alder leaves dosed with 3-8 nm, 50 nm and 60 nm Ag NPs, Ag_2S NPs and $AgNO_3$. The leaves were spiked by soaking in a solution containing a nominal concentration of 10 µg Ag L^{-1}. Also shown are measured concentrations in the leaves (mg Ag kg^{-1}; mean ± standard deviation SD; *n*=3). Common capital letters within a column indicate no statistically significant differences in k1 or k2 values between Ag forms ($X^2_{(1)}$<3.84; p>0.05). Different small letters within a column indicate statistically significant differences in Ag concentrations between Ag forms (one-way ANOVA followed by Holm-Sidak Method, p<0.05).

Exposure route	Ag form	Measured concentration (mg Ag kg^{-1})	k1 (g_{food} $g^{-1}_{organism}$ $hour^{-1}$)	k2 ($hour^{-1}$)
Food	3-8 nm	3.28 ± 2.26 **a**	0.00083 (-0.00080-0.0025) **A**	0.0043 (-0.036-0.045) **A**
	50 nm	1.96 ± 0.22 **a**	0.0086 (-0.0018-0.019) **A**	0.050 (-0.019-0.12) **A**
	60 nm	21.2 ± 6.31 **b**	0.00089 (0-0.0019) **A**	0.013 (-0.017-0.043) **A**
	Ag_2S NPs	3.18 ± 3.56 **a**	0.022 (-0.0040-0.049) **A**	0.0091 (-0.020-0.038) **A**
	$AgNO_3$	13.5 ± 1.95 **b**	0.0014 (-0.00069-0.0035) **A**	0.0038 (-0.030-0.038) **A**

3.5. Discussion

3.5.1. Nanoparticle stability

The hydrodynamic size of all NPs in ASTM medium increased from time point 0h to 48h, most considerably for the 3-8 nm Ag NPs and for the Ag_2S NPs despite their organic/polymer coatings (Table S3.1). This increase was also previously observed in artificial pond water (APW) medium, in which hydrodynamic diameters relatively similar to those obtained in ASTM medium were observed (Silva et al., 2020). For the 50 nm Ag NPs, the hydrodynamic size nearly doubled (89.1 ± 3.45 nm at 48h) compared to the nominal size (Table S3.1), while in UPW the hydrodynamic size remained close to nominal (~58 nm). In APW medium the increase was remarkably higher, with diameters of 1840 ± 503 nm at 48h (Silva et al., 2020). APW and ASTM hard waters are two media with high ionic strength, which promotes the aggregation/agglomeration of NPs, leading to the higher measured hydrodynamic sizes in time. The zeta potentials for the 3-8 nm and 50 nm Ag NPs and Ag_2S NPs were less negative and far from the considered stable range (< -30 mV, > 30 mV) in ASTM medium compared to UPW, revealing the electrostatic inter-particle repulsion was moderate in ASTM medium. For the 60 nm Ag NPs, stability seemed similar in ASTM and APW as equivalent zeta potential values and hydrodynamic diameters were observed (Silva et al., 2020).

Dissolution of the 3-8 nm and the 50 nm Ag NPs was lower in ASTM medium than in either UPW or APW (Silva et al., 2020). Dissolution was higher for the 3-8 nm than for the 50 nm Ag NPs in ASTM medium, as expected due to the higher surface area to size ratio of the 3-8 nm Ag NPs, but the dissolution percentages of these two NPs differed less than in the case of APW (Silva et al., 2020). For the 60 nm Ag NPs dissolution was lower in ASTM medium than in UPW (dissolution around 29%) but slightly higher than in APW and with some evidence of re-precipitation, due to Ostwald ripening or formation of new phases, due to the observed decrease in the dissolved Ag over the 48h period (Table S3.1). For further discussion, see Silva et al. (2020).

3.5.2. Water exposure bioaccumulation test

Ag concentrations and uptake kinetics in larvae exposed to Ag_2S NPs were higher than for the other Ag forms, suggesting higher bioavailability of the simulated aged Ag form and similar but lower bioavailability for the other treatments (Figure 3.1 and Table 3.1). The higher dissolved Ag concentrations in ASTM medium at days 1 and 2 in the 60 nm Ag NP and $AgNO_3$ treatments may be indicative of higher concentrations of available Ag^+ in the

water column (Table S3.2). In our previous study, exposing the freshwater snail *Physa acuta* to the same nominal concentration of the same Ag forms, the 60 nm Ag NPs and $AgNO_3$ also demonstrated higher dissolution in APW, which generally resulted in higher Ag uptake rates from water by the snails (Silva et al., 2020). Thus, considering that uptake rates and k1 values for 60 nm Ag NPs and $AgNO_3$ were significantly lower than those for Ag_2S NPs, dissolution in the water column probably contributed less to Ag uptake in the chironomid larvae. Still, it is likely that the overlying water was an uptake route in this study. Chironomid larvae can be exposed to overlying water when irrigating their burrows or leaving this refuge to feed on superficial sediment. Since this study used inorganic sediment and no food was provided, larvae may have left the burrow more often to search for food, potentially leading to higher exposure to the overlying water than may occur naturally. When accounting for Ag concentrations in the sediment, remarkably higher k1 values were estimated, meaning that larvae had to ingest very high amounts of sediment to reach the observed internal concentrations, which seems unlikely (Table 3.1). This suggests that sediment concentrations were probably too low to explain uptake, thus ingestion of sediment particles probably had only low contribution to total Ag uptake in this test.

The chironomid larvae were exposed to NPs following settlement from the water column into the surface sediment. The higher dissolution of 60 nm Ag NPs and the large proportion of the $AgNO_3$ that existed as free Ag^+ ions (Table S3.2) led to higher availability of Ag^+ ions in the water column and to the formation of complexes with ions in the medium, such as AgCl (Buffet et al., 2014). The fast sedimentation of these complexes may explain the significant reduction of Ag concentrations in water samples at day 1 observed for 60 nm Ag NPs and $AgNO_3$ exposures, and the significant increase in sediment concentrations in the latter. Settlement of NPs and possibly of AgCl complexes may also have occurred in the 3-8 nm and 50 nm Ag NP treatments. In the Ag_2S NP treatment, Ag concentrations were also significantly reduced in water and significantly increased in sediments at day 1, which can be an indication of fast particle sedimentation (Table S3.3). Additionally, adsorption to the glass vial walls could also have caused Ag concentration in the water medium to decrease (Sekine et al., 2015). The absence of organic matter in the sediment used may have contributed to the lower stability of the pristine Ag NPs (Navarro et al., 2008) since they were not protected from dissolution by the binding of natural organic matter and formation of an acquired macromolecule corona (Markiewicz et al., 2018; Xu et al., 2020). Thus, to explain the higher uptake of Ag from the Ag_2S NPs, it can be hypothesised that their high stability resulted in almost null dissolution and weaker association with the sediment particles after settlement, leading to some exchange of Ag_2S NPs to the water, for instance,

due to the reworking activity of larvae. This could have contributed to an additional Ag uptake route for the chironomid larvae, either by exposure to water in the interface with sediment when foraging or to sediment pore water, for instance, through pumping water for burrow irrigation and/or uptake through the integument, since *C. riparius* have a relatively large exposed epithelial surface area for respiration (Buchwalter et al., 2002). The anal papillae of chironomid larvae are permeable to water, therefore intake of water through the anal papillae may also be an uptake route for contaminants in chironomids (Krantzberg and Stokes, 1990). Nevertheless, further investigation is needed to confirm if this a possible uptake route for NPs. In contrast, the lack of passivation of the Ag NP surface in the other treatments may have resulted in stronger association of Ag nanoparticles with sediment particles and/or to increasing dissolution and subsequent adsorption of Ag ions to sediment particles (Rajala et al., 2017). This could have led to lower exchange of Ag to the water/pore water phase resulting in lower uptake when compared to that of the Ag_2S NP treatment. This could also provide a possible explanation for the similar uptake rates observed for the pristine Ag NP and $AgNO_3$ exposures. However, this is merely speculative since the influence of concentrations in pore water was not considered in this test.

The sediment-dwelling oligochaete *Tubifex tubifex* seemed to avoid sediment amended with $AgNO_3$, but not with Ag NPs, at comparable concentrations (Tangaa et al., 2018). In the present study, avoidance behaviour probably does not explain the observed differences in uptake between Ag_2S NPs and the other Ag forms, due to the low concentrations measured in water and sediments compared to previous toxicity studies exposing *C. riparius* larvae to 3-8 nm Ag NPs (the same particles as used in this study) and $AgNO_3$ (see Lopes, 2015).

The chironomid larvae exposed to Ag_2S NPs showed a higher k2 value, thus faster elimination (Figure 3.1, Table 3.1). Such a fast Ag elimination from the body was also seen for *P. acuta* exposed to Ag_2S NPs (Silva et al., 2020). Interestingly, the chironomid larvae revealed similar internal Ag concentrations for all Ag forms at the end of the experiment, even though k2 values and elimination rates were different (Figure 3.1 and Table 3.1). Different cellular uptake pathways have been demonstrated for Ag NPs that determine their intracellular fate and consequently elimination (Khan et al., 2015). One assumption can be that elimination of ionic Ag and NPs operated through different mechanisms in chironomid larvae. For instance, nanoparticulate Ag may have been eliminated faster from the organism, possibly with the excretion of sediment particles, or by some cellular pathway that led to faster efflux (e.g., caveolae-mediated endocytosis was responsible for faster effluxes of Ag NPs (Khan et al., 2015)). Thus, the higher k2 determined in Ag_2S NP

exposure may reflect lower retention and faster excretion of the simulated aged form in the larvae. In turn, the lowest k2 value determined for chironomid larvae exposed to $AgNO_3$ may suggest that the similar Ag concentrations measured in the larvae from the different Ag treatments on the last day of the elimination phase could be related to the portion of internalized Ag (e.g., that was translocated from the gut into other tissues, or absorbed through the integument) (Figure 3.1). Accumulation of Ag in the estuarine polychaete *Nereis diversicolor* exposed to Ag NPs and $AgNO_3$ showed two different strategies of internal Ag distribution, with ionic Ag being mainly associated with metallothioneins (MTs) and Ag NPs associated predominantly with organelles, inorganic granules or heat denatured proteins (García-Alonso et al., 2011). *C. riparius* larvae also revealed different strategies to deal with trace metals, such as reducing arsenate to arsenite in the midgut (Mogren et al., 2013), accumulation in metal-rich granules (MRGs) (Béchard et al., 2008), or sequestration by MTs or MT-like proteins (Arambourou et al., 2013; Gillis et al., 2002; Gimbert et al., 2016; Toušová et al., 2016). Therefore, sequestration of Ag^+ by MTs or other detoxification strategies, such as MRGs, dealing with Ag ions and Ag NPs is likely to have occurred in the present study, yet more research is needed to investigate that.

3.5.3. Sediment exposure bioaccumulation test

3.5.3.1. Uptake and elimination kinetics in chironomid larvae

In the sediment test, internal Ag concentration, uptake rate and k1 value were also substantially higher in chironomid larvae exposed to Ag_2S NPs than the other Ag forms (Figure 3.2, Table 3.2). Again, these results suggest a more efficient uptake of this Ag form. Uptake patterns of Ag in the sediment test were generally similar to the water exposure test, despite the different spiking medium (directly to sediment in this case) and the much higher concentrations than those measured in sediments from the water test. This suggests a similar uptake scenario in both tests. It is possible that sediment pore water was a more important uptake route for chironomid larvae in the sediment exposure test. Similar to what was hypothesized for the water exposure test, the stable Ag_2S NPs could have been weakly bound to the sediment particles and be exchanged easier to the pore water than the Ag NPs and $AgNO_3$. The reworking activity of chironomid larvae creates a microenvironment that could have contributed to further dissolution of the Ag NPs and $AgNO_3$ and further exchange of NPs to the pore water which could have been higher for Ag_2S NPs if less tightly bound to the sediment (Warren et al., 1998). Although Ag concentrations in sediment pore water were the lowest for 60 nm Ag NPs, Ag_2S NPs and $AgNO_3$, the pore water samples

were taken from test vials without organisms, thus without the influence of their reworking activity. It should be noted that this is merely speculative since dissolution in sediments and/or the different metal species in the pore water were not analysed in the present study, nor was the effect of larvae activity on Ag distribution in the system determined explicitly.

Some studies have demonstrated that metal accumulation was better explained by pore water concentrations, for instance, accumulation of perfluoroalkyl compounds from both sediment and pore water by *C. riparius* occurred via dietary and integumentary routes (Bertin et al., 2014). Thus, uptake through the integument may have also occurred in the present test, and uptake through the anal pupillae, as previously suggested. Some freshwater insect larvae ingest water during feeding (Merritt and Cummins, 2008), thus passive uptake of water by chironomid larvae when ingesting sediment particles should not be disregarded. The higher Ag uptake in the Ag_2S NP exposures can mainly result from the exposure to pore water, but also ingestion of sediment particles. Aggregates of Al_2O_3 NPs were visually observed in the gut of *C. riparius*, indicating ingestion of NPs associated with sediment particles (Lorenz et al., 2017).

In both water and sediment exposure tests, lower BCF_ks and BCF_{kspw} were calculated for the 3-8 nm Ag NPs and values were relatively similar between experiments. In turn, BCF_ks and BCF_{kspw} for the other Ag forms were higher, particularly for the Ag_2S NPs in the sediment exposure test (Tables 3.1 and 3.2). The very low k2 values generally observed indicate that Ag was not efficiently eliminated from the body, thus suggesting high Ag bioaccumulation potential by the chironomid larvae. This can be the case for larvae exposed to Ag_2S NPs, that revealed a much higher $BSAF_{ksed}$, as a result of the higher Ag uptake but slow elimination, presenting the second lowest k2 value (Table 3.2). This contradicts the water exposure test result, in which faster elimination of the Ag_2S NPs was observed. In fact, in the sediment exposure test, elimination of Ag seemed to be generally lower than in the water exposure test (but higher for the 3-8 nm Ag NPs), suggesting that Ag was dealt with differently by larvae from water and sediment exposure experiments, in spite of the similar uptake patterns observed in both tests. Two factors should be considered. Firstly, given the much higher sediment concentrations and the reworking behaviour of chironomid larvae, higher exchange of Ag from sediment particles to pore water was a possible scenario, leading to higher Ag uptake. Secondly, in the sediment exposure test ingestion of sediment particles had probably a higher contribution for total Ag uptake, thus greater assimilation from the gut epithelia into tissue could have occurred upon the ingestion of sediment. Intracellular dissolution of Ag NPs can be an additional source of Ag ions (Khan et al., 2015). The gut fluid of deposit feeders contains soft ligands that can mobilize metals

from sediment but the way metals are bound to the sediment particles may also determine their mobilization (Chen et al., 2000). Several studies have suggested Ag NP internalization and subsequent interactions with subcellular compartments in *C. riparius* (Nair et al., 2013, 2011; Park et al., 2015). Although internal fate of Ag was not studied in the present work, multiple mechanisms for Ag uptake and internalization could have occurred in the chironomid larvae.

3.5.3.2. Bioaccumulation in exuviae and imagines

The results showed that pupal exuviae and imagines of chironomids from the $AgNO_3$ treatment contained somewhat higher proportions of Ag relative to the larvae sampled at 48h than those for the other Ag forms (Table 3.3). It is worth mentioning that larvae from the vials from which exuviae and imagines were sampled were kept for a longer time to reach emergence, thus internal Ag concentration in these larvae could have been higher due to the extended exposure. For the Ag_2S NPs only a minor portion (1.11%) of the bioaccumulated Ag seemed to have been transferred to imagines, while 10% were found in exuviae. This may suggest that the form transferred from larvae and/or pupa to exuviae and adult midges observed in the 3-8 nm Ag NP treatment was ionic Ag, and that very low uptake of Ag ions occurred upon exposure to Ag_2S NP which correlates with the low dissolution of these NPs.

Previous studies have shown that only a minor portion of Cu, Cd, Zn and Pb adsorbed to the *C. riparius* larvae exoskeleton (Timmermans et al., 1992). In the present test, adsorption of Ag from the exposure medium to the exuviae may also have been insignificant, although it cannot be ignored. Concentrations of Zn in *C. riparius* have been reported to decrease from larvae to imagines, while a steady increase of Zn concentrations was measured in larval skins and exuviae. In contrast, Cu was not transferred from one life stage to the next, since only very small concentrations were measured in larval skins, pupae, exuviae or imagines. This excluded the exuviae or larval skins as possible routes for Cu elimination and suggested that *C. riparius* efficiently eliminated Cu between larval and pupal stages (Timmermans and Walker, 1989). However, it should be noted that essential metals like Zn and Cu may be dealt with differently by the larvae than non-essential metals such as Ag. Results from the present study indicate that low amounts of Ag were transferred from larvae to the final (imagine) stage. Although Ag was not measured in pupae in the present study, Ag elimination could have occurred before or during the pupal stage. For instance, Ag could have been lost in a meconium (excretion between 4^{th} instar

and pupal stage), as has been reported for As (Mogren et al., 2013). It is possible that accumulated metals associated with the gut epithelium of chironomid larvae can be eliminated upon moulting or metamorphosis, since metals can be shed along with the epithelium (Timmermans et al., 1992).

3.5.4. Food exposure bioaccumulation test

Upon food exposure, only chironomid larvae from the Ag_2S NP treatment revealed Ag uptake. Interestingly, for the 60 nm Ag NPs and $AgNO_3$ significantly higher Ag concentrations were measured in the leaves, indicating higher exposure (Table 3.4). Since the leaves were spiked by soaking in solutions of the different Ag forms, it is likely that the higher dissolution of the 60 nm Ag NPs and $AgNO_3$ contributed to the higher leaf-Ag concentration, also suggesting that mainly Ag ions adsorbed to the leaves. Again, the higher internal Ag concentrations reported point to a higher bioavailability of the Ag_2S NPs. One hypothesis could be that the stable Ag_2S NPs may have been less tightly bound to the leaves than the other Ag NPs leading to higher detachment from the food inside the gut probably leading to higher absorption. A study observed mouthpart deformities in *C. riparius* larvae exposed from the 1st instar to the 4th instar to Ag NP spiked water at 0.002 µg L^{-1} (no sediment) (Tomilina and Grebenyuk, 2020). Considering this, it cannot be ruled out that larvae exposed to Ag NPs and $AgNO_3$ via food developed some mouthpart deformities impeding their feeding.

Leaves were not ground and were possibly more difficult for the chironomid larvae to ingest. *C. riparius* larvae mainly feed on microdetritus fragments and silt particles (Diepens et al., 2016; Ptatscheck et al., 2017). Nevertheless, spiking leaves was chosen in order to study ingestion of contaminated food separately from ingestion of contaminated sediment, thus using leaf disks allowed proper contamination of the food alone and easier handling. Additionally, feeding *C. riparius* larvae with alder leaf disks was performed in a previous test, showing that even 1st instar *C. riparius* larvae can feed on coarse organic matter (Campos et al., 2014). Another aspect that could have contributed to this was the short exposure period in the current food exposure test, which may not be sufficient for proper feeding. Moreover, the potential difficulties *C. riparius* larvae had to feed on the disk leaves could have promoted higher ingestion of uncontaminated sediment particles, which could have assisted elimination of some contaminated leaf particles from the gut.

3.6. Conclusions

Higher Ag uptake was consistently seen in *C. riparius* larvae exposed to Ag_2S NPs than in those exposed to the pristine Ag NPs, while larvae exposed to pristine Ag NPs and $AgNO_3$ generally presented similar kinetics. Interestingly, despite the different spiked media (water or sediment), the uptake patterns of the different Ag forms were similar for both water and sediment exposures, suggesting similar uptake routes. In both water and sediment tests, Ag uptake seemed to be better explained by exposure to water, either sediment pore water or at sediment-water interface, rather than the ingestion of sediment particles, although ingestion of sediment probably may have had some (albeit lower) contribution. The potential trophic link to terrestrial predators is weak since little Ag was transferred to adult midges, although some concerns can be raised for ionic Ag. In the food exposure, only larvae from the Ag_2S NP treatment revealed uptake, although it was very low, supporting the higher bioavailability of this Ag form. Still, the remarkably low accumulation generally observed in the food exposure test was probably due to the food type provided (disk leaves), therefore future experiments should provide ground food. In both water and sediment experiments, the behaviour and bioavailability of the different Ag forms could have been influenced by the absence of organic matter in the sediment. Thus, similar experiments using sediments with organic matter should be performed for comparison, especially to elucidate Ag_2S NP bioavailability and bioaccumulation in chironomid larvae.

In the absence of a food source, such as organic matter, chironomid larvae can take up Ag (by ingesting sediment alone or uptake through water), which indicates that Ag can still be available in environments with low nutritional sources. Using an environmentally relevant scenario (water spiked at 10 µg Ag L^{-1}) showed that *C. riparius* larvae can accumulate relatively high Ag concentrations and, in some cases, elimination can be extremely low, suggesting potential bioaccumulation of Ag in its nanoparticulate and/or ionic form. This may raise concerns about possible adverse effects in terms of chronic exposure and trophic transfer, especially in scenarios of continuous Ag NP/Ag_2S NP exposure such as in water bodies near agricultural settings exposed to sewage sludge or Ag NP based fertilisers or pesticides, or near wastewater treatment plant outfalls. The present study contributes data much needed to support the environmental risk assessment of Ag NPs and their transformation forms in benthic environments.

3.7. References

Arambourou, H., Gismondi, E., Branchu, P., Beisel, J.N., 2013. Biochemical and morphological responses in *Chironomus riparius* (Diptera, Chironomidae) larvae exposed to lead-spiked sediment. Environ. Toxicol. Chem. 32, 2558–2564.

Ardestani, M.M., van Straalen, N.M., van Gestel, C.A.M., 2014. Uptake and elimination kinetics of metals in soil invertebrates: A review. Environ. Pollut. 193, 277–295.

ASTM, 1980. ASTM (E729-80). Standard practice for conducting acute toxicity tests with fishes, macroinvertebrates and amphibians. Am. Stand. Test. Mater. Annu. B. ASTM Stand. 46, 279–280.

Baccaro, M., Undas, A.K., de Vriendt, J., van den Berg, J.H.J., Peters, R.J.B., Van Den Brink, N.W., 2018. Ageing, dissolution and biogenic formation of nanoparticles: How do these factors affect the uptake kinetics of silver nanoparticles in earthworms? Environ. Sci. Nano 5, 1107–1116.

Béchard, K.M., Gillis, P.L., Wood, C.M., 2008. Trophic transfer of Cd from larval chironomids (*Chironomus riparius*) exposed via sediment or waterborne routes, to zebrafish (*Danio rerio*): Tissue-specific and subcellular comparisons. Aquat. Toxicol. 90, 310–321.

Bertin, D., Ferrari, B.J.D., Labadie, P., Sapin, A., Garric, J., Budzinski, H., Houde, M., Babut, M., 2014. Bioaccumulation of perfluoroalkyl compounds in midge (*Chironomus riparius*) larvae exposed to sediment. Environ. Pollut. 189, 27–34.

Bour, A., Mouchet, F., Cadarsi, S., Silvestre, J., Baqué, D., Gauthier, L., Pinelli, E., 2017. CeO_2 nanoparticle fate in environmental conditions and toxicity on a freshwater predator species: a microcosm study. Environ. Sci. Pollut. Res. 24, 17081–17089.

Bour, A., Mouchet, F., Verneuil, L., Evariste, L., Silvestre, J., Pinelli, E., Gauthier, L., 2015. Toxicity of CeO_2 nanoparticles at different trophic levels - Effects on diatoms, chironomids and amphibians. Chemosphere 120C, 230–236.

Buchwalter, D.B., Jenkins, J.J., Curtis, L.R., 2002. Respiratory strategy is a major determinant of [^{3}H]water and [^{14}C]chlorpyrifos uptake in aquatic insects. Can. J. Fish. Aquat. Sci. 59, 1315–1322.

Buffet, P-E., Zalouk-Vergnoux, A., Châtel, A., Berthet, B., Métais, I., Perrein-Ettajani, H., Poirier, L., Luna-Acosta, A., Thomas-Guyon, H., Faverney, C.R., Guibbolini, M., Gilliland, D., Valsami-Jones, E., Mouneyrac, C., 2014. A marine mesocosm study on the environmental fate of silver nanoparticles and toxicity effects on two endobenthic species : The ragworm *Hediste diversicolor* and the bivalve mollusc *Scrobicularia plana*. Sci. Total Environ. 470–471, 1151–1159.

Campos, D., Alves, A., Lemos, M.F.L., Correia, A., Soares, A.M.V.M., Pestana, J.L.T., 2014. Effects of cadmium and resource quality on freshwater detritus processing chains: A microcosm approach with two insect species. Ecotoxicology 23, 830–839.

Cervantes-Avilés, P., Huang, Y., Keller, A.A., 2019. Incidence and persistence of silver nanoparticles throughout the wastewater treatment process. Water Res. 156, 188–198.

Chen, Z., Mayer, L.M., Quetel, C., Donard, O.F.X., Self, R.F.L., Jumars, P.A., Weston, D.P., 2000. High concentrations of complexed metals in the guts of deposit feeders. Limnol.

Oceanogr. 45, 1358–1367.

Clark, N.J., Boyle, D., Handy, R.D., 2019. An assessment of the dietary bioavailability of silver nanomaterials in rainbow trout using an ex vivo gut sac technique. Environ. Sci. Nano 6, 646–660.

Cornelis, G., Kirby, J.K., Beak, D., Chittleborough, D., McLaughlin, M.J., 2010. A method for determination of retention of silver and cerium oxide manufactured nanoparticles in soils. Environ. Chem. 7, 298–308.

Dabrin, A., Durand, C.L., Garric, J., Geffard, O., Ferrari, B.J.D., Coquery, M., 2012. Coupling geochemical and biological approaches to assess the availability of cadmium in freshwater sediment. Sci. Total Environ. 424, 308–315.

Diepens, N.J., Beltman, W.H.J., Koelmans, A.A., van den Brink, P.J., Baveco, J.M., 2016. Dynamics and recovery of a sediment-exposed *Chironomus riparius* population: A modelling approach. Environ. Pollut. 213, 741–750.

Ferrari, B.J.D., Faburé, J., 2017. Field assessment of reproduction-related traits of chironomids using a newly developed emergence platform (E-Board). Ecotoxicol. Environ. Saf. 137, 186–193.

Gallego-Gallegos, M., Doig, L.E., Tse, J.J., Pickering, I.J., Liber, K., 2013. Bioavailability, toxicity and biotransformation of selenium in midge (*Chironomus dilutus*) larvae exposed via water or diet to elemental selenium particles, selenite, or selenized algae. Environ. Sci. Technol. 47, 584–592.

García-Alonso, J., Khan, F.R., Misra, S.K., Turmaine, M., Smith, B.D., Rainbow, P.S., Luoma, S.N., Valsami-Jones, E., 2011. Cellular Internalization of Silver Nanoparticles in Gut Epithelia of the Estuarine Polychaete *Nereis diversicolor*. Environ. Sci. Technol. 45, 4630–4636.

Giese, B., Klaessig, F., Park, B., Kaegi, R., Steinfeldt, M., Wigger, H., von Gleich, A., Gottschalk, F., 2018. Risks, Release and Concentrations of Engineered Nanomaterial in the Environment. Sci. Rep. 8, 1–18.

Gillis, P.L., Diener, L.C., Reynoldson, T.B., Dixon, D.G., 2002. Cadmium-induced production of a metallothioneinlike protein in *Tubifex tubifex* (oligochaeta) and *Chironomus riparius* (diptera): Correlation with reproduction and growth. Environ. Toxicol. Chem. 21, 1836–1844.

Gimbert, F., Geffard, A., Guédron, S., Dominik, J., Ferrari, B.J.D., 2016. Mercury tissue residue approach in *Chironomus riparius*: Involvement of toxicokinetics and comparison of subcellular fractionation methods. Aquat. Toxicol. 171, 1–8.

Gimbert, F., Petitjean, Q., Al-Ashoor, A., Cretenet, C., Aleya, L., 2018. Encaged *Chironomus riparius* larvae in assessment of trace metal bioavailability and transfer in a landfill leachate collection pond. Environ. Sci. Pollut. Res. 25, 11303–11312.

Kaegi, R., Voegelin, A., Sinnet, B., Zuleeg, S., Siegrist, H., Burkhardt, M., 2015. Transformation of AgCl nanoparticles in a sewer system - A field study. Sci. Total Environ. 535, 20–27.

Khan, F.R., Misra, S.K., Bury, N.R., Smith, B.D., Rainbow, P.S., Luoma, S.N., Valsami-Jones, E., 2015. Inhibition of potential uptake pathways for silver nanoparticles in the estuarine snail *Peringia ulvae*. Nanotoxicology 9, 493–501.

Krantzberg, G., Stokes, P.M., 1990. Metal Concentrations and Tissues Distribution in

Larvae of *Chironomus* with Reference to X-ray Microprobe Analysis 93, 84–93.

Kuehr, S., Kaegi, R., Maletzki, D., Schlechtriem, C., 2021. Testing the bioaccumulation potential of manufactured nanomaterials in the freshwater amphipod *Hyalella azteca*. Chemosphere 263, 127961.

Lazareva, A., Keller, A.A., 2014. Estimating potential life cycle releases of engineered nanomaterials from wastewater treatment plants. ACS Sustain. Chem. Eng. 2, 1656–1665.

Lead, J.R., Batley, G.E., Alvarez, P.J.J., Croteau, M.N., Handy, R.D., McLaughlin, M.J., Judy, J.D., Schirmer, K., 2018. Nanomaterials in the environment: Behavior, fate, bioavailability, and effects—An updated review. Environ. Toxicol. Chem. 37, 2029–2063.

Lee, S.W., Park, S.Y., Kim, Y., Im, H., Choi, J., 2016. Effect of sulfidation and dissolved organic matters on toxicity of silver nanoparticles in sediment dwelling organism, *Chironomus riparius*. Sci. Total Environ. 553, 565–573.

Lopes, R.S., 2015. MSc thesis, University of Aveiro, Ecotoxicological assessment of engineered nanoparticles in *Chironomus riparius*. 110 p.

Lorenz, C.S., Wicht, A-J., Guluzada, L., Luo, L., Jager, L., Crone, B., Karst, U., Triebskorn, R., Liang, Y., Anwander, R., Haderlein, S.B., Huhn, C., Kohler, H-R., 2017. Nano-sized Al_2O_3 reduces acute toxic effects of thiacloprid on the non-biting midge *Chironomus riparius*. PLoS One 12, e0176356.

Markiewicz, M., Kumirska, J., Lynch, I., Matzke, M., Köser, J., Bemowsky, S., Docter, D., Stauber, R., Westmeier, D., Stolte, S., 2018. Changing environments and biomolecule coronas: Consequences and challenges for the design of environmentally acceptable engineered nanoparticles. Green Chem. 20, 4133–4168.

McGillicuddy, E., Murray, I., Kavanagh, S., Morrison, L., Fogarty, A., Cormican, M., Dockery, P., Prendergast, M., Rowan, N., Morris, D., 2017. Silver nanoparticles in the environment: Sources, detection and ecotoxicology. Sci. Total Environ. 575, 231–246.

Merritt, R.W., Cummins, K.W., 2008. An Introduction to the aquatic insects of North America. Choice Rev. Online 45, 41-73.

Mogren, C.L., Webb, S.M., Walton, W.E., Trumble, J.T., 2013. Micro x-ray absorption spectroscopic analysis of arsenic localization and biotransformation in *Chironomus riparius* Meigen (Diptera: Chironomidae) and *Culex tarsalis* Coquillett (Culicidae). Environ. Pollut. 180, 78–83.

Nair, P.M.G., Choi, J., 2012. Modulation in the mRNA expression of ecdysone receptor gene in aquatic midge, *Chironomus riparius* upon exposure to nonylphenol and silver nanoparticles. Environ. Toxicol. Pharmacol. 33, 98–106.

Nair, P.M.G., Choi, J., 2011. Identification, characterization and expression profiles of *Chironomus riparius* glutathione S-transferase (GST) genes in response to cadmium and silver nanoparticles exposure. Aquat. Toxicol. 101, 550–560.

Nair, P.M.G., Park, S.Y., Choi, J., 2013. Evaluation of the effect of silver nanoparticles and silver ions using stress responsive gene expression in *Chironomus riparius*. Chemosphere 92, 592–599.

Nair, P.M.G., Park, S.Y., Lee, S.W., Choi, J., 2011. Differential expression of ribosomal protein gene, gonadotrophin releasing hormone gene and Balbiani ring protein gene

in silver nanoparticles exposed *Chironomus riparius*. Aquat. Toxicol. 101, 31–37.

Navarro, E., Baun, A., Behra, R., Hartmann, N.B., Filser, J., Miao, A.J., Quigg, A., Santschi, P.H., Sigg, L., 2008. Environmental behavior and ecotoxicity of engineered nanoparticles to algae, plants, and fungi. Ecotoxicology 17, 372–386.

Niemuth, N.J., Curtis, B.J., Hang, M.N., Gallagher, M.J., Fairbrother, D.H., Hamers, R.J., Klaper, R.D., 2019. Next-Generation Complex Metal Oxide Nanomaterials Negatively Impact Growth and Development in the Benthic Invertebrate *Chironomus riparius* upon Settling. Environ. Sci. Technol. 53, 3860–3870.

OECD, 2017. Test No. 318: Dispersion Stability of Nanomaterials in Simulated Environmental Media. OECD Guideline for the Testing of Chemicals.

OECD, 2010. Test No. 233: Sediment-Water Chironomid Life-Cycle Toxicity Test Using Spiked Water or Spiked Sediment. OECD Guideline for the Testing of Chemicals.

OECD, 2004. Test No. 218: Sediment-Water Chironomid Toxicity Test Using Spiked Sediment. OECD Guideline for the Testing of Chemicals.

Park, S.Y., Chung, J., Colman, B.P., Matson, C.W., Kim, Y., Lee, B.C., Kim, P.J., Choi, K., Choi, J., 2015. Ecotoxicity of bare and coated silver nanoparticles in the aquatic midge, *Chironomus riparius*. Environ. Toxicol. Chem. 34, 2023–2032.

Peixoto, S., Khodaparast, Z., Cornelis, G., Lahive, E., Green Etxabe, A., Baccaro, M., Papadiamantis, A.G., Gonçalves, S.F., Lynch, I., Busquets-Fite, M., Puntes, V., Loureiro, S., Henriques, I., 2020. Impact of Ag_2S NPs on soil bacterial community – A terrestrial mesocosm approach. Ecotoxicol. Environ. Saf. 206, 111405.

Petersen, E.J., Mortimer, M., Burgess, R.M., Handy, R., Hanna, S., Ho, K.T., Johnson, M., Loureiro, S., Selck, H., Scott-Fordsmand, J.J., Spurgeon, D., Unrine, J., van den Brink, N.W., Wang, Y., White, J., Holden, P., 2019. Strategies for robust and accurate experimental approaches to quantify nanomaterial bioaccumulation across a broad range of organisms. Environ. Sci. Nano 6, 1619–1656.

Ptatscheck, C., Putzki, H., Traunspurger, W., 2017. Impact of deposit-feeding chironomid larvae (*Chironomus riparius*) on meiofauna and protozoans. Freshw. Sci. 36, 796–804.

Rajala, J.E., Vehniäinen, E.R., Väisänen, A., Kukkonen, J.V.K., 2017. Partitioning of nanoparticle-originated dissolved silver in natural and artificial sediments. Environ. Toxicol. Chem. 36, 2593–2601.

Ribeiro, F., Gallego-Urrea, J.A., Jurkschat, K., Crossley, A., Hassellöv, M., Taylor, C., Soares, A.M.V.M., Loureiro, S., 2014. Silver nanoparticles and silver nitrate induce high toxicity to *Pseudokirchneriella subcapitata*, *Daphnia magna* and *Danio rerio*. Sci. Total Environ. 466–467, 232–241.

Ribeiro, F., van Gestel, C.A.M., Pavlaki, M.D., Azevedo, S., Soares, A.M.V.M., Loureiro, S., 2017. Bioaccumulation of silver in *Daphnia magna*: Waterborne and dietary exposure to nanoparticles and dissolved silver. Sci. Total Environ. 574, 1633–1639.

Sekine, R., Khurana, K., Vasilev, K., Lombi, E., Donner, E., 2015. Quantifying the adsorption of ionic silver and functionalized nanoparticles during ecotoxicity testing: Test container effects and recommendations. Nanotoxicology 9, 1005–1012.

Selck, H., Handy, R.D., Fernandes, T.F., Klaine, S.J., Petersen, E.J., 2016. Nanomaterials in the aquatic environment: A European Union-United States perspective on the status of ecotoxicity testing, research priorities, and challenges ahead. Environ. Toxicol.

Chem. 35, 1055–1067.

Silva, P. V., van Gestel, C.A.M., Verweij, R.A., Papadiamantis, A.G., Gonçalves, S.F., Lynch, I., Loureiro, S., 2020. Toxicokinetics of pristine and aged silver nanoparticles in *Physa acuta*. Environ. Sci. Nano 7, 3849–3868.

Tangaa, S.R., Selck, H., Winther-Nielsen, M., Croteau, M.N., 2018. A biodynamic understanding of dietborne and waterborne Ag uptake from Ag NPs in the sediment-dwelling oligochaete, *Tubifex tubifex*. NanoImpact 11, 33–41.

Timmermans, K.R., Peeters, W., Tonkes, M., 1992. Cadmium, zinc, lead and copper in *Chironomus riparius* (Meigen) larvae (Diptera, Chironomidae): uptake and effects. Hydrobiologia 241, 119–134.

Timmermans, K.R., Walker, P.A., 1989. The fate of trace metals during the metamorphosis of chironomids (diptera, chironomidae). Environ. Pollut. 62, 73–85.

Tomilina, I.I., Grebenyuk, L.P., 2020. Malformations of Mouthpart Structures of *Chironomus riparius* Larvae (Diptera, Chironomidae) under the Effect of Metal-Containing Nanoparticles. Entomol. Rev. 100, 7–18.

Tourinho, P.S., van Gestel, C.A.M., Morgan, A.J., Kille, P., Svendsen, C., Jurkschat, K., Mosselmans, J.F.W., Soares, A.M.V.M., Loureiro, S., 2016. Toxicokinetics of Ag in the terrestrial isopod *Porcellionides pruinosus* exposed to Ag NPs and $AgNO_3$ via soil and food. Ecotoxicology 25, 267–278.

Toušová, Z., Kuta, J., Hynek, D., Adam, V., Kizek, R., Bláha, L., Hilscherová, K., 2016. Metallothionein modulation in relation to cadmium bioaccumulation and age-dependent sensitivity of *Chironomus riparius* larvae. Environ. Sci. Pollut. Res. 23, 10504–10513.

van den Brink, N.W., Kokalj, A.J., Silva, P. V., Lahive, E., Norrfors, K., Baccaro, M., Khodaparast, Z., Loureiro, S., Drobne, D., Cornelis, G., Lofts, S., Handy, R.D., Svendsen, C., Spurgeon, D., van Gestel, C.A.M., 2019. Tools and rules for modelling uptake and bioaccumulation of nanomaterials in invertebrate organisms. Environ. Sci. Nano 6, 1985–2001.

Warren, L.A., Tessier, A., Hare, L., 1998. Modelling cadmium accumulation by benthic invertebrates in situ: The relative contributions of sediment and overlying water reservoirs to organism cadmium concentrations. Limnol. Oceanogr. 43, 1442–1454.

Xu, L., Xu, M., Wang, R., Yin, Y., Lynch, I., Liu, S., 2020. The Crucial Role of Environmental Coronas in Determining the Biological Effects of Engineered Nanomaterials. Small 16, 1–23.

Yoo, H., Lee, J.S., Lee, B.G., Lee, I.T., Schlekat, C.E., Koh, C.H., Luoma, S.N., 2004. Uptake pathway for Ag bioaccumulation in three benthic invertebrates exposed to contaminated sediments. Mar. Ecol. Prog. Ser. 270, 141–152.

3.8. Supplementary information

Preparation of American Society for Testing and Materials hard water medium (ASTM, 1980)

For the ASTM medium, a 20-L carboy was filled with ultrapure water (UPW) and 200 mL of each of the following stock solutions (prepared in UPW) was added: Calcium sulphate dihydrate (2.4 g L^{-1} $CaSO_4.2H_2O$), potassium chloride (0.8 g L^{-1} KCl), magnesium sulphate (24.57g L^{-1} $MgSO_4.7H_2O$) and sodium hydrogen carbonate (19.20 g L^{-1} $NaHCO_3$). Vitamin (1 mL) was also added to the medium, and pH was corrected to 7.6 ± 0.3. The vitamin was prepared as follows: add 150 mg of thiamine HCl (B1) + 2 mg of cyanocobalamin (B12) + 1.5 mg of biotin (H) to UPW to the final volume of 100 mL.

ASTM, 1980. ASTM (E729-80). Standard practice for conducting acute toxicity tests with fishes, macroinvertebrates and amphibians. Am. Stand. Test. Mater. Annu. B. ASTM Stand. 46, 279–280.

Table S3.1. Characteristics of the Ag NPs dispersed in ASTM medium. Shown are Z-potential values (mV), mean hydrodynamic diameter (nm) measured by Dynamic Light Scattering (DLS); Polydispersity Index (PDI); Dissolved Ag concentration (µg L^{-1}) and percentage of dissolution measured by ICP-MS of 3-8 nm, 50 nm and 60 nm Ag NPs and Ag_2S NPs in ASTM medium at a nominal concentration of 1 mg Ag L^{-1}. All values are given as mean and standard deviation (mean ± SD; *n*=3).

Nanoparticle	Timepoint (h)	Z-potential (mV)	DLS (nm)	PDI	Dissolved Ag concentration (µg L^{-1})	% Dissolution
3-8 nm Ag NP	0	-0.02 ± 0.13	132 ± 0.06	0.27 ± 0.01	44.0 ± 4.89	4.40 ± 0.49
	2	-0.14 ± 0.01	144 ± 3.75	0.29 ± 0.04	61.1 ± 2.04	6.11 ± 0.20
	4	0.01 ± 0.14	144 ± 0.38	0.32 ± 0.03	46.8 ± 5.32	4.68 ± 0.53
	8	-25.1 ± 1.32	151 ± 5.63	0.33 ± 0.05	59.8 ± 3.30	5.98 ± 0.33
	24	0.11 ± 0.04	151 ± 2.02	0.31 ± 0.02	71.1 ± 1.45	7.11 ± 0.14
	48	-0.01 ± 0.03	153 ± 2.01	0.32 ± 0.04	73.7 ± 4.86	7.37 ±0.49
50 nm Ag NP	0	-18.1 ± 0.67	62.7 ± 1.48	0.30 ± 0.02	33.9 ± 6.67	3.39 ± 0.67
	2	-0.05 ± 0.12	84.0 ± 2.90	0.23 ± 0.02	18.8 ± 1.36	1.88 ± 0.14
	4	0.06 ± 0.15	78.8 ± 1.15	0.29 ± 0.05	17.9 ± 0.28	1.79 ± 0.03
	8	0.14 ± 0.05	79.4 ± 2.29	0.25 ± 0.01	15.5 ± 3.24	1.55 ± 0.32
	24	0.04 ± 0.05	84.4 ± 3.52	0.25 ± 0.03	17.2 ± 1.99	1.72 ± 0.20
	48	-0.47 ± 0.9	87.9 ± 1.29	0.27 ± 0.02	23.6 ± 9.44	2.36 ± 0.94
60 nm Ag NP	0	-20.1 ± 0.95	n.a.	0.04	n.a.	n.a.
	2	-21.8 ± 1.59	106.4 ± 3.56	0.20	31.4 ± 2.05	2.30 ± 0.60
	4	-19.3 ± 1.50	94.2 ± 4.53	0.22	23.6 ± 2.14	1.65 ± 0.08
	8	n.a.	n.a.	n.a.	n.a.	n.a.
	24	-20.9 ± 0.00	84.7 ± 4.86	0.26	16.3 ± 0.66	1.12 ± 0.18
	48	-26.0 ± 1.00	88.0 ± 4.76	0.27	19.4 ± 1.86	0.82 ± 0.05
Ag_2S NP	0	-10.1 ± 0.21	n.a.	0.36	n.a.	n.a.
	2	-11.2 ± 1.18	264 ± 19.9	0.36	1.14 ± 1.27	0.32 ± 0.36
	4	-12.0 ± 0.49	278 ± 17.9	0.35	0.02 ± 0.00	0.01 ± 0.00
	8	n.a.	n.a.	n.a.	n.a.	n.a.
	24	-13.7 ± 0.51	302 ± 63.5	0.39	0.02 ± 0.00	0.01 ± 0.00
	48	-12.1 ± 0.57	267 ± 70.9	0.40	0.03 ± 0.02	0.01 ± 0.01

n.a. not analysed at that time point.

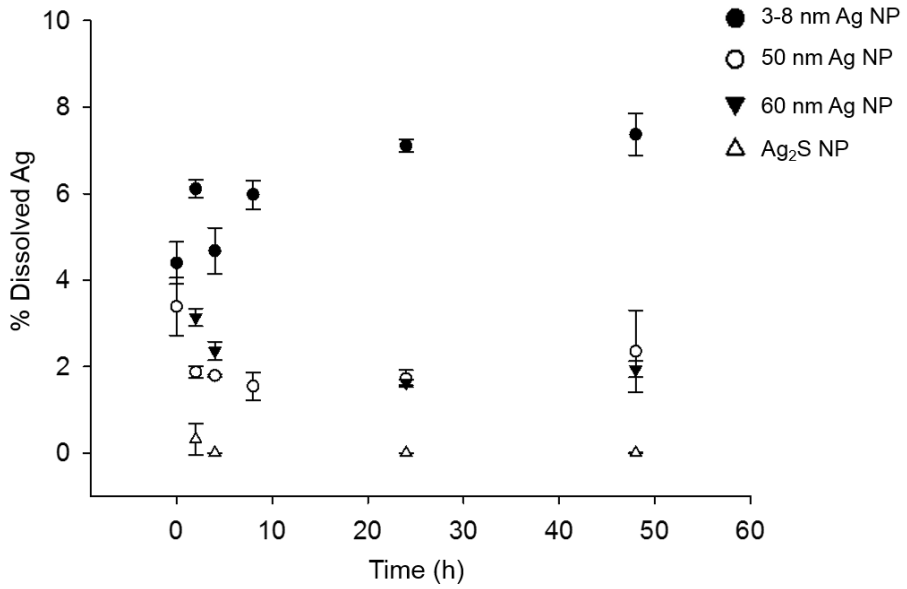

Figure S3.1. Percentage of dissolved Ag at 0, 2, 4, 8, 24 and 48 hours from 3-8 nm and 50 nm Ag NPs and at 2, 4, 24 and 48 hours from 60 nm Ag NPs and Ag_2S NPs, measured by ICP-MS in ASTM medium solutions at a nominal concentration of 1 mg Ag L^{-1}. Error bars indicate the standard deviation (*n*=3).

Table S3.2. Total Ag concentrations (µg Ag L^{-1}) determined at day 0 and dissolved Ag concentrations determined at days 0, 1 and 2 (µg Ag L^{-1}; mean ± standard deviation; *n*=3) in water samples of all treatments of the water exposure bioaccumulation test. Different capital letters in bold within a column indicate statistically significant differences between Ag forms (Kruskall-Wallis test, p<0.05). Different small letters in italics within a row indicate statistically significant differences between sampling times (one-way repeated measures ANOVA followed by Holm-Sidak Method, p<0.05).

Ag form	**Total Ag concentrations (µg Ag L^{-1})**	**Dissolved Ag concentrations (µg Ag L^{-1})**		
	Day 0	**Day 0**	**Day 1**	**Day 2***
3-8 nm Ag NP	10.1 ± 1.09 **A**	0 ± 0 **A** / *a*	0.05 ± 0.01 **A** / *b*	0.06 ± 0.01 **A** / *c*
50 nm Ag NP	11.0 ± 7.64 **A**	0 ± 0 **A** / *a*	0.01 ± 0.01 **A** / *a*	0.07 ± 0.01 **A** / *b*
60 nm Ag NP	12.6 ± 2.11 **A**	0.04 ± 0.04 **A** / *a*	0.83 ± 1.12 **A** / *a*	0.47 ± 0.09 **B** / *a*
Ag_2S NPs	21.8 ± 1.95 **A**	0 ± 0 **A** / *a*	0.04 ± 0.06 **A** / *a*	0.09 ± 0.01 **A** / *a*
$AgNO_3$	8.59 ± 1.29 **A**	0.04 ± 0.07 **A** / *a*	1.94 ± 0.35 **A** / *b*	0.50 ± 0.16 **B** / *a*

***** statistically significant differences between treatments at day 2 by one-way ANOVA followed by Holm-Sidak Method, p<0.05.

Table S3.3. Measured Ag concentrations in water (µg Ag L^{-1}) and sediment (µg Ag kg^{-1}) at days 0, 1 and 2 (mean ± standard deviation SD; *n*=3) of the uptake phase of the toxicokinetic test with *Chironomus riparius* larvae, using water spiked with 3-8 nm, 50 nm, 60 nm Ag NPs, Ag_2S NPs and $AgNO_3$ at a nominal concentration of 10 µg Ag L^{-1}. Different capital letters in bold within a column and different small letters in italics within a row indicate statistically significant differences between Ag forms and sampling times, respectively (two-way ANOVA followed by Holm-Sidak Method, $p<0.05$).

Exposure route	Ag form	Ag concentration at day 0* (µg Ag L^{-1} or µg Ag kg^{-1})	Ag concentration at day 1 (µg Ag L^{-1} or µg Ag kg^{-1})	Ag concentration at day 2 (µg Ag L^{-1} or µg Ag kg^{-1})
Water	3-8 nm	9.87 ± 0.52 **A** / *a*	10.1 ± 0.40 **A** / *a*	2.43 ± 1.22 **A** / *b*
	50 nm	8.34 ± 0.46 **A** / *a*	8.05 ± 0.18 **A,B,C** / *a*	1.34 ± 0.26 **A** / *b*
	60 nm	10.4 ± 0.40 **A** / *a*	7.00 ± 0.31 **B,C** / *b*	3.06 ± 0.36 **A** / *c*
	Ag_2S NPs	13.0 ± 2.69 **B** / *a*	8.56 ± 0.34 **A,B** / *b*	2.11 ± 1.31 **A** / *c*
	$AgNO_3$	9.02 ± 0.96 **A** / *a*	6.18 ± 0.80 **C** / *b*	1.61 ± 0.86 **A** / *c*
Sediment	3-8 nm	1.54 ± 1.40 **A** / *a*	0 ± 0 **A** / *a*	5.18 ± 2.46 **A** / *a*
	50 nm	1.54 ± 1.40 **A** / *a*	3.58 ± 6.20 **A** / *a*	4.34 ± 4.55 **A** / *a*
	60 nm	1.54 ± 1.40 **A** / *a*	7.24 ± 5.70 **A,C** / *a*	14.9 ± 4.57 **B** / *b*
	Ag_2S NPs	1.54 ± 1.40 **A** / *a*	15.2 ± 6.43 **B** / *b*	14.4 ± 0.46 **B** / *b*
	$AgNO_3$	1.54 ± 1.40 **A** / *a*	12.2 ± 1.80 **B,C** / *b*	8.56 ± 3.68 **A,B** / *b*

* background concentration in sediments was considered the same at day 0 for all treatments.

Chapter 4

Bioaccumulation but no biomagnification of silver sulfide nanoparticles in freshwater snails and planarians

Submitted (under review)

Patrícia V. Silva[1], Carlos Pinheiro[1], Rui G. Morgado[1], Rudo A. Verweij[2], Cornelis A. M. van Gestel[2], and Susana Loureiro[1]

[1]CESAM-Centre for Environmental and Marine Studies, Department of Biology, University of Aveiro, Campus Universitário de Santiago, 3810-193 Aveiro, Portugal
[2]Department of Ecological Science, Faculty of Science, Vrije Universiteit Amsterdam, The Netherlands

Bioaccumulation but no biomagnification of silver sulfide nanoparticles in freshwater snails and planarians

4.1. Abstract

Bioaccumulation studies are critical in regulatory decision making on the potential environmental risks of engineered nanoparticles (NPs). The present study evaluated the toxicokinetics of silver sulfide nanoparticles (Ag_2S NPs; simulating an aged Ag NP form) and $AgNO_3$ (ionic counterpart) in the pulmonate snail *Physa acuta* and the planarian *Girardia tigrina*. The snails were first exposed for 7 days to Ag-spiked water, along with the microalgae *Raphidocelis subcapitata* upon which they fed setting up a double route exposure, and subsequently provided as pre-exposed food to the planarians. Ag toxicokinetics and bioaccumulation were assessed in planarians and snails, and potential biomagnification from snail to planarian was evaluated. Gut depuration was also explored to understand whether it constitutes a factor likely to influence Ag toxicokinetics and internal concentrations in the test species. Both species revealed Ag uptake in Ag_2S NP and $AgNO_3$ treatments, with higher uptake from the latter. Uptake by the snails was probably via a combination of water exposure and ingested algae provided as food, but ingestion of algae possibly had higher relevance for Ag uptake from the Ag_2S NPs compared to $AgNO_3$. For planarians, diet probably was the most important exposure route since no Ag uptake was observed in previous waterborne exposures to Ag_2S NPs. Kinetics and internal Ag concentrations did not significantly differ between depurated and non-depurated snails or planarians. The planarians fed on snails revealed no biomagnification. To the best of our knowledge this is the first study investigating the toxicokinetics and biomagnification of NPs in planarians, and with that providing important data on the kinetics and bioaccumulation of NPs in a relevant benthic species.

Keywords: toxicokinetics, nanomaterials, benthic species, dietary uptake, waterborne uptake.

4.2. Introduction

Silver nanoparticles (Ag NPs) exhibit unique properties that enable their application in a large spectrum of products, such as textiles, electronic devices, food, cosmetics, biomedicine and others. Estimated Ag NP global production may reach 800 tons by 2025 (Pulit-Prociak and Banach, 2016). Consequently, the potential interactions of Ag NPs with aquatic and terrestrial environments, including humans, have been extensively investigated (Ferdous and Nemmar, 2020). After usage, Ag NPs may end up in wastewater treatment plants (WWTPs) and are mainly transformed into silver sulfide nanoparticles (Ag_2S NPs). Ag_2S NPs are the predominant Ag form released into surface waters following, mainly, discharge of WWTP effluents (He et al., 2019; Zhao et al., 2021). Once in the water bodies, they will likely experience aggregation and posterior sedimentation (Grün et al., 2018; Spurgeon et al., 2020). Consequently, sediments may become important final sinks for Ag NPs or Ag_2S NPs, as for other NPs (Tangaa et al., 2016). Sun et al. (2016) predicted Ag NP concentrations in sediment to reach about 30 µg kg^{-1} and in surface waters around 1.50 ng L^{-1}. The latter is within the range of 0.3 to 2.5 ng L^{-1} of Ag NPs that was detected in Dutch surface waters (Peters et al., 2018). Therefore, aquatic biota may be at risk, in particular sediment-dwelling organisms.

Several studies demonstrated that different benthic species can accumulate Ag NPs through water and sediment/dietary exposures (Bao et al., 2018; Croteau et al., 2011, 2014; Khan et al., 2015; Silva et al., 2020; Tangaa et al., 2018). One example was the Ag NP internalization by the gut epithelium of the estuarine polychaete *Nereis diversicolor* observed after ingestion of spiked sediments (García-Alonso et al., 2011). The fact that Ag NPs can apparently be endocytosed as intact particles in the gut of common prey species raised concerns about their potential trophic transfer (Tangaa et al., 2016). Studies have reported trophic transfer of NPs, like Ag NP transfer from algae to daphnids (McTeer et al., 2014), TiO_2 NPs from daphnids to zebrafish (Zhu et al., 2010), and Au NPs from algae to mussels (Larguinho et al., 2014). Although substantial attention has been dedicated to this subject, environmental risk assessment of NPs is still in need of adequate studies evaluating the toxicokinetics of engineered NPs in aquatic and terrestrial organisms, specially looking at predators. Understanding the potential for bioaccumulation and biomagnification of engineered NPs is critical for regulatory decision making (Petersen et al., 2019).

The aim of this work was to assess the bioaccumulation and toxicokinetics of Ag_2S NPs (simulating an aged Ag NP form) and $AgNO_3$ (ionic control) in two freshwater epibenthic

species, the pulmonate snail *Physa acuta* and the planarian *Girardia tigrina*. Potential biomagnification was also evaluated in this two-level food chain, simulating a realistic scenario where Ag_2S NPs enter the water body and consequently contaminate the food source, with organisms being exposed through water and diet. Snails (prey) were exposed to spiked water along with the microalgae *Raphidocelis subcapitata* upon which they fed and then were provided to the planarians (predator). Toxicokinetics in both prey and predator were assessed as well as potential bioaccumulation and biomagnification. In addition, the influence of depuration (i.e., gut voidance) on kinetics and internal Ag concentrations of both species was also assessed. The results obtained for snails will be compared with those of a previous study exposing *P. acuta* via different routes to $AgNO_3$ and the same Ag_2S NPs as used in this work (Silva et al., 2020).

P. acuta is a widespread grazer, with key role in freshwater food chains as a trophic link between primary producers and predators (Gonçalves et al., 2017; Musee et al., 2010). *G. tigrina* is a carnivore species, feeding upon small invertebrates such as insect larvae, snails, isopods and oligochaetes (Ilic et al., 2018). They are widespread species having an important position in freshwater food webs both as prey and predator (Saraiva et al., 2020). Planarians possess notable regeneration abilities and a primitive form of the central nervous system, therefore they have mainly been used in neurotoxicity, genotoxicity or carcinogenicity studies (Wu and Li, 2018). Although planarians have been suggested as potential model organisms to be used in environmental toxicology (Wu and Li, 2018), research on the bioaccumulation and toxicokinetics of xenobiotics in planarians is still in its infancy. Therefore, emphasis should be on evaluating the potential bioaccumulation and trophic transfer to planarians due to their important dual role in aquatic food chains. Due to their extremely low solubility, Ag_2S NPs have a low toxicity compared to Ag NPs or Ag ions (He et al., 2019). Nevertheless, Ag_2S NPs showed to be bioavailable and little is known about their toxicokinetics and bioaccumulation in biota (Baccaro et al., 2021; Khodaparast et al., 2021; Kühr et al., 2018). For this reason, Ag_2S NPs were chosen as the nanoparticulate Ag form in the present work. We tested the hypothesis that Ag from Ag_2S NPs and $AgNO_3$ will accumulate and biomagnify in the food chain from snail to planarian.

4.3. Material and Methods

4.3.1. Experimental organisms and culture maintenance

Individuals of *Physa acuta* and *Girardia tigrina* were reared at applEE - applied Ecology and Ecotoxicology laboratory, at the University of Aveiro, Portugal, under controlled

laboratory conditions at 20 ± 1 ºC and 16:8h light: dark photoperiod. Approximately 50 snails were maintained per glass aquarium, filled with 3-L of artificial pond water (APW) medium (Gonçalves et al., 2017; Naylor et al., 1989). The medium was fully renewed once a week and partially renewed every other day. Continuous aeration was provided to maintain oxygen level above 8 mg L^{-1}. To avoid shell fracturing, APW medium was kept at a basic pH of 7.9-8.2. Grounded fish food TetraMin® (Tetrawerke, Melle, Germany) was provided *ad libitum* every other day (Gonçalves et al., 2017). Adult snails of approx. four months old were used in this test. One week prior to the start of the experiment, snails were fed with the microalgae *Raphidocelis subcapitata* to acclimate them to the feeding conditions of the test. *R. subcapitata* was provided at a concentration of $3x10^5$ cells mL^{-1} (Ribeiro et al., 2014, 2015).

Planarians were maintained in plastic containers covered with foil (due to their photonegative nature), filled with American Society for Testing Materials (ASTM) hard water medium (ASTM, 1980) and fed *ad libitum* once a week with bovine liver or *Chironomus riparius* larvae. Bovine liver was grounded and stored at -20 ºC, *C. riparius* larvae were taken from laboratory cultures (see Simão et al. (2020) for details). When feeding, cultures were removed from the dark. Medium was fully renewed immediately after feeding and 2-3 days later (Simão et al., 2020). Adult planarians (size ~1.5 cm) were used and starved 1 week prior to the experiment to ensure uniform metabolic state (Oviedo et al., 2008).

4.3.2. Nanoparticles

Silver sulfide nanoparticles (Ag_2S NPs) were synthetised *ab initio* to simulate an environmentally aged Ag NP form, and were produced and supplied in dispersed solutions (6.56 g Ag L^{-1}; polyvinylpyrrolidone (PVP)), by Applied Nanoparticles (Barcelona, Spain), within the framework of the EU H2020 NanoFASE project (http://www.nanofase.eu/). The batch of Ag_2S NPs used is similar to the batches used by Baccaro et al., (2018), Clark et al., (2019), and Khodaparast et al., (2021). Baccaro et al. (2018) reported a mean size of 20.3 ± 9.8 nm, measured by Transmission Electron Microscopy (TEM). Details on the hydrodynamic size, Zeta-potential and dissolution of the Ag_2S NPs at different time points in UPW (ultra-pure water) and APW medium have been reported by Silva et al. (2020). Tables S4.1 and S4.2 of the supplementary information summarize the latter data. Silver nitrate ($AgNO_3$) was used as the ionic control (Sigma Aldrich; CAS number 7761-88-8; 99% purity; crystalline powder).

4.3.3. Experimental design

4.3.3.1. Physa acuta - water exposure test

The experiment consisted of an uptake phase, exposing snails to Ag_2S NP or $AgNO_3$-spiked APW medium for 7 days, following transfer to clean medium for an elimination phase of 7 days. A negative control in which snails kept in clean APW medium during both phases was also performed. An environmentally relevant concentration of 10 µg Ag L^{-1} was chosen, in order to allow reliable analytical detection of Ag in test medium and test organisms while still being close to predicted and measured total and nanoparticulate Ag concentrations in freshwaters. Measured Ag ENM concentrations in effluents from sewage treatment reached values as high as 1.3 µg L^{-1} (Giese et al., 2018), so being closer to the nominal concentration used in this study. The use of this nominal concentration also allowed the comparison of the toxicokinetics determined for snails with those obtained in a test published by Silva et al. (2020), and ensured bioaccumulation in snails in order to investigate potential trophic transfer to planarians. Two snails per replicate were exposed in 50 mL glass vials filled with the test medium. Stock suspensions were prepared in UPW following the OECD guideline 318 (2017), and diluted in APW to the desired concentration. APW medium was renewed every other day (no need to provide aeration), and snails were fed every other day with *R. subcapitata* at a concentration of $3x10^5$ cells mL^{-1}. Vials were covered with a lid to avoid snails from escaping. The two snails from three replicates per treatment (total of 24 replicates per treatment) were sampled at days 1, 2, 5, 7, 8, 9, 12 and 14. At each sampling time, one of the snails was rinsed three times in UPW and stored, while the other was left in 50 mL clean APW for 24h to depurate before undergoing the same process. Snails were frozen at -80 ºC to allow removing the soft body from the shell according to Silva et al. (2020) as it is known that planarians do not ingest snail shells. Soft bodies were oven-dried for 48h at 60 ºC before being weighted and digested. Water samples (*n*=3 per treatment) were taken at day 0 for total Ag analysis. The experiment was maintained under controlled conditions (20 ± 1 ºC, 16:8h light: dark), vials were inspected every day and pH, temperature and dissolved oxygen (DO) concentration were measured (OECD 2016).

Extra vials were maintained at the same conditions with snails that were used to feed the planarians (see section 4.3.3.2). In a separate experiment, water samples were collected from vials with APW medium spiked at a nominal concentration of 10 µg Ag L^{-1} of Ag_2S NPs or $AgNO_3$ for ultrafiltration and measurement of dissolved Ag concentrations. Water samples (3 mL; *n*=3 per treatment per sampling time) were directly collected from

the same vials at days 0 (meaning at 0h), 1 and 2 of the uptake phase, and filtered through a syringe filter (0.02 µm; AnotopTM, Whatman). To prevent Ag losses to the filter, the filters were previously soaked with a solution of 0.1 M $CuSO_4$ (Cornelis et al., 2010). Table S4.2 shows the dissolved Ag concentrations of Ag_2S NP and $AgNO_3$, also published in Silva et al. (2020).

4.3.3.2. Girardia tigrina - food exposure test

The planarian experiment included an uptake phase and an elimination phase of 72h each. Six planarians were kept in 150 mL glass vials filled with clean ASTM medium (changed daily) and covered with laboratory film. A sheet of foil was placed on top of the vials to provide low ambient lighting to the planarians. Planarians were fed at 0h, 24h and 48h of each phase. For the uptake phase, planarians in each replicate were fed with two snails (pre-exposed during 7 days to Ag_2S NPs or $AgNO_3$), and for the elimination phase with unexposed snails. In the negative control, planarians were fed with unexposed snails during both phases. Pre-exposed snails were directly sampled from the test vials and not depurated or washed before being provided to the planarians. At 12h, 24h, 48h, 72h, 84h, 96h, 120h and 144h planarians were sampled from three replicates per treatment (total of 24 replicates per treatment). Three planarians were rinsed three times in UPW and stored, and the remaining three were left in 50 mL clean ASTM medium to depurate for 24h before undergoing the same process. Planarians were frozen at -80 ºC until digestion. At 0h, 12h and 48h, pre-exposed snails were sampled to measure total Ag concentrations, following the same procedure as described in section 4.3.3.1. Planarians were oven-dried at 60 ºC for 48h and weighted before digestion. Test conditions, vial inspection and parameter monitoring were performed as mentioned in section 4.3.3.1.

4.3.4. Sample digestion for total Ag measurements

Snails (soft body) and planarians were digested following Ribeiro et al. (2017), with minor adaptations, heated on a hotplate inside Teflon beakers with 3 mL concentrated HNO_3 (65%, PanReac AppliChem, trace analysis). After breaking down the tissue, 1 mL concentrated HCl (37%, PanReac AppliChem, trace analysis) was added. Samples were left to evaporate until approximately 1 mL, and then diluted to a final volume of 5 mL with a solution of 1% HCl (37%, PanReac AppliChem, trace analysis). Method accuracy and recovery of each digestion run was assessed by digesting triplicates of blanks and the certified reference material DOLT-5 (Dogfish liver) jointly with the samples. The average Ag

recovery was 90.2 ± 0.52% (mean ± standard deviation SD; *n*=27). For the digestion of the water samples, the methodology described in Ribeiro et al. (2014) was followed. Water samples were digested also on a hotplate inside Teflon beakers with 4 mL of aqua regia (mixture of concentrated HCl (37%):HNO_3 (65%); 3:1 (v/v), PanReac AppliChem, trace analysis). After evaporation until approximately 1 mL, samples were diluted to a final volume of 5 mL with a solution of 1% HCl (37%, PanReac AppliChem, trace analysis). In each digestion run, APW medium was used as blank and recovery controls (with known Ag concentration) were also digested in triplicate, giving an average recovery of Ag of 135 ± 59.3% (mean ± SD; *n*=6). All samples were analysed for total Ag concentration by Graphite furnace Atomic Absorption Spectrometry (AAS; PinAAcle 900Z, PerkinElmer, Singapore). The limit of detection was 0.018 µg Ag L^{-1}.

4.3.5. Toxicokinetic modelling

The toxicokinetics of Ag were described by fitting a one-compartment model to the time-varying internal Ag concentrations measured in snails (soft body) and planarians (model 1) (Ardestani et al., 2014). During the test, planarians revealed a slight increase in weight while snails showed weight loss. An exponential growth rate constant was thus calculated from the planarian or snail dry weight (dw) changes during the respective test duration and included into the toxicokinetics models to account for the effect of biomass changes in estimated internal Ag concentrations. Another model (model 2) that includes a stored fraction (SF) was also used. SF represents a biological site in which metals are stored and not eliminated from the organism (van den Brink et al., 2019). Equations of model 2 are described in the SI.

Model 1 (equations 1 and 2):

$$Q(t) = C_0 + \left(\frac{k1}{(k2 + k_{growth})}\right) * C_{exp} * \left(1 - e^{(-(k2+k_{growth})*t)}\right)$$

(1)

$$Q(t) = C_0 + \left(\frac{k1}{(k2 + k_{growth})}\right) * C_{exp} * \left(e^{(-(k2+k_{growth})*(t-t_c))} - e^{(-(k2+k_{growth})*t)}\right)$$

(2)

Where Q(t) = Ag internal concentration in the organisms at time t days (snails) or hours (planarians) (µg Ag $g^{-1}_{organism}$ dw); C_0 = background internal concentration measured at day 0 (µg Ag $g^{-1}_{organism}$ dw); k1 = uptake rate constant from water (L_{water} $g^{-1}_{organism}$ day^{-1}) or food (g_{food} $g^{-1}_{organism}$ $hour^{-1}$); k2 = elimination rate constant (day^{-1} or $hour^{-1}$); k_{growth} = growth increase or decrease rate constant (day^{-1} or $hour^{-1}$); C_{exp} = Ag exposure concentration in water (µg Ag L^{-1}) or food (µg Ag g^{-1} dw); t = time in days or hours; t_c = time at which organisms were transferred from contaminated to clean medium (day 7 or 72 hours).

Kinetic bioconcentration (BCF_k; L g^{-1}) and biomagnification (BMF_k; g g^{-1}) factors were calculated as:

$$BCF_k / BMF_k = \frac{k1}{k2}$$

Kinetic parameters used to calculate BCF_k and BMF_k were derived from model 1. Estimated BMF_ks > 1 indicate the occurrence of biomagnification.

4.3.6. Statistical analysis

Uptake and elimination kinetics were calculated using non-linear regression in SPSS (version 25). Akaike Information Criteria tests (AIC and AICc) were applied to select the best fitting model (data not shown). Statistical significance of differences between uptake and elimination rate constants for different treatments were tested with Generalised Likelihood Ratio Tests (GLR) in SPSS (version 25). Student *t*-tests (SigmaPlot 12.5 software) were applied to compare exposure concentrations in water (for snails) or diet (for planarians) between Ag_2S NP and $AgNO_3$ treatments. One-way analysis of variance (ANOVA) (SigmaPlot 12.5 software) was used to compare body Ag concentrations of snails provided to planarians at the different times of each treatment. One-way repeated measures ANOVA followed by the Holm-Sidak method ($p<0.05$) (SigmaPlot 12.5 software) was used to compare dissolved Ag concentrations between days in each treatment. Two-way ANOVA (SigmaPlot 12.5 software) with “depuration” and “time” as factors was applied to determine whether depuration and time did influence the internal Ag concentrations and if there was an interaction between both factors. When significant differences were found, all pairwise multiple comparison procedures were performed using the Holm-Sidak method ($p<0.05$). Data transformation (square, square root and log10) was conducted when ANOVA assumptions were not met.

4.4. Results

4.4.1. *Physa acuta* - water exposure test

Concentrations of Ag measured in water of the Ag_2S NP treatment were almost twice the nominal value and significantly higher (*t*-test, $p<0.001$) than for the $AgNO_3$ treatment (Table 4.1). Snail mortality was approximately 10%. The k_{growth} for weight loss was -0.06 ± 0.01 day^{-1} (mean ± SD, *n*=4). During the uptake phase, the internal Ag concentrations in the snails were generally higher for $AgNO_3$ than for Ag_2S NP exposures. Snails from the Ag_2S NP treatment revealed a fast increase in uptake rate during day 1, remaining constant from day 2 onwards. For the elimination phase, a fast decline was observed from day 7 to day 8. In the $AgNO_3$ exposure, uptake gradually increased during the uptake phase and was followed by an extremely slow elimination (Figure 4.1). Using model 1, which gave the best fit, values of k1 and k2 were higher for Ag_2S NP than $AgNO_3$ exposures, but only k2 values significantly differed ($X^2_{(1)}>3.84$; $p<0.05$) (Table 4.1). Toxicokinetic model 2 estimated an SF of zero and identical kinetic curves and rate constants for snails from both the Ag_2S NP and $AgNO_3$ exposures (Figure S4.1, Table S4.3).

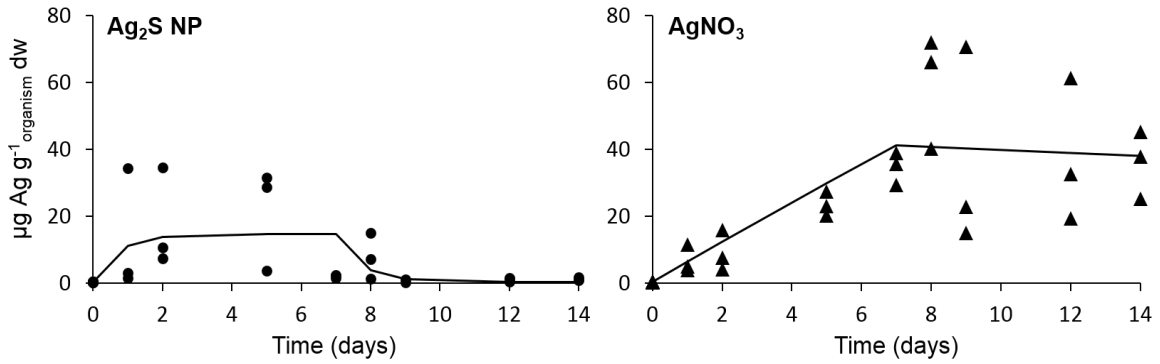

Figure 4.1. Uptake and elimination of Ag in depurated *Physa acuta* exposed for 7 days to water spiked at a nominal concentration of 10 µg Ag L^{-1} of Ag_2S NPs (left) or $AgNO_3$ (right) and transferred to clean water for 7 days. Lines show the fit of the toxicokinetic model 1 to the data points, which represent Ag concentrations determined in snail soft bodies. See Table 4.1 for the resulting kinetics parameter values.

Table 4.1. Uptake (k1) and elimination (k2) rate constants (± 95% confidence interval) of Ag uptake in depurated *Physa acuta* and *Girardia tigrina* exposed to Ag_2S NPs and $AgNO_3$. Bioconcentration factor (BCF_k) for Ag uptake in *P. acuta* exposed through water; biomagnification factor (BMF_k) for Ag uptake in *G. tigrina*. Data was modelled with model 1, see Figures 4.1 and 4.3. Measured exposure concentrations (mean ± standard deviation; *n*=3) in water for *P. acuta* (µg Ag L^{-1}) and in food for *G. tigrina* (µg Ag g^{-1} dw; see Table S4.5 for individual values) are also shown. Different small letters indicate statistically significant differences (*t*-test, p<0.05). Different capital letters indicate statistically significant differences between k1 or k2 values in each species ($X^2_{(1)}$>3.84; p<0.05). Absence of letters indicates no statistically significant differences ($X^2_{(1)}$<3.84; p>0.05).

Species (depurated)	**Ag form**	**Measured exposure concentration** (µg Ag L^{-1} or µg Ag g^{-1})	**k1** (g_{food} $g^{-1}_{organism}$ $hour^{-1}$ or L_{water} $g^{-1}_{organism}$ day^{-1})	**k2** ($hour^{-1}$ or day^{-1})	**BCF_k** (L g^{-1})	**BMF_k** (g g^{-1})
Physa acuta	Ag_2S NPs	17.7 ± 0.59 a	1.13 (-0.43-2.70)	1.45 (-0.60-3.49) A	0.78	
	$AgNO_3$	9.31 ± 0.25 b	0.65 (0.41-0.90)	0.071 (0.013-0.13) B	9.15	
Girardia tigrina	Ag_2S NPs	34.1 ± 25.4	0.001 (0.0003-0.001)	0.016 (0.0046-0.027)		0.063
	$AgNO_3$	41.4 ± 9.44	0.0051 (0.0035-0.0067)	0.012 (0.0048-0.02)		0.43

Internal Ag concentrations were lower in depurated than in non-depurated snails from both treatments at all sampling times (Figure 4.2). In snails exposed to Ag_2S NPs, internal Ag concentrations seemed not to be influenced by depuration or time and no interactions were observed (two-way ANOVA, p>0.05) (Figure 4.2). Even though differences were not significant, a pattern of higher internal Ag concentrations in non-depurated snails can be observed in Figure 4.2, therefore, caution should be taken when interpreting these data. In the $AgNO_3$ treatment, internal Ag concentrations of depurated snails at day 7 were significantly higher (two-way ANOVA, Holm-Sidak method, p<0.05) compared to days 1 and 2. For non-depurated snails, concentrations at day 7 were significantly higher (two-way ANOVA, Holm-Sidak method, p<0.05) than at the other sampling days. At day 7, internal Ag concentrations of depurated snails were significantly lower (two-way ANOVA, Holm-Sidak method, p<0.05) than in non-depurated snails, and no interactions between factors were detected (two-way ANOVA, p>0.05) (Figure 4.2). Uptake and elimination curves for non-depurated and depurated snails showed a similar pattern for both Ag exposures. Uptake curve was higher during the first day in non-depurated snails from the Ag_2S NP treatment and elimination curve decreased faster from day 7 to day 8 (Figure S4.2). Therefore, higher k1 and k2 values were calculated for non-depurated than for depurated snails from Ag_2S NP exposures, although differences were not significant ($X^2_{(1)}$<3.84; p>0.05) because of the large scatter in the data (Table S4.4).

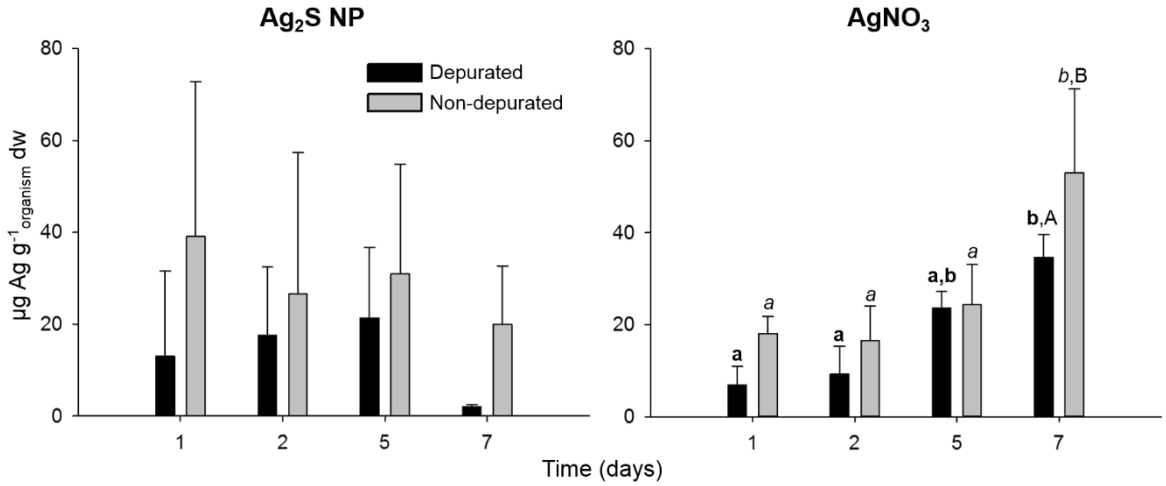

Figure 4.2. Internal Ag concentrations (µg Ag g^{-1} dw; mean ± standard deviation; *n*=3) measured in depurated and non-depurated *Physa acuta* during the 7-day uptake phase of Ag_2S NP and $AgNO_3$ exposures. Different capital letters indicate statistically significant differences between depurated and non-depurated snails within the same day; different small letters in bold and in italics indicate statistically significant differences between days in depurated and non-depurated snails, respectively (two-way ANOVA, followed by Holm-Sidak method, $p<0.05$). Absence of letters indicates no statistically significant differences (two-way ANOVA, $p>0.05$).

Similar k1 and k2 values were determined for depurated and non-depurated snails from the $AgNO_3$ exposure, with non-significantly ($X^2_{(1)}<3.84$; $p>0.05$) higher values for non-depurated ones. BCF_ks values were higher for depurated and non-depurated snails upon $AgNO_3$ exposure, compared to Ag_2S NP (Tables 4.1 and S4.4).

4.4.2. *Girardia tigrina* - food exposure test

Measured Ag concentrations in the diet (pre-exposed snails) given at 48h were significantly lower (*t*-test, $p<0.05$) for Ag_2S NPs than for $AgNO_3$ (Table S4.5).

No mortality occurred in the planarian test. Ag concentrations in the planarians at t=0 were below the detection limit, so C_0 was omitted from the kinetics calculations. Planarians exposed to Ag_2S NPs revealed significantly lower internal Ag concentrations (two-way ANOVA, Holm-Sidak method, $p<0.001$) and lower uptake rate than those exposed to $AgNO_3$. The k_{growth} for the slight increase in weight was 0.004 ± 0.0003 day^{-1} (mean ± SD, *n*=4). Model 1 generally revealed the best fit, and the kinetics derived showed relatively fast elimination in planarians from both exposures (Figure 4.3). Uptake rate constant was lower in planarians exposed to Ag_2S NPs than to $AgNO_3$, while the opposite was observed for k2 values, but differences were not significant in either case ($X^2_{(1)}<3.84$; $p>0.05$) (Table 4.1). The k1 value for Ag_2S NPs determined using model 2 was close to that determined with model 1, for $AgNO_3$ it was higher. Elimination rate constants determined with model 2 were

higher for both exposures, and small stored fractions (SF) of 0.08 and 0.01 were calculated for Ag_2S NPs and $AgNO_3$, respectively (Tables 4.1 and S4.3).

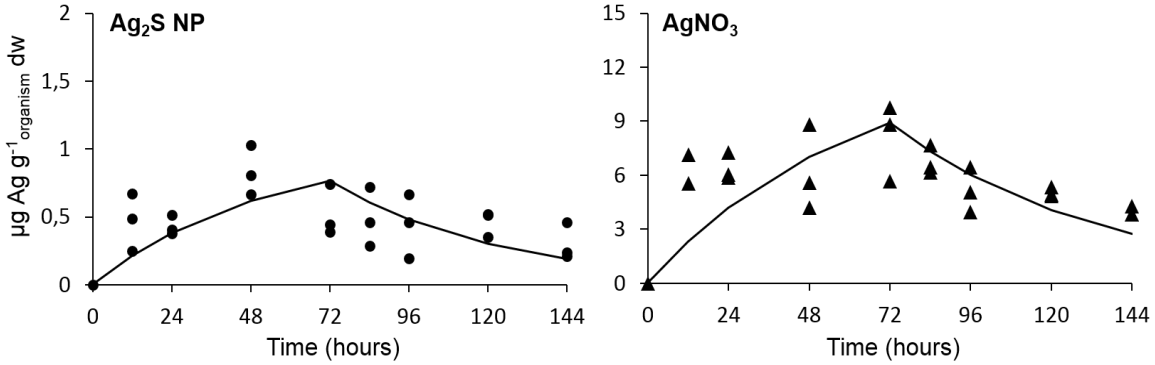

Figure 4.3. Uptake and elimination of Ag in depurated *Girardia tigrina* exposed for 72 hours to food contaminated with Ag_2S NPs (left) and $AgNO_3$ (right), and then fed with clean food for 72 hours. Lines show the fit of model 1 to the data points, which represent Ag concentrations determined in planarians. See Table 4.1 for the resulting kinetics parameter values. Note the differences in the y-axis scales.

In both Ag_2S NP and $AgNO_3$ treatments, concentrations were generally lower in depurated than in non-depurated planarians, even though no significant differences were found, nor interactions (two-way ANOVA, $p>0.05$) (Figure 4.4). The toxicokinetics of Ag in non-depurated planarians showed no significant differences in k1 or k2 values ($X^2_{(1)}<3.84$; $p>0.05$) between treatments (Table S4.4). Furthermore, kinetic patterns and parameters determined for depurated and non-depurated planarians were very similar for $AgNO_3$ and slightly higher for non-depurated ones exposed to Ag_2S NPs, with no significant differences ($X^2_{(1)}<3.84$; $p>0.05$) (Figures 4.3 and S4.2, Tables 4.1 and S4.4). The calculated BMF_ks were below 1 and higher for the ionic than for the nano-Ag exposure (Tables 4.1 and S4.4).

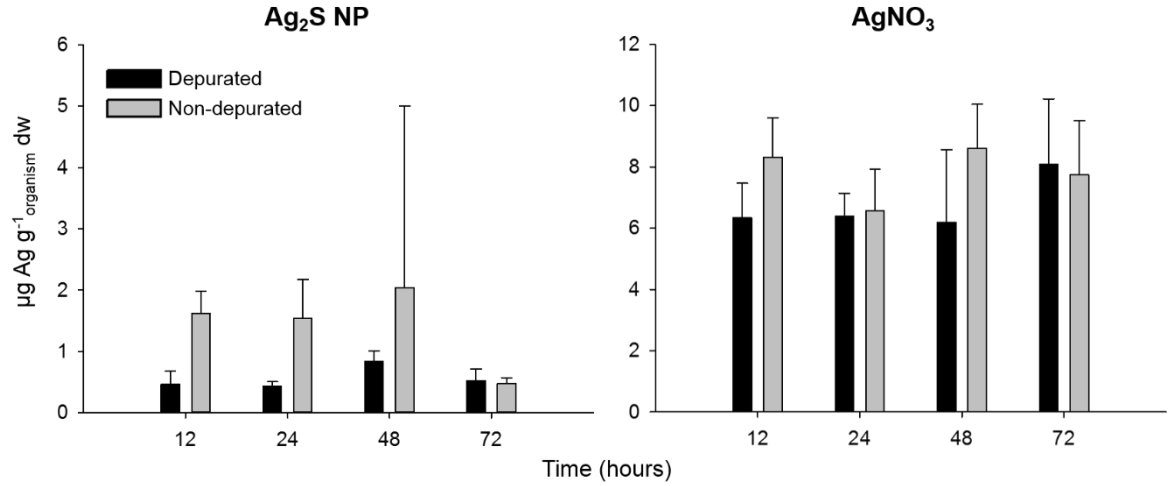

Figure 4.4. Internal Ag concentrations (µg Ag g^{-1} dw; mean ± standard deviation; *n*=3) measured in depurated and non-depurated *Girardia tigrina* during the 72-hour uptake phase of Ag_2S NP and $AgNO_3$ exposures. Absence of letters indicates no statistically significant differences (two-way ANOVA, p>0.05).

Experiments with spiked water (no sediment used) and spiked water and clean sediment were previously conducted, exposing *G. tigrina* to the same Ag_2S NPs and $AgNO_3$ as used in the present work (experimental design described in the SI). Kinetic curves and parameters are displayed in Figure S4.3 and Table S4.6. In these experiments, internal Ag concentrations in the planarians only differed from the control (two-way ANOVA, Holm-Sidak method, p<0.05) upon exposure to $AgNO_3$. No differences were found ($X^2_{(1)}$<3.84; p>0.05) between k1 and k2 values between the two treatments (Table S4.6).

4.5. Discussion

4.5.1. *Physa acuta* - water exposure test

Snails presented distinct uptake and elimination kinetics upon Ag_2S NP and $AgNO_3$ exposures. Due to the extremely low dissolution of Ag_2S NPs in APW medium (Table S4.2), Ag uptake is expected to be predominantly of Ag nanoparticles. Dissolved Ag concentrations measured in water from the $AgNO_3$ treatment (without algae) were 31.3% (day 0) to 39.8% (day 2) of the initial total concentration (Table S4.2), suggesting that Ag was likely bound to the glass walls of the test vials (Sekine et al., 2015) or quickly formed AgCl complexes that settled to the bottom (Ribeiro et al., 2015). Adsorption to the vial walls is also expected to occur for NPs in the Ag_2S NP treatment (Sekine et al., 2015). But this could have contributed to additional uptake by snails, for instance, via dermal uptake across the foot while they are moving on the glass (Bao et al., 2018; Kuehr et al., 2021). Although these measurements were done in water from test vials without *R. subcapitata*, lower

dissolved Ag concentrations in the water column are expected due to Ag uptake by the algae. Ribeiro et al. (2015) observed a fast decrease of Ag concentrations in $AgNO_3$-spiked algae medium (MBL) at 15 µg Ag L^{-1}, which was likely the result of dissolved Ag being readily taken up by *R. subcapitata*. In that study, internalization of Ag by *R. subcapitata* was found to occur only for ionic or dissolved Ag, while Ag NPs were only found adsorbed onto algal cell walls (Ribeiro et al., 2015). Considering this, the combined uptake from water and diet was the most likely scenario for both treatments of the present study. Additionally, Ag uptake of the algae by snails was probably in the form of NPs adsorbed to the algal cell walls in the Ag_2S NP treatment, and likely of internalized Ag ions in the $AgNO_3$ exposure. Although the exposure concentration in the Ag_2S NP treatment was twice that of $AgNO_3$ (Table 4.1), higher internal Ag concentrations were found for snails exposed to $AgNO_3$. This is probably the result of higher bioavailability and the extremely slow elimination observed in the $AgNO_3$ treatment (Figure 4.1). In an earlier work, we found higher internal Ag concentrations in snails from waterborne $AgNO_3$ exposure (Silva et al., 2020). Ag uptake rates in *Lymnaea stagnalis* were faster in $AgNO_3$ than in Ag NP waterborne or dietary (pre-exposed diatoms) exposures (Croteau et al., 2011). For the land snail *Achatina fulica* uptake rate constant from water was much higher upon exposure to $AgNO_3$ than to Ag NPs, while elimination rate constant was lower (Chen et al., 2017). Also, previous studies have reported slower elimination of the ionic than the nanoparticulate Ag form by freshwater invertebrates (Cross, 2017; Silva et al., 2020).

The higher dissolution of Ag from $AgNO_3$ might have contributed to its higher bioavailability to snails from water, explaining, in part, their higher internal Ag concentrations, as has also been suggested for our earlier tests. Ag ions taken up by water and/or transdermal could have been internalized more easily than Ag_2S NPs, since Ag ions can enter cells via ion transport channels (e.g., proton-coupled Na^+ channels) while Ag particles may be too large (Khan et al., 2015). Uptake of metals bound to particulate material has been suggested to mainly occur in the digestive gland of molluscs (Kuehr et al., 2021; Marigómez et al., 2002; Mohammad et al., 2021), which was the major target tissue for Ag accumulation in freshwater snails (Bao et al., 2018). Once contaminated food reached the digestive gland, different processes may occur, such as endocytosis or phagocytosis in digestive cells, potentially leading to different elimination of ionic and nanoparticulate Ag. One hypothesis can be that Ag from $AgNO_3$ and Ag_2S NPs treatments may have been taken up through different cellular pathways, for instance, Ag_2S NPs could have been taken up by pathways that lead to faster efflux (e.g., micropinocytosis or caveolae-mediated endocytosis) (Khan et al., 2015). Another explanation could be the binding of Ag to different

subcellular fractions in the algae. Ribeiro et al. (2015) suggested the binding of Ag to metallothioneins (MTs) to explain the slow elimination upon exposure of *R. subcapitata* to $AgNO_3$. Metals accumulated in the soluble fraction, such as bound to MTs or MT-like proteins, are expected to be trophically available (Rainbow et al., 2011). Thus, another hypothesis for the differences observed between the Ag treatments may be that the Ag potentially internalised by *R. subcapitata* was more trophically available to snails from the $AgNO_3$ treatment, and thus more efficiently assimilated and slowly eliminated. Conversely, since Ag_2S NPs were expected to be adsorbed to the algae cell wall, they may be bound to the insoluble fraction (cellular debris) and be less assimilated by snails, leading to a more efficient elimination (Rainbow et al., 2011). *L. stagnalis* showed high assimilation efficiency (AE) of Ag upon dietary exposure to Ag NPs and $AgNO_3$, but AE was higher when feeding on Ag incorporated in diatoms after exposure to dissolved $AgNO_3$ than for Ag NPs mixed with the diatoms. The authors suggested that less cytosolic Ag (soluble fraction) was present in the diatom cells in the Ag NP treatments, thus the bioavailable Ag form in the diet was reduced (Croteau et al., 2011). For *A. fulica*, AE was similar for Ag NPs and $AgNO_3$, but dietary uptake was generally the dominant route for snails exposed to Ag NPs, while the relative importance of dietary and waterborne exposure depended on Ag concentrations measured in food and water in case of $AgNO_3$ exposure (Chen et al., 2017).

It would be expected that the Ag_2S NPs could be more easily desorbed from the cell walls during digestion, consequently leading to a faster assimilation, with increase of the internal Ag concentrations and uptake rates of snails from this treatment (Pavlaki et al., 2018; Tangaa et al., 2016). However, such scenario was not observed. Considering that the gut pH of freshwater snails may be around neutral (e.g., pH ranging from 6.4 (gizzard) to 7.1 (intestine) in *L. stagnalis* (Carriker, 1946; van der Zande et al., 2020)), dissolution or detachment of Ag_2S NPs from the cell walls was probably less efficient, preventing the Ag_2S NPs from being endocytosed into the gut lumen. These hypotheses would, however, require further confirmation.

Silva et al. (2020) obtained similar uptake and elimination patterns when exposing *P. acuta* to the same Ag_2S NPs in spiked sediment. Although not significantly, internal Ag concentrations in snails from the present test were generally higher during the uptake phase than in snails exposed only to Ag_2S NP-spiked APW medium (no sediment) at similar nominal concentrations and test conditions, but devoid of food (from now on mentioned as the Ag-spiked water test) in Silva et al. (2020). The opposite was observed for internal Ag concentrations in the elimination phase (Silva et al., 2020). Compared with kinetics obtained using model 2, parameters of the Ag_2S NP exposures were not significantly different

between tests (Table S4.3). Nevertheless, the k2 calculated in the present test was much higher and the elimination curve showed a fast drop during the first day of elimination (Figure 4.2), while the decrease of the elimination curve was gradual in the Ag_2S NP treatment of the Ag-spiked water test. This suggests that probably different processes for Ag elimination occurred in snails exposed to Ag_2S NPs in the present test and the Ag-spiked water test (Silva et al., 2020). Therefore, it can be hypothesised that in the presence of algae, uptake of Ag_2S NPs was probably dominated by ingestion of food with adsorbed NPs, which were easily eliminated from the body with the faeces. In turn, the gradual increase of Ag uptake following $AgNO_3$ exposure was identical to that obtained for snails exposed to $AgNO_3$ in the Ag-spiked water test. However, the internal Ag concentrations and k1 value were significantly lower in snails exposed to $AgNO_3$ from the present test (0.65 L_{water} $g^{-1}_{organism}$ day^{-1}) than those from the Ag-spiked water test (1.20 L_{water} $g^{-1}_{organism}$ day^{-1}) (Table S4.3). Even though k2 values were not significantly different, elimination was higher in the present test (Silva et al., 2020). Furthermore, the SF of zero obtained in this test suggests that no Ag was retained in the body of the snails despite the very low k2 (Figure S4.1, Table S4.3), which contradicts the earlier findings (Silva et al., 2020). The similar uptake rates point to similar uptake routes between $AgNO_3$ exposures of the present test and the Ag-spiked water test, which would be from water. However, ingestion of food cannot be ruled out as an uptake route because feeding was observed during the test and there were no significant differences in snail weights between control, Ag_2S NP and $AgNO_3$ exposures (data not shown). Thus, avoidance behaviour was unlikely to occur. Considering this, two hypotheses can be drawn to explain the similar uptake rates but lower internal Ag concentrations in the $AgNO_3$ exposure of the present test and the Ag-spiked water test. First, Ag uptake from water could be more important than from food for snails exposed to $AgNO_3$, but the decrease in water concentrations due to the presence of algae led to a decrease of their uptake. Second, the different ages of snails used in the present work (~4 months old) and in the Ag-spiked water test (~2 months old) may also explain the differences in internal Ag concentrations in $AgNO_3$ exposures. In the work of Croteau et al. (2014), older *L. stagnalis* revealed slower uptake rate constants of waterborne Ag NPs and Ag^+ than younger snails. For *P. acuta*, the lowest metal (Cu, Cd and Pb) concentration in the body was typical for the largest individuals, except for Zn (Spyra et al., 2019).

APW medium was renewed every 48h to keep exposure concentrations relatively constant during the uptake phase, and Ag concentrations in the water during the 48h were not analysed. However, Ag concentrations in water probably decreased due to the potential Ag uptake by *R. subcapitata*, therefore, this lack of measurement of Ag in the water during

the 48h and also in the algae, can be seen as a limitation of the present study. Nevertheless, the exposure of this test did simulate a realistic scenario, where NPs primarily enter the water body and then contaminate the food of benthic invertebrates.

4.5.2. *Girardia tigrina* - food exposure test

The internal Ag concentrations and uptake rate in the planarians were significantly higher upon exposure to $AgNO_3$ compared to Ag_2S NPs (Figure 4.3). Since Ag concentrations in the food were only significantly higher in the ionic treatment than in the Ag_2S NP exposure at 48h, the lower uptake was probably due to differences in availability between the treatments. Planarians capture their prey using mucus secretions, after which it is partially digested by proteolytic enzymes and ingested by the pharynx (Knakievicz, 2014). The pharynx of *Dugesia japonica* showed to be able to sense different chemical stimuli in the food at the same time and decide on its suitability for ingestion (Miyamoto et al., 2020). It could be speculated that particle selection could have occurred when food was ingested by the pharynx and uptake of bigger particles/aggregates such as Ag_2S NPs may have been selectively avoided. According to DLS results, Ag_2S NPs showed strong agglomeration at time 0 in both UPW and APW media (Table S4.1). However, planarians were exposed to the particles in the food, and size/aggregation of Ag_2S NPs inside the snails was not determined. Metal/NP accumulation in the prey may affect their transfer to predators, for instance, if assimilation of metals or NPs is high in the prey, the possible transfer to the predator increases (Tangaa et al., 2016). Hence, to explain the higher Ag accumulation in planarians fed on snails pre-exposed to $AgNO_3$, it can be suggested that Ag was more efficiently assimilated by snails in the $AgNO_3$ treatment, leading to higher Ag availability than for planarians that fed on snails pre-exposed to Ag_2S NPs. Also, more different uptake pathways could have been available for Ag from the $AgNO_3$ treatment than for Ag_2S NPs. Another hypothesis could be that, by the time of capture by planarians, snails pre-exposed to Ag_2S NPs had already been able to eliminate a considerably fraction of the Ag accumulated (see sections 4.5.1 and 4.5.3). Consequently, this led to lower internal Ag concentrations by the time they were predated by the planarians. Snails were provided alive, and they could avoid planarians for some time (personal observation), although it cannot be confirmed that Ag was quickly eliminated by snails during the time they were escaping.

Planarians present two types of intestinal cells: secretory goblet cells (release digestive enzymes into the lumen) and absorptive phagocytes (engulf food particles for intracellular digestion) (Salvetti et al., 2015). In a study injecting boron nitride nanotubes (BNNTs) into

the gut of *D. japonica*, BNNTs were found inside cytoplasmic vesicles of intestinal phagocytes one day after the last injection, probably internalized by endocytosis, but were no longer detected in the planarians three days after of the last injection (Salvetti et al., 2015). Planarians also internalized cerium oxide and cerium fluoride NPs (Ermakov et al., 2019; Salvetti et al., 2020). Intracellular uptake of (waterborne) uncoated and PVP-coated Ag NPs was also observed in *Schmidtea mediterranea*. In that study, a fraction of Ag seemed to accumulate in the gut of *S. mediterranea*, which was probably the result of slow elimination of Ag NPs or low distribution to extra-intestinal tissues (Leynen et al., 2019). This is opposite to the relatively fast elimination rates found in the present work for both exposures. *G. tigrina* exposed to waterborne Cu^{2+} revealed accumulation followed by its rapid removal from the body, which was attributed to some detoxification mechanism of Cu^{2+}, such as MTs (Knakievicz, 2014; Knakievicz and Ferreira, 2008). Different distribution patterns of different metals in the body portions of these organisms have been reported, and were associated with sequestration by MTs (Wu et al., 2011, 2012). The elimination rates and the estimated k2 values for both treatments are similar (Figure 4.3, Table 4.1). Since k2 values depend solely on the organism's ability to eliminate compounds, these results suggest that the planarians eliminated Ag through similar processes in both treatments, although this needs investigation since elimination for non-depurated planarians was faster for the Ag_2S NPs, albeit non-significantly (Figure S4.2, Table S4.4). Still, it can be postulated that intracellular digestion of food occurred in both treatments, possibly explaining the similar elimination rates observed. Possible dissolution of Ag_2S NPs in the digestive system can be another hypothesis to explain the similarity in elimination for the two Ag forms. Intestinal pH of planarians can be slightly acidic (Jennings 1957) (e.g., < 5.5 for *S. mediterranea* (Goupil et al., 2016)), which may lead to potential release of Ag^+ inside the gut and to potential reduction of NP size (Leynen et al., 2019). Still, it should be noted that this is merely speculative since the fate, form and size of Ag_2S NPs inside the snail or planarian bodies were not assessed.

Toxicokinetic parameters were different, especially for $AgNO_3$, when analysing data with model 2. The calculated SF were almost zero and k2 values were higher for both exposures, showing low tendency for Ag to be stored in the planarian body (Figure S4.1, Table S4.3). Previous exposures to waterborne Ag_2S NPs and $AgNO_3$ revealed very low to no Ag uptake by *G. tigrina* (Figure S4.3). Internal Ag concentrations were only significantly different from controls in planarians exposed to $AgNO_3$ (data not shown), but no significant differences were found between kinetic parameters for the uptake of Ag_2S NPs and $AgNO_3$ (Table S4.6). Higher toxicity was observed in *S. mediterranea* upon waterborne exposure to $AgNO_3$

than to uncoated and PVP-coated Ag NPs, suggesting higher bioavailability of the ionic form (Leynen et al., 2019). Uptake of metals, such as Cu, Cd and Zn, by *D. japonica* and *G. tigrina* has been demonstrated to be low and lower than for other freshwater invertebrates (Wu and Li, 2017). The low uptake of waterborne compounds by planarians may be, in part, due to the absence of water-current creating structures and gills. Planarians also secret mucus that can act as a barrier to the entrance of contaminants, which may play a major protection role in water exposures (Wu and Li, 2017). In these waterborne exposures, Ag_2S NPs could have been retained in the mucus and transdermal uptake was probably easier for Ag ions explaining the higher uptake in the $AgNO_3$ treatment. However, upon dietary exposures the uptake of chemicals mainly occurs by the pharynx and not by cutaneous diffusion, which may explain the higher uptake by *G. tigrina* in the food exposure test.

4.5.3. Influence of depuration on the internal Ag concentrations and toxicokinetics of the test organisms

The depuration period is important to consider for a more accurate estimate of bioaccumulation potential. Hence, it is important to determine a depuration time that allows sufficient gut clearance while minimizing the potential elimination of NPs from the tissues (Petersen et al., 2019). In this work, the influence of depuration on the internal Ag concentrations and toxicokinetics of the test species was evaluated. For this, a 24-h depuration period was tested for *P. acuta* and *G. tigrina*. For *P. acuta*, depuration only seemed to influence internal Ag concentrations in snails exposed to $AgNO_3$ at day 7 (Figure 4.2). The minimal gut passage time of food in *L. stagnalis* was around 5h, and gut residence time was determined to be around 22.5h (90% of the ingested label was excreted) (Croteau et al., 2007). To our knowledge, gut residence time was not determined for *P. acuta*. However, assuming that it is similar to that of *L. stagnalis*, this finding suggests that the 24h-depuration period used in this test may be appropriate for complete gut clearance. Other studies have used a 24-hour period of starvation to empty the gut of *P. acuta* before starting exposures (Bernot et al., 2005; Elias and Bernot, 2017). Considering this, our results suggest that the gut content of snails may have been excreted during the depuration without a significant decrease in internal Ag concentrations, except for day 7, indicating that Ag was efficiently assimilated in the $AgNO_3$ treatment. The slow elimination also confirms that likely only a small amount of Ag was egested with faeces, at least for most of the uptake phase of the $AgNO_3$ exposure. Herbivorous snails efficiently assimilate metals from their diet (Croteau et al., 2007). It should be noted that if in the $AgNO_3$ treatment Ag accumulation

also occurred via transdermal uptake, it may not have been eliminated with food through the gut.

For snails exposed to Ag_2S NPs, internal Ag concentrations seemed not to be influenced by time or depuration, even though at day 7 concentrations were clearly lower for depurated than non-depurated snails. For this treatment, even though Ag concentrations were higher at all sampling days for non-depurated snails, statistical comparisons were hindered by the large scatter in the data, preventing drawing reliable conclusions (Figure 4.2). It was previously postulated that Ag_2S NPs could be more efficiently eliminated, likely associated with faeces, therefore, it is possible that Ag_2S NPs were excreted relatively fast with the faeces during the depuration period. Also, based on the minimal gut passage time determined for *L. stagnalis*, it is possible that Ag_2S NPs were excreted faster with the faeces. The significantly higher k2 value of the Ag_2S NP exposure than that of $AgNO_3$ may support this assumption (Table 4.1). Additionally, much lower internal Ag concentrations in the snails were observed in the elimination phase of the Ag_2S NP exposure, while they remained high for $AgNO_3$ (Figures 4.1 and S4.2). Furthermore, the kinetics of depurated and non-depurated snails were similar for the $AgNO_3$ treatment, supporting that elimination during the 24h depuration interval probably did not affect Ag concentrations and kinetics in the snails. For the Ag_2S NP exposure, uptake was highest for non-depurated snails and so were k1 and k2 values, however the large scatter in the data prevented reliable comparisons (Figures 4.1 and S4.2, Tables 4.1 and S4.4).

Even though internal Ag concentrations in non-depurated planarians were higher, no significant differences were found, also not in the kinetic parameters, suggesting that the 24h-depuration period used had limited impact on the results. The excretory system of planarians consists of a protonephridia, which are ciliated and broadly distributed with dual function of osmoregulation and waste expulsion. The highly branched intestine connects to a centrally located pharynx that is used as mouth and anus (Reddien, 2018). The “gut voidance” may not be applicable in this case, given the distinct digestive and excretory systems of planarians, and their very slow digestive process, which can last for 5 days (Sheiman et al., 2002). A more detailed investigation on this subject was beyond the scope of the present work, which only provides a preliminary assessment of depuration in both test species.

4.5.4. Potential bioaccumulation and trophic transfer

Both depurated and non-depurated snails revealed higher BCF_k values upon exposure to $AgNO_3$ than to Ag_2S NPs, indicating that bioaccumulation potential is higher upon ionic

exposure (Tables 4.1 and S4.4). Ag uptake by snails was likely also by ingestion of algae and therefore bioconcentration may not be the appropriate denomination. The term "bioconcentration" is used for snails to indicate that the kinetic parameters used to calculate BCF_ks were based on water exposure concentrations. For the river snail *Cipangopaludina chinensis* BCFs were 0.1 and 0.23 for Ag uptake from citrate and PVP-capped Ag NPs, and 0.92 for $AgNO_3$, after 7 days exposure to a single dose of 60 µg L^{-1} in a paddy microcosm. The biofilm present in the same microcosm revealed much higher BCFs of 1.58, 2.30 and 6.54 upon exposure to citrate and PVP-capped Ag NPs and $AgNO_3$, respectively. The high accumulation observed in biofilms was attributed to the high adsorption ability of extracellular polymeric substances, thus a similar scenario may have happened in the present work (Park et al., 2018). After 7 days of exposure to Ag NPs, the marine snail *Ilyanassa obsoleta* showed BCFs of 0.27-0.33 in an estuarine mesocosm, for biofilms BCFs were 06.2-7.7. In the latter study, the trophic transfer factors (TTFs) from biofilm to snails was 14-270 (at 7 days of exposure: 43), suggesting that ingestion of biofilm was the primary Ag transfer route for snails and not uptake from seawater (Cleveland et al., 2012). Trophic transfer of Ag nanowires was observed in a food chain consisting of a microalgae (*Chlamydomonas reinhardtii*), water flea (*Daphnia magna*) and zebrafish (*Danio rerio*) (Chae and An, 2016). Biomagnification of Ag NPs has been determined in a natural fish food web from a Chinese lake (Xiao et al., 2019).

Biomagnification from snails to planarians did not occur under the present test conditions, and BMF_ks were especially low for the Ag_2S NP exposure. The very similar BMF_ks estimated for depurated and non-depurated planarians further reflect that depuration did not affect their Ag toxicokinetics. Even though biomagnification is usually determined considering only the internal concentrations in the organism, thus excluding possible adsorption to body surfaces, in the environment organisms are predated accounting for contaminants absorbed and adsorbed in the body and their bioavailability for the predator. Therefore, this work provided data considering this more realistic exposure scenario.

4.6. Conclusions

P. acuta was likely exposed through water and food in both treatments, but the ingestion of algae possibly had higher relevance for Ag uptake in the Ag_2S NP treatment compared to $AgNO_3$. Snails revealed Ag uptake and elimination patterns for $AgNO_3$ similar to waterborne exposures in our earlier tests, whereas for Ag_2S NPs distinct kinetics were obtained when compared with water only exposure. Kinetics and internal Ag concentrations generally did not significantly differ between depurated and non-depurated planarians or

snails. For snails, a 24h-depuration period seems appropriate for efficient gut clearance minimizing elimination of internalized Ag in the $AgNO_3$ exposure, however, no reliable conclusion could be drawn for Ag_2S NP elimination. For planarians, the "gut voidance" mechanism may not be applicable, given their distinct digestive process and excretory system. Snails revealed higher bioaccumulation potential in the $AgNO_3$ treatment than those from the Ag_2S NP exposures. Planarians feeding on pre-exposed snails revealed no risk of potential biomagnification, but they did show active uptake and accumulation of Ag in its ionic or nanoparticulate form through previously exposed food under a realistic contamination scenario. Despite the low uptake observed in the Ag_2S NP treatment, dietary intake seemed the most important exposure route for planarians since no uptake was observed in previous waterborne exposures to Ag_2S NPs.

This work provides data on the toxicokinetics and potential bioaccumulation of Ag in benthic communities. This has particularly relevance for planarians due to the scarcity of bioaccumulation and toxicokinetic data for these organisms. To the best of our knowledge, this is the first study investigating the toxicokinetics and biomagnification of NPs in planarians. The evaluation of trophic transfer and potential biomagnification to planarians is of particular relevance due to the position of planarians in aquatic food chains, highlighting their role as a predator, but also as a prey of many aquatic tertiary consumers. Further studies are needed to elucidate the mechanisms following ingestion of contaminated food in planarians and snails, such as in-depth Ag NP/ionic Ag characterization at the cellular level, in order to explain the elimination patterns observed.

4.7. References

Ardestani, M.M., van Straalen, N.M., van Gestel, C.A.M., 2014. Uptake and elimination kinetics of metals in soil invertebrates: A review. Environ. Pollut. 193, 277–295.

ASTM, 1980. ASTM (E729-80). Standard practice for conducting acute toxicity tests with fishes, macroinvertebrates and amphibians. American Society for Testing and Materials. Annu. B. ASTM Stand. 46, 279–280.

Baccaro, M., Berg, J.H.J. Van Den, Brink, N.W. Van Den, 2021. Are long-term exposure studies needed ? Short-term toxicokinetic model predicts the uptake of metal nanoparticles in earthworms after nine months. Ecotoxicol. Environ. Saf. 220, 112371.

Baccaro, M., Undas, A.K., de Vriendt, J., van den Berg, J.H.J., Peters, R.J.B., van den Brink, N.W., 2018. Ageing, dissolution and biogenic formation of nanoparticles: How do these factors affect the uptake kinetics of silver nanoparticles in earthworms? Environ. Sci. Nano 5, 1107–1116.

Bao, S., Huang, J., Liu, X., Tang, W., Fang, T., 2018. Tissue distribution of Ag and oxidative stress responses in the freshwater snail *Bellamya aeruginosa* exposed to sediment-associated Ag nanoparticles. Sci. Total Environ. 644, 736–746.

Bernot, R.J., Kennedy, E.E., Lamberti, G.A., 2005. Effects of ionic liquids on the survival, movement, and feeding behavior of the freshwater snail, *Physa acuta*. Environ. Toxicol. Chem. 24, 1759–1765.

Carriker, M.R., 1946. Observations on the functioning of the alimentary system of the snail *Lymnaea stagnalis* appressa Say. Biol. Bull. 91, 88–111.

Chae, Y., An, Y.J., 2016. Toxicity and transfer of polyvinylpyrrolidone-coated silver nanowires in an aquatic food chain consisting of algae, water fleas, and zebrafish. Aquat. Toxicol. 173, 94–104.

Chen, Y., Si, Y., Zhou, D., Dang, F., 2017. Differential bioaccumulation patterns of nanosized and dissolved silver in a land snail *Achatina fulica*. Environ. Pollut. 222, 50–57.

Clark, N.J., Boyle, D., Eynon, B.P., Handy, R.D., 2019. Dietary exposure to silver nitrate compared to two forms of silver nanoparticles in rainbow trout: Bioaccumulation potential with minimal physiological effects. Environ. Sci. Nano 6, 1393–1405.

Cleveland, D., Long, S.E., Pennington, P.L., Cooper, E., Fulton, M.H., Scott, G.I., Brewer, T., Davis, J., Petersen, E.J., Wood, L., 2012. Pilot estuarine mesocosm study on the environmental fate of silver nanomaterials leached from consumer products. Sci. Total Environ. 421–422, 267–272.

Cornelis, G., Kirby, J.K., Beak, D., Chittleborough, D., McLaughlin, M.J., 2010. A method for determination of retention of silver and cerium oxide manufactured nanoparticles in soils. Environ. Chem. 7, 298–308.

Cross, R.K., 2017. The fate of engineered nanomaterials in sediments and their route to bioaccumulation. PhD Thesis. University of Exeter. 210 p.

Croteau, M.N., Dybowska, A.D., Luoma, S.N., Misra, S.K., Valsami-Jones, E., 2014. Isotopically modified silver nanoparticles to assess nanosilver bioavailability and toxicity at environmentally relevant exposures. Environ. Chem. 11, 247–256.

Croteau, M.N., Luoma, S.N., Pellet, B., 2007. Determining metal assimilation efficiency in aquatic invertebrates using enriched stable metal isotope tracers. Aquat. Toxicol. 83, 116–125.

Croteau, M.N., Misra, S.K., Luoma, S.N., Valsami-Jones, E., 2011. Silver bioaccumulation dynamics in a freshwater invertebrate after aqueous and dietary exposures to nanosized and ionic Ag. Environ. Sci. Technol. 45, 6600–6607.

Elias, D., Bernot, M.J., 2017. Effects of individual and combined pesticide commercial formulations exposure to egestion and movement of common freshwater snails, *Physa acuta* and *Helisoma anceps*. Am. Midl. Nat. 178, 97–111.

Ermakov, A., Popov, A., Ermakova, O., Ivanova, O., Baranchikov, A., Kamenskikh, K., Shekunova, T., Shcherbakov, A., Popova, N., Ivanov, V., 2019. The first inorganic mitogens: Cerium oxide and cerium fluoride nanoparticles stimulate planarian regeneration via neoblastic activation. Mater. Sci. Eng. C 104, 109924.

Ferdous, Z., Nemmar, A., 2020. Health impact of silver nanoparticles: A review of the biodistribution and toxicity following various routes of exposure. Int. J. Mol. Sci. 21, 2375.

García-Alonso, J., Khan, F.R., Misra, S.K., Turmaine, M., Smith, B.D., Rainbow, P.S., Luoma, S.N., Valsami-Jones, E., 2011. Cellular internalization of silver nanoparticles

in gut epithelia of the estuarine polychaete *Nereis diversicolor*. Environ. Sci. Technol. 45, 4630–4636.

Giese, B., Klaessig, F., Park, B., Kaegi, R., Steinfeldt, M., Wigger, H., Von Gleich, A., Gottschalk, F., 2018. Risks, release and concentrations of engineered nanomaterial in the environment. Sci. Rep. 8, 1–18.

Gonçalves, S.F., Pavlaki, M.D., Lopes, R., Hammes, J., Gallego-Urrea, J.A., Hassellöv, M., Jurkschat, K., Crossley, A., Loureiro, S., 2017. Effects of silver nanoparticles on the freshwater snail *Physa acuta*: The role of test media and snails' life cycle stage. Environ. Toxicol. Chem. 36, 243–253.

Goupil, L.S., Ivry, S.L., Hsieh, I., Suzuki, B.M., Craik, C.S., O'Donoghue, A.J., McKerrow, J.H., 2016. Cysteine and aspartyl proteases contribute to protein digestion in the gut of freshwater planaria. PLoS Negl. Trop. Dis. 10, e0004893.

Grün, A.Y., App, C.B., Breidenbach, A., Meier, J., Metreveli, G., Schaumann, G.E., Manz, W., 2018. Effects of low dose silver nanoparticle treatment on the structure and community composition of bacterial freshwater biofilms. PLoS One 13, e0199132.

He, D., Garg, S., Wang, Z., Li, L., Rong, H., Ma, X., Li, G., An, T., Waite, T.D., 2019. Silver sulfide nanoparticles in aqueous environments: Formation, transformation and toxicity. Environ. Sci. Nano 6, 1674–1687.

Ilic, M.D., Tubic, B.P., Marinkovic, N.S., Markovic, V.M., Popovic, N.Z., Zoric, K.S., Rakovic, M.J., Paunovic, M.M., 2018. First report on the non-indigenous triclad *Girardia tigrina* (Girard, 1850) (Tricladida, Dugesiidae) in Serbia, with notes on its ecology and distribution. Acta Zool. Bulg. 70, 39–43.

Jennings, J.B., 1957. Studies on feeding, digestion, and food storage in free-living flatworms (Platyhelminthes: Turbellaria). Biol. Bull. 112, 63–80.

Khan, F.R., Misra, S.K., Bury, N.R., Smith, B.D., Rainbow, P.S., Luoma, S.N., Valsami-Jones, E., 2015. Inhibition of potential uptake pathways for silver nanoparticles in the estuarine snail *Peringia ulvae*. Nanotoxicology 9, 493–501.

Khodaparast, Z., van Gestel, C.A.M., Papadiamantis, A.G., Gonçalves, S.F., Lynch, I., Loureiro, S., 2021. Toxicokinetics of silver nanoparticles in the mealworm *Tenebrio molitor* exposed via soil or food. Sci. Total Environ. 777, 146071.

Knakievicz, T., 2014. Planarians as invertebrate bioindicators in freshwater environmental quality: the biomarkers approach. Ecotoxicol. Environ. Contam. 9, 1–12.

Knakievicz, T., Ferreira, H.B., 2008. Evaluation of copper effects upon *Girardia tigrina* freshwater planarians based on a set of biomarkers. Chemosphere 71, 419–428.

Kuehr, S., Kosfeld, V., Schlechtriem, C., 2021. Bioaccumulation assessment of nanomaterials using freshwater invertebrate species. Environ. Sci. Eur. 33, 1-36.

Kühr, S., Schneider, S., Meisterjahn, B., Schlich, K., Hund-Rinke, K., Schlechtriem, C., 2018. Silver nanoparticles in sewage treatment plant effluents: chronic effects and accumulation of silver in the freshwater amphipod Hyalella azteca. Environ. Sci. Eur. 30, 1–11.

Larguinho, M., Correia, D., Diniz, M.S., Baptista, P.V., 2014. Evidence of one-way flow bioaccumulation of gold nanoparticles across two trophic levels. J. Nanoparticle Res. 16, 1–11.

Leynen, N., Van Belleghem, F.G.A.J., Wouters, A., Bove, H., Ploem, J.P., Thijssen, E., Langie, S.A.S., Carleer, R., Ameloot, M., Artois, T., Smeets, K., 2019. In vivo toxicity assessment of silver nanoparticles in homeostatic versus regenerating planarians. Nanotoxicology 13, 476–491.

Marigómez, I., Soto, M., Cajaraville, M.P., Angulo, E., Giamberini, L., 2002. Cellular and subcellular distribution of metals in molluscs. Microsc. Res. Tech. 56, 358–392.

McTeer, J., Dean, A.P., White, K.N., Pittman, J.K., 2014. Bioaccumulation of silver nanoparticles into *Daphnia magna* from a freshwater algal diet and the impact of phosphate availability. Nanotoxicology 8, 305–316.

Miyamoto, M., Hattori, M., Hosoda, K., Sawamoto, M., Motoishi, M., Hayashi, T., Inoue, T., Umesono, Y., 2020. The pharyngeal nervous system orchestrates feeding behavior in planarians. Sci. Adv. 6, 1–10.

Mohammad, W.A., Ali, S.M., Farhan, N., Said, S.M., 2021. The toxic effect of zinc oxide nanoparticles on the terrestrial slug *Lehmannia nyctelia* (Gastropoda-Limacidae). J. Basic Appl. Zool. 1, 1–9.

Musee, N., Oberholster, P.J., Sikhwivhilu, L., Botha, A.M., 2010. The effects of engineered nanoparticles on survival, reproduction, and behaviour of freshwater snail, *Physa acuta* (Draparnaud, 1805). Chemosphere 81, 1196–1203.

Naylor, C., Maltby, L., Calow, P., 1989. Scope for growth in *Gammarus pulex*, a freshwater benthic detritivore. Hydrobiologia 188/189, 517–523.

OECD, 2017. Test No. 318: Dispersion Stability of Nanomaterials in Simulated Environmental Media. OECD Guideline for the Testing of Chemicals. Organization for Economic Co-operation and Development, Paris.

OECD, 2016. Test No. 243: *Lymnaea stagnalis* Reproduction Test. OECD Guideline for the Testing of Chemicals. Organization for Economic Co-operation and Development, Paris. https://doi.org/10.1787/9789264264335-en

Oviedo, N.J., Nicolas, C.L., Adams, D.S., Levin, M., 2008. Establishing and maintaining a colony of planarians. Cold Spring Harb. Protoc. 3, 1–6.

Park, H.G., Kim, J.I., Chang, K.H., Lee, B.-C., Eom, I.-C., Kim, P., Nam, D.H., Yeo, M.K., 2018. Trophic transfer of citrate, PVP coated silver nanomaterials, and silver ions in a paddy microcosm. Environ. Pollut. 235, 435–445.

Pavlaki, M.D., Morgado, R.G., Soares, A.M.V.M., Calado, R., Loureiro, S., 2018. Toxicokinetics of cadmium in *Palaemon varians* postlarvae under waterborne and/or dietary exposure. Environ. Toxicol. Chem. 37, 1614–1622.

Peters, R.J.B., van Bemmel, G., Milani, N.B.L., den Hertog, G.C.T., Undas, A.K., van der Lee, M., Bouwmeester, H., 2018. Detection of nanoparticles in Dutch surface waters. Sci. Total Environ. 621, 210–218.

Petersen, E.J., Mortimer, M., Burgess, R.M., Handy, R., Hanna, S., Ho, K.T., Johnson, M., Loureiro, S., Selck, H., Scott-Fordsmand, J.J., Spurgeon, D., Unrine, J., van den Brink, N.W., Wang, Y., White, J., Holden, P., 2019. Strategies for robust and accurate experimental approaches to quantify nanomaterial bioaccumulation across a broad range of organisms. Environ. Sci. Nano 6, 1619–1656.

Pulit-Prociak, J., Banach, M., 2016. Silver nanoparticles - A material of the future...? Open Chem. 14, 76–91.

Rainbow, P.S., Luoma, S.N., Wang, W.X., 2011. Trophically available metal - A variable feast. Environ. Pollut. 159, 2347–2349.

Reddien, P.W., 2018. The cellular and molecular basis for planarian regeneration. Cell 175, 327–345.

Ribeiro, F., Gallego-Urrea, J.A., Goodhead, R.M., van Gestel, C.A.M., Moger, J., Soares, A.M.V.M., Loureiro, S., 2015. Uptake and elimination kinetics of silver nanoparticles and silver nitrate by *Raphidocelis subcapitata*: The influence of silver behaviour in solution. Nanotoxicology 9, 686–695.

Ribeiro, F., Gallego-Urrea, J.A., Jurkschat, K., Crossley, A., Hassellöv, M., Taylor, C., Soares, A.M.V.M., Loureiro, S., 2014. Silver nanoparticles and silver nitrate induce high toxicity to *Pseudokirchneriella subcapitata*, *Daphnia magna* and *Danio rerio*. Sci. Total Environ. 466–467, 232–241.

Ribeiro, F., van Gestel, C.A.M., Pavlaki, M.D., Azevedo, S., Soares, A.M.V.M., Loureiro, S., 2017. Bioaccumulation of silver in *Daphnia magna*: Waterborne and dietary exposure to nanoparticles and dissolved silver. Sci. Total Environ. 574, 1633–1639.

Salvetti, A., Gambino, G., Rossi, L., De Pasquale, D., Pucci, C., Linsalata, S., Degl'Innocenti, A., Nitti, S., Prato, M., Ippolito, C., Ciofani, G., 2020. Stem cell and tissue regeneration analysis in low-dose irradiated planarians treated with cerium oxide nanoparticles. Mater. Sci. Eng. C 115, 111113.

Salvetti, A., Rossi, L., Iacopetti, P., Li, X., Nitti, S., Pellegrino, T., Mattoli, V., Golberg, D., Ciofani, G., 2015. In vivo biocompatibility of boron nitride nanotubes: Effects on stem cell biology and tissue regeneration in planarians. Nanomedicine 10, 1911–1922.

Saraiva, A.S., Sarmento, R.A., Gravato, C., Rodrigues, A.C.M., Campos, D., Simão, F.C.P., Soares, A.M.V.M., 2020. Strategies of cellular energy allocation to cope with paraquat-induced oxidative stress: Chironomids vs Planarians and the importance of using different species. Sci. Total Environ. 741, 140443.

Sekine, R., Khurana, K., Vasilev, K., Lombi, E., Donner, E., 2015. Quantifying the adsorption of ionic silver and functionalized nanoparticles during ecotoxicity testing: Test container effects and recommendations. Nanotoxicology 9, 1005–1012.

Sheiman, I.M., Zubina, E. V., Kreshchenko, N.D., 2002. Regulation of the feeding behavior of the planarian *Dugesia (Girardia) tigrina*. J. Evol. Biochem. Physiol. 38, 414–418.

Silva, P. V., van Gestel, C.A.M., Verweij, R.A., Papadiamantis, A.G., Gonçalves, S.F., Lynch, I., Loureiro, S., 2020. Toxicokinetics of pristine and aged silver nanoparticles in *Physa acuta*. Environ. Sci. Nano 7, 3849–3868.

Simão, F.C.P., Gravato, C., Machado, A.L., Soares, A.M.V.M., Pestana, J.L.T., 2020. Toxicity of different polycyclic aromatic hydrocarbons (PAHs) to the freshwater planarian *Girardia tigrina*. Environ. Pollut. 266, 115185.

Spurgeon, D.J., Lahive, E., Schultz, C.L., 2020. Nanomaterial transformations in the environment: effects of changing exposure forms on bioaccumulation and toxicity. Small 16, 1–12.

Spyra, A., Cieplok, A., Strzelec, M., Babczyńska, A., 2019. Freshwater alien species *Physella acuta* (Draparnaud, 1805) - A possible model for bioaccumulation of heavy metals. Ecotoxicol. Environ. Saf. 185, 109703.

Sun, T.Y., Bornhöft, N.A., Hungerbühler, K., Nowack, B., 2016. Dynamic probabilistic

modeling of environmental emissions of engineered nanomaterials. Environ. Sci. Technol. 50, 4701–4711.

Tangaa, S.R., Selck, H., Winther-Nielsen, M., Croteau, M.N., 2018. A biodynamic understanding of dietborne and waterborne Ag uptake from Ag NPs in the sediment-dwelling oligochaete, *Tubifex tubifex*. NanoImpact 11, 33–41.

Tangaa, S.R., Selck, H., Winther-Nielsen, M., Khan, F.R., 2016. Trophic transfer of metal-based nanoparticles in aquatic environments: A review and recommendations for future research focus. Environ. Sci. Nano 3, 966–981.

van den Brink, N.W., Jemec Kokalj, A., Silva, P.V., Lahive, E., Norrfors, K., Baccaro, M., Khodaparast, Z., Loureiro, S., Drobne, D., Cornelis, G., Lofts, S., Handy, R.D., Svendsen, C., Spurgeon, D., van Gestel, C.A.M., 2019. Tools and rules for modelling uptake and bioaccumulation of nanomaterials in invertebrate organisms. Environ. Sci. Nano 6, 1985–2001.

van der Zande, M., Kokalj, A.J., Spurgeon, D., Loureiro, S., Silva, P. V., Khodaparast, Z., Drobne, D., Clark, N.J., van den Brink, N., Baccaro, M., van Gestel, C.A.M., Bouwmeester, H., Handy, R.D., 2020. The gut barrier and the fate of engineered nanomaterials: a view from comparative physiology. Environ. Sci. Nano 7, 1874–1898.

Wu, J.P., Chen, H.C., Li, M.H., 2012. Bioaccumulation and toxicodynamics of cadmium to freshwater planarian and the protective effect of N-Acetylcysteine. Arch. Environ. Contam. Toxicol. 63, 220–229.

Wu, J.P., Chen, H.C., Li, M.H., 2011. The preferential accumulation of cadmium in the head portion of the freshwater planarian, *Dugesia japonica* (Platyhelminthes: Turbellaria). Metallomics 3, 1368–1375.

Wu, J.P., Li, M.H., 2018. The use of freshwater planarians in environmental toxicology studies: Advantages and potential. Ecotoxicol. Environ. Saf. 161, 45–56.

Wu, J.P., Li, M.H., 2017. Low uptakes of Cd, Cu, and Zn in *Dugesia japonica*, a freshwater planarian with higher tolerance to metals. Chem. Ecol. 33, 257–269.

Xiao, B., Zhang, Y., Wang, X., Chen, M., Sun, B., Zhang, T., Zhu, L., 2019. Occurrence and trophic transfer of nanoparticulate Ag and Ti in the natural aquatic food web of Taihu Lake, China. Environ. Sci. Nano 6, 3431–3441.

Zhao, J., Li, Y., Wang, X., Xia, X., Shang, E., Ali, J., 2021. Ionic-strength-dependent effect of suspended sediment on the aggregation, dissolution and settling of silver nanoparticles. Environ. Pollut. 279, 116926.

Zhu, X., Wang, J., Zhang, X., Chang, Y., Chen, Y., 2010. Trophic transfer of TiO_2 nanoparticles from daphnia to zebrafish in a simplified freshwater food chain. Chemosphere 79, 928

4.8. Supplementary information

Table S4.1. Z-potential values (mV), polydispersity Index (PDI) and mean hydrodynamic diameter (nm) measured by Dynamic Light Scattering (DLS); dissolved Ag concentrations (µg L^{-1}) and percentage of dissolution of Ag_2S NPs dispersed in ultrapure water (UPW) and artificial pond water (APW) medium at a nominal concentration of 1 mg Ag L^{-1}, measured by Inductively Coupled Plasma Mass Spectrometry (ICP-MS). Values are given as mean and standard deviation (mean ± SD; *n*=3). Data published in Silva et al. (2020).

Medium	Timepoint (h)	Z-potential (mV)	DLS (nm)	PDI	Dissolved Ag concentration (µg L^{-1})	% Dissolution
UPW	0	-33.9 ± 0.74	215 ± 9.76	0.34	n.a.	n.a.
	2	-33.1 ± 14	206 ± 22.3	0.41	0.13 ± 0.05	0.04 ± 0.02
	4	-36.2 ± 5.64	206 ± 23.1	0.38	0.03 ± 0.01	0.01 ± 0.002
	24	-44.4 ± 3.36	207 ± 32.9	0.4	0.02 ± 0.005	0.01 ± 0.001
	48	-42.1 ± 4.37	212 ± 18.2	0.37	0.05 ± 0.01	0.01 ± 0.003
APW	0	-9.55 ± 0.66	191 ± 6.55	0.33	n.a.	n.a.
	2	-9.31 ± 2.51	213 ± 30.6	0.4	0.71 ± 0.06	0.20 ± 0.02
	4	-8.93 ± 0.49	206 ± 16.8	0.41	0.15 ± 0.16	0.04 ± 0.05
	24	-8.35 ± 2.18	183 ± 20.6	0.37	0.12 ± 0.17	0.03 ± 0.05
	48	-7.97 ± 3.68	159 ± 13.5	0.35	0.01 ± 0.002	0.002 ± 0.0005

n.a. not analysed at that time point.

Table S4.2. Total Ag concentrations determined at day 0 and dissolved Ag concentrations (µg Ag L^{-1}; mean ± standard deviation; *n*=3) determined at days 0, 1 and 2 in APW medium from Ag_2S NP and $AgNO_3$ treatments. Different capital letters within a column indicate statistically significant differences between treatments (*t*-test, p<0.05). Different small letters within a line indicate statistically significant differences between days in each treatment (one-way repeated measures ANOVA followed by Holm-Sidak Method, p<0.05). Data published in Silva et al. (2020); statistical analysis redone to apply to the two Ag forms used in this study.

Ag from	Total Ag concentrations (µg Ag L^{-1})	Dissolved Ag concentrations (µg Ag L^{-1})		
	Day 0	Day 0	Day 1	Day 2
Ag_2S NPs	16.8 ± 0.72 **A**	0.08 ± 0.1 **A / a**	0.17 ± 0.09 **A / a**	0.05 ± 0.08 **A / a**
$AgNO_3$	7.51 ± 0.26 **B**	2.35 ± 0.2 **B / a**	2.49 ± 0.16 **B / a,b**	2.99 ± 0.12 **B / b**

Toxicokinetic models – model 2 (equation S1 and S2)

The toxicokinetics of Ag were also described fitting a one-compartment model to the internal Ag concentrations measured in snails (soft body) and planarians, accounting for a stored fraction (SF) (van den Brink et al., 2019):

$$Q(t) = C_0 + \left(C_{exp} * k1 * SF * t\right) + \left(C_{exp} * \left(\frac{k1}{(k2 + k_{growth})}\right) * \left(1 - e^{\left(-(k2+k_{growth})*t\right)}\right) * (1 - SF)\right)$$

(S1)

$$Q(t) = C_0 + \left(C_{exp} * k1 * SF * t_c\right) + \left(C_{exp} * \left(\frac{k1}{(k2+k_{growth})}\right) * \left(1 - e^{\left(-(k2+k_{growth})*t_c\right)}\right) * e^{\left(-(k2+k_{growth})*(t-t_c)\right)} * (1 - SF)\right)$$

(S2)

Where Q(t) = Ag internal concentration in the organisms at time t days (snails) or hours (planarians) (µg Ag $g^{-1}_{organism}$ dw); C_0 = background internal concentration measured at day 0 (µg Ag $g^{-1}_{organism}$ dw); k1 = uptake rate constant from water (L_{water} $g^{-1}_{organism}$ day^{-1}) or food (g_{food} $g^{-1}_{organism}$ $hour^{-1}$); k2 = elimination rate constant (day^{-1} or $hour^{-1}$); SF= stored fraction (ranging from 0 to 1; unit less); k_{growth} = growth decrease rate constant (day^{-1} or $hour^{-1}$); C_{exp} = Ag exposure concentration in water (µg Ag L^{-1}) or food (µg Ag g^{-1} dw); t = time in days or hours; t_c = time at which organisms were transferred from contaminated to clean media (day 7 or 72 hours).

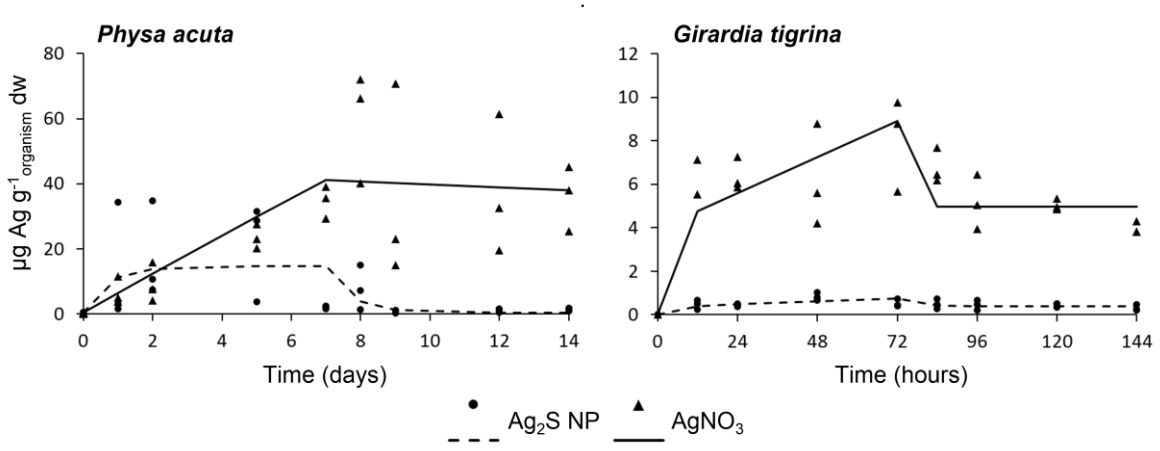

Figure S4.1. Uptake and elimination of Ag in depurated *Physa acuta* and *Girardia tigrina* exposed to Ag_2S NPs and $AgNO_3$. Snails were exposed for 7 days to water spiked at a nominal concentration of 10 µg Ag L^{-1}, and transferred to clean water for 7 days; planarians were exposed for 72 hours to contaminated food and then fed with clean food for 72 hours. Lines show the fit of model 2 to the data points, which represent Ag concentrations determined in planarians and snails (soft body). See Table S4.3 for the resulting kinetics parameter values.

Table S4.3. Uptake (k1) and elimination (k2) rate constants and stored fraction (SF) (± 95% confidence intervals) of Ag uptake in depurated *Physa acuta* and *Girardia tigrina* exposed to Ag_2S NPs and $AgNO_3$. Also shown are toxicokinetic parameters from a test (Ag-spiked water test) with *P. acuta* exposed to waterborne Ag_2S NPs and $AgNO_3$ at a nominal concentration of 10 µg Ag L^{-1} from Silva et al. (2020). Data was modelled with model 2, see Figure S4.1. Measured exposure concentrations (mean ± standard deviation; *n*=3) in water for *P. acuta* (µg Ag L^{-1}) and in food for *G. tigrina* (µg Ag g^{-1} dw; see Table S4.5 for individual values) are also shown. Different capital letters in bold within a column indicate statistically significant differences in k1 or k2 values between Ag_2S NPs and $AgNO_3$ in each species ($X^2_{(1)}$>3.84; p<0.05). Different capital letters in italics indicate statistically significant differences between k1 or k2 of each treatment in *P. acuta* from present work and from the Ag-spiked water test ($X^2_{(1)}$>3.84; p<0.05). Absence of letters indicates no statistically significant differences ($X^2_{(1)}$<3.84; p>0.05).

Species (depurated)	**Ag form**	**Measured concentration** (µg Ag L^{-1} or µg Ag g^{-1} dw)	**k1** (L_{water} $g^{-1}_{organism}$ day^{-1} or g_{food} $g^{-1}_{organism}$ $hour^{-1}$)	**k2** (day^{-1} or $hour^{-1}$)	**SF**
Physa acuta	Ag_2S NPs	17.7 ± 0.59	1.13 (-0.67-2.94)	1.45 (-1.18-4.08) **A**	0 (-0.051-0.051)
	$AgNO_3$	9.31 ± 0.25	0.65 (0.056-1.25) *A*	0.071 (-4.71-4.85) **B**	0 (-)
Physa acuta (Silva et al. (2020))	Ag_2S NPs	2.46 ± 0.48	1.07 (-0.97-3.10)	0.44 (-0.79-1.67)	0 (-0.52-0.52)
	$AgNO_3$	9.46 ± 0.59	1.20 (0.69-1.70) *B*	0.02 (n.d.)	1 (-)
Girardia tigrina	Ag_2S NPs	34.1 ± 25.4	0.0021 (-0.0017-0.0058)	0.17 (-0.22-0.56)	0.076 (-0.053-0.21)
	$AgNO_3$	41.4 ± 9.44	0.15 (n.d.)	1.52 (n.d.)	0.011 (-)

(-) very wide 95% confidence intervals.
(n.d.) not possible to determine 95% confidence intervals.

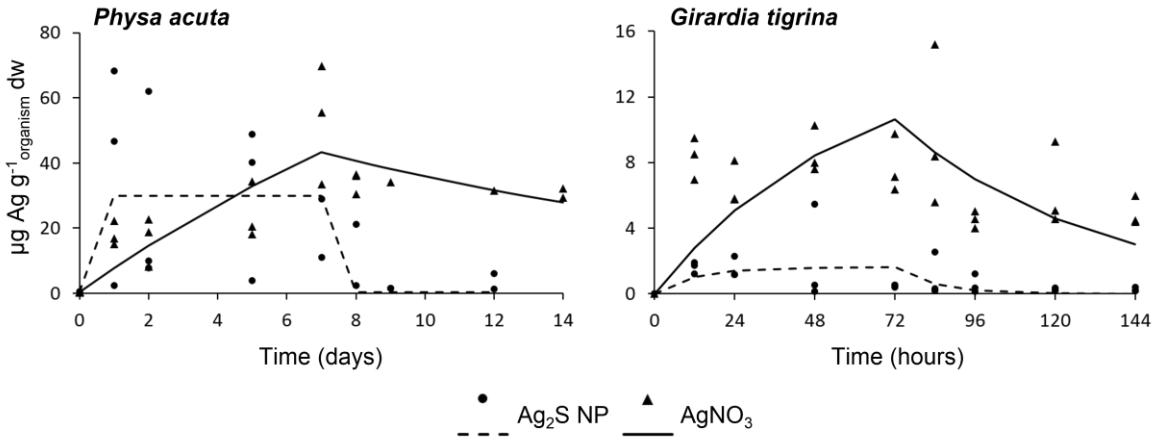

Figure S4.2. Uptake and elimination of Ag in non-depurated *Physa acuta* and *Girardia tigrina* exposed to Ag_2S NPs and $AgNO_3$. Snails were exposed for 7 days to water spiked at a nominal concentration of 10 µg Ag L^{-1}, and transferred to clean water for 7 days; planarians were exposed for 72 hours to contaminated food and then fed with clean food for 72 hours. Lines show the fit of model 1 to the data points, which represent Ag concentrations determined in planarians and snails (soft body). See Table S4.4 for the resulting kinetics parameter values.

Table S4.4. Uptake (k1) and elimination (k2) rate constants (± 95% confidence intervals) of Ag uptake in non-depurated *Physa acuta* and *Girardia tigrina* exposed to Ag_2S NPs and $AgNO_3$. Bioconcentration factor (BCF_k) for Ag uptake in *P. acuta* exposed through water; biomagnification factor (BMF_k) for Ag uptake in *G. tigrina*. Data was modelled with model 1, see Figure S4.2. Measured exposure concentrations (mean ± standard deviation; *n*=3) in water for *P. acuta* (µg Ag L^{-1}) and in food for *G. tigrina* (µg Ag g^{-1} dw; see Table S4.5 for individual values) are also shown. Different small letters indicate statistically significant differences (*t*-test, p<0.05). Absence of letters indicates no statistically significant differences ($X^2_{(1)}$<3.84; p>0.05).

Species (non-depurated)	**Ag form**	**Measured concentration** (µg Ag g^{-1} dw or µg Ag L^{-1})	**k1** (g_{food} $g^{-1}_{organism}$ $hour^{-1}$ or L_{water} $g^{-1}_{organism}$ day^{-1})	**k2** ($hour^{-1}$ or day^{-1})	**BCF_k** (L g^{-1})	**BMF_k** (g g^{-1})
Physa acuta	Ag_2S NPs	17.7 ± 0.59 a	19.6 (n.d.)	11.8 (n.d.)	1.66	
	$AgNO_3$	9.31 ± 0.25 b	0.82 (0.59-1.04)	0.13 (0.076-0.19)	6.31	
Girardia tigrina	Ag_2S NPs	34.1 ± 25.4	0.0041 (-0.0012-0.0094)	0.081 (-0.037-0.20)		0.051
	$AgNO_3$	41.4 ± 9.44	0.0063 (0.0036-0.009)	0.014 (0.0038-0.025)		0.45

(n.d.) not possible to determine 95% confidence intervals.

Table S4.5. Total Ag concentrations (µg Ag g^{-1} dw; mean ± standard deviation; *n*=3) determined in pre-exposed *Physa acuta* soft bodies (for 7 days), given as food item to *Girardia tigrina* at 0, 24 and 48 hours. Different small letters within a column indicate statistically significant differences between Ag concentrations measured in snails from Ag_2S NP and $AgNO_3$ treatments (*t*-test, p<0.05). Absence of letters within a line indicates no statistically significant differences between internal concentrations of snails provided at the different times of each treatment (one-way ANOVA, p>0.05).

Ag form	**Measured concentration** (µg Ag g^{-1} dw)		
	0h	**24h**	**48h**
Ag_2S NPs	26.9 ± 15	62.1 ± 29.5	18.2 ± 15.3 **a**
$AgNO_3$	38.8 ± 11.7	38.8 ± 3.10	48.4 ± 7.95 **b**

Experimental design – *Girardia tigrina* waterborne experiments

The experiments consisted of an uptake phase of 7 days, following transfer to clean medium for a 7-day elimination phase. Stock solutions were prepared following the guideline OECD 318 (2017). Experiments were maintained at 16:8h light: dark photoperiod and 20 ± 1 ºC. During the tests, pH, temperature, and dissolved oxygen (DO) concentrations were measured to ensure parameter quality. Organisms with a length of ~1.5 cm were selected and exposed to a nominal concentration of 10 µg Ag L^{-1} in Ag_2S NP and $AgNO_3$ treatments. No food was provided during the experiments and vial inspection was performed daily.

Girardia tigrina – water exposure (no sediment) test

Stock suspensions were prepared in ultrapure water and diluted in ASTM test medium to the required concentration. Planarians were individually exposed in plastic containers

filled with 40 mL of the spiked ASTM medium. ASTM medium was renewed every other day. Planarians were sampled at 1, 2, 5, 7, 8, 9, 12 and 14 days, from three replicates per treatment, washed three times in UPW and frozen at -80 ºC until analysis. Prior to digestion, planarians were oven-dried at 60 ºC for 48h and individually weighted. Water samples were taken at day 0 (*n*=3 per treatment) for total Ag measurements.

***Girardia tigrina* – water exposure and clean sediment test**

Planarians were individually exposed in 50 mL glass vials, with ASTM:sediment depth ratio of 4:1 and assembled 24h prior to spiking. Inorganic fine sediment (<1 mm), previously burned for 4h at 500 ºC, was used. ASTM was spiked according to the OECD 233 guideline (2010), with adaptations (see description also in Silva et al. (2020)). Vials were covered with a lid. Water and sediment were sampled (*n*=3 per treatment) at days 0, 3 and 7 for total Ag measurements. Sampling times and procedure as described above.

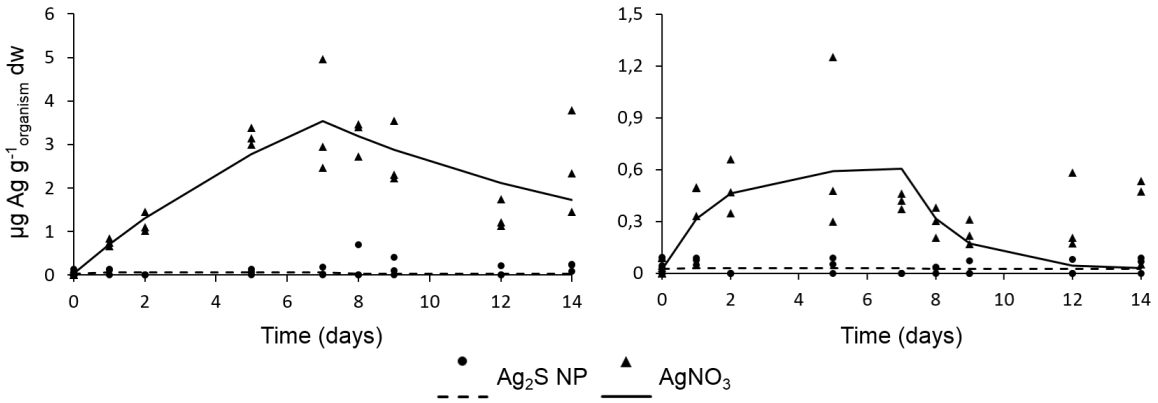

Figure S4.3. Uptake and elimination of Ag in *Girardia tigrina* exposed to Ag_2S NPs and $AgNO_3$ in a test with spiked water (no sediment) (left) and in a test with spiked water and clean sediment (right), at a nominal concentration of 10 µg Ag L^{-1}. Lines show the fit of model 1 to the data points, which represent Ag concentrations determined in planarians. See Table S4.6 for the resulting kinetics parameter values.

Table S4.6. Uptake (k1) and elimination (k2) rate constants (± 95% confidence intervals) of Ag uptake in *Girardia tigrina* exposed in a test with spiked water (no sediment) and a test with spiked water and clean sediment, at a nominal concentration of 10 µg Ag L^{-1} of Ag_2S NPs and $AgNO_3$. Data was modelled with model 1, see Figure S4.3. Measured concentrations in water are also shown (µg Ag L^{-1}; mean ± standard deviation; *n*=3). Different small letters within a column indicate statistically significant differences between Ag exposure concentrations in each test (*t*-test, p<0.05). Absence of letters indicates no statistically significant differences ($X^2_{(1)}$<3.84; p>0.05).

Girardia tigrina	**Ag form**	**Measured concentration** (µg Ag L^{-1})	**k1** (L_{water} $g^{-1}_{organism}$ day^{-1})	**k2** (day^{-1})
Spiked water (no sediment)	Ag_2S NPs	10.9 ± 0.73 **a**	0.04 (n.d.)	15.8 (n.d.)
	$AgNO_3$	7.46 ± 0.41 **b**	0.09 (0.07-0.12)	0.12 (0.08-0.17)
Spiked water and clean sediment	Ag_2S NPs	3.91 ± 5.26 **a**	0.02 (n.d.)	23.7 (n.d.)
	$AgNO_3$	3.00 ± 4.12 **a**	0.13 (0.05-0.22)	0.70 (0.24-1.18)

(n.d.) not possible to determine 95% confidence intervals.

4.8.1. Supplementary references

OECD, 2017. Test No. 318: Dispersion Stability of Nanomaterials in Simulated Environmental Media. OECD Guideline for the Testing of Chemicals. Organization for Economic Co-operation and Development, Paris.

OECD, 2010. Test No. 233: Sediment-Water Chironomid Life-Cycle Toxicity Test Using Spiked Water or Spiked Sediment. OECD Guideline for the Testing of Chemicals. Organization for Economic Co-operation and Development, Paris.

Silva, P. V., van Gestel, C.A.M., Verweij, R.A., Papadiamantis, A.G., Gonçalves, S.F., Lynch, I., Loureiro, S., 2020. Toxicokinetics of pristine and aged silver nanoparticles in *Physa acuta*. Environ. Sci. Nano 7, 3849–3868.

van den Brink, N.W., Jemec Kokalj, A., Silva, P.V., Lahive, E., Norrfors, K., Baccaro, M., Khodaparast, Z., Loureiro, S., Drobne, D., Cornelis, G., Lofts, S., Handy, R.D., Svendsen, C., Spurgeon, D., van Gestel, C.A.M., 2019. Tools and rules for modelling uptake and bioaccumulation of nanomaterials in invertebrate organisms. Environ. Sci. Nano 6, 1985–2001.

Chapter 5

Toxicokinetics and bioaccumulation of silver sulfide nanoparticles in benthic invertebrates in an indoor stream mesocosm

To be submitted

Patrícia V. Silva[1], Ana Rita R. Silva[1], Nathaniel J. Clark[2], Joanne Vassallo[2], Marta Baccaro[3], Neja Medvešček[4], Magdalena Grgić[5], Abel Ferreira[1], Martí Busquets-Fité[6], Kerstin Jurkschat[7], Anastasios G. Papadiamantis[8,9], Victor Puntes[10,11,12], Iseult Lynch[8], Claus Svendsen[13], Nico W. van den Brink[3], Richard D. Handy[2], Cornelis A. M. van Gestel[14] and Susana Loureiro[1]

[1]Department of Biology and CESAM, University of Aveiro, Campus Universitário de Santiago, 3810-193 Aveiro, Portugal
[2]School of Biological and Marine Sciences, University of Plymouth, Plymouth, UK
[3]Department of Toxicology, Wageningen University, Wageningen, The Netherlands
[4]Department of Biology, Biotechnical Faculty, University of Ljubljana, Večna pot 111, 1000 Ljubljana, Slovenia
[5]Department of Biology, Josip Juraj Strossmayer University of Osijek, Cara Hadrijana 8/A, 31000 Osijek, Croatia
[6]Applied Nanoparticles SL, C Alaba 88, 08018 Barcelona, Spain
[7]Department of Materials, Oxford University Begbroke Science Park, Begbroke, United Kingdom
[8]School of Geography, Earth and Environmental Sciences, University of Birmingham, Edgbaston, B15 2TT Birmingham, UK
[9]NovaMechanics Ltd., 1065, Nicosia, Cyprus
[10]Institut Català de Nanociència i Nanotecnologia (ICN2), CSIC, The Barcelona Institute of Science and Technology (BIST), Campus UAB, Bellaterra, Barcelona, Spain
[11]Institució Catalana de Recerca i Estudis Avançats (ICREA), 08010 Barcelona, Spain
[12]Vall d'Hebron Institut de Recerca (VHIR), 08035 Barcelona, Spain
[13]Centre of Ecology and Hydrology (CEH-NERC), Wallingford, UK
[14]Department of Ecological Science, Faculty of Science, Vrije Universiteit Amsterdam, The Netherlands

Toxicokinetics and bioaccumulation of silver sulfide nanoparticles in benthic invertebrates in an indoor stream mesocosm

5.1. Abstract

Mesocosms allow the simulation of environmentally relevant conditions and can be used to establish more realistic scenarios of organisms' exposure to NPs. A mesocosm experiment was conducted to assess the toxicokinetics and bioaccumulation of silver sulfide NPs (Ag_2S NPs) in a simulated, indoor stream environment. The main objectives were to: 1) determine toxicokinetics of Ag_2S NPs as a model for environmentally aged Ag NPs and $AgNO_3$ in the freshwater benthic invertebrates *Girardia tigrina*, *Physa acuta* and *Chironomus riparius*, 2) determine if single-species tests can predict bioaccumulation in the mesocosm test, and 3) evaluate potential Ag bioaccumulation and biomagnification. Silver was bioaccumulated by the test species in both Ag_2S NP and $AgNO_3$ exposures, with 1.5 to 11 times higher body Ag concentrations upon $AgNO_3$ exposure. In the Ag_2S NP exposure, the observed uptake was probably of the particulate form, indicating the bioavailability of this more environmentally persistent and relevant Ag nanoparticulate form. Interspecies interactions were observed, namely predation, which probably influenced Ag uptake and bioaccumulation. Single-species tests generally were not able to reliably predict Ag bioaccumulation in the more complex mesocosm test scenario. Biomagnification under environmentally realistic exposure seemed to be low, even though it was likely to occur in the food chain *P. acuta* → *G. tigrina* in the $AgNO_3$ treatment. To our knowledge, this is the first study evaluating the toxicokinetics of Ag_2S NPs in benthic invertebrates in a freshwater mesocosm experiment.

Keywords: mesocosm, silver sulfide nanoparticles, bioaccumulation, biomagnification, exposure routes, benthic invertebrates, single-species tests.

5.2. Introduction

The increasing application of engineered nanoparticle in products and processes, and their inevitable release into the environment has highlighted the need to understand the effects of these materials on ecosystems (Lead et al., 2018). Silver nanoparticles (Ag NPs) are one of the most produced NPs, being widely applied in medical and consumer products due to their broad-spectrum antibacterial properties (Jiang et al., 2017). Therefore, an increasing body of research has been conducted on Ag NP fate and toxicity in the different environmental compartments (Lead et al., 2018; Selck et al., 2016). Wastewater effluents are one of the main sources of Ag NPs into aquatic systems (Azimzada et al., 2017) which during wastewater treatment may react with sulfur to form silver sulfide NPs (Ag_2S NPs) (He et al., 2019; Kaegi et al., 2011). In surface waters, these NPs tend to aggregate and settle from the water column to the sediment phase. Therefore, the sediment compartment can be an important sink for Ag NPs (Furtado et al., 2015; Lowry et al., 2012) with predicted concentrations going up to 30 µg Ag NP kg^{-1} (Sun et al., 2016). The accumulation in sediments may lead to subsequent exposure of biofilms and benthic species, with risk for toxicity and biomagnification across aquatic food webs (Clark et al., 2019). In soft freshwaters in the presence of natural organic matter, Ag NPs may form relatively stable dispersions in the water column and can migrate over long distances, posing risks to pelagic organisms (Li et al., 2020; Tangaa et al., 2016). While hard waters with higher ionic strength, especially those impacted by effluent discharges show particle settling. Therefore, understanding exposure, toxicokinetics and bioaccumulation potential of NPs has become crucial for assessing their environmental risk (Petersen et al., 2019). The bioaccumulation potential of NPs has recently been reviewed (Handy et al., 2018; Kuehr et al., 2021; Petersen et al., 2019). However, most studies involved single-species tests under standard laboratory conditions (Kuehr et al., 2021). Such studies can provide important mechanistic information on the effects of individual organisms, but do not reflect the complexity of environmental systems (Bernhardt et al., 2010; Lead et al., 2018). Moreover, most studies used pristine Ag NPs, while Ag_2S NPs can be considered as a more persistent and relevant Ag nanoparticulate form in the environment (Clark et al., 2019).

Recent studies have attempted to replicate more complex scenarios to assess the fate and effects of NPs under more realistic conditions (Bour et al., 2015). In the environment, exposure can be complex, especially in aquatic systems where organisms can be simultaneously exposed to sediments, water and food (Warren et al., 1998). Furthermore, the bioaccumulation of substances, including NPs, not only depends on their characteristics

but also on the exposure pathway, feeding habits and physiology of the exposed organisms (Brooks et al., 2009). Interspecies interactions (e.g., competition, predation, avoidance) can influence bioaccumulation by altering the organism's behaviour (Diepens et al., 2015). Experimental designs such as mesocosms are used to simulate more complex exposure scenarios to increase environmental relevance, while allowing replication (Nikinmaa, 2014). The need for mesocosm studies to enhance environmental realism and improve NP assessment has been raised (Lead et al., 2018; Selck et al., 2016), as well as the importance of using toxicokinetic tools to understand their potential bioaccumulation and risk (Petersen et al., 2019).

Considering this, a mesocosm experiment simulating a natural stream environment was conducted indoors to assess the toxicokinetics and bioaccumulation of Ag_2S NPs and $AgNO_3$ in freshwater organisms. The main objectives were to: 1) determine the toxicokinetics of Ag_2S NPs to simulate an environmentally aged Ag NP form, and compared to $AgNO_3$ as a metal salt control in freshwater benthic invertebrates, 2) determine if single-species tests can predict bioaccumulation in the mesocosm test scenario and 3) evaluate potential Ag bioaccumulation and biomagnification. Several species were used in the mesocosm and here the focus was on the planarian, *Girardia tigrina*; the snail, *Physa acuta* and the midge larvae, *Chironomus riparius*.

5.3. Materials and Methods

5.3.1. Test species and cultures maintenance

The species *Girardia tigrina*, *Physa acuta* and *Chironomus riparius* were bred and maintained under controlled laboratory conditions (20 ± 1 ºC and 16:8h light: dark photoperiod) at the University of Aveiro, Portugal. Due to their photonegative nature (Saraiva et al., 2020), *G. tigrina* were maintained in plastic containers covered with foil. These containers were filled with American Society for Testing Materials (ASTM) hard water (ASTM, 1980), having a pH between 7.5 and 7.8. The planarians were fed *ad libitum* once a week with bovine liver or *C. riparius* larvae. ASTM medium was fully renewed immediately after feeding and 2 days after. Adult planarians (size 1.5 to 2 cm) used in the present experiment were unfed 1 week prior to the experiment to ensure a uniform metabolic state (Oviedo et al., 2008). Snails were kept in groups of approx. 50 individuals per glass aquarium, filled with 3 L of artificial pond water (APW) (Naylor et al., 1989), with continuous aeration and a basic pH between 7.9 and 8.2 to avoid shell fracturing. The medium was partially renewed every other day and fully renewed once a week. The animals were fed *ad*

libitum every other day with ground fish food, TetraMin® (Tetrawerke, Melle, Germany). Snails of approx. two months old were used in the experiment. *C. riparius* larvae were cultured in plastic containers with inorganic fine sediment (<1 mm grain size, previously burned at 500 °C for 4 h) and ASTM hard water, at a depth ratio of 1:4, respectively. Continuous aeration was provided to the cultures. Sediment was fully renewed monthly, and ASTM hard water was fully renewed every two weeks. Larvae were fed *ad libitum* three times a week with a suspension of ground TetraMin® (Tetrawerke, Melle, Germany). For the experiment, egg ropes were isolated from the main *C. riparius* culture. After hatching, larvae were fed every other day and second instar larvae (6 to 7 days post-hatching) were used in the mesocosm test.

5.3.2. Nanoparticles

Silver sulfide nanoparticle were obtained as a colloid suspension [Ag_2S NPs in polyvinylpyrrolidone (PVP), 1.32 g Ag_2S L^{-1}; reported size 20.4 ± 11.9 nm] and were supplied by Applied Nanoparticles (Barcelona, Spain), a partner of the EU H2020 NanoFASE project (http://www.nanofase.eu/). These NPs were synthetised *ab initio* to simulate an environmentally aged Ag NP form in order to increase the realism of the exposure. Detailed characterization of the Ag_2S NP colloids is described in the supplementary information (SI). Silver nitrate ($AgNO_3$, Sigma Aldrich, CAS number 7761-88-8, 99% purity, as crystalline powder) was used as the metal salt control.

5.3.3. Experimental design

5.3.3.1. Mesocosm experiment

The experiment used an indoor modular mesocosm system at the Applied Ecology and Ecotoxicology group, at the University of Aveiro, Portugal, maintained at 15 ± 1 ºC (air temperature) and 16:8h light: dark photoperiod. The system was composed of 36 artificial streams made of glass (each of 2 m length, 0.200 m width and 0.225 m depth) arranged in triplicates. Each triplicate was supplied with water from a shared sump (Figure 5.1 A and B). The system was divided into 12 sets of triplicates, with 4 sets being randomly assigned to each treatment: control, Ag_2S NPs and $AgNO_3$. The final water volume of each triplicate (3 streams and the sump) was approx. 207 L, and the water was operated in recirculation mode. The bottom of each stream was covered with a layer of sediment (<2 mm grain size, previously burned at 500 ºC for 4h) mixed with ground alder leaves (*Alnus glutinosa*; 1% w/w), giving a total of 7 kg of sediment per stream. Then, each stream was filled with 35 L

of APW (Naylor et al., 1989), freshly prepared and enriched with sodium metasilicate nonahydrate (0.028 g L^{-1} $NaSiO_3.9H_2O$), dipotassium hydrogen phosphate (0.008 g L^{-1} K_2HPO_4) and sodium nitrate (0.085 g L^{-1} $NaNO_3$), to simulate the mineral concentrations of the Mau river, located in an unpolluted area in Sever do Vouga, Portugal (Vidal et al., 2014). At day zero, APW medium pH was 7.81-7.90. Alder leaves collected from the riparian vegetation at São Pedro de Alva, Portugal, were used to provide organic matter to the sediment and food for the test organisms. In all streams, water was maintained at a constant flow rate of approx. 4 L/min, as measured in the Mau River. Unglazed ceramic tiles (20 cm^2) were incubated in the Mau River two weeks prior to the start of the experiment, to allow natural colonization of biofilm, which served as food source for snails. Ceramic tiles also served as shelter for planarians.

The systems were acclimated for 2 days to allow equilibration of the water chemistry, after which organisms were introduced into each stream: the invertebrates *G. tigrina* (planaria, 50/stream), *P. acuta* (snail, 60/stream), *C. riparius* (midge larvae, 150/stream) and *Lumbriculus variegatus* (blackworm, approx. 900 mg/stream). In addition, *Daphnia magna* (water flea; 0.25% ration for the fish equating to approximately 13 *Daphnia*/river/day) and the rainbow trout *Oncorhynchus mykiss* (3/stream) were kept separately in submerged plastic chambers in the streams, with a plastic mesh-covered aperture (1 mm) on two opposite sides to prevent other organisms from entering the container but allowing water flow. Ceramic tiles with biofilm were placed in the inflow, middle, and outflow of each stream (Figure 5.1 C). One day after all organisms were introduced, each triplicate of Ag_2S NP and $AgNO_3$ treatments was spiked daily at the shared sump, to maintain the required nominal concentration of 10 µg Ag L^{-1}. This concentration (sub-lethal) was selected based on previous bioaccumulation experiments with the test species and to ensure reliable Ag measurements in the different compartments. The mesocosm experiment lasted for 14 days and organisms were exposed for the entire test duration, so including only the uptake phase and excluding an elimination phase. In this work, the sampling procedure and results for *G. tigrina*, *P. acuta* and *C. riparius* are presented, data for the other organisms are reported elsewhere (manuscript in preparation).

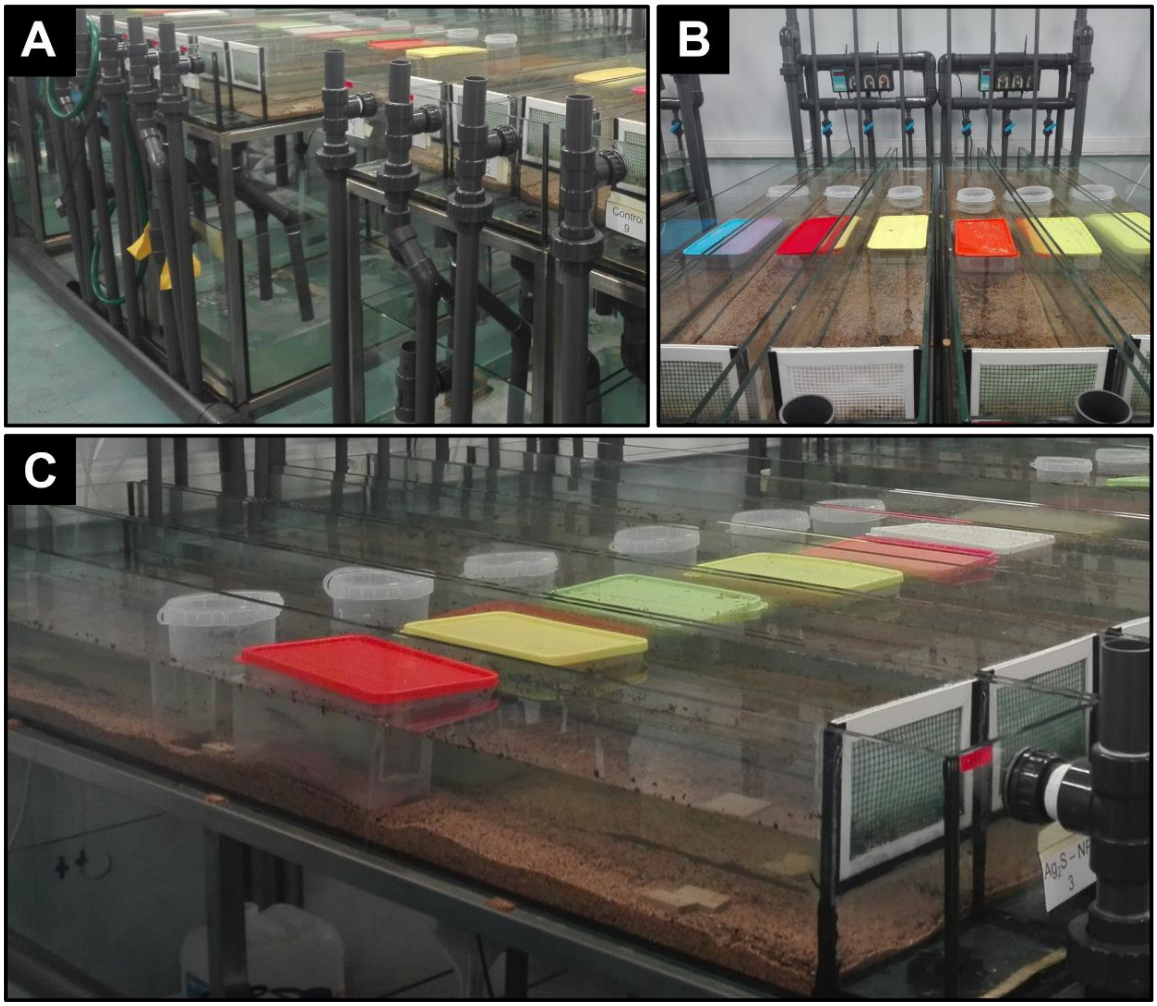

Figure 5.1. Photographs of the mesocosm system. A) triplicates of streams connected to the shared sump, B) closer image to the triplicate streams, C) closer image of a stream. Fish were kept in the rectangular boxes with lids and daphnids in the cylindrical boxes.

5.3.3.2. Single-species experiments

Single-species tests were previously conducted with *P. acuta* (Silva et al., 2020), *G. tigrina* and *C. riparius* to determine the toxicokinetics of Ag_2S NPs and $AgNO_3$ through different exposure routes. The three species were exposed in independent single-species tests to waterborne Ag_2S NPs and $AgNO_3$ at a nominal concentration of 10 µg Ag L^{-1} and clean sediment. The detailed description of the *P. acuta* single-species test can be found in Silva et al. (2020). Briefly, *P. acuta* was exposed to Ag-spiked APW medium and clean sediment for 7 days and then transferred to clean APW and sediment for another 7 days. No food was provided, and the snails were samples at days 1, 2, 5 and 7 of each phase, 3 replicates per sampling time. The *G. tigrina* experiments followed the same procedure as

for the snails, but the medium used was ASTM hard water (ASTM, 1980). For *C. riparius* the design was similar to that of *P. acuta* and *G tigrina*, with some adaptations. Chironomids (ten 4th instar larvae per replicate) were exposed to ASTM medium and the uptake and elimination phases lasted for 48h each. After sampling at 12h intervals for 96h, the larvae were left to depurate for 4h. Sampling procedure, samples digestion and total Ag analysis followed the protocols described in Silva et al. (2020). To compare with the mesocosms result, only the uptake phase of these single-species tests was considered.

5.3.3.3. Sampling procedure

One stream of each set of 4 triplicates assigned to each treatment was destructively sampled at days 2, 7 and 14. On each sampling day, water (10 mL; *n*=4 per treatment) and sediment (20-30 g; *n*=4 per treatment) were collected near the inflow, middle, and outflow of each stream for total Ag analysis. Sampled organisms were left to depurate for 24h in containers with clean APW medium. Some snails were stored without depuration or washing to allow the evaluation of potential biomagnification considering a more realistic scenario, which includes any adsorbed Ag on the organism and Ag in the digestive tract. Organisms were rinsed in ultra-pure water, pooled and frozen at -80 ºC until total Ag analysis. Snail shells and soft bodies were separated and analysed separately. Prior to digestion, samples were freeze-dried and weighted. Water samples were daily taken from each stream for total Ag analysis, and for routine measurements of water chemistry parameters, such as temperature, pH, dissolved oxygen (DO), electrolytes and total ammonia. On days 1, 6 and 13, water was sampled from each stream at 10min, 1h, 2h, 4h and 24h after dosing to outline the exposure profile between spiking periods. Water was also sampled on days 1, 2, 6, 7, 8, 10, 13 and 14 to determine particulate Ag, by single particle inductively coupled plasma mass spectrophotometry (sp-ICP-MS). On days 2 and 14, water, sediment and sediment pore water samples were taken for Transmission Electron Microscopy (TEM) analysis (see SI for the methodology).

5.3.4. Sample digestion and Ag analysis of biota samples

Total metal analysis in biota followed the methodology of Clark et al. (2019). Samples were digested in Eppendorf tubes with 0.5 mL of neat nitric acid (Fisher, Primar Plus Trace Metals Analysis Grade), for 2h in a water bath at 65 ºC. After cooling, samples were diluted to 1.5 mL using ultrapure deionised water and stored in the dark until analysis. Samples were analysed for total Ag by ICP-MS. To assess accuracy and recovery of the procedure,

the certified reference material DORM-4 (National Research Council Canada) was analysed as described above, with a recovery of 80.9% ± 15.2%; *n*=20.

5.3.5. Sample digestion and Ag analysis of water and sediment samples

Water samples were immediately acidified with 0.5 mL of neat nitric acid (Fisher, Primar Plus Trace Metals Analysis Grade), and stored in the dark at 4 ºC until total Ag analysis, by ICP-MS. Particulate Ag content of the water was measured using an iCAP RQ ICP-MS in time resolved analysis. Sample analysis was conducted over 60 seconds at a flow rate of 0.25-0.35 mL min^{-1}. The transport efficiency was calculated using well characterised particles from BBI solution (UK). The instrument was calibrated using dissolved standards ranging from 0.5 to 4 µg L^{-1}.

Total Ag concentrations in sediment samples were determined at days 0, 2, 7 and 14. About 30 g moist sediment (*n*=12 *per* treatment) was dried at 85 ºC. Sub-samples of around 250 mg dry sediment were digested in covered 50 mL glass beakers using 10 mL neat nitric acid. The acid mixture was gently simmered at 110 ºC on a hotplate for at least 2h in the fume hood adapted from Chen and Ma (2001). The digests were then cooled, diluted with 2 % (*v/v*) nitric acid into 25 mL volumetric flasks, transferred to polypropylene tubes and then stored in the dark until analysis. The reference material *Enviro*MAT Contaminated Soil (SS-2) was digested and analysed using the same procedure, giving a recovery of 51.5% ± 8.7%; *n*=6. The extractable Ag fractions in all dried sediment samples were determined by a two-step sequential extraction method at days 0, 2, 7 and 14, following the method described by Tatsi et al. (2018). The first extraction was with ultrapure deionised water (MilliQ water, Elga, 18.2 Ω) to release the water soluble fraction of Ag and followed by the dilute acid extractable fraction of Ag with 0.1 M nitric acid; both at ratios 1:10 (soil:solution) in 15 mL polypropylene centrifuge tubes. The tubes were shaken (IKA Labortechnik KS250) for 1h, followed by centrifugation for 10 min at 4500 × *g* (Harrier 18/80). Each solution was decanted, then acidified with 2 % nitric acid and stored in the dark until analysis by ICP-MS. A more detailed description of the sampling and analysis of biota, water and sediment samples can be found in a separate article.

5.3.6. Toxicokinetic modelling

To describe Ag toxicokinetics in the test organisms, one-compartment models were fitted to the measured body Ag concentrations in *G. tigrina*, *P. acuta* and *C. riparius*. A model commonly used to determine toxicokinetics of metals was applied (model 1 – single

exposure route), using the total Ag concentration in the water or sediment as separate exposure routes (Ardestani et al., 2014). Model 2 was also used to understand toxicokinetics using a model accounting for sediment and water as simultaneous exposure routes (double exposure route) (van den Brink et al., 2019). Organisms increased in weight during the test. Therefore, exponential growth rate constants were calculated from the organism dry weight (dw) changes during the experiment and included in both models to account for the effect of biomass changes in the estimated body Ag concentrations.

Model 1

$$Q(t) = C_0 + \left(\frac{k1}{(k2+k_{growth})}\right) * C_{exp} * \left(1 - e^{(-(k2+k_{growth})*t)}\right)$$

Model 2

$$Q(t) = C_0 + \left(\frac{(C_{\exp water}*kw+C_{\exp sed}*ks)}{(k2+k_{growth})}\right) * \left(1 - e^{(-(k2+k_{growth})*t)}\right)$$

Where Q(t) = Ag internal concentration in the organisms at time t days (µg Ag $g^{-1}_{organism}$ dw); k1 = uptake rate constant from water or sediment (L_{water} $g^{-1}_{organism}$ day^{-1} or $g_{sediment}$ $g^{-1}_{organism}$ day^{-1}); k2 = elimination rate constant (day^{-1}); C_0 = background internal concentration measured at day 0 (µg Ag $g^{-1}_{organism}$ dw); $C_{exp\ water}$ = Ag exposure concentration in water (µg Ag L^{-1}); $C_{exp\ sed}$ = Ag exposure concentration in sediment (mg Ag kg^{-1}); ks = uptake rate constant from sediment ($g_{sediment}$ $g^{-1}_{organism}$ day^{-1}); k_{growth} = growth rate constant (day^{-1}).

For model 2, the relative contribution (in %) of each uptake route to the total Ag uptake was determined as follows:

Water uptake route:

$$\left(\frac{(C_{\exp water} * kw)}{(C_{\exp water} * kw + C_{\exp sed} * ks)}\right) * 100$$

Sediment uptake route:

$$\left(\frac{(C_{\exp sed} * ks)}{(C_{\exp water} * kw + C_{\exp sed} * ks)}\right) * 100$$

Ag uptake patterns and toxicokinetic parameters derived from the mesocosm test were compared with results from previous single-species tests (Silva et al., 2020). To enable reliable comparison, data of the single-species tests were modelled considering only the uptake phase and applying the same models as described above.

5.3.7. Calculation of bioconcentration, bioaccumulation and biomagnification factors

Kinetic bioconcentration (BCF_k; L g^{-1}), kinetic biota-to-sediment accumulation ($BSAF_k$; g g^{-1}) and biomagnification factors (BMF), were calculated to relate body concentrations to Ag exposure levels in water, sediment and food, respectively, using the equations (Arnot and Gobas, 2006):

$$BCF_k/BSAF_k = \frac{k1}{k2} \qquad BMF = \frac{C_o}{C_d}$$

Where k1 and k2 are the uptake and elimination rate constants described above; C_o is the concentration in the organism (predator) (µg Ag $g^{-1}_{organism}$ dw) and C_d is the concentration in the diet (prey) (µg Ag $g^{-1}_{organism}$ dw) after 7 or 14 days of exposure. Values of BMF >1 indicate biomagnification potential.

5.3.8. Statistical analysis

Equations were fitted to the data and toxicokinetic parameters and corresponding 95% confidence intervals (CI) were estimated by non-linear regression in SPSS (version 25). Akaike Information Criteria tests (AIC and AICc) were applied for the selection of the best fitting models (data not shown). Generalised Likelihood Ratio Tests (GLR) were applied to determine the significance of differences of k1 and k2 parameters between Ag forms, species, or between mesocosm and single-species tests. Two-way analysis of variance (ANOVA) followed by the Holm-Sidak method ($p<0.05$) (SigmaPlot 12.5 software) was also applied for analysis of treatment and time as factors in Ag concentrations of water or sediment samples, organisms, and shells of depurated snails. Additionally, two-way ANOVA followed by the Holm-Sidak method ($p<0.05$) was applied considering depuration and time as factors to determine differences in body Ag concentrations of depurated and non-depurated snails/shells in time. Since no non-depurated snails were sampled at day 2, this day was not included in the two-way ANOVA comparison. Data transformations were conducted whenever ANOVA assumptions were not fulfilled.

5.4. Results

5.4.1. Nanoparticle characterization

The characterization of the Ag_2S NP colloids in the stock solution is summarized in Tables S5.1 and S5.2, along with the TEM images (Figures S5.1 and S5.2). Characterization showed an average measured particle diameter of 20.4 ± 11.9 nm determined by TEM and a zeta-potential value of -23.8 ± 4.5 mV in milli-Q water (Figure S5.1, Table S5.1). The particle elemental composition by TEM-EDX showed high Ag%, from 70% to 85% (Figure S5.2, Table S5.2). In APW medium, Ag_2S NPs revealed almost no dissolution using a test concentration of 1 mg Ag L^{-1} (Table S5.3). DLS values indicated strong agglomeration at time 0, with a hydrodynamic size of 336 nm, that remained relatively constant throughout the 48h. Z-potential values also revealed stable values during the 48h (Table S5.3).

5.4.2. Exposure medium: water and sediment

Total Ag concentrations in water from the $AgNO_3$ treated mesocosms gradually increased until day 7 after which they stayed close to the nominal concentration of 10 µg Ag L^{-1} (data not shown), at around 13 µg Ag L^{-1} until the end of the experiment (Table 5.1). In the Ag_2S NP treated mesocosms, Ag concentrations increased until day 11, reaching a peak of around 28 µg Ag L^{-1}, followed by a decrease until the end of the experiment (data not shown), with concentrations of about 13 µg Ag L^{-1} (Table 5.1). Total Ag concentrations in water from control streams were below the detection limit. Concentrations at days 7 and 14 differed significantly from day 2 (two-way ANOVA, Holm-Sidak method, $p<0.05$) in both treatments and no significant differences (two-way ANOVA, $p>0.05$) were detected between concentrations of Ag_2S NPs and $AgNO_3$ (Table 5.1). Measurements by sp-ICP-MS detected Ag particles in water from Ag_2S NP and $AgNO_3$ treatments which increased over time (data not shown). No particulate Ag was detected in control water samples. Figure S5.3 and Table S5.4 show the TEM image and Ag and S composition (%) in the Ag_2S NP treatment at day 2. Particulate Ag was detected in APW in this treatment. No particulate Ag was found by TEM analysis in the other treatments or sampling days. No particulate Ag was detected by TEM in sediment pore water of the Ag_2S NP and $AgNO_3$ treatments (data not shown).

Table 5.1. Measured total Ag concentrations in water (µg Ag L^{-1}) and sediment (mg Ag kg^{-1}) (mean ± SD; *n*=4) of Ag_2S NP and $AgNO_3$ treatments of the mesocosm test. Different capital letters within a line indicate significant differences between treatments of water (italics) or sediment (non-italics) samples; different small letters within a row indicate significant differences between sampling days of each treatment of water (italics) or sediment (non-italics) samples (two-way ANOVA followed by Holm-Sidak method, p<0.05).

Medium		**Water (µg Ag L^{-1})**		**Sediment (mg Ag kg^{-1})**	
Ag treatment		**Ag_2S NP**	**$AgNO_3$**	**Ag_2S NP**	**$AgNO_3$**
Measured concentration (mean±SD)	**day 0**	< LOD	< LOD	0.005 ± 0.001* / ** / **a**	
	day 2	0.95 ± 1.22 *a* / *A*	2.80 ± 3.79 *a* / *A*	0.052 ± 0.013 b / A	0.053 ± 0.016 b / A
	day 7	12.8 ± 4.02 *b* / *A*	9.71 ± 0.93 *b* / *A*	0.14 ± 0.021 c / A	0.10 ± 0.020 c / A
	day 14	13.4 ± 4.32 *b* / *A*	12.8 ± 3.41 *b* / *A*	0.30 ± 0.13 d / A	0.20 ± 0.085 d / A

* background concentration in sediments was considered the same at day 0 for sediments of Ag_2S NP and $AgNO_3$ treatments.
** *n* = 3; < LOD: below limit of detection.

Total Ag concentrations in sediment revealed a background concentration of 4.87 µg Ag kg^{-1} at day 0, which increased throughout the test period. For Ag_2S NP and $AgNO_3$ treatments, total Ag concentrations in sediment significantly increased (two-way ANOVA, Holm-Sidak method, p<0.05) from day 0 to day 14 (Table 5.1). No significant interactions were found between treatment and time (two-way ANOVA, p>0.05) in water or sediment samples. A small fraction of Ag was extracted from sediment by water in all treatments, and around 12% and 28% of the total Ag were extracted by diluted acid from sediment sampled at day 14 in Ag_2S NP and $AgNO_3$ treatments, respectively (data not shown).

5.4.3. Toxicokinetics of Ag in benthic invertebrate species in mesocosm test

Of the *G. tigrina* introduced in the mesocosms, 76%, 74% and 72% were recovered at day 7 and 75%, 87% and 86% after 14 days, in control, Ag_2S NP and $AgNO_3$ treatments, respectively. For snails, recovery of animals in control, Ag_2S NP and $AgNO_3$ exposures was 50%, 71% and 70% at day 7 and 35%, 45% and 61% after 14 days, respectively. At day 7, only 6.5%, 5.8% and 3.2% of chironomid larvae were recovered in the control, Ag_2S NP and $AgNO_3$ treatments, respectively, and 0% at day 14.

Figure 5.2 shows the uptake kinetics of Ag in *G. tigrina* and *P. acuta* (soft body) when exposed for 14 days to Ag_2S NP and $AgNO_3$ in the mesocosm test. Chironomid larvae were not found in the streams on the last sampling day, therefore Ag uptake concentrations are only shown till day 7. The uptake curves shown in Figure 5.2 were obtained through modelling with water as exposure route (model 1), which are identical when modelling considering sediment exposure (model 1) or double exposure (model 2). For planarians,

toxicokinetics were only determined accounting for water as (single) exposure route, as no indication was found that planarians do ingest sediment.

For all invertebrates, highest Ag uptake rates and body Ag concentrations were observed in the $AgNO_3$ treated mesocosms. In general, higher body Ag concentrations were found in snails, followed by planarians, but in the Ag_2S NP exposures chironomid larvae revealed higher body concentrations than planarians. For planarians and chironomid larvae, body Ag concentrations in both treatments gradually increased over time (Figure 5.2). For snails exposed to Ag_2S NPs, body concentrations stabilized slowly over the 14-day exposure period, while following $AgNO_3$ exposure the snails presented a steep increase until day 2, after which body concentrations levelled off followed by a decrease from day 7 to 14 (Figure 5.2). Body Ag concentrations of planarians exposed to $AgNO_3$ were significantly higher (two-way ANOVA, Holm-Sidak method, $p<0.001$) than in individuals from the Ag_2S NP exposure at days 7 and 14. For chironomids, body concentrations were significantly higher (two-way ANOVA, Holm-Sidak method, $p<0.05$) for $AgNO_3$ compared to Ag_2S NP treatments at days 2 and 7. Silver concentrations in snails peaked at day 7 upon Ag_2S NP (body burden, 53 µg Ag g^{-1} dw) and $AgNO_3$ (body burden, 119 µg Ag g^{-1} dw) exposures, and were significantly higher (two-way ANOVA, Holm-Sidak method, $p<0.001$) in the $AgNO_3$ treatment. At day 14, internal Ag concentrations in snails exposed to $AgNO_3$ were not significantly different from those exposed to Ag_2S NPs, being of 59.2 and 41.3 µg Ag g^{-1} dw, respectively (Figure 5.2).

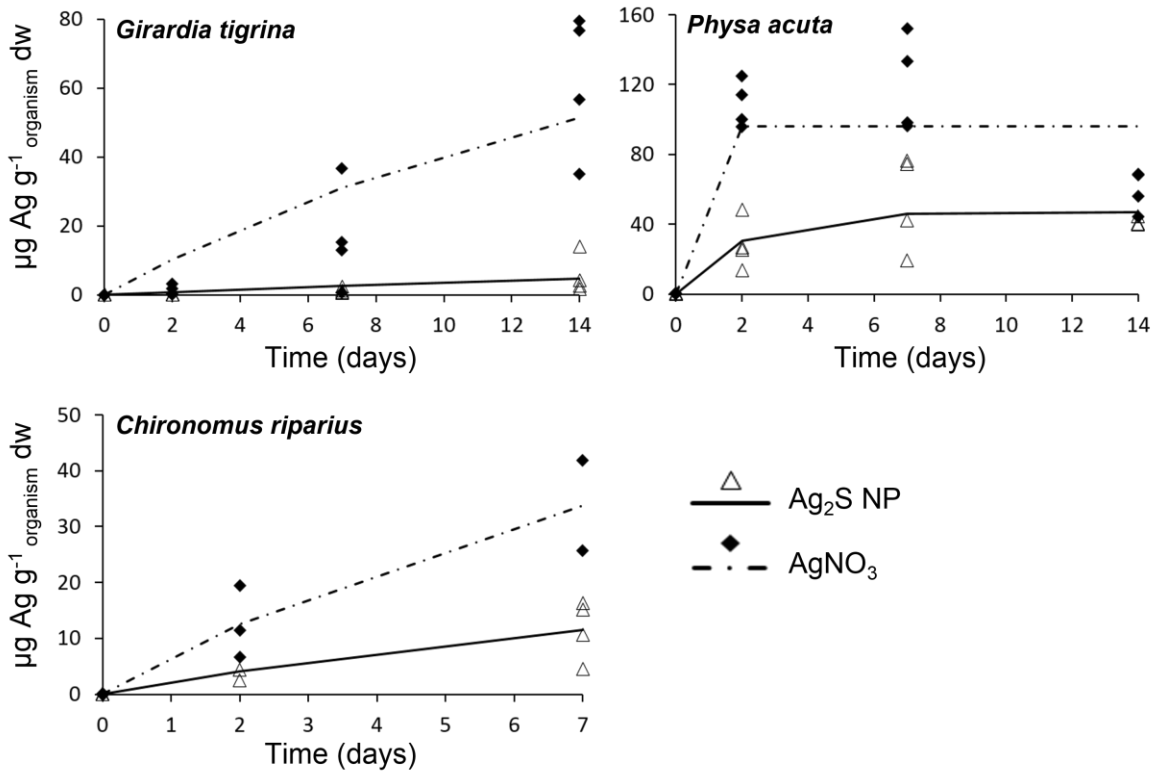

Figure 5.2. Uptake kinetics of Ag in the invertebrates *Girardia tigrina*, *Physa acuta* (soft body) and *Chironomus riparius*, exposed to Ag_2S NPs or $AgNO_3$ at a nominal concentration of 10 µg Ag L^{-1} in mesocosms for 14 days. Lines show the fit of a one-compartment model (model 1 – single exposure route) to the total Ag concentrations measured in replicate samples of organisms. Chironomid data is only available till day 7 as they were no longer found on day 14. Note the differences in the y-axis scales and x-axis scales.

Table 5.2 displays the toxicokinetic parameters calculated when considering water or sediment as exposure routes. All organisms revealed higher k1 values in the $AgNO_3$ exposures. Snails revealed the highest k1 water and k1 sediment values (Table 5.2), showing remarkably high k1 sediment, especially for $AgNO_3$. Significant differences were only found between k1 water values of planarians and chironomids in the Ag_2S NP treatment ($X^2_{(1)}$>3.84; p<0.05). Snails had higher k2 values, especially for $AgNO_3$, while planarians and larvae presented k2 values of zero or almost zero. Considering the double exposure (water and sediment), the same k1 water and k2 values as for single water exposure were determined, except for snails exposed to $AgNO_3$. In turn, much lower k1 sediment values were obtained from double exposure modelling than in single-exposure, however differences were not significant as no 95% CI could be estimated (Table S5.5). Water seemed to be responsible for almost 100% of the Ag uptake by snails and chironomid larvae (Table S5.5).

Table 5.2. Toxicokinetic parameters for the uptake of Ag in the freshwater invertebrates *Girardia tigrina*, *Physa acuta* (soft body) and *Chironomus riparius* exposed for 14 days to Ag_2S NPs and $AgNO_3$ in the mesocosm test. Data was modelled with model1, considering water or sediment as single exposure routes. Mean measured Ag exposure concentrations in water and sediment until day 7 (for chironomids) and day 14 (for planarians and snails) used in the models are also shown. k1 is the uptake rate constant and k2 the elimination rate constant. 95% CI are given in brackets. Absence of letters indicate no significant differences ($X^2_{(1)}$<3.84; p>0.05) in: k1 or k2 values between Ag_2S NPs vs $AgNO_3$ of water or sediment exposures in each species; between k1 or k2 values of Ag_2S NPs of water or sediment exposures between species; between k1 or k2 values or $AgNO_3$ of water or sediment exposures between species. Different capital letters indicate significant differences ($X^2_{(1)}$>3.84; p<0.05) between k1 of Ag_2S NPs of water exposures between species.

Species	Ag form	Mean exposure concentrations water ($\mu g\ Ag\ L^{-1}$)	Mean exposure concentrations sediment ($mg\ Ag\ kg^{-1}$)	k1 water ($L_{water}\ g^{-1}_{organism}\ day^{-1}$)	k1 sediment ($g_{sediment}\ g^{-1}_{organism}\ day^{-1}$)	k2 (day^{-1})
Girardia tigrina	**Ag_2S NP**	9.05 ± 6.76	0.13 ± 0.12	0.05 (-0.05-0.15) A	n.a.	0 (-0.36-0.36)
	$AgNO_3$	8.45 ± 5.14	0.10 ± 0.085	0.64 (0.01-1.28)	n.a.	0 (-0.19-0.19)
Physa acuta	**Ag_2S NP**	9.05 ± 6.76	0.13 ± 0.12	2.65 (0.24-5.07)	183 (16.3-351)	0.47 (-0.06-1.00)
	$AgNO_3$	8.45 ± 5.14	0.10 ± 0.085	80.4 (n.d.)	6041 (n.d.)	7.06 (n.d.)
Chironomus riparius	**Ag_2S NP**	6.88 ± 6.91	0.071 ± 0.059	0.32 (-0.21-0.86) B	31.3 (-20.8-83.3)	0 (-0.55-0.55)
	$AgNO_3$	6.25 ± 4.49	0.057 ± 0.042	1.12 (0.28-1.96)	123 (30.1-215)	0.02 (-0.25-0.29)

(n.d.) not possible to determine 95% CI, and therefore also no comparison made with other Ag forms, species or exposure routes.
n.a. not applicable – toxicokinetics accounting for sediment as exposure route was not determined for planarians.

Figure S5.4 shows the body Ag concentrations in depurated and non-depurated snails. Non-depurated snails from the Ag_2S NP treatment showed a significant increase in body Ag concentrations from day 7 to 14, and body concentrations of depurated snails exposed to $AgNO_3$ significantly decreased at day 14 (two-way ANOVA, Holm-Sidak method, $p<0.05$). In both treatments, non-depurated snails had significantly higher body Ag concentrations than depurated individuals at day 14, and treatment and time showed a significant interaction (two-way ANOVA, Holm-Sidak method, $p<0.05$) (Figure S5.4). Caution should, however, be taken when interpreting this data since it did not pass equal variance test for the two-way ANOVA analysis and no reliable transformations were possible. Total Ag concentrations in shells of depurated *P. acuta* exposed to Ag_2S NPs did not significantly differ (two-way ANOVA, $p>0.05$) between sampling days, while for $AgNO_3$ exposure shell concentrations were significantly higher (two-way ANOVA, Holm-Sidak method, $p<0.001$) at days 7 and 14. Ag concentrations significantly differed (two-way ANOVA, Holm-Sidak method, $p<0.05$) between the two Ag forms at days 7 and 14, and interaction was significant (two-way ANOVA, Holm-Sidak method, $p<0.001$) between treatment and time (Figure S5.5). Shells from non-depurated snails from Ag_2S NP exposures had higher Ag concentrations than shells from depurated snails at days 7 and 14, while the opposite was observed in the $AgNO_3$ treatment. No significant differences (two-way ANOVA, $p>0.05$) were found between shells from depurated and non-depurated snails within each treatment (Figure S5.6).

5.4.4. Comparison of toxicokinetics between mesocosm and single-species tests

In general, planarians and snails reached higher body Ag concentrations at respective times in the mesocosm test compared to the single-species tests, while the chironomid larvae reached similar or higher concentrations in the single-species test (Figure 5.3). Table 5.3 presents data of the three species exposed in independent single-species tests, which contained non-spiked sediment and water spiked to a nominal concentration of 10 µg Ag L^{-1}. In these single-species tests, Ag concentrations in sediments increased during the uptake phase due to settlement from the water column, so sediment exposure was also accounted for in the toxicokinetics calculations for snails and chironomid larvae. The table also presents data from the mesocosm tests modelled with water or sediment as exposure routes to enable direct comparison. Mesocosm data was modelled considering equivalent exposure times as for the single-species data, i.e. for planarian and snails' data was modelled until day 7 and for chironomids until 48h. Since chironomid larvae were sampled

every 12h in the single-species tests, graphs and kinetic parameters of both single-species and mesocosm tests are presented in hours (Figure 5.3, Table 5.3). For *G. tigrina* exposure to $AgNO_3$, mesocosm and single-species tests showed an increasing Ag uptake pattern, although uptake was much lower in the single-species experiment (Figure 5.3), being significantly lower at day 7 (two-way ANOVA, Holm-Sidak method, $p<0.05$), and k1 and k2 values did not differ ($X^2_{(1)}<3.84$; $p>0.05$) between tests (Table 5.3). But, for Ag_2S NP, *G. tigrina* revealed no significant Ag uptake compared with the control in the single-species Ag_2S NP exposure, while in mesocosms the total Ag concentrations in planarians reached 2.35 µg Ag g^{-1}dw (Figure 5.3, Table 5.3).

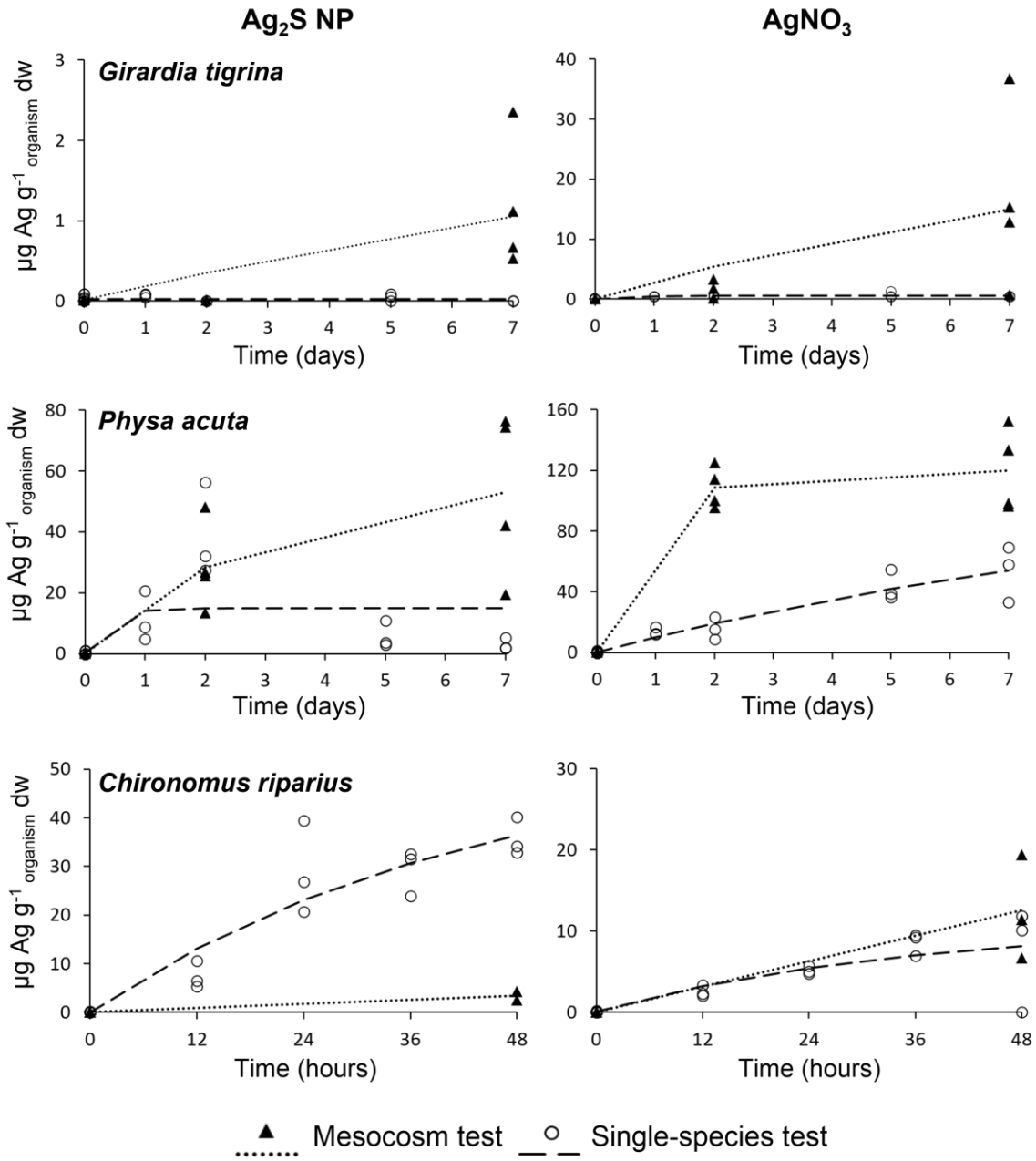

Figure 5.3. Uptake kinetics of Ag_2S NPs (left) and $AgNO_3$ (right) in *Girardia tigrina*, *Physa acuta* and *Chironomus riparius*. Graphs shows the data from the mesocosm test and from single-species tests for each species. The species were individually exposed in single-species tests for 7 days (*G. tigrina* and *P. acuta*) or 48h (*C. riparius*) to water spiked at a nominal concentration of 10 µg Ag L^{-1} and non-spiked sediment. Lines show the fit of a one-compartment model (model 1 – single exposure route) to the total Ag concentrations measured in replicate samples of organisms. Note the differences in the y-axis and x-axis scales.

Snails exposed to Ag_2S NPs in both mesocosm and single-species tests showed a fast Ag uptake during the first day, which continued until day 2 in the mesosoma test. In snails from single-species tests the uptake curve reached steady state from day 1 until the end of the uptake phase, while for snails in the mesocosm test, steady state was reached later,

from day 7 to 14 (Figures 5.2 and 5.3). Snails from the mesocosm test revealed significantly higher body Ag concentrations (two-way ANOVA, Holm-Sidak method, $p<0.05$) at day 7 in the Ag_2S NP exposure, and at days 2 and 7 (two-way ANOVA, Holm-Sidak method, $p<0.001$) in the $AgNO_3$ exposure than snails from the single-species test. Upon $AgNO_3$ exposures, snails in the single-species test exhibited a very different uptake pattern, showing a gradual increase with time (Figure 5.3), with k1 and k2 values being significantly lower ($X^2_{(1)}>3.84$; $p<0.05$) than for the mesocosm exposure (Table 5.3). In turn, for snails exposed to Ag_2S NPs in single-species test, values of k1 sediment and k2 were significantly higher ($X^2_{(1)}>3.84$; $p<0.05$) than for mesocosm test (Table 5.3). In single-species tests of the three species, remarkably high k1 sediment were also generally obtained, particularly for snails.

Chironomid larvae showed similar gradual Ag uptake patterns for $AgNO_3$ exposures in both mesocosm and single-species tests during the first 24h, after which uptake in the single-species test slowed down. Still, body Ag concentrations were not different between mesocosm and single-species tests in larvae from this exposure (two-way ANOVA, $p>0.05$). Uptake rates increased gradually upon exposures to Ag_2S NPs, but body Ag concentrations in larvae from the single-species test reached values around 10 times higher (two-way ANOVA, Holm-Sidak method, $p<0.001$) at day 2 (35.7 µg Ag g^{-1} dw) than those from the mesocosm (3.42 µg Ag g^{-1} dw) (Figure 5.3). For chironomid larvae, no significant differences were found in kinetic parameters between mesocosm and single-species tests ($X^2_{(1)}<3.84$; $p>0.05$) (Table 5.3).

Table 5.3. Toxicokinetic parameters for Ag uptake in the freshwater invertebrates *Girardia tigrina*, *Physa acuta* (soft body) and *Chironomus riparius* exposed to Ag_2S NPs and $AgNO_3$ in single-species tests and compared with mesocosm exposures. In single-species tests, organisms were exposed to water spiked at a nominal concentration of 10 µg Ag L^{-1} and non-spiked sediment. Data was modelled with model 1, considering water or sediment as exposure routes. Measured Ag exposure concentrations (mean ± SD) in water and sediment until day 2 (for chironomids) and day 7 (for planarians and snails) used in the models are also shown. k1 is the uptake rate constant (from water or sediment) and k2 is the elimination rate constant. 95% CI are given in brackets. Significant differences ($X^2_{(1)}$>3.84; p<0.05) are given within a column with different: small letters - Ag_2S NPs vs $AgNO_3$ of the single-species test (bold) or mesocosm test (italics) in each species; capital letters - mesocosm vs single-species tests for Ag_2S NPs (bold) or $AgNO_3$ (italics) in each species.

Species	Ag form	Test type	Measured water exposure concentrations (µg Ag L^{-1})	Measured sediment exposure concentrations (mg Ag kg^{-1})	k1 water (L_{water} $g^{-1}_{organism}$ day^{-1})*	k1 sediment ($g_{sediment}$ $g^{-1}_{organism}$ day^{-1})*	k2 (day^{-1})*
Girardia tigrina	**Ag_2S NP**	Mesocosm	6.88 ± 6.91	0.071 ± 0.059	0.03 (-0.03-0.08) *a*	n.a.	0 (-0.69-0.69) *a*
		Single-species	4.03 ± 5.26	0.014 ± 0.007	0	n.a.	0
	$AgNO_3$	Mesocosm	6.25 ± 4.49	0.057 ± 0.042	0.47 (-0.64-1.59) *a* / *A*	n.a.	0 (-0.80-0.80) *a* / *A*
		Single-species	3.12 ± 4.12	0.012 ± 0.006	0.25 (-0.10-0.60) *A*	n.a.	1.56 (-0.83-3.94) *A*
Physa acuta	**Ag_2S NP**	Mesocosm	6.88 ± 6.91	0.071 ± 0.059	2.79 (-0.02-5.61) *a* / **A**	271 (-1.91-543) *a* / **A**	0.24 (-0.26-0.73) *a* / **A**
		Single-species	5.50 ± 5.23	0.018 ± 0.007	7.65 (-47.1-62.4) **a** / **A**	2340 (-14399-19079) **a** / **B**	2.86 (-18.5-24.2) **a** / **B**
	$AgNO_3$	Mesocosm	6.25 ± 4.49	0.057 ± 0.042	22.6 (5.49-39.7) *b* / *A*	2478 (602-4355) *b* / *A*	1.10 (0.10-2.10) *a* ***I*** *A*
		Single-species	3.52 ± 4.03	0.020 ± 0.014	2.95 (1.44-4.47) **a** ***I*** *B*	520 (253-787) **b** / *B*	0.13 (-0.06-0.32) **b** / *B*
Chironomus riparius*	**Ag_2S NP**	Mesocosm	0.95 ± 1.22	0.032 ± 0.027	0.07** *a* / **A**	2.02** *a* / **A**	0.001 (-0.01-0.01) *a* ***I*** **A**
		Single-species	7.90 ± 4.99	0.010 ± 0.007	0.16 (0.09-0.23) **a** / **A**	125 (67.2-182) **a** / **A**	0.01 (-0.02-0.04) **a** / **A**
	$AgNO_3$	Mesocosm	2.80 ± 3.79	0.032 ± 0.028	0.10** *a* / *A*	8.54** *a* / *A*	0.001 (-0.02-0.02) *a* ***I*** *A*
		Single-species	5.60 ± 3.32	0.007 ± 0.005	0.06 (0.01-0.11) **a** / *A*	44.5 (3.79-85.2) **a** / *A*	0.02 (-0.04-0.08) **a** / *A*

**Chironomus riparius* from mesocosm and single-species tests: k1 water in L_{water} $g^{-1}_{organism}$ $hour^{-1}$; k1 sediment in $g_{sediment}$ $g^{-1}_{organism}$ $hour^{-1}$; k2 in $hour^{-1}$.
**not possible to calculate 95% CI.
n.a. not applicable – toxicokinetics accounting for sediment as exposure route was not determined for planarians.

5.4.5. Evaluation of potential bioaccumulation and biomagnification

Table 5.4 shows the BCF_k or $BSAF_k$ for the uptake of Ag in the snails and chironomid larvae and the BMF for planarians. BMFs were calculated considering: 1) chironomid larvae (at day 7) as diet, 2) depurated snails (at days 7 and 14) as diet, 3) non-depurated/non-washed snails (at days 7 and 14) as diet, and 4) accounting with both organisms (mean body Ag concentrations of non-depurated snails and larvae) as diet, as planarians probably fed on both organisms. For planarians, no BCF_k values could be determined for both treatments as no elimination was seen, so k2=0 (Table 5.4).

Table 5.4. Bioconcentration (BCF_k; water; L g^{-1}) and bioaccumulation ($BSAF_k$; sediment; g g^{-1}) factors of Ag in *Physa acuta* and *Chironomus riparius* exposed to Ag_2S NPs and $AgNO_3$ in mesocosm tests. Biomagnification factors (BMFs) accounting for ingestion of larvae (at day 7), snails (at days 7 and 14) and ingestion of snails and larvae (at day 7) in *Girardia tigrina* exposed to Ag_2S NPs and $AgNO_3$ in mesocosm tests.

	Girardia tigrina		***Physa acuta***		***Chironomus riparius***	
	Ag_2S NP	**$AgNO_3$**	**Ag_2S NP**	**$AgNO_3$**	**Ag_2S NP**	**$AgNO_3$**
BCF_k	n.d.	n.d.	5.64	11.4	n.d.	56
$BSAF_k$	n.a.	n.a.	389	856	n.d.	6150
BMF (larvae)	0.1 (7 d)	0.49 (7 d)	n.a.	n.a.	n.a.	n.a.
BMF (depurated snails)	0.02 (7 d)	0.14 (7 d)	n.a.	n.a.	n.a.	n.a.
	0.14 (14 d)	1.05 (14 d)	n.a.	n.a.	n.a.	n.a.
BMF (non-depurated snails)	0.03 (7 d)	0.14 (7 d)	n.a.	n.a.	n.a.	n.a.
	0.06 (14 d)	0.36 (14 d)	n.a.	n.a.	n.a.	n.a.
BMF (non-depurated snails and larvae)	0.04 (7 d)	0.22 (7 d)	n.a.	n.a.	n.a.	n.a.

n.d. not determined, k2 is 0.
n.a. not applicable to these species.

Chironomid larvae exposed to Ag_2S NPs also had k2=0 making it impossible to determine BCF_k or $BSAF_k$ values, but they showed to bioaccumulate Ag following $AgNO_3$ exposure. Snails seemed to bioaccumulate Ag from both Ag forms. For *G. tigrina*, BMFs considering chironomid larvae or snails (depurated and non-depurated) as diet were higher in the $AgNO_3$ exposure. Planarians revealed BMF > 1 when considering depurated snails as their food in the $AgNO_3$ treatment (Table 5.4). The BMF values (non-depurated snails and larvae) at day 7 were similar to those calculated accounting only for snails, in both Ag_2S NP and $AgNO_3$ exposures (Table 5.4).

5.5. Discussion

5.5.1. Exposure medium: water and sediment

Total Ag concentrations in water showed a gradual increase in time, stabilizing towards the end of the experiment, suggesting that during the initial spiking days Ag was rapidly removed from the water column and partitioned to sediments and glass walls, and probably organisms. The increasing Ag concentrations in the sediment (Table 5.1) confirmed the tendency of Ag to partition from the water to the sediment in both treatments, with sediments becoming a sink for Ag. This is in accordance with other studies where sediment was the main sink for Ag in Ag NP and $AgNO_3$ treatments (Jiang et al., 2017). The small fraction of Ag extracted with water suggests that most of the Ag was adsorbed onto sediment particles and/or organic matter. However, approx. 12% (Ag_2S NPs) and 28% ($AgNO_3$) of total Ag was extracted by diluted acid, suggesting some Ag was present in a labile fraction that may become bioavailable to organisms. The detection of particulate Ag in water indicates that organisms were also exposed to particles via water in both treatments (Figure S5.3, Table S5.4; data not shown). The increase in particulate Ag concentrations over time is probably justified by the spiking routine. Particles detected in water from the $AgNO_3$ treatments probably resulted from the complexation of Ag with chloride present in the APW medium and remaining in the water column (data not shown) (Buffet et al., 2014). A more detailed analysis of Ag fate in the mesocosms is beyond the scope of this paper and will be the subject of a separate paper.

5.5.2. Toxicokinetics of Ag in invertebrate species in the mesocosm test

5.5.2.1. Girardia tigrina

Values of k1 water for the uptake of Ag in the planarians were lower than those for chironomid larvae and snails (Table 5.2). A study reported the k1 values for Cd, Cu and Zn uptake in the planarians *Dugesia japonica* and *G. tigrina* being up to 10 times lower compared with molluscs, crustaceans and oligochaetes (Wu and Li, 2017). It was suggested that the absence of gills and water current-creating structures may lead to lower metal uptake from water (Wu and Li, 2017). *G. tigrina* revealed significantly higher body Ag concentrations upon exposure to $AgNO_3$ compared to Ag_2S NP exposure, even though the measured Ag concentrations in water indicate that exposure was similar for both Ag forms (Figure 5.2, Table 5.1). This suggests a higher bioavailability in the $AgNO_3$ treatment and thus uptake was likely mainly of the ionic form. Similarly, Ag from the $AgNO_3$ treatment also

seemed more available and more toxic to *Schmidtea mediterranea*, belonging also to the family of Dugesiidae (Leynen et al., 2019). However, it cannot be confirmed that the major uptake was of ionic Ag because particulate Ag was also detected in water from both treatments, which is indicative of particle exposure. Particles in the $AgNO_3$ treatment are probably soluble AgCl complexes, which could also have been taken up and/or their re-solubilisation could have led to the release of Ag ions (Buffet et al., 2014). Planarian cells phagocyte food, and the internalisation of other nanoparticles has also been demonstrated (Ermakov et al., 2019; Salvetti et al., 2020). For instance, boron nitride nanotubes were found inside cytoplasmic vesicles of intestinal phagocytes in *D. japonica*, likely internalized by endocytosis (Salvetti et al., 2015). In the present test particles, including Ag_2S NPs, could have also been internalized by endocytic processes. Furthermore, Ag ions could have been taken up by metallothioneins (MTs) as suggested for other metals in planarians (Wu et al., 2011, 2012).

Planarians primarily take up chemicals from the water by cutaneous diffusion (Kapu and Schaeffer, 1991), but uptake can also occur by the pharynx when feeding (Balestrini et al., 2014). Additionally, these organisms secret mucus that can prevent the entrance and diffusion of contaminants into the body (Calevro et al., 1998; Wu and Li, 2017). The planarian *Dugesia etrusca* secreted abnormal amounts of mucus upon exposure to waterborne Al^{3+} and Cr^{3+} (Calevro et al., 1998). Nevertheless, similar to this study, time-dependent increasing body concentrations were observed in planarians exposed to metals in water (Calevro et al., 1998; Indeherberg et al., 1999; Wu and Li 2017). Although mucus may have prevented uptake to a certain extent, it seems that some uptake was still possible, especially of Ag ions. Ag was detected at concentrations up to 0.083 µg L^{-1} in the epidermal mucus of the planarian *S. mediterranea* after 2 days of exposure to 15 mg L^{-1} of uncoated and PVP-coated Ag NPs (Leynen et al., 2019). A study attributed the additional transdermal uptake observed in *L. variegatus* exposed to PEG-coated Ag NPs to associations of the NPs with the epidermis, resulting in localised dissolution and uptake of Ag soluble forms across the organisms skin (Cross, 2017). If Ag gets retained in the mucus, gradual transdermal uptake of Ag ions (either waterborne ions or from dissolution of AgCl particles), may have occurred in planarians from the $AgNO_3$ exposures, while the almost null dissolution of Ag_2S NPs may have resulted in a much lower transdermal uptake.

For planarians, sediments are probably not an exposure route because no evidence was found of planarians ingesting sediment particles. Thus, no toxicokinetics calculations accounting for Ag concentrations in the sediment were made. The pharynx of planarians has shown the ability to simultaneously sense different chemical stimuli in the food and

decide whether to feed or reject its ingestion (Miyamoto et al., 2020). This may help avoiding accidental ingestion of sediment particles when feeding selectively on their preys. Nevertheless, planarian movement on the sediment surface could have also contributed to transdermal uptake from sediment pore water. Sediment particles can get trapped in the mucus (personal observation in mesocosm and single-species tests), therefore one may hypothesize possible transdermal uptake from retained sediment particles. Metal accumulation in predator epibenthic organisms was related to metal concentrations in their preys (De Jonge et al., 2010). Higher body Ag concentrations upon $AgNO_3$ exposures were also found for snails, chironomid larvae (Figure 5.2) and blackworms (data not shown). These organisms are natural preys of planaria (Guecheva et al., 2003), thus food exposure may also have contributed to the higher Ag uptake observed in $AgNO_3$ exposures. The high loss of chironomid larvae from the mesocosms (see results) may be an indication that *C. riparius* were predated by *G. tigrina*. In the present mesocosm study, planarians showed no elimination of Ag in neither treatment (Table 5.2). However, the mesocosm test did not include an elimination phase, therefore Ag elimination cannot be evaluated properly.

5.5.2.2. Physa acuta

Bioaccumulation tests performed with *P. acuta* with the same age as those used in the present study showed no toxicity in exposures to water spiked at 10 µg Ag L^{-1} and sediment contaminated at 10 mg Ag kg^{-1} (Silva et al., 2020). Higher LC_{50} and EC_{50} were determined for *P. acuta* in waterborne exposures (Gonçalves et al., 2017). Although mortality cannot be disregarded, the decreasing numbers can mainly be attributed to predation by planarians.

Silver concentrations in the snails were in general considerably higher than in planarians (Figure 5.2). Although both are epibenthic species, this emphasizes that bioavailability of Ag was different and not entirely dependent on its fate in water/sediment but also on species-specific traits such as ecology, feeding strategies and physiology (Brooks et al., 2009; De Jonge et al., 2010; Diepens et al., 2015). The calculation of the contribution from water and sediment for total Ag uptake revealed that water contributed with nearly 100% in both treatments (Table S5.5). This outcome was also verified in our previous study (Silva et al., 2020). Like planarians, *P. acuta* are likely more exposed to the water phase. Uptake of metal-contaminated suspended particles from water can be a food source for *P. acuta* (De Jonge et al., 2010). The remarkably high k1 values estimated when accounting for Ag concentrations in the sediment may suggest that exposure to sediment may not have contributed much to Ag uptake in both treatments. Nevertheless, exposure to sediments

may have happened, as snails probably fed on sediment organic matter, and accidental ingestion of sediment particles probably occurred, albeit with very low contribution to uptake. Adsorption to the foot and consequent transdermal uptake may also be a possible uptake route for snails (Marigómez et al., 2002), which could have happened during snail movement on the sediment surface. Snails probably also fed on the biofilm on the ceramic tiles, and biofilm possibly growing on the sediment/glass walls. Biofilms have shown a high bioaccumulation of Ag from Ag NP and $AgNO_3$ exposures (Park et al., 2018) and constitute relevant exposure routes to snails (Cleveland et al., 2012). Diet (diatoms) was the main Ag uptake route for *Lymnaea stagnalis* in Ag NP and $AgNO_3$ exposures (Croteau et al., 2011).

In the present study, body Ag concentrations were significantly higher in $AgNO_3$ than in Ag_2S NP exposed snails, except at day 14. The fast increase observed until day 2 may be reflected by the very high k1 value obtained for the $AgNO_3$ treatment, while snails exposed to Ag_2S NPs showed a more gradual increase in Ag uptake, suggesting that Ag in the $AgNO_3$ exposure was more easily available for uptake by snails (Figure 5.2 and Table 5.2). This gradual increase can also result from a balance between uptake and elimination, since Ag_2S NPs were previously shown to be easily taken up and eliminated by *P. acuta* (Silva et al., 2020). Freshwater snails efficiently accumulate Ag from Ag NPs and $AgNO_3$ in water or sediment (Ramskov et al., 2015; Stoiber et al., 2015), with some studies reporting higher Ag uptake following $AgNO_3$ exposures (Bao et al., 2018; Dai et al., 2013). On the other hand, approx. 80% of the Ag bioaccumulated in *L. stagnalis* from waterborne citrate-coated Ag NPs was estimated to be of the particulate form (Croteau et al., 2014). In our earlier bioaccumulation tests with waterborne exposure (no sediment) Ag_2S NPs revealed to be available probably as particles for uptake as almost no dissolution took place (Silva et al., 2020). This almost null dissolution was also found for Ag_2S NPs in the mesocosm test (Tables S5.3), which indicates that the Ag uptake observed for the three species was likely of the nanoparticulate form.

In a previous study, 24h of depuration seemed to be generally appropriate for gut clearance minimizing elimination of internalized Ag in snails exposed for 7 days to $AgNO_3$, while results were less conclusive for the Ag_2S NPs treatment (unpublished work). However, in the present work non-depurated snails were also not washed, thus the possible contribution of Ag adsorbed on snails' body should be also considered for interpretation of the data. In the present mesocosm test, at day 7 internal Ag concentrations of snails did not significantly differ between both treatments, suggesting no effect of depuration and/or a low contribution of Ag adsorbed onto the body of non-depurated snails to total soft body concentrations. However, concentrations in depurated snails were significantly lower than

non-depurated at day 14 from both exposures (Figure S5.4). This can mean that for both treatments, some of the ingested Ag was in the digestive tract and was eventually excreted, or that some internalized Ag was being eliminated, or even that Ag adsorbed to the body of non-depurated snails contributed to higher internal Ag concentrations at this day, probably as a result of adsorbed Ag accumulated in time.

Shells accumulated little Ag compared with soft bodies. At the end of the mesocosm test, shells of depurated *P. acuta* had accumulated 3.6% of Ag in Ag_2S NP and 13.8% in $AgNO_3$ treatments compared to the soft body Ag concentrations. As observed in the work of Silva et al. (2020), no pattern in concentration changes in snail soft bodies and shells was apparent thus making redistribution from tissues to shells unlikely. Moreover, no significant differences were found between Ag concentrations in shells from depurated and non-depurated animals, suggesting that for shells depuration had no effect in Ag concentrations (Figure S5.6), while soft bodies revealed significantly lower body Ag concentrations in depurated snails at the end of the experiment in both treatments (Figure S5.4). Concentrations in shells are likely to have been the result of Ag adsorption to shells from the exposure medium. This adsorption was significantly higher in the $AgNO_3$ treatment and showed to increase during exposure, unlike in the nanoparticulate treatment (Figure S5.5). For further analysis, see Silva et al. (2020).

5.5.2.3. Chironomus riparius

The very low control survival of *C. riparius* larvae is likely due to predation by the planarians rather than toxicity. Thus, in the Ag_2S NP and $AgNO_3$ exposures, the low larvae recovery was also ascribed to predation rather than to toxicity. In another mesocosm experiment, less than 7% of *C. riparius* larvae were recovered at the end of the test, which was also attributed to predation rather than to toxicity of CeO_2 NPs (Bour et al., 2016). For *C. riparius*, the same trend of higher Ag accumulation in $AgNO_3$ than in Ag_2S NP exposures was observed (Figure 5.2). Silver uptake by *C. riparius* larvae exposed in water spiked with Ag NPs and sulfide was slower and lower than in water spiked only with Ag NPs (Lee et al., 2016). Chironomids are deposit-feeders, that live in the surface layer of sediments and have considerable burrowing activity, therefore sediments are considered their dominant exposure route (Bour et al., 2014; Ferrari et al., 2019). However, the very high k1 sediment values, especially for the $AgNO_3$ exposure, may indicate that contribution from sediment was too low to explain uptake (Table 5.2). From the double exposure modelling, uptake rate constants from sediment of almost zero were determined and water contributed for all Ag uptake in the chironomid larvae (Table S5.5). Still, caution should be taken when

considering the contribution of water or sediment to total uptake because no 95% CI could be determined for kw and ks. Chironomid larvae can be vulnerable to water exposure when leaving the tube for feeding on surface sediments or when pumping water for tube irrigation (De Haas et al., 2005). It was demonstrated that chironomids can accumulate metals from the overlying water and pore water (Bervoets et al., 1997; Gimbert et al., 2018).

Ag NPs rapidly deposit onto sediments and accumulate or attach to the organic matter (Park et al., 2018). As mentioned earlier, complexation and sedimentation of AgCl is also expected. Considering that chironomid larvae probably fed on sediment organic matter and particles, higher contribution from sediments would be expected. Aggregates of CeO_2 NPs (Bour et al., 2014) and Al_2O_3 NPs (Lorenz et al., 2017) were observed in the digestive tract of *C. riparius* larvae, indicating uptake of NPs alone and/or associated with sediment particles. After settling into the sediment phase, Ag was probably mostly adsorbed onto sediment particles and organic matter, but some labile pool of Ag was expected to be available for both Ag forms (see above). This suggests that at some point some Ag may have been exchanged to the pore water to become available, for instance, for transdermal uptake, which seemed to be easier for ionic Ag than for the nanoparticulate form, explaining the higher accumulation and uptake in the $AgNO_3$ treatment. This was also observed in a study exposing *C. riparius* to both sediment and pore water which resulted in transdermal uptake of perfluoroalkyl compounds (Bertin et al., 2014). Exchange of dissolved Ag to the pore water phase could have been further promoted by the intense reworking activity of the chironomid larvae (Warren et al., 1998). As mentioned above, possible re-solubilisation of AgCl particles should be considered (Buffet et al., 2014). In another study with *L. variegatus,* no transdermal or dietary uptake was observed upon exposure to Ag_2S NPs, while exposure to $AgNO_3$ resulted in transdermal uptake of Ag dissolved in sediment pore water (Cross, 2017). Lower body Ag concentrations found in the nanoparticle exposure could be generally attributed to faster Ag elimination of NPs, for instance, with excreted food and/or due to cellular processes that promoted faster elimination of the NPs than of the Ag ions (Khan et al., 2015). However, k2 values of zero or almost zero were determined for both treatments and the absence of an elimination phase hinders proper evaluation of Ag elimination by organisms from the mesocosm test, as mentioned earlier.

5.5.3. Interspecies interactions in the mesocosm test

As demonstrated in the present study, benthic organisms can accumulate Ag differently following exposure to $AgNO_3$ or Ag_2S NPs, which may depend on their feeding behaviour, feeding and excretion rates, biotransformation or gut physiology (Brooks et al., 2009; De

Jonge et al., 2010). Bioaccumulation may have also been affected by external factors such as species interactions. Competition for space was shown to result in a decrease of food uptake by *M. balthica* exposed to polychlorinated biphenyls and chlorpyrifos in sediments (Diepens et al., 2015). Since most of the species used in our mesocosm test were benthic, some competition for space was possible. Interspecies interactions (e.g., competition and avoidance behaviour) between *Physa* and *Chironomus* have also been reported, resulting in high snail density negatively affecting chironomid larvae abundance (Devereaux and Mokany, 2006; Gresens, 1995). During depuration, blackworms were observed to break and remove the shell from live snails, resulting in their death, but it cannot be confirmed if the same happened during the exposure in the presence of sediment.

Predation may have had a considerable impact, for example, the presence of planarians could have hampered feeding behaviour of chironomid larvae that must leave their tube to feed on surface sediment particles. Although fish were kept in chambers, their chemical cues could have affected the invertebrates' behaviour (Paterson et al., 2013). The presence of predator fish significantly reduced the foraging activities of *C. riparius* (Hölker and Stief, 2005). *P. acuta* avoided natural cues of the fish predator *Lepomis gibbosus*. However, for the first 6 hours of exposure, snails exhibited 30-47% less predator avoidance behaviour in treatments at a nominal Ag NP concentration of 0.03 µg L^{-1} than in controls (Justice and Bernot, 2014). It is possible that cues released from the rainbow trout could have altered the behaviour of *P. acuta* in our mesocosm test, although the detection of fish cues could also have been impaired by Ag exposure.

5.5.4. Comparison of toxicokinetics between mesocosm and single-species tests

5.5.4.1. Girardia tigrina

The significantly higher body Ag concentrations in planarians from $AgNO_3$ treated mesocosms (~40 times higher) point to higher Ag bioavailability and uptake than in single-species tests, even though the k1 values did not differ significantly. While k2 was zero in $AgNO_3$ treatments of the mesocosm test, planarians seemed to be able to eliminate Ag following $AgNO_3$ exposure in single-species test, even though k2 values were not significantly different (Table 5.3). Importantly, no uptake seemed to have occurred in the single-species Ag_2S NP exposure, as body Ag concentrations did not differ from the controls. Considering this, the observed Ag uptake in the Ag_2S NP treated mesocosms relative to single-species studies indicates a higher bioavailability of this Ag form to the

planarians in the mesocosms. The apparently higher bioavailability and uptake of Ag_2S NP and $AgNO_3$ in the mesocosm test is most likely related to the simultaneous exposure to different routes (water, food and sediment pore water) and to the continuous spiking, which contributed to relatively constant Ag concentrations in water. The absence of Ag uptake in Ag_2S NP exposures in single-species test may be an indication that for planarians water is a less important uptake route to this Ag form compared to uptake via food. *G. tigrina* revealed Ag uptake upon feeding on snails pre-exposed to both Ag_2S NP and $AgNO_3$ (unpublished work), suggesting that dietary exposure may be more important for Ag uptake in this organism. Furthermore, Ag uptake from Ag_2S NP and $AgNO_3$ exposures seemed to be faster in the single-species test upon dietary exposure since body Ag concentrations at 48h were 0.83 (Ag_2S NPs) and 6.20 ($AgNO_3$) µg Ag g^{-1} dw, while in mesocosm body Ag concentrations at the equivalent time were 0.01 (Ag_2S NPs) and 1.35 ($AgNO_3$) µg Ag g^{-1} dw.

5.5.4.2. Physa acuta

The k1 water values did not significantly differ between Ag_2S NP-mesocosm and single-species tests however, internal Ag concentrations in snails at day 7 were around 18 times higher in the mesocosm, indicating underestimation of bioaccumulation by the single-species test. Although the Ag uptake from Ag_2S NPs showed a different pattern until day 7 between both experiments, the single-species test seemed to predict the steady state obtained in the mesocosms after 7 days (Figures 5.2 and 5.3). However, this is probably related to the snail´s ability to eliminate these NPs, and the steady state level is much higher than expected based on the single-species assay. Also, for single-species tests, very high k1 values from sediment were determined suggesting that sediments probably had a minor contribution to uptake.

The overall significantly higher k1 and k2 values found in the mesocosm relative to the single-species tests in both treatments suggests that uptake and elimination was different between the experiments (Table 5.3). Even though exposure concentrations (mean values) in water were relatively similar between the experiments (Table 5.3), the increase in body Ag concentrations in snails exposed to Ag_2S NPs from the mesocosms may be, in part, the result of the increasing Ag concentrations in water (Table 5.1), while in the single-species test concentrations in water decreased over time likely due to sedimentation. In the $AgNO_3$ treatment, uptake patterns were distinct and body Ag concentrations of snails from the mesocosm were significantly higher than from the single-species test at day 2 (Figure 5.3), but Ag concentrations in water at day 2 were still low (Table 5.1) and similar to those in the

single-species exposure at the equivalent time (Silva et al., 2020). Thus, although Ag concentrations were not measured in biofilms due to their very low biomass, feeding on them could have constituted another uptake route for snails in mesocosms. Another aspect that was never observed in the single-species tests with *P. acuta* exposed to $AgNO_3$ is the considerable decrease in internal Ag concentrations already starting during the uptake phase, but this was seen in snails exposed to $AgNO_3$ in the mesocosms at day 14 (Figure 5.2). As previously mentioned, simultaneous exposure to different uptake routes in the mesocosms may explain the higher accumulation and the differences in elimination kinetics.

5.5.4.3. Chironomus riparius

Very different uptake rates and body Ag concentrations were obtained between single-species and mesocosm tests for the Ag_2S NP exposures. In the single-species treatment, body Ag concentrations were 10 times higher at 48h than in the mesocosm test (Figure 5.3). However, total Ag concentrations in sediment at day 2 were around 4 times lower in the single-species test than in the mesocosms. This may confirm that ingestion of sediment particles did not contribute much for Ag uptake in the mesocosm test. In the single-species test, body Ag concentrations were much higher for Ag_2S NP than for $AgNO_3$ exposures, whereas the opposite was observed in the mesocosms. Since the sediment used in single-species tests was inorganic, the higher stability of Ag_2S NPs could have resulted in weaker attachment onto sediment particles and subsequent easier exchange to pore water. Therefore, Ag_2S NPs was probably more bioavailable in the single-species test than in the mesocosms. This can also be an indication that the labile pool extracted from Ag_2S NP treated mesocosms was probably not bioavailable to chironomid larvae, for instance, due to lower exchange to sediment pore water as a result of the organic matter present in this sediment, resulting in lower Ag uptake even at higher total sediment concentrations. Additionally, temperature affects biological processes, thus the 5 ºC difference between experiments (15 ºC in mesocosm and 20 ºC in single-species tests) could have influenced the results. The higher temperature in the single-species tests is expected to promote uptake and accumulation (Péry and Garric, 2006).

Interestingly, body Ag concentrations and uptake curves are very similar between $AgNO_3$ treatments of the single-species and mesocosm tests, suggesting that single-species test may predict bioaccumulation until 48h. This points to a similar bioavailability of Ag in the $AgNO_3$ treatment from both experiments, even though sediments from single-species test did not have organic matter. In turn, it may also support the fact that Ag uptake by the chironomid larvae was more important through water than via sediment. However,

the uptake rate in the single-species test seemed to slow down before 48h, thus it is not clear if it can predict bioaccumulation at longer exposure times considering the increase in body Ag concentrations at day 7 in the mesocosms. Additionally, k1 and k2 parameters of chironomids did not differ. It should be noted, however, that due to the low number of replicates and only two time points available for the chironomids in the mesocosm experiment (to match the exposure times of single-species) kinetic parameters were probably not reliably estimated, which may have affected the reliability of these conclusions, including the predictability of the $AgNO_3$ exposures. Nevertheless, such data limitation can be expected when dealing with more complex scenarios such as mesocosm or field experiments.

The different ages of the chironomid larvae used may also be a factor to consider in explaining the differences observed, as 2nd instar larvae were used in the mesocosms while 4th instar larvae were used in the single-species tests. Thus, larvae grew during the mesocosm experiment and moulted. Moulting and metamorphosis were associated with the elimination of Cd and Zn during larval growth of *C. riparius* (Timmermans and Walker, 1989). Ag NPs strongly adsorbed to the chironomid larvae surface (Asztemborska et al., 2014), therefore elimination through moulting was likely to happen. The mealworm *Tenebrio molitor* eliminated Ag by shedding exuviae upon exposure to $AgNO_3$ and Ag_2S NPs (Khodaparast et al., 2021). In a previous study exposing *C. riparius* larvae to Ag-spiked sediment, adult midges from the $AgNO_3$ treatment revealed a higher fraction of Ag (~21 %) than adults from the Ag_2S NP treatment (1%) relative to the Ag concentrations measured in larvae. This suggests that some ionic Ag can be transferred to adult midges, while NPs may be mostly eliminated, for instance, through shedding (unpublished work).

5.5.5. Predicting bioaccumulation in complex exposure

One of the aims of the present study was to assess whether bioaccumulation tests with single exposure routes and single organisms can predict bioaccumulation in a complex but more realistic scenario such as a mesocosm. Overall, even though some toxicokinetic parameters did not differ between the two experiments, these single-species tests seemed not to be able to reliably predict Ag bioaccumulation in the mesocosms for the following reasons: first, body Ag concentrations were significantly higher in both Ag_2S NP and $AgNO_3$ treatments in the mesocosms pointing to underestimation of the bioaccumulation, while for chironomids were much lower in the Ag_2S NP treated mesocosms; second, in some cases the large scatter in the data leading to very wide 95% CI hampered reliable comparisons; third, interspecies interactions probably affected their behaviour and consequently their

exposure and uptake of Ag. Although Ag uptake in chironomids exposed to $AgNO_3$ in mesocosms seemed to be predicted by the single-species test, the very short exposure time (48h) may not be realistic or robust enough to build conclusions, especially considering the increasing in the internal Ag concentrations in the chironomids observed at day 7 in the mesocosm. This seems to confirm previous studies that concluded that standardized laboratory assays hardly are able to reflect mesocosm tests (Bone et al., 2015; Mikó et al., 2015).

5.5.6. Evaluation of potential bioaccumulation and biomagnification

In an environmentally realistic scenario, Ag adsorbed on the body surface and present in the digestive system of the preys may also contribute to Ag accumulation in predators (Bour et al., 2016). Therefore, some snails were not depurated or washed before sampling. The results suggest that Ag remaining in the gut (or even internalised) in the snails may have been excreted during the 24h depuration of sampling day 14 and/or that Ag adsorbed to the body of non-depurated snails contributed for the total Ag body concentrations measured (Figure S5.4). Calculations only considered snail soft body concentrations because planarians do not ingest the shell. At day 7, higher BMFs were calculated considering chironomid larvae rather than snails as the food source for dietary exposure, probably due to the higher body Ag concentrations measured in the snails (Table 5.4). Likewise, BMFs values calculated with snails and larvae as food sources were approximately the same as when accounting only with snails as single diet (Table 5.4), due to the very low body Ag concentrations found in chironomid larvae. This is an important aspect, as trophic transfer is dependent on the exposure routes of the prey and the feeding habits of the predator (Brooks et al., 2009). At day 14, body Ag concentrations in snails (depurated) decreased in $AgNO_3$ exposures and BMF of 1.05 was calculated for planarians, suggesting biomagnification (Table 5.4). Biomagnification of fullerenol nanoparticles occurred in the food chain *Scenedesmus obliquus* → *Daphnia magna* but not from *D. magna* → *Danio rerio* (Shi et al., 2020). In a natural aquatic food web from a Chinese lake, Ag NPs revealed higher bioaccumulation potential than total Ag. Furthermore, Ag NPs were biomagnified in a fish food web (Xiao et al., 2019).

In our study, higher BCF_ks and $BSAF_k$s were found for *P. acuta* exposed to $AgNO_3$ than to Ag_2S NP exposures (Table 5.4). BCFs were also higher for the freshwater snail *Cipangopaludina chinensis* after 7 days of exposure to $AgNO_3$ (0.92) than to citrate (0.1) and PVP-capped (0.23) Ag NPs in a paddy microcosm (Park et al., 2018). The freshwater snail *Potamopyrgus antipodarum* clone B revealed much higher BSAF (~2) upon exposure

to Ag NPs than to $AgNO_3$ (~0.3), while *P. antipodarum* clone A showed similar and low BSAF in both treatments (Ramskov et al., 2015). Chironomids revealed $BSAF_k$ in exposure to $AgNO_3$ around 7 times higher than snails. However, it should be kept in mind that sediment may not have contributed much to uptake in the mesocosms, therefore BSAFs should be interpreted with caution. Furthermore, the k2 values were determined in the absence of an elimination phase, making them a bit less certain.

Although our results demonstrate that Ag was bioaccumulated in the three test species, most BMFs were < 1 indicating that Ag was not biomagnified and probably was biodiluted along the food chain. Park et al., (2018) although finding BMFs < 1, suggested that Ag may bioaccumulate and be transferred through aquatic food chains exposed to Ag NPs and $AgNO_3$. Nevertheless, since steady state was generally not achieved in the different mesocosm compartments (water, sediment, and biota), it is not possible to determine reliable biomagnification factors. It should be noted, however, that steady state may be difficult to realize in natural dynamic environmental conditions (Petersen et al., 2019).

5.6. Conclusions

This study investigated the toxicokinetics of Ag in benthic freshwater invertebrates exposed to Ag_2S NPs and $AgNO_3$ in mesocosm experiments. Toxicokinetic parameters were compared with those derived from single-species tests and Ag bioaccumulation and potential biomagnification were evaluated. Higher Ag accumulation and uptake rates were found for all invertebrates upon exposure to $AgNO_3$. Uptake of the nanoparticulate Ag form by the three test species seemed to have occurred in Ag_2S NP treatments, which suggests that this most relevant and persistent Ag nanoform is likely to be bioavailable for uptake in benthic organisms. Water seemed to be the most important uptake route. Predation may have influenced chironomid larvae behaviour, as a significant number was probably predated by planarians. Even though some toxicokinetic parameters did not differ significantly and some uptake patterns were similar between single-species and mesocosm tests, the single-species tests generally seemed not able to reliably predict Ag bioaccumulation in the more complex environment of the mesocosms. Biomagnification under this environmentally realistic exposure scenario seemed to be low, even though it seemed to occur in the food chain *P. acuta* → *G. tigrina* in the $AgNO_3$ treatment. This mesocosm study allowed determination of toxicokinetics and bioaccumulation in complex scenarios, including simultaneous exposure routes and species interactions, that cannot be observed in single-species assays, providing a crucial bridge between laboratory and field conditions. To our knowledge, this is the first study evaluating the toxicokinetics of Ag_2S

NPs in benthic invertebrates in a freshwater mesocosm experiment. The present work provides ecologically relevant data that may contribute to improvements of nano regulation.

5.7. References

Arambourou, H., Gismondi, E., Branchu, P., Beisel, J.N., 2013. Biochemical and morphological responses in *Chironomus riparius* (Diptera, Chironomidae) larvae exposed to lead-spiked sediment. Environ. Toxicol. Chem. 32, 2558–2564.

Ardestani, M.M., Van Straalen, N.M., van Gestel, C.A.M., 2014. Uptake and elimination kinetics of metals in soil invertebrates: A review. Environ. Pollut. 193, 277–295.

Arnot, J.A., Gobas, F.A.P.C., 2006. A review of bioconcentration factor (BCF) and bioaccumulation factor (BAF) assessments for organic chemicals in aquatic organisms. Environ. Rev. 14, 257–297.

ASTM, 1980. ASTM (E729-80). Standard practice for conducting acute toxicity tests with fishes, macroinvertebrates and amphibians. Am. Stand. Test. Mater. Annu. B. ASTM Stand. 46, 279–280.

Asztemborska, M., Jakubiak, M., Ksiazyk, M., Stęborowski, R., Polkowska-Motrenko, H., Bystrzejewska-Piotrowska, G., 2014. Silver nanoparticle accumulation by aquatic organisms - Neutron activation as a tool for the environmental fate of nanoparticles tracing. Nukleonika 59, 169–173.

Azimzada, A., Tufenkji, N., Wilkinson, K.J., 2017. Transformations of silver nanoparticles in wastewater effluents: links to Ag bioavailability. Environ. Sci. Nano 4, 1339–1349.

Balestrini, L., Isolani, M.E., Pietra, D., Borghini, A., Bianucci, A.M., Deri, P., Batistoni, R., 2014. Berberine exposure triggers developmental effects on planarian regeneration. Sci. Rep. 4, 4914, 9–11.

Bao, S., Huang, J., Liu, X., Tang, W., Fang, T., 2018. Tissue distribution of Ag and oxidative stress responses in the freshwater snail *Bellamya aeruginosa* exposed to sediment-associated Ag nanoparticles. Sci. Total Environ. 644, 736–746.

Bernhardt, E.S., Colman, B.P., Hochella, M.F., Cardinale, B.J., Nisbet, R.M., Richardson, C.J., Yin, L., 2010. An Ecological Perspective on Nanomaterial Impacts in the Environment. J. Environ. Qual. 39, 1954–1965.

Bertin, D., Ferrari, B.J.D., Labadie, P., Sapin, A., Garric, J., Budzinski, H., Houde, M., Babut, M., 2014. Bioaccumulation of perfluoroalkyl compounds in midge (*Chironomus riparius*) larvae exposed to sediment. Environ. Pollut. 189, 27–34.

Bervoets, L., Blust, R., De Wit, M., Verheyen, R., 1997. Relationships between river sediment characteristics and trace metal concentrations in tubificid worms and chironomid larvae. Environ. Pollut. 95, 345–356.

Bone, A.J., Matson, C.W., Colman, B.P., Yang, X., Meyer, J.N., Di Giulio, R.T., 2015. Silver nanoparticle toxicity to Atlantic killifish (*Fundulus heteroclitus*) and *Caenorhabditis elegans*: A comparison of mesocosm, microcosm, and conventional laboratory studies. Environ. Toxicol. Chem. 34, 275–282.

Bour, A., Mouchet, F., Cadarsi, S., Silvestre, J., Verneuil, L., Baqué, D., Chauvet, E., Bonzom, J.M., Pagnout, C., Clivot, H., Fourquaux, I., Tella, M., Auffan, M., Gauthier,

L., Pinelli, E., 2016. Toxicity of CeO2 nanoparticles on a freshwater experimental trophic chain: A study in environmentally relevant conditions through the use of mesocosms. Nanotoxicology 10, 245–255.

Bour, A., Mouchet, F., Silvestre, J., Gauthier, L., Pinelli, E., 2015. Environmentally relevant approaches to assess nanoparticles ecotoxicity: A review. J. Hazard. Mater. 283, 764–777.

Bour, A., Mouchet, F., Verneuil, L., Evariste, L., Silvestre, J., Pinelli, E., Gauthier, L., 2015. Toxicity of CeO_2 nanoparticles at different trophic levels - Effects on diatoms, chironomids and amphibians. Chemosphere 120C, 230–236.

Brooks, A.C., Gaskell, P.N., Maltby, L.L., 2009. Importance of prey and predator feeding behaviors for trophic transfer and secondary poisoning. Environ. Sci. Technol. 43, 7916–7923.

Buffet, P.-E., Zalouk-Vergnoux, A., Châtel, A., Berthet, B., Métais, I., Perrein-Ettajani, H., Poirier, L., Luna-Acosta, A., Thomas-Guyon, H., Faverney, C.R., Guibbolini, M., Gilliland, D., Valsami-Jones, E., Mouneyrac, C., 2014. A marine mesocosm study on the environmental fate of silver nanoparticles and toxicity effects on two endobenthic species : The ragworm *Hediste diversicolor* and the bivalve mollusc *Scrobicularia plana*. Sci. Total Environ. 470–471, 1151–1159.

Calevro, F., Filippi, C., Deri, P., Albertosi, C., Batistoni, R., 1998. Toxic effects of aluminium, chromium and cadmium in intact and regenerating freshwater planarians. Chemosphere 37, 651–659.

Chen, M., Ma, L.Q., 2001. Comparison of Three Aqua Regia Digestion Methods for Twenty Florida Soils. Soil Sci. Soc. Am. J. 65, 491–499.

Clark, N.J., Boyle, D., Handy, R.D., 2019. An assessment of the dietary bioavailability of silver nanomaterials in rainbow trout using an *ex vivo* gut sac technique. Environ. Sci. Nano 6, 646–660.

Cleveland, D., Long, S.E., Pennington, P.L., Cooper, E., Fulton, M.H., Scott, G.I., Brewer, T., Davis, J., Petersen, E.J., Wood, L., 2012. Pilot estuarine mesocosm study on the environmental fate of Silver nanomaterials leached from consumer products. Sci. Total Environ. 421–422, 267–272.

Cross, R.K., 2017. The fate of engineered nanomaterials in sediments and their route to bioaccumulation. PhD Thesis. University of Exeter. 210 p.

Croteau, M.N., Dybowska, A.D., Luoma, S.N., Misra, S.K., Valsami-Jones, E., 2014. Isotopically modified silver nanoparticles to assess nanosilver bioavailability and toxicity at environmentally relevant exposures. Environ. Chem. 11, 247–256.

Croteau, M.N., Misra, S.K., Luoma, S.N., Valsami-Jones, E., 2011. Silver bioaccumulation dynamics in a freshwater invertebrate after aqueous and dietary exposures to nanosized and ionic Ag. Environ. Sci. Technol. 45, 6600–6607.

Dai, L., Syberg, K., Banta, G.T., Selck, H., Forbes, V.E., 2013. Effects, Uptake, and Depuration Kinetics of Silver Oxide and Copper Nanoparticles in a Marine Deposit Feeder, *Macoma balthica*. ACS Sustain. Chem. Eng. 1, 760−767.

de Haas, E.M., Kraak, M.H.S., Koelmans, A.A., Admiraal, W., 2005. The impact of sediment reworking by opportunistic chironomids on specialised mayflies. Freshw. Biol. 50, 770–780.

De Jonge, M., Blust, R., Bervoets, L., 2010. The relation between Acid Volatile Sulfides (AVS) and metal accumulation in aquatic invertebrates: Implications of feeding behavior and ecology. Environ. Pollut. 158, 1381–1391.

Devereaux, J.S.L., Mokany, A., 2006. Visual and chemical cues from aquatic snails reduce chironomid oviposition. Aust. J. Zool. 54, 79–86.

Diepens, N.J., Van Den Heuvel-Greve, M.J., Koelmans, A.A., 2015. Modeling of Bioaccumulation in Marine Benthic Invertebrates Using a Multispecies Experimental Approach. Environ. Sci. Technol. 49, 13575–13585.

Ermakov, A., Popov, A., Ermakova, O., Ivanova, O., Baranchikov, A., Kamenskikh, K., Shekunova, T., Shcherbakov, A., Popova, N., Ivanov, V., 2019. The first inorganic mitogens: Cerium oxide and cerium fluoride nanoparticles stimulate planarian regeneration *via* neoblastic activation. Mater. Sci. Eng. C 104, 109924.

Ferrari, B.J.D., Vignati, D.A.L., Roulier, J.L., Coquery, M., Szalinska, E., Bobrowski, A., Czaplicka, A., Dominik, J., 2019. Chromium bioavailability in aquatic systems impacted by tannery wastewaters. Part 2: New insights from laboratory and in situ testing with *Chironomus riparius* Meigen (Diptera, Chironomidae). Sci. Total Environ. 653, 1–9.

Furtado, L.M., Norman, B.C., Xenopoulos, M.A., Frost, P.C., Metcalfe, C.D., Hintelmann, H., 2015. Environmental Fate of Silver Nanoparticles in Boreal Lake Ecosystems. Environ. Sci. Technol. 49, 8441–8450.

Gimbert, F., Geffard, A., Guédron, S., Dominik, J., Ferrari, B.J.D., 2016. Mercury tissue residue approach in *Chironomus riparius*: Involvement of toxicokinetics and comparison of subcellular fractionation methods. Aquat. Toxicol. 171, 1–8.

Gimbert, F., Petitjean, Q., Al-Ashoor, A., Cretenet, C., Aleya, L., 2018. Encaged *Chironomus riparius* larvae in assessment of trace metal bioavailability and transfer in a landfill leachate collection pond. Environ. Sci. Pollut. Res. 25, 11303–11312.

Gonçalves, S.F., Pavlaki, M. D., Lopes, R., Hammes, J., Gallego-Urrea, J.A., Hassellöv, M., Jurkschat, K., Crossley, A., Loureiro, S., 2017. Effects of silver nanoparticles on the freshwater snail *Physa acuta*: The role of test media and snails' life cycle stage. Environ. Toxicol. Chem. 36, 243–253.

Gresens, S.E., 1995. Grazer Diversity, Competition and the Response of the Periphyton Community. Oikos. 73, 336–346.

Guecheva, T.N., Erdtmann, B., Benfato, M.S., Henriques, J.A.P., 2003. Stress protein response and catalase activity in freshwater planarian *Dugesia* (*Girardia) schubarti* exposed to copper. Ecotoxicol. Environ. Saf. 56, 351–357.

Handy, R.D., Ahtiainen, J., Navas, J.M., Goss, G., Bleeker, E.A.J., Von Der Kammer, F., 2018. Proposal for a tiered dietary bioaccumulation testing strategy for engineered nanomaterials using fish. Environ. Sci. Nano 5, 2030–2046.

He, D., Garg, S., Wang, Z., Li, L., Rong, H., Ma, X., Li, G., An, T., Waite, T.D., 2019. Silver sulfide nanoparticles in aqueous environments: Formation, transformation and toxicity. Environ. Sci. Nano 6, 1674–1687.

Hölker, F., Stief, P., 2005. Adaptive behaviour of chironomid larvae (*Chironomus riparius*) in response to chemical stimuli from predators and resource density. Behav. Ecol. Sociobiol. 58, 256–263.

Indeherberg, M.B.M., Van Straalen, N.M., Schockaert, E.R., 1999. Combining life-history

and toxicokinetic parameters to interpret differences in sensitivity to cadmium between populations of *Polycelis tenuis* (Platyhelminthes). Ecotoxicol. Environ. Saf. 44, 1–11.

Jiang, H.S., Yin, L., Ren, N.N., Xian, L., Zhao, S., Li, W., Gontero, B., 2017. The effect of chronic silver nanoparticles on aquatic system in microcosms. Environ. Pollut. 223, 395–402.

Justice, J.R., Bernot, R.J., 2014. Nanosilver Inhibits Freshwater Gastropod (*Physa acuta*) Ability to Assess Predation Risk. Am. Midl. Nat. 171, 340–349.

Kaegi, R., Voegelin, A., Sinnet, B., Hagendorfer, H., Burkhardt, M., 2011. Behavior of Metallic Silver Nanoparticles in a Pilot Wastewater Treatment Plant. Environ. Sci. Technol. 3902–3908.

Kapu, M.M., Schaeffer, D.J., 1991. Planarians in toxicology. Responses of asexual *Dugesia dorotocephala* to selected metals. Env. Contam Toxicol 47, 302–307.

Khan, F.R., Misra, S.K., Bury, N.R., Smith, B.D., Rainbow, P.S., Luoma, S.N., Valsami-Jones, E., 2015. Inhibition of potential uptake pathways for silver nanoparticles in the estuarine snail *Peringia ulvae*. Nanotoxicology 9, 493–501.

Khodaparast, Z., van Gestel, C.A.M., Papadiamantis, A.G., Gonçalves, S.F., Lynch, I., Loureiro, S., 2021. Toxicokinetics of Silver Nanoparticles in the Mealworm *Tenebrio molitor* Exposed via Soil or Food. Sci. Total Environ. 777, 146071

Kuehr, S., Kaegi, R., Maletzki, D., Schlechtriem, C., 2021a. Testing the bioaccumulation potential of manufactured nanomaterials in the freshwater amphipod *Hyalella azteca*. Chemosphere 263, 127961.

Kuehr, S., Kosfeld, V., Schlechtriem, C., 2021b. Bioaccumulation assessment of nanomaterials using freshwater invertebrate species. Environ. Sci. Eur. 33, 1-36.

Lead, J.R., Batley, G.E., Alvarez, P.J.J., Croteau, M.N., Handy, R.D., McLaughlin, M.J., Judy, J.D., Schirmer, K., 2018. Nanomaterials in the environment: Behavior, fate, bioavailability, and effects—An updated review. Environ. Toxicol. Chem. 37, 2029–2063.

Lee, S.W., Park, S.Y., Kim, Y., Im, H., Choi, J., 2016. Effect of sulfidation and dissolved organic matters on toxicity of silver nanoparticles in sediment dwelling organism, *Chironomus riparius*. Sci. Total Environ. 553, 565–573.

Leynen, N., Van Belleghem, F.G.A.J., Wouters, A., Bove, H., Ploem, J.P., Thijssen, E., Langie, S.A.S., Carleer, R., Ameloot, M., Artois, T., Smeets, K., 2019. *In vivo* Toxicity Assessment of Silver Nanoparticles in Homeostatic versus Regenerating Planarians. Nanotoxicology 13, 476–491.

Li, P., Su, M., Wang, X., Zou, X., Sun, X., Shi, J., Zhang, H., 2020. Environmental fate and behavior of silver nanoparticles in natural estuarine systems. J. Environ. Sci. (China) 88, 248–259.

Lorenz, C.S., Wicht, A.-J., Guluzada, L., Luo, L., Jäger, L., Crone, B., Karst, U., Triebskorn, R., Liang, Y., Anwander, R., Haderlein, S.B., Huhn, C., Kohler, H.-R., 2017. Nano-sized Al_2O_3 reduces acute toxic effects of thiacloprid on the non-biting midge *Chironomus riparius*. PLoS One 12, e0176356.

Lowry, G. V, Espinasse, B.P., Badireddy, A.R., Richardson, C.J., Reinsch, B.C., Bryant, L.D., Bone, A.J., Deonarine, A., Chae, S., Therezien, M., Colman, B.P., Hsu-kim, H., Bernhardt, E.S., Matson, C.W., Wiesner, M.R., 2012. Long-Term Transformation and

Fate of Manufactured Ag Nanoparticles in a Simulated Large Scale Freshwater Emergent Wetland. Environ. Sci. Technol. 46, 7027−7036.

Marigómez, I., Soto, M., Cajaraville, M.P., Angulo, E., Giamberini, L., 2002. Cellular and Subcellular Distribution of Metals in Molluscs. Microsc. Res. Tech. 56, 358–392.

Mikó, Z., Ujszegi, J., Gál, Z., Imrei, Z., Hettyey, A., 2015. Choice of experimental venue matters in ecotoxicology studies: Comparison of a laboratory-based and an outdoor mesocosm experiment. Aquat. Toxicol. 167, 20–30.

Miyamoto, M., Hattori, M., Hosoda, K., Sawamoto, M., Motoishi, M., Hayashi, T., Inoue, T., Umesono, Y., 2020. The pharyngeal nervous system orchestrates feeding behavior in planarians. Sci. Adv. 6, 1–10.

Naylor, C., Maltby, L., Calow, P., 1989. Scope for growth in *Gammarus pulex*, a freshwater benthic detritivore. Hydrobiologia 188, 517–523.

Nikinmaa, M., 2014. Chapter 5: The Most Important Experimental Designs and Organisms in Aquatic Toxicology, in: An Introduction to Aquatic Toxicology. Elsevier Inc., pp. 53–63.

Oviedo, N.J., Nicolas, C.L., Adams, D.S., Levin, M., 2008. Establishing and maintaining a colony of planarians. Cold Spring Harb. Protoc. 3, 1–6.

Park, H.G., Kim, J.I., Chang, K.H., Lee, B.C., Eom, I.C., Kim, P., Nam, D.H., Yeo, M.K., 2018. Trophic transfer of citrate, PVP coated silver nanomaterials, and silver ions in a paddy microcosm. Environ. Pollut. 235, 435–445.

Paterson, R.A., Pritchard, D.W., Dick, J.T.A., Alexander, M.E., Hatcher, M.J., Dunn, A.M., 2013. Predator cue studies reveal strong trait-mediated effects in communities despite variation in experimental designs. Anim. Behav. 86, 1301–1313.

Péry, A.R.R., Garric, J., 2006. Modelling effects of temperature and feeding level on the life cycle of the midge *Chironomus riparius*: An energy-based modelling approach. Hydrobiologia 553, 59–66.

Petersen, E.J., Mortimer, M., Burgess, R.M., Handy, R., Hanna, S., Ho, K.T., Johnson, M., Loureiro, S., Selck, H., Scott-Fordsmand, J.J., Spurgeon, D., Unrine, J., Van Den Brink, N.W., Wang, Y., White, J., Holden, P., 2019. Strategies for robust and accurate experimental approaches to quantify nanomaterial bioaccumulation across a broad range of organisms. Environ. Sci. Nano 6, 1619–1656.

Ramskov, T., Forbes, V.E., Gilliland, D., Selck, H., 2015. Accumulation and effects of sediment-associated silver nanoparticles to sediment-dwelling invertebrates. Aquat. Toxicol. 166, 96–105.

Salvetti, A., Gambino, G., Rossi, L., De Pasquale, D., Pucci, C., Linsalata, S., Degl'Innocenti, A., Nitti, S., Prato, M., Ippolito, C., Ciofani, G., 2020. Stem cell and tissue regeneration analysis in low-dose irradiated planarians treated with cerium oxide nanoparticles. Mater. Sci. Eng. C 115, 111113.

Salvetti, A., Rossi, L., Iacopetti, P., Li, X., Nitti, S., Pellegrino, T., Mattoli, V., Golberg, D., Ciofani, G., 2015. *In vivo* biocompatibility of boron nitride nanotubes: Effects on stem cell biology and tissue regeneration in planarians. Nanomedicine 10, 1911–1922.

Saraiva, A.S., Sarmento, R.A., Gravato, C., Rodrigues, A.C.M., Campos, D., Simão, F.C.P., Soares, A.M.V.M., 2020. Strategies of cellular energy allocation to cope with paraquat-induced oxidative stress: Chironomids vs Planarians and the importance of using

different species. Sci. Total Environ. 741, 140443.

Selck, H., Handy, R.D., Fernandes, T.F., Klaine, S.J., Petersen, E.J., 2016. Nanomaterials in the aquatic environment: A European Union-United States perspective on the status of ecotoxicity testing, research priorities, and challenges ahead. Environ. Toxicol. Chem. 35, 1055–1067.

Shi, Q., Wang, C.L., Zhang, H., Chen, C., Zhang, X., Chang, X.L., 2020. Trophic transfer and biomagnification of fullerenol nanoparticles in an aquatic food chain. Environ. Sci. Nano 7, 1240–1251.

Silva, P. V., van Gestel, C.A.M., Verweij, R.A., Papadiamantis, A.G., Gonçalves, S.F., Lynch, I., Loureiro, S., 2020. Toxicokinetics of pristine and aged silver nanoparticles in *Physa acuta*. Environ. Sci. Nano 7, 3849–3868.

Stoiber, T., Croteau, M.N., Romer, I., Tejamaya, M., Lead, J.R. Luoma, S.N., 2015. Influence of hardness on the bioavailability of silver to a freshwater snail after waterborne exposure to silver nitrate and silver nanoparticles. Nanotoxicology 9, 918–927.

Sun, T.Y., Bornhöft, N.A., Hungerbühler, K., Nowack, B., 2016. Dynamic Probabilistic Modeling of Environmental Emissions of Engineered Nanomaterials. Environ. Sci. Technol. 50, 4701–4711.

Tangaa, S.R., Selck, H., Winther-Nielsen, M., Khan, F.R., 2016. Trophic transfer of metal-based nanoparticles in aquatic environments: A review and recommendations for future research focus. Environ. Sci. Nano 3, 966–981.

Tatsi, K., Shaw, B.J., Hutchinson, T.H., Handy, R.D., 2018. Copper accumulation and toxicity in earthworms exposed to CuO nanomaterials: Effects of particle coating and soil ageing. Ecotoxicol. Environ. Saf. 166, 462–473.

Timmermans, K.R., Walker, P.A., 1989. The fate of trace metals during the metamorphosis of chironomids (diptera, chironomidae). Environ. Pollut. 62, 73–85.

Toušová, Z., Kuta, J., Hynek, D., Adam, V., Kizek, R., Bláha, L., Hilscherová, K., 2016. Metallothionein modulation in relation to cadmium bioaccumulation and age-dependent sensitivity of *Chironomus riparius* larvae. Environ. Sci. Pollut. Res. 23, 10504–10513.

van den Brink, N.W., Kokalj, J.A., Silva, P. V., Lahive, E., Norrfors, K., Baccaro, M., Khodaparast, Z., Loureiro, S., Drobne, D., Cornelis, G., Lofts, S., Handy, R.D., Svendsen, C., Spurgeon, D., van Gestel, C.A.M., 2019. Tools and rules for modelling uptake and bioaccumulation of nanomaterials in invertebrate organisms. Environ. Sci. Nano 6, 1985–2001.

Vidal, T., Santos, J.I., Marques, C.R., Pereira, J.L., Claro, M.T., Pereira, R., Castro, B.B., Soares, A., Gonçalves, F., 2014. Resilience of the macroinvertebrate community of a small mountain river (Mau River, Portugal) subject to multiple stresses. Mar. Freshw. Res. 65, 633–644.

Warren, L.A., Tessier, A., Hare, L., 1998. Modelling cadmium accumulation by benthic invertebrates *in situ*: The relative contributions of sediment and overlying water reservoirs to organism cadmium concentrations. Limnol. Oceanogr. 43, 1442–1454.

Wu, J.P., Chen, H.C., Li, M.H., 2012. Bioaccumulation and toxicodynamics of cadmium to freshwater planarian and the protective effect of N-Acetylcysteine. Arch. Environ.

Contam. Toxicol. 63, 220–229.

Wu, J.P., Chen, H.C., Li, M.H., 2011. The preferential accumulation of cadmium in the head portion of the freshwater planarian, *Dugesia japonica* (Platyhelminthes: Turbellaria). Metallomics 3, 1368–1375.

Wu, J.P., Li, M.H., 2017. Low uptakes of Cd, Cu, and Zn in *Dugesia japonica*, a freshwater planarian with higher tolerance to metals. Chem. Ecol. 33, 257–269.

Xiao, B., Zhang, Y., Wang, X., Chen, M., Sun, B., Zhang, T., Zhu, L., 2019. Occurrence and trophic transfer of nanoparticulate Ag and Ti in the natural aquatic food web of Taihu Lake, China. Environ. Sci. Nano 6, 3431–3441.

5.8. Supplementary information

Characterization of Ag_2S NP colloids

Images were acquired using a JEOL1010 transmission electron microscope (JEOL, Japan) working at 80keV. For sample preparation, formvar-coated and carbon stabilized 200-mesh copper grids (Ted-pella Inc., USA) were dipped in aliquots of Ag_2S NP stock solution with 1:10 dilution in milli-Q water and left to dry for at least 12h. ImageJ software (NIH, USA) was used to process the acquired Transmission Electron Microscopy (TEM) images to calculate mean size and size distribution. The hydrodynamic diameter and the surface charge of the nanomaterial (NM) colloids were measured by Dynamic Light Scattering (DLS) and Zeta Potential (Z-Potential) on a Malvern Zetasizer Nano ZS90 which incorporates a Zeta potential analyser (Malvern Instruments Ltd, Worcestershire, UK). In order to be within the technical experimental limits, samples had to be diluted 1:10 in milli-Q water. UV-Visible absorption spectra of the Ag_2S NP colloids were measured using an Agilent Cary 60 UV-Vis Spectrophotometer setting spectra measuring limits between 300 and 800 nm.

Table S5.1: Characterization summary table showing core NP size by analysis of TEM images, hydrodynamic size by Dynamic Light Scattering (DLS) presented as both Intensity and Number, polydispersity Index (PDI) and Zeta-Potential for the Ag_2S NP colloids used in the mesocosm test. Conductivity, pH and the exact dilution factor of the stock solution in milli-Q water used to conduct the measurement are given to complement the measured Zeta-Potential value (Peixoto et al., 2020).

Nanomaterial	Size by TEM (nm)	DLS size			Zeta-Potential			
		By intensity (nm)*	By number (nm)*	PDI	Mean (mV)*	Conductivity (mS/cm)	Dilution factor	pH
20 nm Ag_2S NP colloid	20.4 ± 11.9	340 ± 15	132 ± 20	0.240	-23.8 ± 4.5	0.174	1:10	8.72

* SD of the mean within 3 replicates.

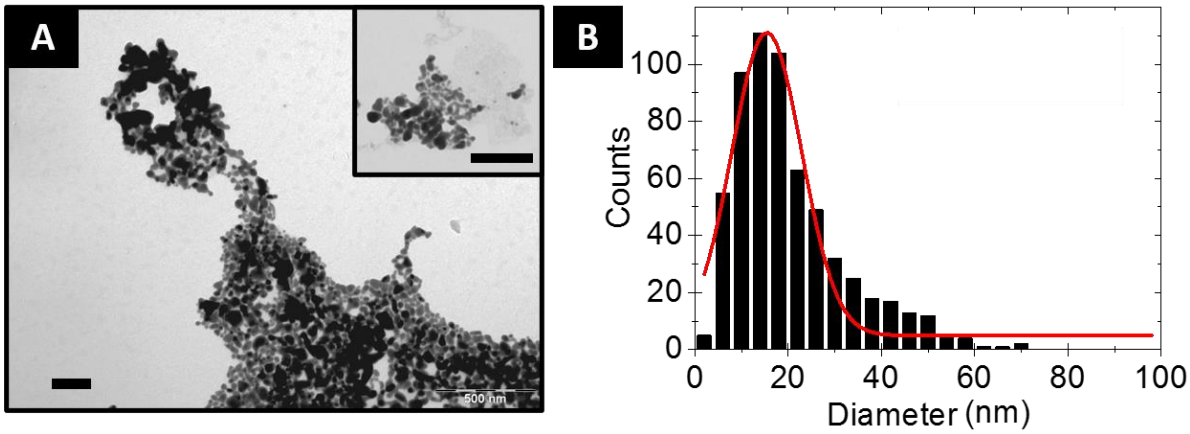

Figure S5.1: Characterization data of the Ag_2S NP colloids used in this study. A) a low magnification TEM image with a higher magnification shown in the inset at the top-right (scale bar equalling 200 nm), B) the corresponding size distribution by analysis of the TEM images (20.4 ± 11.9 nm; particle number counted =613) (Peixoto et al., 2020).

Table S5.2. Ag and S composition, in percentage, of the Ag_2S NP colloids used in this study, measured by TEM-EDX.

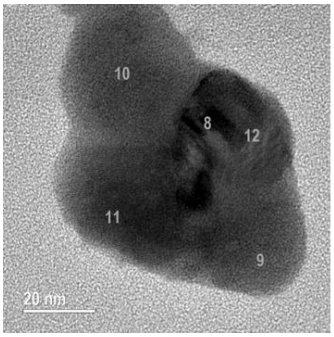

Spectrum Label	Spectrum 8	Spectrum 9	Spectrum 10	Spectrum 11	Spectrum 12
S	14.8	20.3	28.2	30.3	29.8
Ag	85.2	79.7	71.8	69.7	70.2
Total	100	100	100	100	100

Figure S5.2. High resolution TEM image of Ag_2S NP colloids.

Characterization of Ag_2S NPs in APW medium

The stability of Ag_2S NPs in APW medium was assessed by measuring the dissolution, hydrodynamic size and Z-potential at different time points: 0, 0.5, 1, 2, 4, 8, 24 and 48 hours, in suspensions of 10 µg Ag L^{-1} and 1 mg Ag L^{-1}. NP dissolution monitoring was performed according to the protocol of Avramescu et al. (2017), based on the European Committee for Standardisation (CEN) guidance EN 71-3:2019 on "Safety of toys - Part 3: Migration of certain elements" (European's Committee for Standardisation, 2019), which is commonly used in metal bioaccessibility assays (Dodd et al., 2013). Dissolution of Ag_2S NPs was measured at 0, 0.5, 1, 2, 4, 8, 24 and 48 hours in 1 mg L^{-1} suspensions of APW, and at each sampling time, part of each sample was filtered using 0.02 µm pore-diameter syringe filters (AnotopTM, Whatman) and directly acidified with pure ICP-grade HNO_3 (Sigma Aldrich; CAS Number 7697-37-2) to a final concentration of 2% HNO_3. Dissolved Ag^+

concentrations were measured by Inductively Coupled Plasma Mass Spectrometry (ICP-MS, PerkinElmer, Nexion 3000). Results are reported as percentage dissolution (%Diss), determined as the amount of dissolved Ag ([DAg^+]) divided by the original Ag concentration ([Ag^+]) used for the experiment (%Diss=([DAg^+]/[Ag^+])×100%). The rest of each sample was, simultaneously, analysed to measure the hydrodynamic size and Z-potential, using a Malvern Zetasizer (Nano ZS) equipped with a LASER of 632.8 nm and a scattering angle of 173º. All measurements were performed at 20 ºC following a 2-minute equilibration, using Sarstedt polystyrene (Ref: 67.742, 10 x 4 x 45 mm) cuvettes and Malvern Zetasizer DTS0170 disposable folded capillary cells, for size and zeta potential measurements, respectively. The operation procedures used the built-in values for the refractive indices (η) and absorption coefficients (α) for Ag and Ag_2S from the Malvern Zetasizer Software (version 7.13).

Table S5.3. Characteristics of the Ag_2S NPs used in the mesocosm test in terms of Zeta-potential (mV), polydispersity Index (PDI) and mean hydrodynamic diameter (nm) measured by Dynamic Light Scattering (DLS); Dissolved Ag concentration (µg L^{-1}) and percentage of dissolution of Ag_2S NPs in APW solutions at a nominal concentration of 1 mg Ag L^{-1} determined by ICP-MS. All values are given as mean and standard deviation (mean ± SD; *n*=3).

Timepoint (h)	Z-potential (mV)	Hydrodynamic diameter by DLS (nm)	PDI	Dissolved Ag concentration (µg L^{-1})	Dissolution (%)
0	-6.32 ± 0.62	336 ± 26.6	0.58 ± 0.06	0.04 ± 0.07	0.004 ± 0.007
0.5	-7.02 ± 2.35	359 ± 58.2	0.57 ± 0.10	0 ± n.d.	0 ± n.d.
1	-5.93 ± 1.52	344 ± 23.5	0.56 ± 0.07	1.27 ± 2.21	0.13 ± 0.22
2	-8.34 ± 0.88	322 ± 22.3	0.55 ± 0.08	0.79 ± 0.60	0.08 ± 0.06
4	-9.09 ± 0.52	334 ± 17.8	0.52 ± 0.08	0.07 ± 0.08	0.01 ± 0.01
8	-7.56 ± 0.60	330 ± 15.8	0.54 ± 0.07	0 ± n.d.	0 ± n.d.
24	-5.40 ± 0.77	430 ± 61.9	0.66 ± 0.08	0 ± n.d.	0 ± n.d.
48	-8.67 ± 1.38	301 ± 16.1	0.53 ± 0.05	0 ± n.d.	0 ± n.d.

n.d. not possible to determine the standard deviation.

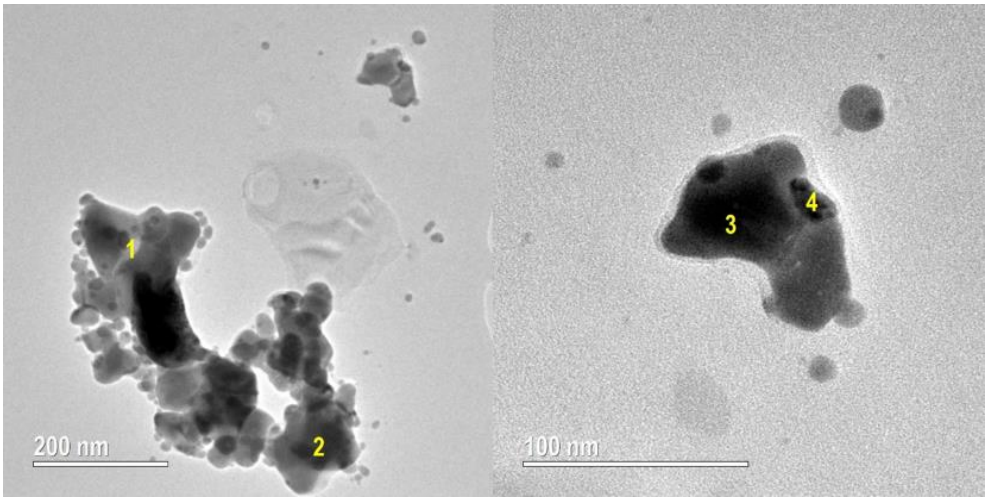

Figure S5.3. TEM images of Ag_2S NPs in APW medium at sampling time day 2 of the mesocosm test.

Table S5.4. Ag and S composition, in percentage, by TEM-EDX of Ag_2S NPs in APW medium at sampling time day 2 of the mesocosm test (spectrum numbers correspond to the numbers on the Ag_2S NPs in Figure S5.3).

Spectrum Label	Spectrum 1	Spectrum 2	Spectrum 3	Spectrum 4
S	31.51	32.25	28.54	28.16
Ag	68.49	67.75	71.46	71.84
Total	100	100	100	100

Table S5.5. Toxicokinetic parameters for the uptake of Ag, and the relative contribution of uptake from water (APW) and sediment to the total uptake of Ag in the freshwater invertebrates *Physa acuta* (soft body) and *Chironomus riparius*, exposed to Ag_2S NPs and $AgNO_3$ in the mesocosm test. Data was modelled considering water and sediment as simultaneous exposure routes. kw is the uptake rate constant from water, ks is the uptake rate constant from sediment and k2 is the elimination rate constant. 95% Confidence intervals (CI) are given in brackets. Absence of letters indicates no significant differences between k2 values ($X^2_{(1)}$<3.84; p>0.05).

Species	**Ag form**	**kw** (L_{water} $g^{-1}_{organism}$ day^{-1})	**ks** ($g_{sediment}$ $g^{-1}_{organism}$ day^{-1})	**k2** (day^{-1})	**% uptake from water**	**% uptake from sediment**
Physa acuta	Ag_2S NP	2.58 (n.d.)	5.32 (n.d.)	0.47 (-1.27-2.21)	97.10	2.90
	$AgNO_3$	128 (n.d.)	1.72 (n.d.)	11.3 (n.d.)	99.98	0.02
Chironomus riparius	Ag_2S NP	0.32 (n.d.)	0.01 (n.d.)	0 (n.d.)	99.96	0.04
	$AgNO_3$	1.12 (n.d.)	0.02 (n.d.)	0.02 (n.d.)	99.98	0.02

(n.d.) not possible to determine 95% confidence intervals.

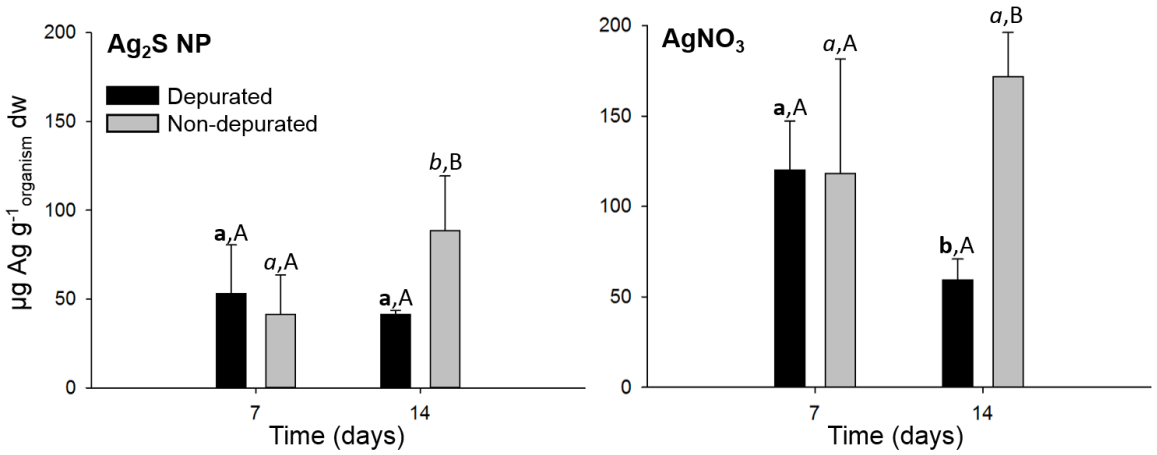

Figure S5.4. Silver concentrations (mean ± SD; *n*=4; µg Ag g^{-1} dw) of depurated and non-depurated *Physa acuta* (soft body) exposed to Ag_2S NP (left) and $AgNO_3$ (right). Different small letters in bold and in italics indicate a significant difference between sampling days within Ag_2S NP and $AgNO_3$ treatments, respectively; different capital letters indicate a significant difference between depurated and non-depurated organisms on the respective sampling day (two-way ANOVA followed by Holm-Sidak Method, $p<0.05$).

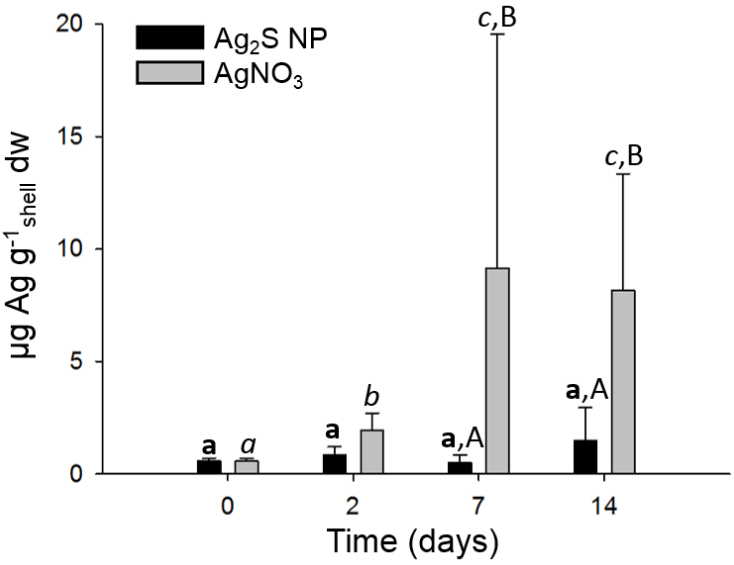

Figure S5.5. Silver concentrations (mean ± SD; *n*=4; µg Ag g^{-1} dw) in the shells of depurated *Physa acuta* exposed to Ag_2S NPs and $AgNO_3$. Different small letters in bold and in italics indicate a significant difference between sampling days within Ag_2S NP and $AgNO_3$ treatments, respectively; different capital letters indicate a significant difference between treatments on the respective sampling day (two-way ANOVA followed by Holm-Sidak Method, $p<0.05$).

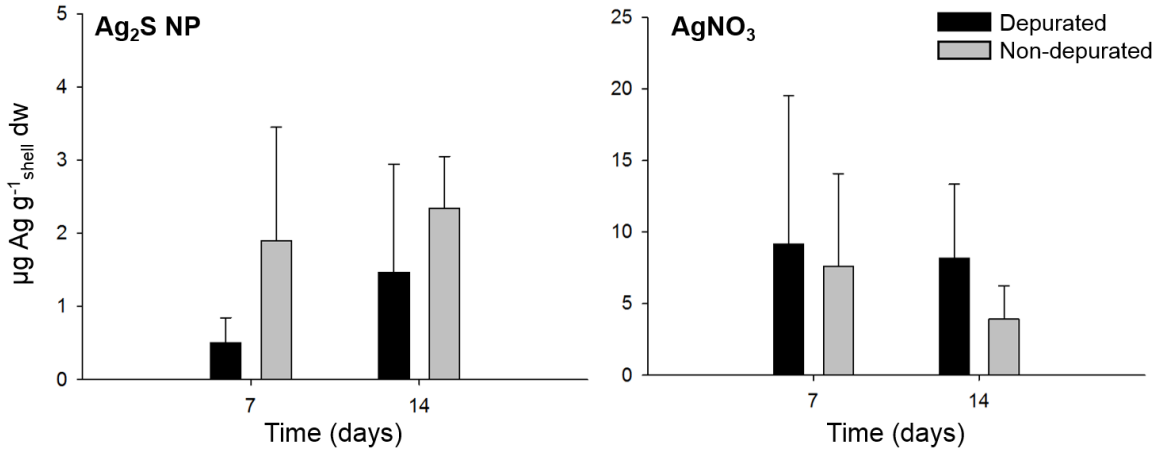

Figure S5.6. Silver concentrations (mean ± SD; *n*=4; µg Ag g^{-1} dw) in shells of depurated and non-depurated *Physa acuta* exposed to Ag_2S NPs (left) and $AgNO_3$ (right). Absence of letters indicates no significant differences between sampling days within the same treatment and between depurated and non-depurated shells within each sampling day (two-way ANOVA, p>0.05).

5.8.1. Supplementary references

Avramescu, M.L., Rasmussen, P.E., Chénier, M., Gardner, H.D., 2017. Influence of pH, particle size and crystal form on dissolution behaviour of engineered nanomaterials. Environ. Sci. Pollut. Res. 24, 1553–1564.

Dodd, M., Rasmussen, P.E., Chénier, M., 2013. Comparison of Two *In Vitro* Extraction Protocols for Assessing Metals' Bioaccessibility Using Dust and Soil Reference Materials. Hum. Ecol. Risk Assess. 19, 1014–1027.

European's Committee for Standardisation (CEN), 2019. CEN/TC 52. Safety of toys - Part 3: Migration of certain elements. guidance EN 71-3:2019.

Peixoto, S., Khodaparast, Z., Cornelis, G., Lahive, E., Green Etxabe, A., Baccaro, M., Papadiamantis, A.G., Gonçalves, S.F., Lynch, I., Busquets-Fite, M., Puntes, V., Loureiro, S., Henriques, I., 2020. Impact of Ag_2S NPs on soil bacterial community – A terrestrial mesocosm approach. Ecotoxicol. Environ. Saf. 206, 111405.

Chapter 6

General Discussion and Conclusions

6. General Discussion and Conclusions

6.1. Summary and highlights

The demand for engineered nanomaterial (ENM)-enabled products increases in parallel with ENMs environmental risk, consequently increasing the pressure on the scientific community to tackle this concern. Quantifying the uptake and elimination of ENMs by organisms and determine their bioaccumulation potential are key components to understand their mechanism of toxicity (van den Brink et al., 2019).

As addressed in **Chapter 1**, the general aim of the present thesis was to determine and understand the toxicokinetics and bioaccumulation of pristine and (simulated) aged silver nanoparticles (Ag NPs) and $AgNO_3$ to freshwater benthic invertebrates. Because of discharges of Ag NPs, mainly in their sulfidised form (Ag_2S NP), into aquatic environments and subsequent settlement into sediments, this thesis focused on ecologically relevant benthic invertebrate species, which can be simultaneously exposed to NPs and/or their transformation product through water, sediment, and food. This study used several Ag NPs with different characteristics, including a simulated aged form (Ag_2S NPs), to account for the most environmental relevant Ag NP form. Considering these arguments, **Chapters 2 to 5** focused on studying the toxicokinetics and potential bioaccumulation and biomagnification of the different Ag NP forms in three benthic invertebrate species. **Chapter 6**, provides the general summary of the thesis and its main findings (highlights). This chapter also provides proposals for uptake and elimination routes in the three test species, based on the findings of the thesis and hypotheses raised, integrating information from the different chapters. These schematic proposals will use representations of the test organisms that are not in accordance with their real anatomy and proportions, but may be helpful in visualising the hypotheses based on current scientific insights. To finalise this work, final conclusions and future perspectives will be addressed.

In **Chapter 2**, the toxicokinetics of 3-8 nm, 50 nm and 60 nm Ag NPs, Ag_2S NPs and $AgNO_3$ were evaluated in the freshwater snail *Physa acuta*. Snails were exposed to 1) contaminated water without sediment (Ag-spiked water test), 2) contaminated water with clean sediment (Ag-spiked water with clean sediment test), and 3) spiked sediment with clean water (Ag-spiked sediment test). Firstly, results showed that the **characteristics of the different Ag forms greatly influenced the bioavailability of Ag to the snails in all tests**, as snails showed different uptake and elimination kinetics of the different Ag forms within the same exposure route. Uptake of the different Ag forms was comparable in both

waterborne exposure tests (Ag-spiked water test and Ag-spiked water with clean sediment test) but was different from those obtained for snails exposed in the Ag-spiked sediment test. Thus, **exposure route may also determine the bioavailability of Ag to *P. acuta*.** When considering the more **realistic exposure scenario with water and sediment as simultaneous exposure routes** (Ag-spiked water with clean sediment test), **water was the predominant route for Ag uptake in all treatments**. Even though Ag settled from the water column to the sediment phase, the movement of snails probably promoted resuspension of Ag at the sediment-water interface facilitating uptake via water, which could be easier in the inorganic sediment used. This scenario was also likely to have happened in the Ag-spiked sediment test, also with low contribution of sediment particle ingestion to Ag uptake.

In Figure 6.1, different routes of uptake from water are suggested for *P. acuta* exposed to dissolved and NP Ag forms. In the figures, the Ag forms are placed next to the arrow to show the importance of the uptake or elimination route for that Ag form. The "dissolved Ag" indicated in the figures may account for Ag^+ and for other dissolved Ag species resulting from the complexation of Ag^+ (e.g., AgCl) that might also be present in solution and available for uptake by the organisms. Transdermal uptake from the surrounding water was probably an uptake route and seemed to be more important for dissolved Ag. Transdermal uptake through the foot may also be an uptake route when the snails are gliding over the sediment (e.g., sediment pore water) (Figure 6.1). Oral uptake of water is another possible uptake route. It was observed that oral water ingestion can be a consequence of swallowing and bite cycles in *Lymnaea stagnalis* (De With, 1996). Accidental oral uptake of sediment particles likely occurred in both tests with sediment, albeit with minor contribution for Ag uptake (Figure 6.1). This is supported by personal observation of sediment particles during the snail soft tissue digestion. This work also revealed that the **Ag_2S NPs were available for uptake but were easily eliminated from the organism in the three experiments**. Snails **dealt differently with the different Ag forms**, since different eliminations were observed between the treatments.

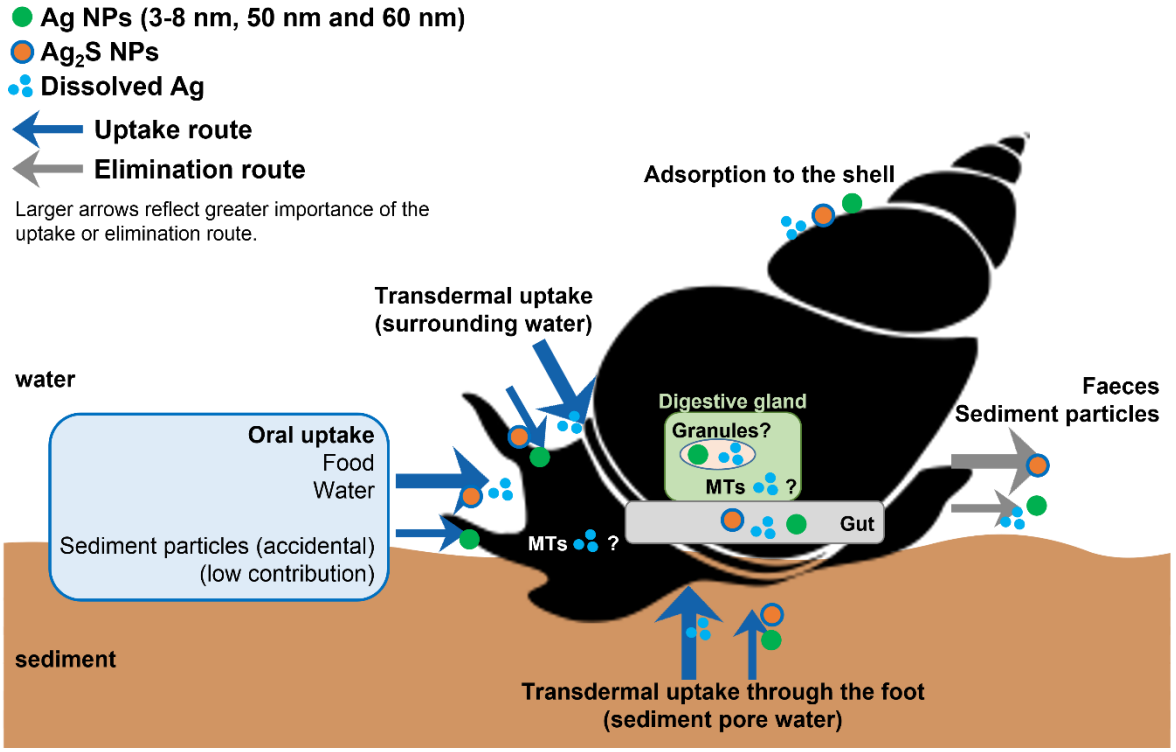

Figure 6.1. Schematic proposal for uptake and elimination routes of Ag in *Physa acuta* exposed to 3-8 nm, 50 nm and 60 nm Ag NPs, Ag_2S NPs and $AgNO_3$ in the different exposure route tests (Chapters 2, 4 and 5).

Overall, **elimination was faster for Ag_2S NPs** suggesting that this Ag form was not retained in the body, whereas for the pristine Ag NP and $AgNO_3$ treatments slower elimination was generally seen in the different exposures. In some cases, a stored fraction (SF) of 1 was calculated for $AgNO_3$ and pristine NPs. This suggests that the **accumulated Ag was retained in the body, which may raise concerns regarding bioaccumulation in snails and possibly trophic transfer.** This could be the result of the sequestration of NPs and ionic Ag in the digestive gland, for instance, in metal-containing granules or the binding of ionic Ag to metallothioneins (MTs) as exemplified in Figure 6.1 (Croteau et al., 2007; Desouky, 2006). To explain the higher Ag elimination observed in the $AgNO_3$ treatment in tests with sediment, especially in the Ag-spiked sediment, it was postulated that some ionic Ag was excreted with sediment particles, although this needs confirmation. Lastly, Ag concentrations measured in the **shells of snails from all tests were low** and were possibly the result of **Ag (either ionic or nanoparticulate Ag) adsorption to the shells** (Figure 6.1).

In **Chapter 3**, the toxicokinetics and bioaccumulation of the same pristine Ag NPs, Ag_2S NPs and $AgNO_3$ were explored in larvae of the non-biting midge *Chironomus riparius*. The

aim was also to evaluate the uptake of Ag via different separate exposure routes: water, sediment and food. Interestingly, a pattern was observed in the three experiments: **higher internal Ag concentrations and uptake rates were found in larvae exposed to Ag_2S NPs**, and similar but lower uptake for Ag NPs and $AgNO_3$. Moreover, **uptake patterns of all Ag forms were similar in the water and sediment exposure tests, suggesting similar uptake routes**. In this chapter, results also point to a **higher contribution to Ag uptake from water** rather than from sediment. It was hypothesised that due to the absence of organic matter in the sediment, the more stable Ag_2S NP form was more easily exchanged to pore water or to water at the interface with sediment than the other Ag forms, in both water and sediment exposure route tests. These exchanges were probably enhanced by the reworking activity of the larvae. In turn, in the mesocosm test using sediment with organic matter (ground leaves) Ag uptake from $AgNO_3$ was much higher than from Ag_2S NPs, and uptake from water (oral or transdermal) also seemed to have higher contribution than sediments (Chapter 5) (Figure 6.2).

The chironomid larvae in the water exposure route test were **likely exposed via water, for instance, when foraging at the sediment-water interface or to sediment pore water**. Oral uptake of sediment particles can be another uptake route, even if with a minor contribution for uptake in this experiment (Figure 6.2). When sediment was the spiked media, Ag uptake was probably the result of the **combination of pore water exposure and ingestion of sediment particles,** even though it seems that water was more important as the uptake patterns were quite similar in the water and sediment exposure tests. In both water and sediment exposure route tests, the suggested uptake from water is via transdermal uptake from sediment pore water and also from overlying water when foraging. Passive oral uptake of water (e.g., when feeding on sediment particles and when pumping water for tube irrigation) and uptake through the anal papillae were also suggested (Figure 6.2). However, more research is needed to confirm these uptake routes for the different Ag forms tested.

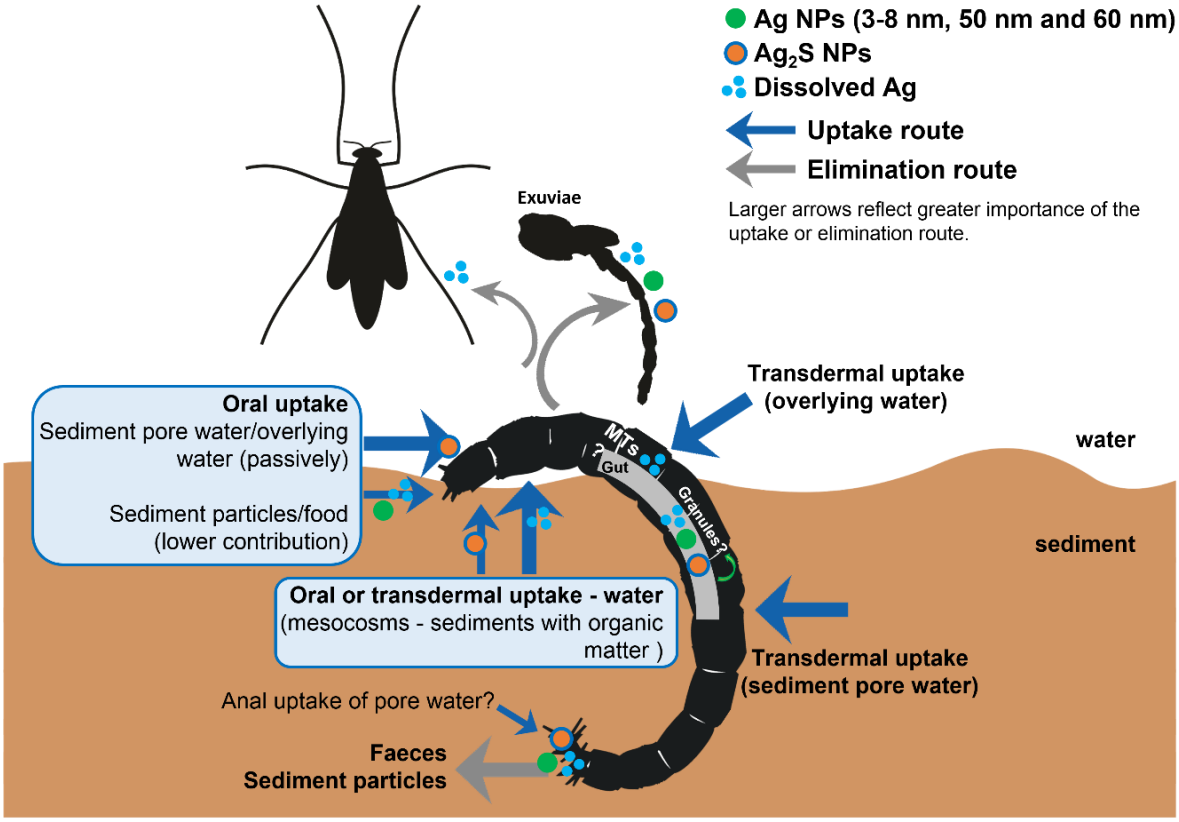

Figure 6.2. Schematic proposal for uptake and elimination routes of Ag in *Chironomus riparius* exposed to 3-8 nm, 50 nm and 60 nm Ag NPs, Ag_2S NPs and $AgNO_3$ in the different exposure route tests (Chapters 3 and 5).

In the water exposure route test, the chironomid larvae showed to eliminate Ag faster in the Ag_2S NP exposure and slower in the $AgNO_3$ treatment, reaching similar internal Ag concentrations at the end of the elimination phase. It was hypothesised that in this test, the nanoparticulate form was eliminated faster from the organism than ionic Ag (and was faster for Ag_2S NPs), and then reached similar values may be due to some ionic Ag being retained in the body. A possible elimination route can be through the egestion of sediment particles (Figure 6.2). Conversely**, elimination in the sediment exposure route test was slower**, also for Ag_2S NPs, even though the results suggest similar uptake routes for both experiments. This can, however, be the result of the higher sediment concentrations, which could have led to a higher exchange of Ag to pore water. Even though ingestion of sediment particles contributed less to the total Ag uptake, its contribution was probably higher in the sediment exposure route test than in the water exposure test. This could have resulted in a higher internalization of nanoparticulate and ionic Ag in the gut lumen upon sediment ingestion (Figure 6.2), as seen in the estuarine polychaete *Nereis diversicolor* (García-Alonso et al., 2011). Sequestration by MTs or metal-rich granules were postulated as reported for other cationic metals in chironomid larvae (Figure 6.2) (Béchard et al., 2008;

Gimbert et al., 2016; Toušová et al., 2016). Again, this is merely speculative and should be addressed in the future. Results from the test with **spiked food were inconclusive as no significant uptake occurred when compared to the control, except for the Ag_2S NPs**. Ag_2S NPs could have been slightly bound to the leaves, consequently leading to higher detachment from the food in the gut and likely to higher absorption into the gut lumen. Nonetheless, this can also be the result of the food type, offered in disks, instead of, for instance, as ground food.

This study showed that **pupal exuviae is also a Ag elimination route** and so was the **transfer of some Ag to adult midges** (Figure 6.2). However, the **potential trophic link to terrestrial predators seems to be weak**, although the percentage of Ag found in adult midges of the $AgNO_3$ treatment should not be ignored (20.9% of the Ag content in larvae). To the best of our knowledge, this is the first study determining the toxicokinetics of NPs in chironomids.

In **Chapter 4**, a **more realistic scenario was investigated**, where Ag_2S NPs reached aquatic ecosystems and consequently contaminated food sources, potentially exposing organisms to water and food. Briefly, *P. acuta* were exposed to Ag_2S NPs or $AgNO_3$-spiked water and fed with clean microalgae (*Raphidocelis subcapitata*). Some snails were maintained in extra vials of each treatment and provided as food item to the planarian *Girardia tigrina*. Toxicokinetics and bioaccumulation were evaluated in both organisms as well as the potential of Ag biomagnification in the food chain *P. acuta* → *G. tigrina*. In this test, ingestion of food was also an uptake route for the snails (Figure 6.1) and the **combined uptake via water and food was the likely exposure scenario**. Ag in the water was probably taken up by *R. subcapitata*, possibly by NP adsorption to the algal cell walls in the Ag_2S NP treatment and internalized Ag in the $AgNO_3$ exposure (Ribeiro et al., 2015). Toxicokinetics of Ag in *P. acuta* were distinct between the two treatments, with **higher uptake but lower elimination following exposure to $AgNO_3$ compared to Ag_2S NPs**. To explain this, it was postulated that Ag could have been internalised in algae (e.g., bound to MTs (Ribeiro et al., 2015)) and therefore was more trophically available, and so it was more easily assimilated in the $AgNO_3$ treatment. The higher Ag ion concentration in the water of the $AgNO_3$ exposure can also explain the higher Ag uptake in the snails. Additionally, once ingested food reaches the digestive gland, different cellular processes can occur, consequently leading to different elimination rates for nanoparticulate and ionic Ag (Figure 6.1). These results were compared with the Ag-spiked water test from Chapter 2. Ag uptake and elimination of snails upon exposure to Ag_2S NPs in this test differed from those

observed in the Ag-spiked water test. Possibly, **Ag uptake from Ag_2S NPs was mainly by ingestion of algae and the Ag was rapidly eliminated with the faeces,** which seemed to be an important elimination route for Ag_2S NPs in this test (Figure 6.1). In turn, the gradual Ag uptake and slow elimination obtained in the $AgNO_3$ treatment resembled those of the Ag-spiked water test, however, internal Ag concentrations and uptake rate constant (k1) values were significant lower in the test of Chapter 4. Two explanations were suggested: 1) uptake from water was more important but the reduction of Ag concentrations in the water due to the presence of algae could have led to lower uptake; 2) the difference in age between the snails used in this test and those used in the Ag-spiked water test influenced uptake, as seen in other studies (Croteau et al., 2014; Spyra et al., 2019).

For ***G. tigrina*, uptake was much higher upon exposure to $AgNO_3$**, even though similar Ag concentrations were measured in the snails provided as food. Thus, three hypotheses were drawn: 1) the possible higher Ag assimilation in snails pre-exposed to $AgNO_3$ may have led to higher Ag availability to planarians than when fed on snails pre-exposed to Ag_2S NPs; 2) more different Ag uptake pathways could have been involved for $AgNO_3$ than for Ag_2S NPs; 3) snails pre-exposed to Ag_2S NPs previously showed efficient elimination, so they may have been able to eliminate a considerable amount of Ag before being predated by the planarians. An important finding was that **food exposure had a higher contribution to Ag uptake from the nanoparticles by the planarians** (Figure 6.3). *G. tigrina* were previously exposed to waterborne 3-8 nm, 50 nm and 60 nm Ag NPs (same Ag NPs as Chapters 2 and 3), Ag_2S NPs and $AgNO_3$ through spiked water (no sediment) and spiked water and clean sediment. Planarians revealed uptake (albeit low) only in exposures to 60 nm Ag NPs and $AgNO_3$ (data on 3-8 nm, 50 nm and 60 nm Ag NPs are not shown in the thesis). Since the 60 nm Ag NPs revealed higher dissolution, it seems that **waterborne uptake by planarians was of dissolved Ag,** possible due to the epidermal mucus layer that can act as a protective barrier (Figure 6.3). Transdermal uptake from pore water may also happen when moving on the sediment surface, even though epidermal mucus may mitigate uptake (Figure 6.3). Although *P. acuta* and *G. tigrina* are epibenthic species, mostly exposed to the water phase, **uptake of water had much higher contribution to Ag uptake for the snails than for the planarians**.

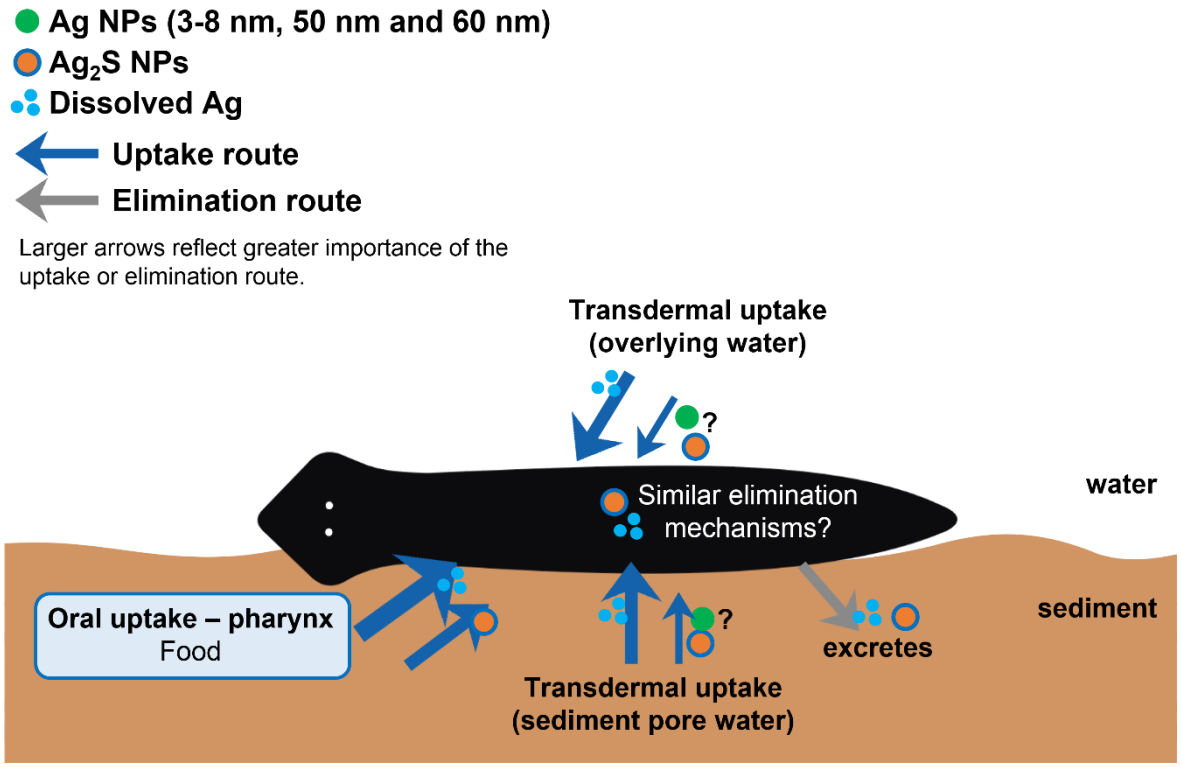

Figure 6.3. Schematic proposal for uptake and elimination routes of Ag in *Girardia tigrina* exposed to 3-8 nm, 50 nm and 60 nm Ag NPs, Ag_2S NPs and $AgNO_3$ in the different exposure route tests (Chapters 4 and 5).

Planarians revealed similar elimination in both treatments, suggesting that the Ag taken up from both $AgNO_3$ and Ag_2S NP treatments could have been eliminated through similar mechanisms (Figure 6.3). However, this hypothesis needs investigation. For **snails, the 24h-depuration time may be sufficient for proper gut clearance, minimizing elimination of internalized Ag,** although in the case of snails exposed to **Ag_2S NP the results were not conclusive.** For **planarians, "gut voidance" may not be applicable** due to their distinct digestive and excretory systems, and their very slow digestive process. **No biomagnification of Ag_2S NPs occurred in the two-level food chain *P. acuta* → *G. tigrina*** under the present test conditions. This was the first study investigating the toxicokinetics and biomagnification of Ag NPs in planarians, hence it provides useful data, especially looking at benthic predator's perspective. This work shows that further toxicokinetics studies should be conducted with planarians in order to better understand their Ag uptake and elimination mechanisms, and also highlights the role of planarian as a predator in bioaccumulation/biomagnification studies.

For the final study of the thesis, **Chapter 5**, an indoor mesocosm experiment was conducted **simulating a stream environment**. The three aims of this chapter were: 1) to determine toxicokinetics of Ag_2S NPs and $AgNO_3$ in the freshwater benthic invertebrates *P. acuta*, *C. riparius* and *G. tigrina*; 2) to determine if single-species tests (Chapter 2 to 4) can predict bioaccumulation in the more complex scenario of a mesocosm; and 3) assess Ag bioaccumulation in the three invertebrates and potential biomagnification. The **three invertebrate species showed higher uptake rates and Ag accumulation upon exposure to $AgNO_3$**, but revealed uptake of Ag_2S NPs, indicating that the **more relevant and persistent Ag nanoform may be bioavailable** in benthic environments. **Water seemed the most important uptake route for the three species**. For snails and planarians, exposure to water and food may have contributed to Ag uptake for both $AgNO_3$ and Ag_2S NP treatments (Figures 6.1 and 6.3). For planarians, the occurrence of transdermal uptake is hypothesised in both treatments, albeit higher in organisms exposed to $AgNO_3$. However, transdermal uptake of NPs in planarians needs confirmation (Figure 6.3). Moreover, the observed uptake of Ag_2S NPs by the planarians supports the importance of the dietary uptake of nanoparticulate Ag to this organism since the very **low recovery of chironomid larvae suggests that were predated by planarians**. Predation therefore may have influenced chironomid behaviour and consequently their Ag uptake patterns. *C. riparius* significantly reduced their foraging activities in the presence of fish predators (Hölker and Stief, 2005). Snails also respond to predator cues, therefore may also have changed their behaviour to escape planarians (and probably rainbow trout that were kept in cages in the mesocosms). This leads to an important aspect: since **interspecies interactions can greatly affect organism exposure to contaminants,** and it cannot be verified in single-species tests.

It was concluded that **overall, the single-species tests could not reliably predict Ag bioaccumulation in a more complex scenario, such as the mesocosm experiment**. The reasons are: 1) for planarians, internal Ag concentrations in the mesocosms were around 40 times higher than in single-species test (for Ag_2S NPs there was no uptake in the single-species test). Even though kinetics did not significantly differ, it may be due to the large confident intervals; 2) for snails, the kinetic parameters differed overall, except for k1 water in the Ag_2S NP exposure, but internal Ag concentrations were 18 times higher in snails from mesocosm in this treatment. Uptake patterns were quite different between the two experiments in the $AgNO_3$ treatment and internal Ag concentrations were significantly higher in the mesocosm test; 3) chironomids from the Ag_2S NP-spiked mesocosms showed around 10 times lower internal Ag concentrations than those from the single-species test.

In turn, similar uptake patterns during the first 48h were obtained in the $AgNO_3$ treatments, even though this very short exposure time (48h) may not predict uptake levels reached upon longer-term exposure; 4) the scarcity of data (especially in the case of chironomids) and the very wide 95% CI determined for the calculated uptake and elimination rate constants hampered reliable comparisons and conclusions.

Biomagnification potential under these mesocosm conditions was apparently low. However, a **BMF of 1.05** was estimated for the **food chain *P. acuta* → *G. tigrina* upon $AgNO_3$ exposure**. To our knowledge, this is the first time that the toxicokinetics of Ag_2S NPs in benthic invertebrates in a freshwater mesocosm experiment were investigated. Thus, this work provided important data to **help predicting the potential exposure, uptake, bioaccumulation and biomagnification of the most relevant Ag forms in more realistic benthic environments.**

6.2. Final conclusion and future perspectives

The present thesis provides information and parameters that can be used to better understand the fate of Ag NPs within the biota compartment, such as its interactions and bio-uptake in benthic freshwater ecosystems. The use of different benthic species highlights the importance of using benthic organisms from different functional feeding groups to be representative of the multiple exposure scenarios that exist within benthos. Information obtained for the Ag_2S NPs has particular relevance since few studies have addressed its bioaccumulation. As verified, this Ag nanoform is bioavailable and may be bioaccumulate in some conditions, alerting for research on its environmental fate and effects. Determining bioavailability and bioaccumulation of Ag_2S NPs in the more realistic environment of the mesocosm experiment was crucial to provide more realistic data to predictive models, especially considering that in some cases standard laboratory tests may not be able to reliably predict bioaccumulation in more complex environments. Furthermore, it also provides methodologies that can help in adapting current test guidelines, or to develop new ones, for the evaluation of the toxicokinetics and bioaccumulation of ENMs in benthic environments. There is a lack of standardized methods for bioaccumulation testing of ENMs. Priority can be given to the development of guidelines for mesocosm experiments, and so this work may contribute for that. Handy et al. (2018) suggested the use of *in silico* models with bioaccumulation data on invertebrate species as part of a proposal for a tiered approach to bioaccumulation testing of ENMs using fish. This places great emphasis on animal welfare (3 R's - Reduce, Refine and Replace). Investigations on how to use invertebrate data to reduce the need for fish testing are undergoing within the

NanoHarmony project (https://nanoharmony.eu/). In this regard, the data on the bioaccumulation of Ag NPs in invertebrate species in this thesis showed increasing relevance and urgency.

This study highlights the need for future complementary studies to better understand NP bioavailability and bioaccumulation in different scenarios, such as quantifying and tracking Ag NP (and other NP) distribution, forms, and concentrations in the organisms. For this is also fundamental to fully characterize the exposure medium and quantify different exposure routes. Evaluation of internal pathways that determine the fate of the ionic and nanoparticulate forms inside the organism is crucial to understand their bioaccumulation, as mentioned throughout this thesis. The formation of coronas by the accumulation of organic molecules, inside or outside the organisms, on ENMs may strongly affect their fate, bioavailability, uptake and internal processing. In this respect, it can be mentioned that samples of snail faeces derived from this work (Chapter 4) will soon provide information on the formation on a possible bio-corona by these organisms.

To conclude, priority should be given to performing more realistic exposures, accounting for simultaneous exposure routes and species interactions, and focusing on exposures to all relevant forms in which ENMs and ENM-derived metals may be encountered. Organisms can act as bio-reactors for ENMs, hence it is important to also evaluate their transformations and internal processing following uptake.

6.3. References

Béchard, K.M., Gillis, P.L., Wood, C.M., 2008. Trophic transfer of Cd from larval chironomids (*Chironomus riparius*) exposed via sediment or waterborne routes, to zebrafish (*Danio rerio*): Tissue-specific and subcellular comparisons. Aquat. Toxicol. 90, 310–321.

Croteau, M.N., Dybowska, A.D., Luoma, S.N., Misra, S.K., Valsami-Jones, E., 2014. Isotopically modified silver nanoparticles to assess nanosilver bioavailability and toxicity at environmentally relevant exposures. Environ. Chem. 11, 247–256.

Croteau, M.N., Luoma, S.N., Pellet, B., 2007. Determining metal assimilation efficiency in aquatic invertebrates using enriched stable metal isotope tracers. Aquat. Toxicol. 83, 116–125.

De With, N.D., 1996. Oral water ingestion in the pulmonate freshwater snail, *Lymnaea stagnalis*. J Comp Physiol B. 166, 337–343.

Desouky, M.M.A., 2006. Tissue distribution and subcellular localization of trace metals in the pond snail *Lymnaea stagnalis* with special reference to the role of lysosomal granules in metal sequestration. Aquat. Toxicol. 77, 143–152.

García-Alonso, J., Khan, F.R., Misra, S.K., Turmaine, M., Smith, B.D., Rainbow, P.S., Luoma, S.N., Valsami-Jones, E., 2011. Cellular Internalization of Silver Nanoparticles

in Gut Epithelia of the Estuarine Polychaete *Nereis diversicolor*. Environ. Sci. Technol. 45, 4630–4636.

Gimbert, F., Geffard, A., Guédron, S., Dominik, J., Ferrari, B.J.D., 2016. Mercury tissue residue approach in *Chironomus riparius*: Involvement of toxicokinetics and comparison of subcellular fractionation methods. Aquat. Toxicol. 171, 1–8.

Handy, R.D., Ahtiainen, J., Navas, J.M., Goss, G., Bleeker, E.A.J., von der Kammer, F., 2018. Proposal for a tiered dietary bioaccumulation testing strategy for engineered nanomaterials using fish. Environ. Sci. Nano 5, 2030–2046.

Hölker, F., Stief, P., 2005. Adaptive behaviour of chironomid larvae (*Chironomus riparius*) in response to chemical stimuli from predators and resource density. Behav. Ecol. Sociobiol. 58, 256–263.

Ribeiro, F., Gallego-Urrea, J.A., Goodhead, R.M., van Gestel, C.A.M., Moger, J., Soares, A.M.V.M., Loureiro, S., 2015. Uptake and elimination kinetics of silver nanoparticles and silver nitrate by *Raphidocelis subcapitata*: The influence of silver behaviour in solution. Nanotoxicology 9, 686–695.

Spyra, A., Cieplok, A., Strzelec, M., Babczyńska, A., 2019. Freshwater alien species *Physella acuta* (Draparnaud, 1805) - A possible model for bioaccumulation of heavy metals. Ecotoxicol. Environ. Saf. 185, 109703.

Toušová, Z., Kuta, J., Hynek, D., Adam, V., Kizek, R., Bláha, L., Hilscherová, K., 2016. Metallothionein modulation in relation to cadmium bioaccumulation and age-dependent sensitivity of *Chironomus riparius* larvae. Environ. Sci. Pollut. Res. 23, 10504–10513.

van den Brink, N.W., Kokalj, A.J., Silva, P. V., Lahive, E., Norrfors, K., Baccaro, M., Khodaparast, Z., Loureiro, S., Drobne, D., Cornelis, G., Lofts, S., Handy, R.D., Svendsen, C., Spurgeon, D., van Gestel, C.A.M., 2019. Tools and rules for modelling uptake and bioaccumulation of nanomaterials in invertebrate organisms. Environ. Sci. Nano 6, 1985–2001.